Adherence interactions between milk proteins and human intestinal surface layer components

A thesis presented in partial fulfilment of the requirements for the degree of

Doctor of Philosophy

Massey University

Palmerston North, New Zealand.

Christiane Schmidmeier

2016

Abstract

Recent research suggests a number of food-derived proteins may be used as orally delivered functional components. The native structure is often vital to their activity and requires protection during the digestive process. Nutrient vehicles are used as protective envelopes and as a mechanism for targeting specific sites of activity, e.g. the small intestine. This study evaluated molecules which adhere to one or more *in vitro* models of three human intestinal surface layers. Successful candidates could then be incorporated into nutrient vehicles, promoting adhesion to the surface layers and resulting in prolonged retention of the active ingredient at the site of action or absorption.

To identify molecules that adhere to models of the intestinal surface, an adhesion protocol was developed to screen the proteome of whole milk, skim milk and whey for candidate proteins. Molecules adhering to model layers of the human gastrointestinal tract (intestinal epithelial cells, mucin or bacteria with the propensity to form a biofilm) were screened by SDS-PAGE analysis and identified by mass spectrometry and Western blot. The binding behaviour of selected proteins was further investigated by flow cytometry. The combined results showed that milk and whey proteins exhibit different binding affinities to the models of individual surface layers. α-Lactalbumin was found to adhere to a model of the intestinal epithelial cells, while β-lactoglobulin showed binding to the protective mucin layer. Lactoferrin and various components of immunoglobulins showed highest binding affinity to bacteria. Finally, IgM appeared to adhere to all three tested model layers of the human gastrointestinal surface. Least binding was observed to the intestinal epithelial cells in culture. The validity of the developed adhesion protocol was demonstrated by replicating adhesion of immune-related proteins, lactoferrin and immunoglobulins, to bacterial cells.

This work reveals new important characteristics of milk-derived proteins in their ability to adhere to models of the gastrointestinal surface. These may be further utilised in site-specific targeting of functional foods.

Acknowledgements

Although doing experiments for and writing on a doctoral thesis is a project for one's own hands and development, I have not been alone on my journey. There have been many people offering guidance, support and friendship for which I am very grateful.

First I would like to thank the Riddet Institute and Massey University for giving me the opportunity to work on this great project. It has been a pleasure to contribute to the extension of knowledge and to be part of an intellectually stimulating community.

My thesis was sponsored by the Earle Food Scholarship. For making me one of their fellows I am very thankful to Professors Dick and Mary Earle.

Further I would like to thank AgResearch who generously provided me with the facilities and equipment for my experimental work and also an office at their Ruakura Campus.

My gratitude goes to my supervisors Distinguished Professor Harjinder Singh, Dr Brendan Haigh and Dr Nicole Roy who provided me great support and never failed to encourage me to find the right answers and stay focussed and motivated.

During my time, I was fortunate to meet and work with a lot of great people from the Dairy Science Building and the Dairy Foods Team. A big "Thank you" to everybody who helped me in the lab, took time for discussions and advice and above all that you gave me home away from home. Particularly, I would like to thank Robert for sharing an office and for being a good friend.

Thank you, Marty.

Liebe Eltern, ich kann euch nicht genug für eure unerschöpfliche und bedingungslose Unterstützung danken. Ich weiß, dass es nicht immer einfach für euch war und ihr euch bei

Zeiten gefragt hab, weshalb ich diese oder jene Entscheidung getroffen habe – auch wenn ihr mich das nie habt spüren lassen. Vielen Dank.

Auch meinen Großeltern möchte ich danken. Besonders für euch muss es schwer gewesen sein, mich gehen zu sehen. Dennoch wart ihr immer für mich da, habt mich unterstützt und mir geschrieben. Ich hoffe wir können die verlorenen Jahren jetzt nachholen. Alles Liebe.

... aus Lorbeeren macht man Kränze keine Betten.

- Steady Fremdkörper (Muff Potter)

I have been impressed with the urgency of doing

Knowing is not enough; we must apply.

Being is not enough; we must do

- Leonardo da Vinci

Meiner Familie.

Table of contents

List of abbreviations

90/10	Co-culture of Caco-2 and HT29-MTX cells in ratio 90:10
α-LA	α-Lactalbumin
β-LG	β-Lactoglobulin
BSA	Bovine serum albumin
CAPS	*N*-cyclohexyl-3-aminopropanesulfonic acid
CBB	Coomassie brilliant blue
CFU	Colony forming units
DL594	DyLight594
DMEM	Dubelco's modified Eagle medium
DMSO	Dimethyl sulfoxide
DTT	Dithiothreitol, Cleland's Reagent
ECL	Enhanced chemiluminescence
E. coli	*Escherichia coli*
ESI	Electrospray ionisation
EtOH	Ethanol
FCS	Foetal calf serum
FITC	Fluorescein isothiocyanate
Fuc	Fucose
Gal	Galactose
GalNAc	N-acetyl-galactosamine
GIT	Gastrointestinal tract
GlcNAc	N-acetyl-glucosamine
HCl	Hydrochloric acid
HPLC	High performance liquid chromatography
hr	Hour
HRP	Horseradish peroxidase
IEC	Intestinal epithelial cells

IgA/G/M	Immunoglobulin A/G/M
(IgG) hc	(Immunoglobulin G) heavy chain
kDa	kilo Dalton
LC-MS/MS	Liquid chromatography tandem mass spectrometry
LF	Lactoferrin
LiCl	Lithium chloride
Man	Mannose
MeOH	Methanol
MFGM	Milk fat globule membrane
min	Minute
MTX	Methotrexate
MUC(2)	Mucin(2) protein
NaCl	Sodium chloride
NaOH	Sodium hydroxide
NeuNAc / Neu5Ac	N-acetyl-neuraminic acid, sialic acid
NHS	N-hydroxysuccinimide
OD_{600}	Optical density at 600 nm
PBS	Phosphate buffered saline
PBS-T	PBS with 0.05% Tween20
PBS 5.5	10:6 diluted PBS used during the wash cycle, pH 5.5
PIA	Polysaccharide intercellular adhesion, poly N-acetyl-glucosamine
PTS-domain	Proline, threonine, and serine rich region in mucin protein backbone
Rhd	Rhodamine
rpm	Revolutions per minute
SDS-PAGE	Sodium dodecyl sulfate polyacrylamide gel electrophoresis
S. epidermidis	*Staphylococcus epidermidis*
sec	Second

sIgA	Secretory Immunoglobulin A
SLB	Sample loading buffer
STD	Standard
TBS	Tris-buffered saline
TT	Tris-tricine
V	Volts
WGA	Wheat germ agglutinin

List of figures

List of tables

Introduction

Supplementing foods with potentially beneficial ingredients is not new. In the 1920s the US government initiated the fortification of salt with iodine to fight iodine deficiency and goiter and maintain public health [19, 20]. Since then, more nutrients have been described to have functions besides their nutritional value (e.g. vitamins) and have been added to food as functional ingredients. This led to the development of the functional food market about 20 years ago which is now worth US$ 43.27 billion and continues to grow rapidly [21]. Nowadays, integrating additional nutrients, often as a functional ingredient, or beneficial bacteria into food products is creating a unique selling position for new products. With the exception of probiotics, the added molecules, such as minerals or vitamins, are less prone to premature degradation in the upper gastrointestinal tract (GIT). Consequently, a relatively large proportion of the added functional ingredients would reach the site of absorption in an active state.

Recent research has identified molecules of predominantly food origin, which confer beneficial effects to the human body (e.g. lactoferrin (LF), reviewed in [22]). Many of these have already been approved as a food supplements [23]. Some of these molecules are of larger size than traditional food supplements such as vitamins. Due to their complexity and tertiary structure, protein molecules are susceptible to degradation in the GIT environment [23].

To protect protein molecules, and at times to also avoid undesirable flavours (e.g. unsaturated fatty acids from fish oil), methods have been developed to protect them. This could be done, for example, by encapsulation or using liposomes or micelles as vehicles. However, this generates an additional step in the delivery process. The body has to degrade the protective carrier before it can access the functional molecule. If the degradation takes longer than expected, the nutrient vehicles will pass the site of absorption (or function) of the functional nutrients they carry and the functional nutrients are ineffective once they are released. To address this, research is focusing on “controlled release”, i.e. the development of nutrient delivery systems that release the carried nutrient under pre-determined conditions. Presently the method of choice is to coat

several layers around the functional nutrients, each of which is stable in one milieu (e.g. in the stomach) but dissolves in another (e.g. the small intestine). Thus the combination of coatings results in a controlled release of the nutrient at the site of absorption (interaction), e.g. the small intestine.

To date, a number of food-derived molecules are known for their ability to bind to one or several of the (inner) surface layers in the human GIT. These layers are epithelial cells, mucin and bacteria and their biofilms. Free milk oligosaccharides (from human colostrum [24-29]) and glycoproteins (e.g. porcine LF [30] or caseins [31]) have been found to bind to bacteria [32]. For example, *Escherichia coli* (*E. coli*) adhesion was inhibited mainly due to fucosyloligosaccharides, oligosaccharides which contain fucose [33-35]. The involvement of glycosides in bacterial adhesion suggests that binding could be lectin-mediated [36]. Further, some molecules from plant extracts have been ascribed bacterial anti-adhesive properties, for example from cranberries [37-39] or tea [40]. However, here it was not clear whether the anti-adherence was due to binding to bacterial or epithelial cells. Not much information regarding adhesion to intestinal epithelial cells (IEC) was found, probably due to the absorptive character of these cells. Finally, the negatively charged glycoside side chains of mucins can bind chitosan polymers or other positively charged molecules, while in the presence of divalent cations, such as Ca^{2+}, also negatively charged molecules show muco-adhesion [41]. The large mucin polymers can also entangle with other polymers (chain interpenetration [41, 42]) or retain smaller molecules which enter into the glycoprotein network.

The binding properties of these molecules could be harnessed to generate targeted delivery systems for functional ingredients. If the molecules were incorporated as anchor molecules into the surfaces of nutrient delivery vehicles, this would cause the nutrient delivery vehicles to "stick" and accumulate on the GIT surface. Thus the retention time would increase and more functional ingredients could be released close to their site of absorption compared to the current nutrient delivery systems which only provide a protective layer around the functional ingredients.

As indicated above, different molecules adhere through various types of interactions, including receptor binding [24], protein-protein interactions [43], lectin-carbohydrate interactions [36] and electrostatic interactions or through bridging by multivialent ions [41]. Physical interactions, such as chain interpenetration of large molecules [41] or entrapment of smaller molecules, are also possible. Understanding these interactions could further support the development of improved targeted delivery systems by tailoring anchor molecules, for example, through processing, and thus increasing their binding affinity to the GIT surface layer of interest.

These examples show that there is a wide spectrum of food molecules which have the potential to bind to one or several layers of the GIT surface. However, most of the studies have been conducted with isolated components. Further research is required to determine whether the passage of the upper GIT (i.e. low pH and proteolytic enzymes in the stomach), the conditions of the small intestine (i.e. almost neutral pH and ionic strength) and the competitive binding environment (i.e. other food molecules) have an impact on the binding ability and affinity of these components.

No information could be found in the literature suggesting that a systematic screening of foods, for example milk or whey, has been conducted to identify all molecules that have the potential to adhere to one or several layers of the small intestinal surface, or how these molecules bind in a simulated intestinal environment. However, it would be desirable to have a library of food-derived molecules which specifically adhere to one of the GIT surface layers.

As to date, there are no alternatives to targeted delivery of nutrients via the oral route, it is desirable to improve the efficacy of the existing targeted delivery systems and avoid loss of functional ingredients due to premature degradation or delayed release. Therefore, the objective of this dissertation is to develop an adhesion protocol which will then be used to screen milk and whey to identify molecules which adhere to one or several layers of the human intestinal surface. These molecules can be used as anchors for nutrient delivery vehicles. Thus, the time available to degrade the vehicles will increase, and the nutrients will be released at their site of

absorption. This strategy allows for the preparation of efficient delivery vehicles for functional ingredients.

Chapter 1 Review of literature

This review intends to give an overview of the human gastrointestinal physiology with focus on properties of the small intestine as this section of the GIT is most relevant for nutrient absorption and thus the targeted site for most nutrient delivery systems. The individual surface layers, IEC, mucin layer and bacterial biofilm, will be presented in detail. Finally molecules and nutrient delivery systems with known binding properties to the GIT surface or individual layers thereof will be summarised to provide an impression of the current progress in the field of targeted delivery of functional nutrients.

1.1 Physiology of the human gastrointestinal tract

The human digestive tract is made up of a series of linked functional units for the digestion and absorption of food [44]. As shown in Figure 1.1, food is first processed in the mouth (oral cavity) and then passed through the oesophagus and cardiac valve (lower esophageal sphincter) into the stomach where the food is transformed into a viscous paste [45] which is released through the pyloric valve into the small intestine. In the duodenum, the first part of the small intestine, secretions from liver and gallbladder are added. The digested food is then transported through jejunum and ileum where most nutrients are absorbed [45] before entering the caecum through the ileocecal valve. Finally, in the colon, the food is fermented by the colonic microbiota and remaining water is absorbed, leaving a thick digesta which is passed into the rectum before defecation.

The single units have structural similarity (e.g. tube like) but differ crucially in distinct features like cell lining [44], mucus layer (Figure 1.2) or resident bacteria (Figure 1.3). The addition of secretions further contributes to specific functions of the distinct regions [46]. The main functions of the GIT are motility, secretion, digestion and absorption [47, 48].

1.1.1 The stomach

After passing through the oral cavity, including primary size reduction and mixing with enzyme (e.g. amylase) and mucin containing saliva, the ingested food is transported through the oesophagus into the stomach. The stomach, which has a volume from 50 ml (empty) up to 1.5 L

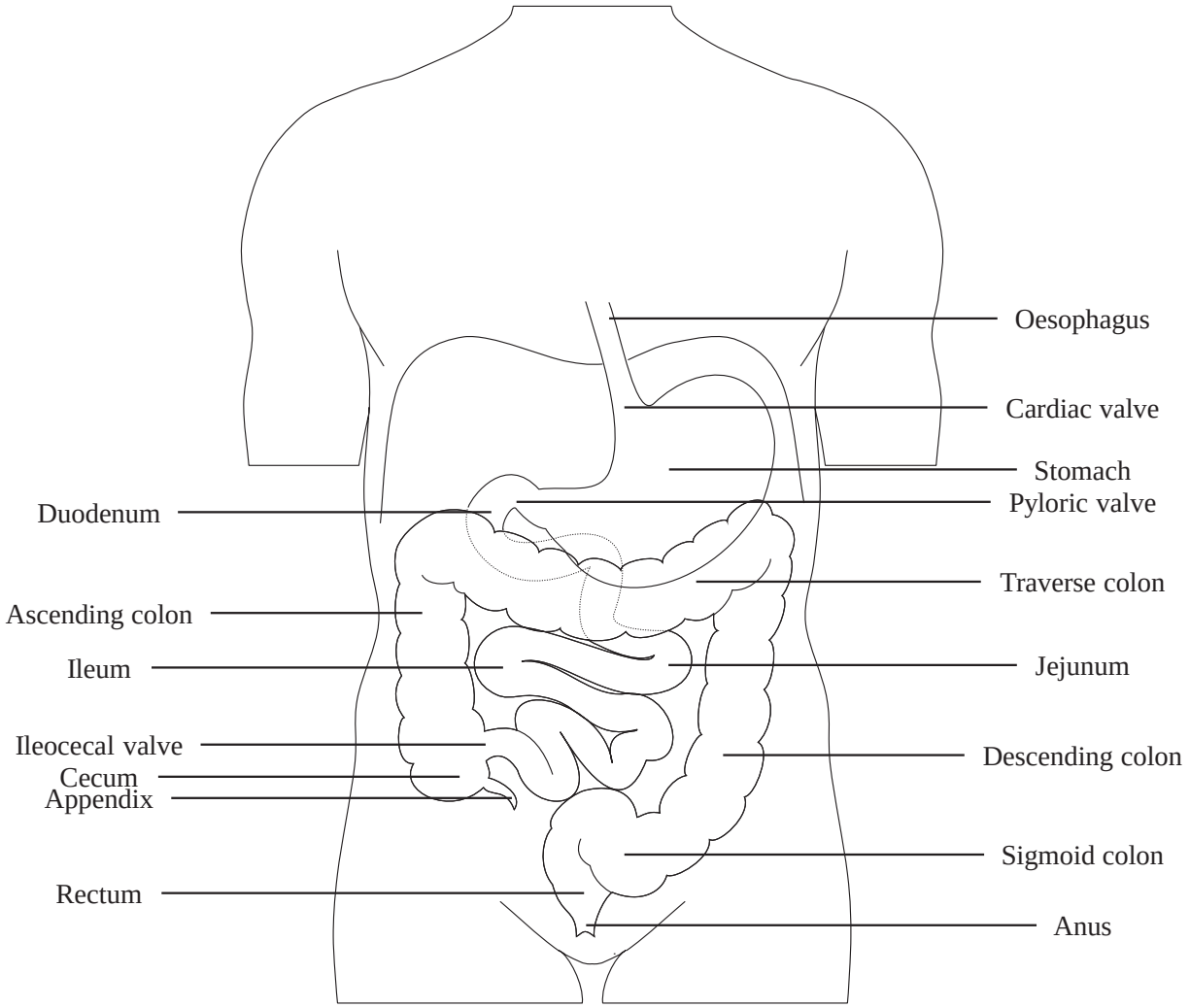

Figure 1.1: Schematic representation of the human digestive tract. Adapted from Javadzahdeh and Hamedeyazdan [49]

(stretched), serves as a reservoir for food. The food is partially neutralised and macronutrients are degraded (digestion). During digestion, food is mixed with gastric secretions and moved through contractions of the gastric wall, leading to the formation of highly viscous chyme [45].

One of the key functions of the stomach is the inactivation of dangerous components ingested with the food such as bacteria. Therefore, the pH in the stomach is as low as 2 [45]. The low pH is created by the secretion of hydrochloric acid (HCl) from parietal cells [50]. HCl is one of the main components of gastric acid, which is also responsible for activating pepsin. Pepsin is an endopeptidase which hydrolyses peptide bonds with the aromatic amino acids phenylalanin or tyrosine. Pepsin activity results in large peptides with are further digested in the small intestine [45].

In order to protect the gastric epithelial cells from the harsh environment in the stomach, mucins are secreted by foveolar cells or cardiac tubular glands [51] which form a up to 0.6 mm thick mucin layer [45] (Figure 1.2). The normal mucin layer contains mucin 5AC (MUC5AC), MUC6 and the membrane bound MUC1 [52]. In a healthy human the epithelial cell lining of the stomach does not get in contact with the gastric contents as all molecules need to penetrate and diffuse through the mucin layer before reaching the epithelial cells.

1.1.2 The small intestine - duodenum, jejunum and ileum

The first part of the human intestinal tract is the five to six meter long small intestine [48, 53-55]. The small intestine is the major organ for nutrient absorption due to its length and surface (transit time 2 to 4 hr) [56]. The topography of its luminal surface is characterised by apical microvilli, crypts and villi as well as Keckring and half-moon folds which enlarge the contact surface to 200 m^2 to enhance absorption [57, 58]. Peristalsis leads to a permanent movement and mixing of its contents [59].

As the epithelial cells of the small intestine form a permeable membrane, they are additionally protected by a mucus layer [54]. The thickest mucus layer is found in the early duodenum to protect against the highly acidic chyme coming from the stomach. The chyme is then mixed

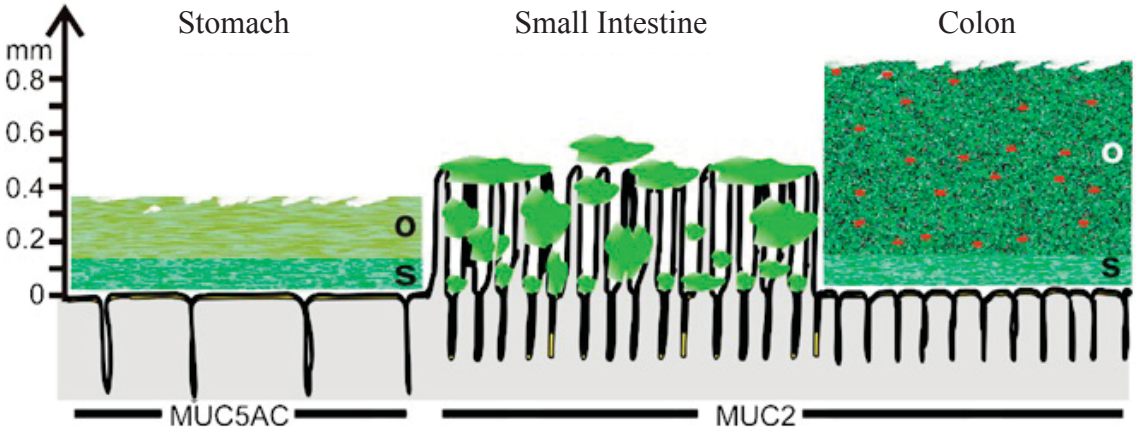

Figure 1.2: Schematic representation of the mucus coverage of the gastrointestinal tract [60].
Green layers represent expression of genes encoding the outer loose mucus (o) and inner stratified (s) layer, respectively. Red dots represent microorganisms in the outer mucus layer of the colon. Variation of mucus thickness and villi length along the GIT is not shown [60].

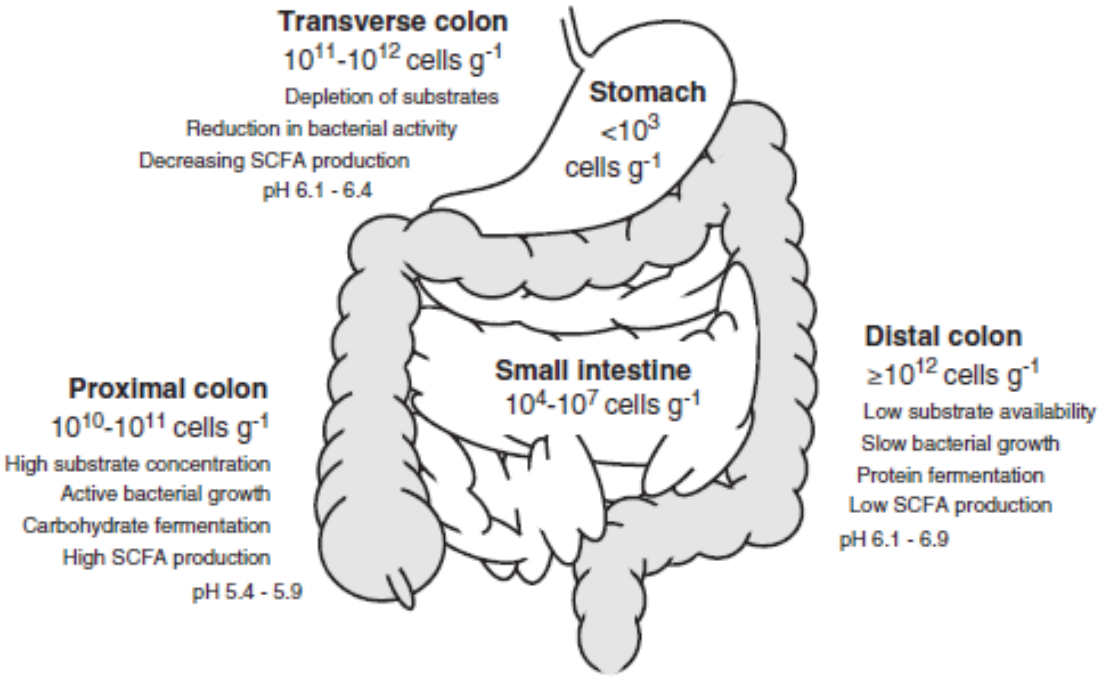

Figure 1.3: Schematic representation of the microbiota of the human gastrointestinal tract [18]
Schematic representation of the amount of bacteria per gram of intestinal contents, nutrient availability and bacterial fermentative activity typically found in different sections of healthy individuals.

with sodium-bicarbonate, bile salts, phospholipids and enzymes in the duodenum [61]. Bile salts, amphipathic molecules synthesised in the liver [62], enable the diffusion of post-digestion emulsions through the (*ex vivo* porcine) intestinal mucus due to the high negative charge the bio-surfactants impart to the droplets [63]. The lower parts of the small intestine are the jejunum, the main site of nutrient absorption and detection which has the most elongated villi, and the ileum for absorption of the remaining nutrients before passing the yet undigested food to the colon [64].

The small intestine has several functions [46], the major of which are absorption, barrier, and signal recognition and transduction. The combination of all processes is required to efficiently absorb nutrients while preventing harmful lumen contents, like bacteria or toxins, from entering the circulatory system [65]. Absorption, barrier, and signal recognition and transduction are illustrated in Figure 1.4 and are discussed below [66-68].

1.1.2.1 Absorption

The central function of the GIT is degradation of food and absorption of released nutrients [57]. The apical cell membrane has various transport systems for specific nutrients (e.g. glucose, amino acids or peptides) and also facilitates the uptake of non-nutrient food compounds. Membrane transport occurs mainly in three ways (Figure 1.4): (I) Paracellular transport is passive diffusion and utilises the gap at intercellular junctions between IEC [66]. This flexible and sometimes leaky (e.g. after interferon-γ treatment) pathway even allows transport of large solutes up to 10 kDa, including small proteins and bacterial lipopolysaccharides [69-71]. (II) Transcellular diffusion happens against an electrochemical gradient. It is the principal transport system for substances that can penetrate cell membranes, e.g. minerals [72]. (III) Intracellular vesicle transport is transcytosis of high molecular compounds like proteins [66].

Further, osmotic or electrochemical gradients can enable transport, e.g. water transport is related to osmotic processes (transcellular or paracellular) [45]. This is also linked to substance transport by solvent-drag whereby water carries off particles paracellularly [73, 74].

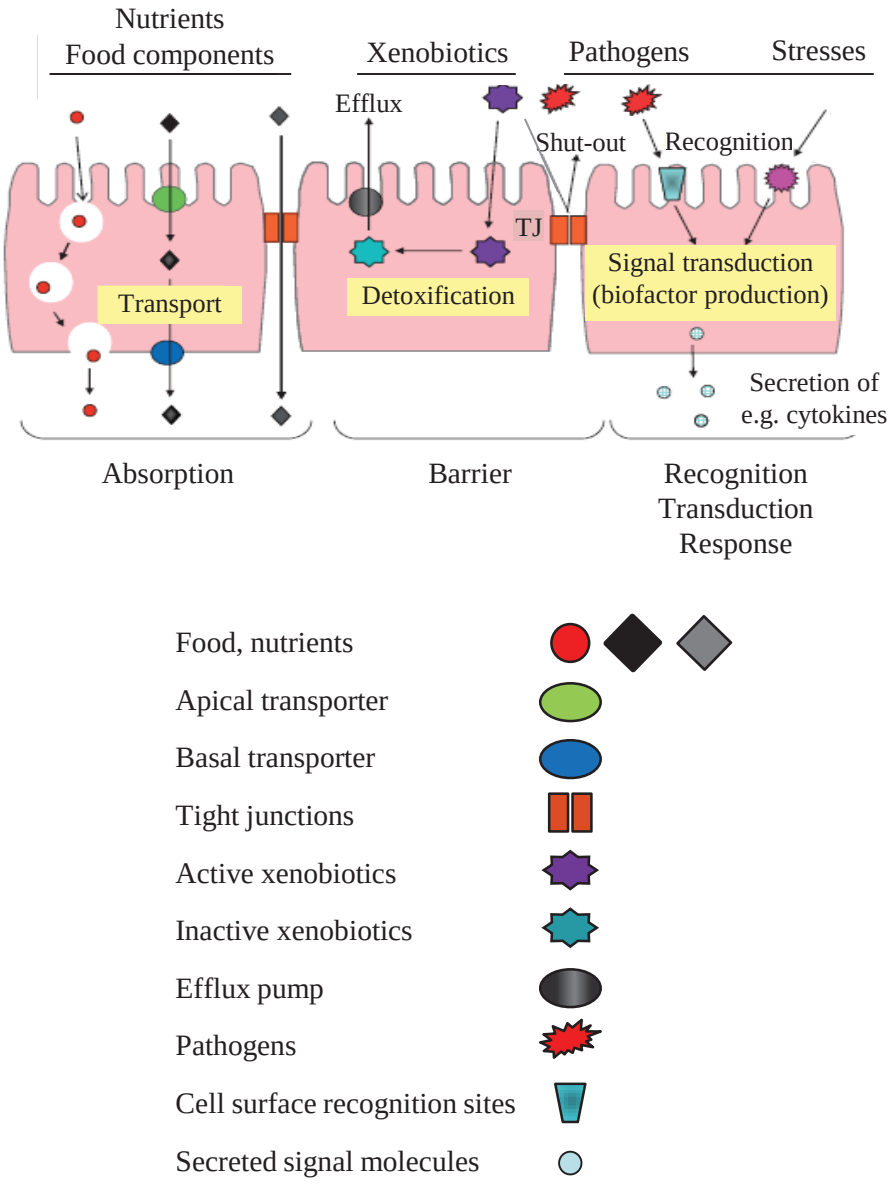

Figure 1.4: Three major functions of the intestinal epithelial cell monolayer. Adapted from Shimizu [66].

1.1.2.2 Barrier

The GIT interface is protected by several means: (I) a physical barrier that includes tight junctions which seal the IEC together [66, 75] and motility (peristalsis) to control the bacterial growth and to "clean off" chyme residues [57, 76]; (II) the biological barrier (innate immunity) including detoxification enzymes [77], secreted antiviral immunoglobulin A (IgA) antibodies and antimicrobial peptides [78-82]; (III) the harsh environment in the stomach and small intestine can also be considered a chemical barrier [83]; (IV) a last barrier is the commensal microbiota which deter exogenous bacteria from colonising the GIT surface [84].

1.1.2.3 Signal recognition and transduction

Signal recognition and transduction is carried out by the enteroendocrine cells which recognise food-derived nutrients [66] but also non-nutrient chemicals. The cells release hormones and paracrine factors to control digestion and food intake [85].

1.1.2.4 Duodenum as designated site for targeted delivery of nutrients

To date, the limited strategies that exist to control the release or retention of orally administered functional ingredients within the small intestine rely on pH (controlled release) or adhesion [59]. When moving from the stomach into the small intestine, the chyme is exposed to sudden changes in the environment, particularly an increase in pH-value from as low as 1 in the stomach up to 6.5 in the upper small intestine (Table 1.1). Further, glands attached to the duodenum start secreting digestive juices when food enters the small intestine, and this results for example in a 2-fold increase in bile salt concentration and changes in the ionic strength which also depend on the food. The combination of these milieu changes the chyme is exposed to, and a patchy mucus layer (Figure 1.2) make the duodenum the site of choice for studies of targeted delivery to the small intestine. The small intestine has only loose mucin coverage in discrete patches which are distributed along the villi. In-between the mucin islands, epithelial cells are exposed to the lumen contents to enable absorption of nutrients. In contrast, the mucin layers in the stomach and the colon are thick, two-layered blankets to protect the epithelial cells from hostile gastric conditions and dangerous food components or colonic microorganisms,

respectively (Figure 1.2). The difference in mucin layer structure and thickness is only one of the physical and physiological changes observed through the GIT. These changes are summarised in Table 1.2 and are detailed in Section 1.1.4.

1.1.3 The large intestine – caecum, colon and rectum

After absorption of water and salts and addition of lubricating mucus in the caecum [86], the chyme mix enters the colon. The main processes in the colon are further water and electrolyte absorption and thickening of the faeces, the microbial degradation of non-absorbable food components, such as fibre, carbohydrates and lipids and the degradation of remaining proteins and amino acids. Upon reaching the rectum, defecation and continence are regulated by propulsive motility [46].

An efficient protection of the epithelial surface is necessary, especially in the colon due to the extensive bacterial load, even if the majority are living in a mutualistic relationship with the host [87]. Thus, a thick mucin barrier guards the epithelial monolayer / S-layer (Figure 1.2) [60].

1.1.4 Physiological differences throughout the intestinal tract

One of the most striking differences across the length of the GIT is the pH-value. It rises from very low in the stomach to almost neutral in the duodenum [88, 89], increasing further to pH 7 to 8 in the ileum [53, 54], then decreasing again in the colon with a pH-value around 6.0 [90]. Another element of difference can be found in the mucin layer covering the IEC. A thick MUC5AC layer resides in the stomach, changing to a patchy, thin and soluble MUC2 monolayer in the small intestine where it follows the villi surface and is not firmly attached to the underlying cells. Finally, the colon is covered by a firm and thick two layered mucus barrier which has definite attachment to the underlying epithelia (Figure 1.2) [60, 91, 92]. The physiological changes throughout the intestine were summarised by Shoaf-Sweeney and Hutkins [24] and are shown in Table 1.2.

Table 1.1: Milieu changes in the upper gastrointestinal tract induced by the ingestion of food

	Fasted	Post-prandial
Ionic strength	Duodenum: 140 mM [93]	Increase and additional ions from food
Bile salts	Duodenum: 4.3 to 6.4 mM	Increase: 6 to 15 mM [94]
pH value	pH 1 to 2 in stomach	pH 5.8 to 6.5 in duodenum [89]

Table 1.2: Physical and physiological changes throughout the intestinal tract

	Proximal Intestine	Distal Intestine
Surface topography	High villi (10 to 40 per mm^2)	Smooth surface
Mucin coverage	Few mucus patches	Thick mucus layer
Chyme flow	High flux	Long residence time
pH-value	Close to neutral	Rising in distal small intestine direction
Digestive enzymes & bile components	High prevalence	Decrease or inactivation
Epithelial cells [95]	Proportion of goblet cells duodenum 4%	Proportion of goblet cells distal colon 16%
Bacteria (Figure 1.3)	Few bacteria in the apical parts [96]	Increase [95, 97]

The distribution of bacterial phyla throughout the human GIT is still a controversial topic: Carroll et al. [98] showed that probiotic bacteria were mainly located in the colon while pathogens colonise the upper regions of the GIT. In contrast, Bongaerts et al. [99] state that *Lactobacilli* are among the dominant bacteria in the proximal small intestine where easily available carbohydrates derived from host diet are used as the primary nutrient source. Other studies report that all identified phyla are discontinuously distributed across the GIT [100]. Generally, metagenomic studies looking at the microbial population in the GIT agree that the bacterial community in the jejunum is remarkably diverse compared to that found in the distal ileum, ascending colon or rectum in terms of composition and phylogenetic distribution (samples were taken as mucosal biopsies) [101]. However, this type of study should be considered with caution as most studies use faecal samples as a proxy of the *in vivo* bacterial community inside the human intestinal tract. Thus the phylotypes identified may not necessarily represent the microbial diversity in the colon [102-105].

1.1.5 Modes of interactions between food molecules and intestinal surfaces

The surrounding physico-chemical environment is important for interactions between food molecules and the intestinal surface as they influence the conformation and surface charge of molecules and adhesins. Additionally, cell shedding, mucus turnover and chyme flux lead to erosion of the adhering particles.

Potential bonding mechanisms include chemical (covalent, electrostatic, H-bridges, hydrophobic) and physical (e.g. chain interpenetration) interactions. Receptor based adhesion is also likely to play a role. The main types of adhesion-receptor interactions [24] include:

- Lectin-carbohydrate interactions appear along the surface of the host cell. They involve glycolipids, glycoproteins and proteoglycans that can be found in the glycocalyx layer [36].

- Protein-protein interactions involving the extracellular matrix components of the host cell. They are associated with basolateral surface structures of the mucosa (e.g.

fibronectin, laminin, collagen or elastin, which all bind to microbial surface components recognising adhesive matrix molecules [43]).

- Hydrophobin (fungal adhesins)-protein interactions occur during the early stages of fungi-host contact before specific lectin-carbohydrate or protein-protein interactions are formed. Although they are often thought to be nonspecific, there might be a degree of specificity [106, 107].

Although these interactions relate to microbial adhesion, the principal modes of adherence (of both host and bacteria) are also applicable to the interactions between food components and bacteria or IEC. For example, generation of low-molecular size digestion products in the small intestine leads to enhanced anti-adhesion effect of tempeh and tofu *in vitro* [108]. Thereby agglomerates of soy bean extracts and bacteria were accumulated in the supernatant of tempeh-extract treated piglet intestinal brush borders, among which the carbohydrate-based anti-adhesion bioactive component [109] was present. This indicates that the food molecules bind to the bacteria, and it is possible that one or several of the above mentioned adhesion-mechanisms are involved. However, this does not exclude that the digested food components also adhere to the human intestinal surface.

1.1.6 Processes and structural changes during food digestion

Throughout the GIT, the food is exposed to different physical environments, specific enzymatic processes and other conditions which lead to a step by step degradation of the complex food to individual nutrients, such as monosaccharides or amino acids, which can be absorbed through the intestinal wall. As the chemical structure and properties of the individual food groups (carbohydrates, proteins and lipids) vary, each group has its own site and systems for digestion [110]. However, some mechanisms like chewing and grinding in the mouth affect all nutrients [111].

Initially, in the oral cavity, the food is mixed with saliva and exposed to friction, causing dilution, access to salivary enzymes, and potential interactions with electrolytes and

biopolymers like mucins. This occurs within a few seconds (sec) to minutes (min), and with a moderate change in pH and temperature [112-115]. The degree of interaction between proteins and salivary components mainly depends on the charge on the proteins [116].

Passing into the stomach, nutrients enter a highly acidic (pH 2) environment accompanied by peristaltic movement. Here the chyme is mixed with pepsin (aspartic protease) and gastric lipase, mucins, salts and little amounts of detergents, such as lecithin and bile salts [111, 117]. Gass et al. [118] suggest that, due to fluctuation in gastric emptying times, gastric pH, pepsin activity levels and the extent of emulsification, the hydrolysis of protein in the stomach can be incomplete.

Digestion is progressed in the small intestine where five pancreatic enzymes with broad specificity are secreted [111]. The digestion is determined by surface active bile salts, inorganic salts which increase the pH-value to 6.0 to 7.5, and lipolytic and proteolytic enzymes. Intestinal digestion is a highly complex process as remnants of the earlier digestive phases are present [111, 119-121]. Gastric and small intestinal proteolysis results in breakdown products consisting of 30% amino acids and 70% oligopeptides. Remaining peptides are hydrolysed at the N-terminus by brush border membrane amino peptidases [122, 123].

Studies suggest that the small intestinal absorption of peptides is mainly transcellular, commencing with selective or nonselective endocytic uptake at the luminal membrane, followed by intracellular degradation by the lysosomal system and transport of degraded products to the extracellular space [124-128]. The absorption rate follows Michealis-Menten kinetics whereby the rate of absorption is limited in the order protein < fat < carbohydrate [129]. It was demonstrated that the passage of bovine β-lactoglobulin (β-LG) across enterocytes is mostly transcellular [130-132] with more than 90% of bovine β-LG being transported via a degradative pathway and 10% transported directly [130]. Despite a number of mechanisms for the exclusion of undigested macromolecules from systemic compartments, experimental evidence strongly suggests that antigenically active macromolecules can be transported from the lumen into the

circulation. This implies that protein can escape complete digestion, however, in nutritionally irrelevant quantities. Thereby absorption appears to be related to the concentration of ingested protein [133-136]. For example, oral administration of 1.9 to 2.5 g of β-LG resulted in antigen levels of 1.5 to 4.4 $ng.ml^{-1}$ serum [137]. Further, bovine milk immunoglobulins (Igs), which are degraded by small intestinal proteases into $F(ab')_2$, Fab and Fc fragments [138] can evade proteolysis. The secretory component of IgA makes it more resistant to proteolysis. Also bovine IgG and IgM are relatively resistant to hydrolysis and can survive the passage through the GIT in significant amounts [139, 140]. The resistance to proteolysis of some specific protein domains seems to be a prerequisite for crossing the small intestinal mucosal barrier to sensitise the immune system [141-143]. In contrast, the study of Bernasconi et al. [144] indicates that, besides transformation of nutrients for efficient absorption, one of the main functions of small intestinal processing is to reduce food immunoreactivity.

Although the uptake of particles (e.g. in targeted delivery systems) in the small intestine is now widely established, there is still controversy regarding the uptake mechanism and extent [145] which occurs transcellularly and to a lesser extent through paracellular pathways or resorption [146-151]. Research in this field is on-going, with considerable focus on the performance of targeted delivery systems during the passage through the stomach and small intestine. Often *in vitro* models of the GIT are used for these experiments. One major drawback in the evaluation of these digestive systems *in vitro* is that these are not able to simulate the magnitude of variables in real digestive systems. The dilution with saliva and the salivary flow, the amount of gastric juice released and the quantities of surface-active compounds and enzymes present in the small intestine vary markedly according to the type of food, the individual's physiology and within the same human subject at different times of the day [111].

1.2 Intestinal surface layers

The inner surface of the GIT is lined by several layers (Figure 1.5 and Figure 1.6). The first is the epithelial S-layer [152] covered by the glycocalyx, itself covered by one or two layers of secreted mucin (Figure 1.2) [92, 153, 154]. The interplay of layers can be described as a

dynamic fluid state with continuous movement and transposition [155], due to secretion and absorption, epithelial replacement and villous motility [156]. For example, the unstirred mucus layer is permeable to ions and products of low molecular weight via slow diffusion or retention of nutrients [71], but impermeable to larger molecules, such as proteases and certain toxins. It is further impregnated with IgA [157-159]. Lastly, bacteria inhabiting the GIT can be considered the top layer. These are also able to colonise the other layers. Savage [155] describes bacterial filaments which adhere tightly to the epithelium and also mucin glycoproteins. The latter can be used by several commensal bacteria, as an initial binding site [24, 160, 161] as well as carbohydrate source [162]. Epithelial secretions can also be used as nutrients [155, 163].

Together with the inter-meshed mucus layer [164], the glycocalyx is crucial for a functioning of the barrier and to maintain the relationship between host and microbiota [78, 165]. The functional integrity of the layer system depends on the single layers acting together, and each contributing to the protective and absorptive function of the complex barrier by coordinated regulation of mucus, epithelial cells and immunity responses [166, 167] (Figure 1.5).

1.2.1 Epithelial cell layer and glycocalyx

The IEC and the monolayer they form play a particularly important role in the intestinal functions. This is the first cell population that comes into direct contact with lumen contents, digest and intestinal microbial components and the final cell layer for absorptive or secretory processes in the epithelium [66, 168, 169]. The S-layer (single cell thick monolayer) is capable of regulating the permeability [170] by expression of a variety of digestive enzymes, transporters and receptors.

The IEC layer is composed of distinct cell lineages, each contributing uniquely to mucosal defense and maintenance of barrier integrity [171-174]. To enable a barrier, polarised IEC are sealed by intercellular junctions to their adjacent cells at the most apical region and bound to the extracellular matrix via several multi-protein complexes [24, 152, 169, 175]. Further, the cells show distinct polarisation by site-specific expression of transport proteins which allows

vectorial absorption and secretion [168, 176]. All mature cells of the absorptive, goblet and enteroendocrine cell lines are evolved from the lower crypt compartments consisting of stem cells [164, 177]. During their migration towards the villus, these cells proliferate, turn into transit amplifying cells and finally differentiate into the different lineages. They migrate within one to four days along the vertical axis of the functional villus where they are segregated into the mucus layer [24, 57, 156, 178-180], generating a fast and constant cell turnover [152]. Thereby a balance between proliferation and cell loss is maintained while preserving the structural continuity and functional integrity of the IEC surface [181]. Evidence has been found that apoptosis is activated specifically in villus cells residing at the top of the villi [182]. The most abundant cell types among IEC are enterocytes and goblet cells [183]:

- Absorptive enterocytes with a luminal brush-border [57, 184] are the most prevalent cells, they form a layer of columnar-shaped cells or microvillus epithelium to separate the lumen from the sub-epithelial lamina propria or basolateral domain in which the mucosal immune cells reside [173, 185].

- Goblet cells are unicellular glands which secret mucins as lubricant for protection of IEC and to bind pathogens [57, 171, 186]. They comprise between 4% and 16% of the cells on the villi [95, 164].

Less abundant cells include paneth cells (antimicrobial defence cells in the small intestine [57, 164, 187, 188]), microfold cells without glycocalyx or mucin layer [97, 189] (transepithelial vesicular trafficking of antigens and bacteria [190, 191]), Peyer's patches (tertiary lymphoid tissue [78]), chemosensory enteroendocrine cells [168] and the undifferentiated crypt cells [184].

The glycocalyx is a dense extracellular zone (0.5 µm thickness [192]) on the apical surface of IEC which is composed of carbohydrate-rich transmembrane and secreted and vesicular bound molecules (e.g. glycoproteins, glycolipids, proteoglycans or collagen) [193-195]. Because of

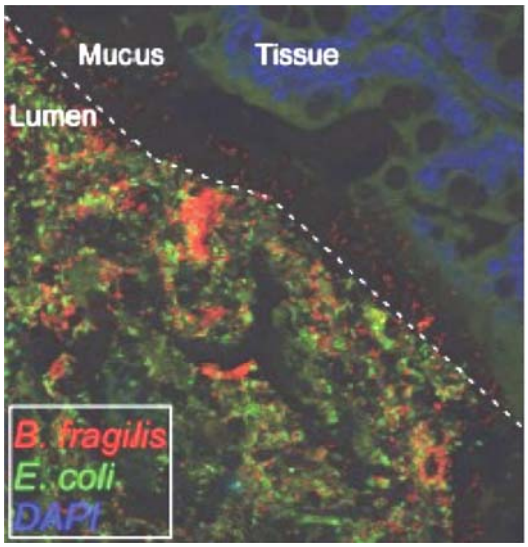

Figure 1.5: Intestinal layers [196]

Intact intestinal layer system: Lumen with bacteria on the left / bottom part of the picture and IEC in the top-right corner in blue. The two domains are separated by a mucin coat (black diagonal zone) which shows only few bacteria (red) in the outer layer. Colours enhanced to increase contrast.

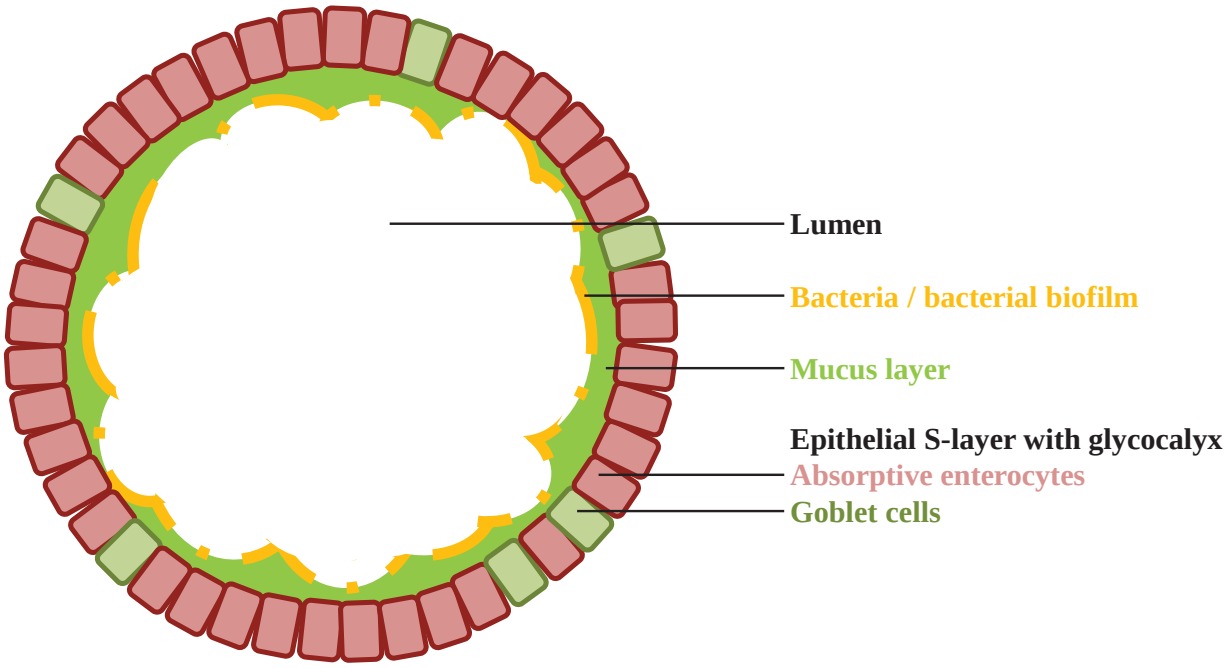

Figure 1.6: Scheme of the human intestinal layers

densly glycosylated transmembrane mucins [197] and a relatively fast extracellular release of polysaccharides and proteins from the cell surfaces [198] the cell coat is constantly renewed and acts as reinforcement of the physical barrier. It shows an affinity for lectins, toxins and bacteria [199] and is capped by and integrated within a secreted mucus gel [43, 78, 200-204]. The glycocalyx is thought to play a role in cell growth, differentiation, metabolism and cell-cell interactions [205-210], modulation of receptor-mediated membrane processing [211, 212] and acts as selective molecular sieve and depot region for nutrients [213]. Its diversity and density of saccharides make it an appealing site for lectin-bearing bacteria [24, 214-216].

Levine et al. [213] showed that the total average diffusion times of molecules are increased, and reaction rates decreased, due the anisotropic (density gradient) structure of the extracellular matrix and glycocalyx when compared with isotropic (constant density) transfer media.

1.2.1.1 Cell culture of epithelial cells

To date there have been no reports on the successful culture of freshly dissociated IEC. The most likely explanation lies in the intrinsic properties of the villus enterocytes: they are terminally differentiated cells, destined to undergo apoptosis [182, 217]. Further, the small intestine is one of the most uncommon sites for cancer in humans and experimental animals, and the few cell lines derived from this tissue proved of little use, due to their fibroblastic nature (ovine) [218], slow multiplication rates (10 days) or oncogenic metabolic characteristics (human) [219]. Most well-established tumour derived cell lines originate from colon cancers (e.g. Caco-2 and HT29) [164]. Both Caco-2 and HT29 cells display a marked heterogeneity in morphology and function [220]. Nevertheless, using established cell lines has the advantage that the cells are available and easy to handle, whereas primary cells normally are derived from different individuals and thus may lead to poor reproducibility [55]. However, one should keep in mind that established cell lines are derived from a progressive oncogenic progress and exhibit many chromosomal abnormalities. Further, the cells are from the colon and cannot be assumed to reliably display the properties of normal enterocytes. This demands careful analysis of each

individual application, particularly with respect to making meaningful *in vitro-in vivo* correlations [55, 164].

1.2.1.2 HT29-MTX cells

The parental cell line HT29 is an isolate of a colon tumour (adenocarcinoma) of a 44-year old Caucasian female [55]. Contrary to earlier assumptions, that the parental HT29 cell line has properties of intestinal stem cells [221], more recent research shows that HT29 cells contain a small proportion of cells which differentiate spontaneously as either enterocytic or mucus secreting cell types. These cells can be selected by special culture conditions, such as applying the cytotoxic drug methotrexate (MTX), deriving a population of clones which maintain a different (mucus secreting) phenotype in the absence of the selective agent [222]. Through stably adapting HT29 cells to MTX, HT29-MTX cells have been generated [221, 222]. Monolayers, grown from sub-clones of HT29-MTX, consist mainly of mature goblet cells with a discrete brush border with the presence of villi and characteristic proteins and form a continuous mucus layer on their apical surface. The thickness of the mucus layer is between 142±51 µm and 53±52 µm, consistent with the range of the human mucus layer [29, 221-223]. Mucin production is dependent on growth phase and starts with confluence and increases post-confluently [224, 225]. At late confluence, HT29-MTX cells show a dense mucus gel with numerous mucus buds on their apical surface [226]. Differentiated HT29-MTX cells secrete several types of mucin, including MUC5AC and MUC6 which are highly expressed in the stomach and upper small intestine [225, 227]. Caution is required, however, as the levels of MUC2, MUC3, MUC4 and MUC5AC mRNA were found to differ from one population to another and within each population according to the confluence stage [225].

Compared to the human small intestine, which secrets mainly MUC2, HT29-MTX cells predominantly produce MUC5AC. Both are secreted sialomucins [228, 229], encoded by a gene cluster on the 11p15 chromosome [230-232]. They can form networks due to cysteine rich N- and C-termini with a minimum of one large proline, threonine and serine rich region (PTS-domain). O-linked glycoside side chains make up <70% of the molecular weight [233, 234].

Consensus tandem repeat apo-mucin sequences of the two glycoproteins are PTTTPISTTTTVTPTPTPTGTQT (MUC2) and TTSTTSAP (MUC5AC) [235]. However, differences in the protein structure are of minor importance as interactions are most likely to happen with the easier accessible glycoside side chains which are modified due to malignancy [236, 237]. This manifests in an increase in sialomucin, a decrease in O-acetylated sialic acid (NeuNAc) and sulfomucin or alterations in the expression of blood group antigens [235, 238]. Also a reduction of the molecular weight (due to an approximate 50% reduction in carbohydrate content and chain length), simplification of glycoside chains and aberrant glycosylation in (pre) neoplastic mucins can be observed [235, 237]. The changes which have been described in colon carcinoma cells *in vivo*, have also been found in mucin-secreting colon carcinoma cells in culture. For example, mucins of the HT29 cell line have truncated glycoside-side chains due to prematurely stopped elongation due to sialation [239]. Malignant transformation of IEC is also associated with abnormal glycosylation of the cell surface (e.g. gp190 [240] or $\alpha_{2,6}$-sialation [241]). Despite these variations, HT29 cells and their mucin producing subpopulations are a widely used model for the human intestinal mucin producing cells.

1.2.1.3 Caco-2 cells

Caco-2 cells are the most widely used commercially available cell line (ATCC and ECACC). They were isolated from the colon adenocarcinoma of a 72-year old Caucasian male and express functions of enterocytes upon reaching confluence [242-246]. The cells form a polarised monolayer of well differentiated columnar absorptive cells [164, 247-249]. Thus they are particularly useful for the study of absorption [247, 250], cell polarisation and biosynthesis of brush border enzymes [246, 251-253]. The brush borders (microvilli covered apical cell surface) can be well organised on some cells but quite irregular on others [220]. In addition to brush border enzymes, Caco-2 cells express other features like tight junction proteins [254], the P-glycoprotein drug efflux pump and the di/tripeptide transporter [255-257] which are found in the small intestine.

Caco-2 cells have glycosaminoglycans as receptors which can be used for adhesion by microorganisms, e.g. *E. coli*. As enterococci adherence can be inhibited by treatment with heparin or heparan sulfate [215, 258], polysaccharides seem to be involved. Similar results are found for eukaryotic cells. Quaroni [259] found that monoclonal antibodies raised against Caco-2 cells recognised antigens specific to normal villus cells of human colon tissue. However, a Caco-2 monolayer, composed of solely absorptive cells, cannot resemble the small intestinal S-layer by itself. The tightness of the monolayer resembles more the colon [164, 247, 260], about 5- to 10-fold higher transepithelial electric resistance than in the small intestine, resulting in poor permeability for hydrophilic compounds via the paracellular pathway. Furthermore, it is widely accepted that Caco-2 cells show other colonocytic features like the expression of surfactant protein A [261].

1.2.2 Mucin layer

Intestinal mucus consists of approximately 95% water. The remaining components are mucins, electrolytes, proteins, trefoil-peptides, antibodies and nucleic acids [88, 262]. The polymer weight of mucins is up to 10 MDa [263] and the natural concentration in pig duodenum is between 30 to 50 $mg.ml^{-1}$ [233, 264]. Mucins are highly sialated, gel forming glycoproteins which provide for the characteristic viscoelasticity of the mucus layer throughout the entire GIT. They can be divided into cell-surface or membrane-bound mucins and secreted mucins [173, 200, 265, 266]. Current knowledge about mucus structure is not extensive as *in vivo* studies on these layers are difficult. Atuma et al. [91] and Johansson et al. [267] found that, in live intestinal tissue preparations, mucus is thicker than expected.

1.2.2.1 Gel layer properties

The gel-like mucus layer covers the intestinal lumen and thus widely restricts contact between microorganisms and IEC (Figure 1.5). It serves as a medium for protection, lubrication and transport between lumen and IEC surface. Furthermore, the large filamentous gel-forming glycoproteins block binding sites at the IEC surface and contain anti-adherence molecules [53, 92, 160, 173, 268-270]. The tight adherence of mucin to the apical surfaces of IEC is due to the

existence of the specific complex between mucin oligosaccharides and the mucin binding protein of the apical membrane [271]. The thickness of the mucus layer is balanced between replacement secretion and enzymatic degradation, shear forces [91, 272] and a constant motion down the GIT [160, 273]. Of crucial importance to the integrity of the gel-network [274] is the resistance of MUC2 to digestive enzyme cleavage. The protein core is protected by dense glyoside-side chains which are linked via O-glycosidic bonds whereas the domains responsible for the formation of di- and trimers at the N- and C-termini are protected by a trypsin-resistant fragment.

A layer of phospholipids, primary phosphatidylcholine, covers the mucin layer. It provides a hydrophobic barrier and greatly limits the penetration of macromolecular water-soluble luminal contents [275-279]. These phospholipids are arranged in lamellar structures associated with specific proteins. As the mucin-network is strongly negatively charged, the phosphatidylcholine head group is believed to be electrostatically bound to the mucin network, forming a monolayer with the fatty acid chains extending into the lumen [280], transforming the hydrophilic mucus surface into a hydrophobic one [280] which also prevents adherence and penetration of bacteria [281, 282]. Csaki [175] hypothesises a permeability enhancing effect of surfactants on the intestinal mucus layer. Some proteins, for example β-casein or β-LG, but also whey protein isolates and caseinates and hydrolysates thereof were shown to possess surfactant like properties [283], and thus may exhibit a permeability enhancing effect. In this case an adhesive carrier made of β-LG would fulfil two tasks: (I) potentially enhanced adhesion to the intestinal surface and (II) decrease the barrier function and thus support of macromolecule transition through the mucin layer.

The viscosity of mucus varies from the crypts to the villi tips. A low viscosity was observed in the low goblet cells, the crypt basis and close to the lumen, whereas mucus adjacent to the columnar epithelium has a higher viscosity. Throughout the GIT, the mucus viscosity increases towards the distal colon. Results from Tanaka et al. [284] were unexpected as they showed a relative low mucus viscosity with low diffusion coefficient for H^+ and HCO_3^- in the duodenum

(compared with gastric mucus). This indicates that duodenal mucus may play a more important role in inhibiting ion diffusion than its gastric counterpart, and also that factors other than viscosity are involved in diffusion.

The mucus gel is relatively permeable to ions and low molecular weight solutes (m_R<1.3 kDa) with a measured rate of diffusion close to that in an unstirred layer of solution. High molecular weight enzymes like pepsin (ca. 35 kDa) cannot diffuse through the mucus at a physiologically significant rate. So the intact adherent mucus layer will act as a protective barrier [285]. On the contrary, more recent data showed that protein up to the molecular size of human IgA (ca. 162 kDa) can move freely through the network [286]. The authors hypothesised that the experimental set up of the earlier studies reduced the diffusion rate. Results from Macierzanaka et al. [287] show that mucus diffusion ability and velocity of monodisperse latex particles and a sodium-caseinate stabilised oil-in-water emulsion are dependent on particle size, but more on the presence of bile salts. The diffusion coefficient has a higher value for small particles and in the presence of bile salts, which lower the ζ-potential of the particles, this may increases the repulsion from negatively charged mucins. For lipophilic substances, mucin is a permeable diffusion barrier [288].

Bertolazzi et al. [289] found that the hydrophobicity is reduced from the proximal to distal duodenum. Hydrophobicity affects the adhesion of macromolecules, bacteria and toxins to the epithelia. They further showed that a high hydrophobicity is necessary to maintain the bio-physical barrier properties of the mucus layer, as a decreased hydrophobicity leads to an increased permeability of macromolecules as can be observed in caeliac patients.

1.2.2.2 Mucin molecules

Mucins are chemically and structurally diverse molecules, which all contain large quantities of galactose (Gal) and hexosamines with lesser amounts of fucose (Fuc) and strongly polar groups such as neuraminic acids or sulfate. The O-glycosylation is clustered in mucin domains that are rich in the amino acids serine, threonine and proline. Carbohydrates occur as linear and

branched oligosaccharides, which make up to 80 to 85% of the molecule weight and are attached to proteins *via* serine or threonine residues. The attachment of sulfate and NeuNAc to mucin oligosaccharides confers resistance to digestion by glycosidases [290].

Humans possess at least 18 to 21 mucin-type glycoproteins of which MUC2 is predominant in the small intestine [173, 291]. Differences between mucin types appear to be related to their respective functions within the GIT barrier system. Their surface charge, neutral or acidic, depends on glycosylation modifications [291]. The number of sugar-monomers in the carbohydrate side chains varies depending on the mucin origin. Chain lengths from 12 to 19 sugars can be found in mucins from the stomach and colon whereas those from saliva or small intestine are decorated with shorter chains of only five to eight monomers. Nevertheless, the glycoside side chains from different mucins have common structural patterns which divide into three regions: (I) at the reducing end of the carbohydrate chain, N-acetyl-galactosamine (GalNAc) connects the side chain via O-glyosidic linkage to Threonine or Serine in the protein core region. The core region of the protein backbone is formed by numerous tandem repeats of the same amino acid sequence with mostly Threonine and Serine [285, 292]. (II) The GalNAc residue is extended into the backbone region of the side chain consisting of alternating β-linked Gal and N-acetyl-glucosamine (GlcNAc) residues. (III) The frequently branched terminal (peripheral) region of the sugar chains is characterised by fucose, NeuNAc and GalNAc, in addition to GlcNAc and Gal. Due to ester-sulphate and NeuNAc residues in the glycoside side chains, mucins have an overall negative charge. This negative charge also increases the stiffness of the “bottle brush” around the mucin’s polypeptide core and confers a large hydration sphere in solution [153, 154, 293]. Finally, the biochemically-specific moieties contribute widely to the binding functionality [285, 294, 295]. The GlcNAc present in human mucin is a binding site for many bacterial proteins, e.g. an extracellular protein from *Lactobacillus plantarum* [296].

Membrane-bound mucins in human colonic goblet cells are MUC1, MUC3A/B, MUC4 and MUC12. They possess a membrane spanning domain and a heavily O-glycosylated tandem repeat domain [285], and may play a role in modulating the effects of bacterial interactions with

the epithelial membrane when the secretory mucin matrix is bypassed [166]. The monomeric mucins are components of the enterocyte apical brush border and therefore located primarily at the cell surface. However, they can be found in the mucus layers after being proteolytically cleaved just outside the cell membrane [153, 293]. MUC3 is the most abundantly expressed membrane mucin in the small intestine. It consists of two subunits: an extracellular subunit containing heavily O-glycosylated tandem repeat domains and two epidermal growth factor-like domains. It extends rod-like 200 to 1500 nm above the cell surface and forms the glycocalyx [297-299].

There are at least five gel-forming mucins: MUC2, MUC5AC, MUC5B, MUC6 and MUC19 [200, 265, 266, 291, 293]. The size of the protein backbone is at least 4500 amino acids. Both the C- and the N-terminal end of the protein core as well as the portion between the two heavily glycosylated segments are cysteine-rich with the potential for forming disulphide bridges [285]. Their PTS-domains become densely O-glycosylated by the glycosylation machinery of the Golgi apparatus and consequently form "mucin domains" [157]. MUC2, one of the most important representatives of this group [300], forms trimers by disulphide bonding in cysteine-rich N-terminal von-Willebrand-Factor domains. These domains are resistant to trypsin digestion [60, 274]. Macromolecules are up to and exceeding 10 µm in length [301-303]. Due to the formation of disulfide bridges the final polymers have molecular weights up to $m_R=10^7$ Da, with the monomeric mucin molecules having molecular weights of 2 to 3 x 10^6 Da [157].

The network like structure enables the formation of different layers of mucus [153, 154] as occurring in the colon [92]. When released from storage in goblet cell, granulate MUC2 expands in volume and spreads out under the outer mucus layer resulting in a lamellar stratified appearance of the inner mucus layer. Further, volume expansion to outer layer MUC2 is probably due to cleavages in the cysteine-rich parts that do not disrupt the polymer but increase the water binding capacity [154].

1.2.2.3 Mucins and adherence interaction

Mucoadhesive mechanisms are well summarised by Jacobs [41]:

- Chain inter-penetration occurs between mucin glycoside side chains and muco-adhesive polymers [41, 42].
- Hydrogen bonds can form between functional groups on either side, e.g. hydroxyl, carboxyl, amine or amide endings. Thereby anionic and neutral polymers appear to be well equipped for muco-adhesion at lower pH values. However, their carboxyl groups are protonated at intestinal pH-value and can only bind via poly-cationic salts (e.g. Ca^{2+}).
- Cationic polymers like chitosan can bind to mucins due to their opposite charges. This phenomenon can, however, not be generalised for all positively charged polymers.
- Adhesion of nanoparticles depends on their size: smaller particles bind better.

The strong negative charges of mucin glycoside tips due to NeuNAc and ester sulphate [157, 304] influence the overall interaction characteristics of mucin. NeuNAc is often the terminal monosaccharide in the oligosaccharide chain attached to glycoproteins. It is a relatively strong acid (pK_s=2.6) and completely deprotonated at physiological pH-value [304, 305]. Thus it generates an acidic micro-environment around mucin glycoside ends.

The negative charge leads to a high calcium affinity of glycoproteins wherein the glycoside side chains (mainly NeuNAc) probably "wrap around the Ca^{2+}" [306]. There are indications that a 1:1 complex between one sialate and one calcium ion is formed [304]. Forstner and Forstner [307] found that binding of Ca^{2+} to rat small intestinal goblet cell mucin was found to reach saturation at a concentration of free Ca^{2+} of 0.1 to 1.0 mM (max. 0.14 $M.kg^{-1}$ mucin) and to be independent of time and temperature in the physiological relevant range from pH 6.5 to 7.5. This indicates a pK of binding groups of approximately 7 which is higher than the pK_S of other NeuNAc groups. Thus it is likely that NeuNAc groups have artificially elevated pK_S-values as

they are buried in hydrophobic areas. Further, treatment of goblet cell mucin with neuraminidase decreases Ca^{2+} binding by almost 90%. Finally, a decrease in the viscosity of mucin was observed, suggesting that $CaCl_2$ may cause the mucin molecules to become smaller or more symmetrical.

Mucoadhesive properties *in vitro* have been shown for polymers, e.g. chitosan, using a BIACORE device [308, 309] or oral delivery studies [310]. Further lectins, like wheat germ agglutinin (WGA) or soy bean agglutinin, can be used as mucin adhesives [311, 312]. Pectins are a polymer group with known mucoadhesive properties [313] and some chatechins (tea polyphenols) were found to bind to different mucins. Likely the presence of a gallyol ring plays a vital role in this interaction as only epigallocatechin but not epicatechin seem to show this behaviour [314].

A last group of functional molecules which has been investigated regarding its mucin interactions are pharmaceuticals. Specific drugs have been shown to bind to mucins, often in a pH-dependent manner, thus reducing diffusion coefficients [315].

1.2.3 Biofilms

Several decades ago the first reports of the existence of so called “biofilms” appeared [316]. Biofilms are “structured communities of bacterial cells enclosed in a self-produced polymeric matrix and adherent to an inert or living surface” [316-320]. The matrix can be described as a “dynamic environment in which the constituent bacterial cells appear to reach a homeostatic state and are organised to make optimal use of all available nutrients” [321].

It is generally considered that the majority (95 to 99%) of microorganisms live in such a community [320, 322]. Also in the human GIT, where the microorganisms can find a variety of surfaces to adhere to, biofilms seem to be the preferred form of existence. Biofilms are in a carefully balanced equilibrium and small variations in exo- and endogenous parameters cause changes in matrix composition, architecture and microorganisms [318]. Therefore, to date all

standard *in vitro* laboratory models create a reductionist picture of the *in vivo* situation [319, 323].

1.2.3.1 Biofilm formation

The initial events that make microorganisms change their metabolism mode from planktonic to biofilm-associated are not completely understood [324-326]. A likely initiation factor for building extra polymeric substances might be the high availability of the respective substrates in the culture-environment [327]. In order to avoid chemical or physical stress factors which might affect the membrane lateral pressure, excess solutes are used to aid in colonisation of the GIT [328]. This is similar to the hypothesis by Creti et al. [329] that bacteria, in non-optimal growth conditions (e.g. excess of carbon sources), start the accumulation of reducing equivalents to dispose molecules out of the cell. The requirements for the formation of a biofilm are the existence of any kind of surface (liquid-liquid, liquid-solid, liquid-air or solid-air), water, available nutrients and the bacteria itself [316]. This complexity implies that there is no general valid adhesion mechanism for all microorganisms. However, a common five stage model was identified as shown for *E. coli* and *Staphylococcus epidermidis* (*S. epidermidis*) biofilms [316, 330-332] (Figure 1.7):

Stage 1: Initial reversible attachment: the native tissue or biomaterial, generally covered with a conditioning film [333], is attached by planktonic bacteria via adhesive surface molecules which overcome repulsive forces between the cell and the surface [24, 43, 332, 334-338]. This is possible even in turbulent streams as close proximity to the surface drastically decreases the fluid velocity [316, 330]. The forces include nonspecific van-der-Waals, hydrophobic [339] and electrostatic [334] interactions. Specific binding is mediated by a capsular polysaccharide adhesion or a cell wall-associated protein [332, 333, 340, 341]. Extra polymeric substances are not needed for the first attachment phase [163, 342].

Stage 2: Transformation of reversible to irreversible attachment: interaction between the bacteria and the surface is strengthened by production of extracellular polymers or specific

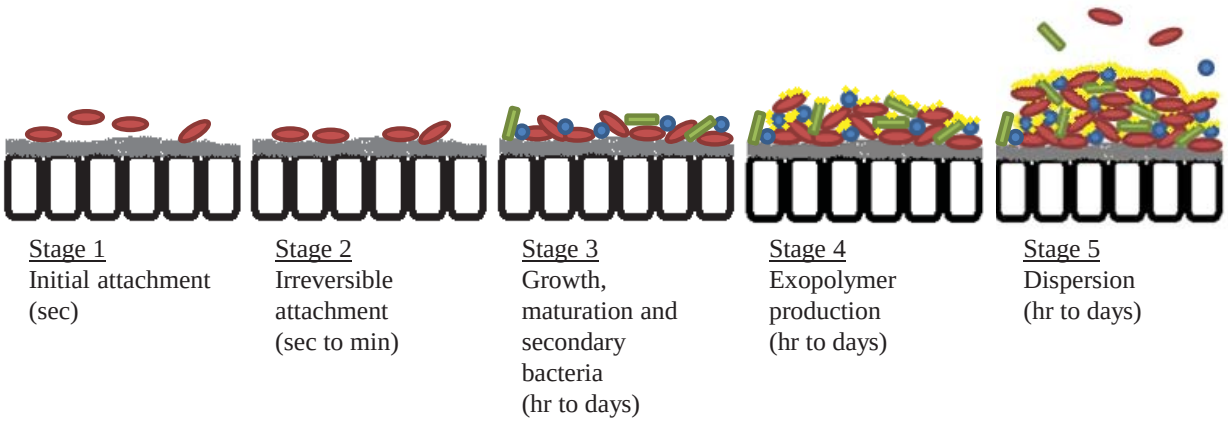

Figure 1.7: Scheme of the development of a bacterial biofilm on a native tissue

Pictures assembled with information from Costerton et al. and Sauer [339, 343]

adhesins often located on pili, fimbriae or flagella. The latter are of higher importance for Gram-negative bacteria like *E. coli*. In *staphylococcal* biofilm formation, the primary determinant of the accumulation phase is the polysaccharide intercellular adhesion (PIA) [344].

Stage 3: Early development of biofilm architecture: secondary bacteria, also of other types, can co-adhere to the primary colonising bacteria. After this, the microbial accumulation starts which can take place either by bacterial growth or by further addition of new bacteria out of the liquid phase [339, 345].

Stage 4: Development of microcolonies into a mature biofilm: initiation of extra polymeric substance production is characteristic for this step, leading to the formation of a three-dimensional growth of the biofilm [321, 333]. In a biofilm, the contribution of each type of interaction – London dispersion forces, electrostatic interactions (involving particularly Ca^{2+}) and hydrogen bonds – varies [316, 331, 346, 347]. Also bacterium-bacterium interactions induce growth and lead to a heterogeneous physicochemical environment [333].

Stage 5: Dispersion of cells from biofilm: some cells are released into the surrounding environment and return to the planktonic state, especially under shear force. Bacteria showing biofilm specific phenotype display crucially different surface properties at the boundary layer compared to planktonic cells [348].

Sauer et al. [343] found that most (stage specific) proteins are overexpressed. Some of these are involved in production of extra polymeric substances, metabolism and membrane transport. Due to the rapid passage of material through the GIT, biofilms must form rapidly [156]. A short video showing a biofilm development was published online by Sanders et al. [322] describing the work from Berk et al. [349] who modelled the development of a *Vibrio cholera* biofilm recorded with four-color confocal imaging.

1.2.3.2 Biofilm structure

A mature biofilm is composed of three layers [318, 332]. The bottom layer ("cement") is formed by the linking film which binds the biofilm to the surface and consists of glycoproteins and exopolysaccharides secreted by bacteria to bind the entire biofilm to the surface. Its strength is crucial for that of the whole biofilm [350]. The middle layer is made up of a compact bacterial population. It is a collection of microorganisms secreting extracellular matrix. On top is the surface layer from which free-floating bacteria can rise and spread. The majority of surface layer is made up of exopolysaccharide matrix which defines the surface properties of the biofilm [351].

The charged groups in bacterial polymers influence physico-chemical properties, such as solidness, viscosity, water binding capacity or binding of inorganic ions. Extra polymeric substances can also be hydrophobic or possess localised hydrophilic and hydrophobic regions. Thus they confer various properties to the matrices in which they are found and account for the wide differences in properties characteristic for biofilms [321, 331]. Enzymatic alteration of extra polymeric substances is believed to change their physicochemical properties and thus biofilm structure [352]. In order to minimise energy and material, the forces which keep the biofilm matrix together are not covalent, but weaker interactions [316] (compare Section 2.3.3.1, biofilm phase 4). The majority of extra polymeric substances present in biofilms can interact in a variety of ways, and *in silico* models reveal that charged groups are mostly on the exterior of the molecular chains [331]. Large channels and pores allow the entry of colonising cells and their establishment within the biofilm; they also enable the flow of nutrients, enzymes, metabolites, waste products and other solutes [321].

1.2.3.3 Biofilm community

Living in a co-existence with same or different bacteria bears several advantages for a microorganism. The cells are relatively immobilised and exist in direct proximity with each other. This allows the establishment of numerous interactions which make a biofilm a symbiotic

habitat [316, 353] and justifies the energy expenditure in synthesising the extracellular matrix [354, 355]:

- Accumulation, disproportion and reuse of nutrients: the extracellular matrix has a gel-like constitution. Therefore, convective transport is inhibited whereas diffusion is possible and nutrient gradients emerge. For example, varying oxygen levels allow microenvironments for aerobic and anaerobic bacteria in close proximity [316, 318, 356]. Further, products of certain microorganisms' metabolism might serve as substrates for others [357]. So the close spatial relation of different specialised bacteria allows the degradation and utilisation of otherwise indigestible or difficult to digest substances. These processes can also take place in dispersion but due to transport processes they take more time [316].

- Protection: a biofilm can serve as protection in many ways, e.g. extreme pH-values, high salt concentrations, biocides and antibiotics as well as host immune reactions and dehydration [321, 358].

- Transport of signals and genes: compared to planktonic populations, the bacterial cell density is high and therefore allows the transport and interchange of information by gene transfer or low molecular signal molecules [316, 318].

Biofilms are not to be associated solely with pathogens and disadvantageous effects. Hancock et al. [359] demonstrated that *E. coli* Nissle 1917, a major probiotic strain (benefits were observed for a number of intestinal conditions) and excellent coloniser of the human GIT, is able to colonise and establish itself *in vitro* in the presence of urinary tract isolates. Also, as it is covering the mucosal layer(s) of the GIT, a biofilm can mask original surface properties. It might, for example, change hydrophobic surface properties into hydrophilic ones [360].

1.2.3.4 Well studied biofilm forming bacteria

Along the GIT, the characteristics of residing bacteria differ markedly, e.g. cell count, species and function (Figure 1.3). *E. coli*, a Gram-negative facultative anaerobe, is one of the minor components of the commensal microbiota, with 1% of total biomass after establishment of a stable microbial population. However, it reaches concentrations up to 10^8 cells.ml^{-1} and the biology of *E. coli* in the GIT is well characterised, so it is often used as an example organism for studies of the microbiota [361]. Isolates with pathogenic potential are distinct from commensal *E. coli*, the latter displaying a lower frequency of virulence traits such as adherence factors and toxins [333, 362, 363]. For biofilm formation, GlcNAc, cellulose, colanic acid and antigen 43 are utilised [330, 333, 364, 365]. Thereby pGlcNAc, cellulose and colanic acid are the major components. Colonic acid seems to be produced at lower temperatures [366] and thus is not relevant for biofilms growth in the human GIT. Probiotic *E. coli* Nissle 1917 was isolated by Alfred Nissle in 1917 from faeces of a soldier who did not develop diarrhoea, in contrast to other soldiers in the same area. This strain does not exhibit any virulence factors, but has genomic islands responsible for the synthesis of several fitness-factors which contribute to the strain's probiotic nature. Its serotype is O6:K5:H1 which indicates that *E. coli* Nissle 1917 produces lipopolysaccharides with short polysaccharide side-chains (type O6), an extracellular capsule (type K5) and H1 flagella (type H1) for motility. Further, it has fimbriae and curli which mediate adhesion to IEC or to the mucus layer. Its outer cell membrane contains a lipopolysaccharide unique to *E. coli* Nissle 1917, and may explain why this strain exhibits immunomodulation properties without showing immunotoxic effects [367]. *E. coli* Nissle 1917 requires cellulose to adhere to HT29 cells contrary to other *E. coli* strains e.g. commensal *E. coli* TOB1 [368]. Also, unlike other strains, *E. coli* Nissle 1917 shows no co-regulation of curli and cellulose expression [368-370] and it can form biofilms at 37°C, whereas other *E. coli* strains need temperatures under 30°C [367].

S. epidermidis 1457, a human skin pathogen, is a facultative anaerobe which was isolated from an infected catheter. However, the composition and structure of its pGlcNAc are similar to that

of GIT bacteria. This strain is useful for adherence studies because it displays a large percentage of pGlcNAc and less protein in the biofilm matrix [371, 372]. In *S. epidermidis* 1457, pGlcNAc is called PIA (polysaccharide intercellular adhesion) and it has an important role in the establishment of the biofilm structure [371]. *S. epidermidis* 1457 M10 is a pGlcNAc depleted strain, due to an *icaADBC* knock-out [345, 373].

The *S. epidermidis* 1457 wild-type expresses PIA in fibrous strands at the cell surface whereas the M10 mutant releases pGlcNAc into the culture filtrate resulting in a complete loss of the extracellular matrix. By expressing PIA, bacteria can efficiently change the electrostatic properties of their cell surface, a likely reason for the resistance against antibacterial peptides as these are usually cationic. The extracellular matrix has been suggested to mediate immune evasion. Hence, the mutant strain is more susceptible to killing by major antibacterial peptides of human skin, cationic human β-defensin 3, LL-37 and anionic dermcidin [374, 375].

1.2.3.5 Bacterial cellulose

Cellulose is one of the main components of bacterial biofilms [376] of e.g. *E. coli* strains [377], *Salmonella* [378], *Enterobacter* [365, 379] and *Pseudomonas* [380, 381]. The co-expression with fimbriae, as observed in some *E. coli* strains, leads to the formation of a highly hydrophobic and rigid network, whereas the sole expression of cellulose results in a relatively hydrophilic and elastic surface [379].

Bacterial cellulose is structurally different from rigid plant cellulose, and cellulose networks themselves differ between bacteria (Figure 1.8). The cellulose produced by *Enterobactereaceae* seems to be structurally different from the cellulose produced by *Gluconacetobacter*, formerly *Acetobacter*, strains (*Gluconacetobacter xylinus* serves as model organism for cellulose biosynthesis) [379, 382, 383]. While the cellulose of *Gluconacetobacter* has a maximum degree of crystallinity of 70%, giving it a lower mechanical strength, cellulose of *Enterobacter* CJF002 has a crystallinity of 70% up to over 90%. Further, the Iα-fraction of the water-insoluble cellulose material of *Enterobacter* CJF002 cellulose is around 50%, which is smaller than that

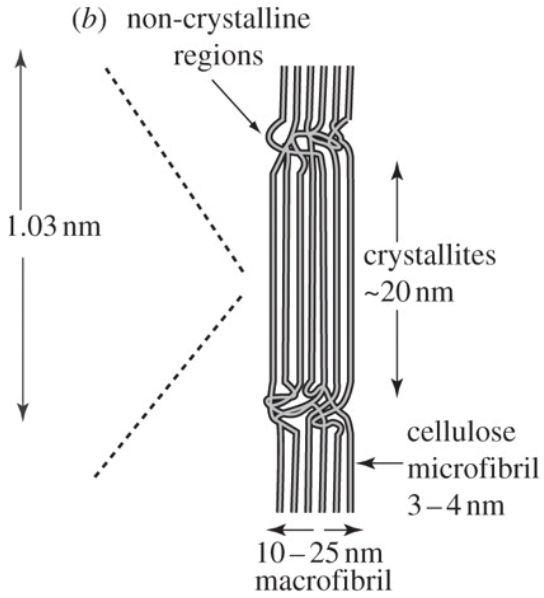

A

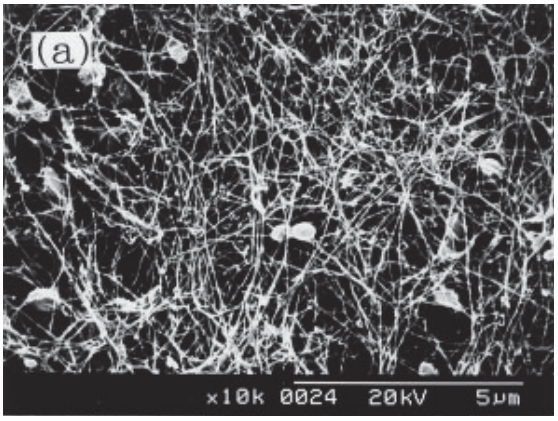

B

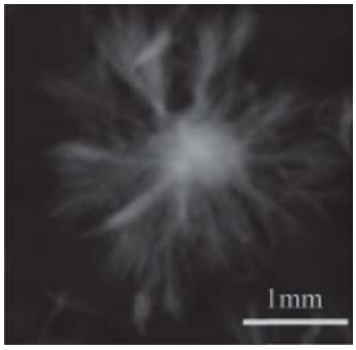

C

Figure 1.8 A-B: Cellulose of different origins

(A) Plant cellulose microfibrils, aggregated to a macrofibril [384]. (B) Scanning electron micrographs of bacterial cellulose, agitated culture (*G. xylinum*) [385]. (C) Optical picture of *enterobacterial* cellulose obtained under agitation [386]

of *Gluconacetobacter* (U.S. Pat. No. 5,144,021 in [383]). The Iα-fraction is a meta-stable phase; it has the same conformation of the heavy atom skeleton but different hydrogen bonding patterns to Iβ-cellulose. The lower percentage of this polymorph might be a reason for the increased surface interaction of *Enterobacter* CJF002 cellulose, as it leads to an altered balance in the orientation of OH-groups of the cellulose material, and so a higher density of OH-groups on the surface [383, 387]. Although the different forms of cellulose are chemically identical, glucose units are bound together to produce a long straight unbranched polymer chain [388], the variations in packing and orientation of the microfibrils result in marked differences in mesoscopic and macroscopic properties of the fibres, rendering enterobacterial cellulose with a large specific surface area of 50 to 150 $m^2.g^{-1}$ [389]. CJF002 cellulose may therefore be a good carrier material with excellent protein absorptivity due to especially strong interactions with proteins.

1.2.3.6 Poly-β(1,6)-N-acetyl-D-glucosamine

Genetic studies and polysaccharide analyses indicate that another cell-bound polysaccharide, pGlcNAc, of *E. coli* and *Staphylococci* is required for biofilm formation [390, 391]. pGlcNAc serves as a biofilm adhesin, responsible for mediating cell-cell adhesion [335, 392] in phylogenetically diverse species which exploit diverse hosts and environmental niches. It has structural similarities to cellulose in being an amorphous exopolysaccharide produced during the active growth phase. It also shields the growing colony from host immune defences and is an important virulence factor [391-396].

There are various forms of pGlcNAc which appear to differ in their molecular weight, in the degree of N-deacetylation of the GlcNAc residues and in the presence of O-succinate substituents (Figure 1.9) [334, 391, 397, 398]. The deacetylation is an uncommon feature for extra polymeric substances and the resulting cationic character (theoretical pK 6.9) of pGlcNAc presumably is essential for biofilm formation, immune evasion and the attachment of pGlcNAc to the negatively charged bacterial cell surface. Further, the solubility in aqueous environment is

affected. Mutant PIA (100% acetylated) has a high tendency to precipitate in aqueous solution, in contrast to the partly deacetylated soluble wild-type PIA [334].

Data indicate that deacetylation sites in wild-type pGlcNAc are randomly distributed and deacetylation by the surface-attached IcaB occurs in the cell surface matrix, whereas other steps in pGlcNAc biosynthesis take place inside the cell [334, 352, 399]. pGlcNAc is the main biofilm matrix component of *S. epidermidis* 1457 [400]. It is located in fibrous strands on the cell surface where it serves as an essential factor in biofilm formation [335, 401].

Purification of PIA led to the separation of two polysaccharide fractions [334], polysaccharide I and polysaccharide II. Chemical analysis and NMR spectroscopy of these two fractions showed that polysaccharide I (>80%) is a linear homoglycan of β-(1,6)-linked 2-acetamido-2-D-glucopyranosyl residues. On average 80 to 85% are N-acetylated while the remaining non-acetylated polysaccharide I is positively charged (Figure 1.9). The minor fraction, polysaccharide II (<20%), is structurally related to polysaccharide I but has a lower content of non-N-acetylated D-glucosaminyl residues. It also contains phosphate and ester-linked succinate, rendering it moderately anionic. The combination of these modifications leads to the simultaneously positive and negative charges in the polysaccharide. For the PIA-chains, an average molecular weight of 30 kDa has been calculated [334, 338, 402]. The basic structure has also been shown for pGlcNAc from other bacteria [338, 390, 403].

1.3 Adherence mediating structures and transport systems

Throughout the GIT, each site has its specific function and corresponding physical and chemical impact on the chyme. Nutrient carriers must therefore be constructed to transit all sites until their site of absorption and ensure that the carried nutrients keep their function. Further, the associated adherence factors must remain intact.

There are several oral delivery vehicles, such as liposomes (Figure 1.10), capsules, dendrimers, multiple emulsions or biodegradable polymers, and targeting molecules are incorporated into these structures [404-408]. It was shown that addition of polymers, such as chitosan, might

increase the interaction with the GIT surface [404, 405]. Generally a variety of parameters is crucial for particle uptake: particle size, ratio and quantity of chemical components, amount of encapsulated antigen, hydrophobicity, surface charge, type of associated adjuvants and dose of administration [409].

The advantages of specific delivery systems are prolonged retention time at the site of drug absorption, intensified contact to the underlying mucosal epithelial barrier and enhancement of epithelial transport of usually poorly absorbed drugs like peptides or proteins. Mucoadhesive polymers can also modulate the permeability of IEC by loosening the tight intercellular junctions or act as inhibitors of proteolytic enzymes [176].

1.3.1 First generation of adhesives: mucoadhesives

The first attempt to design drug vehicles for enhancing absorption are mucoadhesives which specifically and robustly bind to mucins, modulate epithelial permeability and inhibit proteolytic enzymes [176]. Mucoadhesion of polymers increases with molecular weight / chain length and anionic character (carboxyl groups preferred over sulphate groups) but decreases with crosslinking density [410]. Typical mucoadhesins are lectins [411], chitosan or derivates thereof [412], polymer networks with thiolated moieties [413] or polymers with mucin penetrating tethers [414, 415]. The possibility also exists for pH sensitive microspheres for duodenum specific delivery [416]. These systems however, involve little specificity in that adhesins bind randomly to any mucin and do not distinguish between adherent and shed-off mucus or surfaces of other lumen contents. Further, retention time at the target site is limited due the relatively fast mucus turnover [176].

1.3.2 Receptor-based interactions

The next development in the field of targeted delivery is cytoadhesins which are molecules (e.g. lectins) that bind directly to the epithelial cell surface instead of the mucus layer. Beyond receptor-mediated binding, lectins could trigger the active vesicular uptake of large molecules or small vehicles [176].

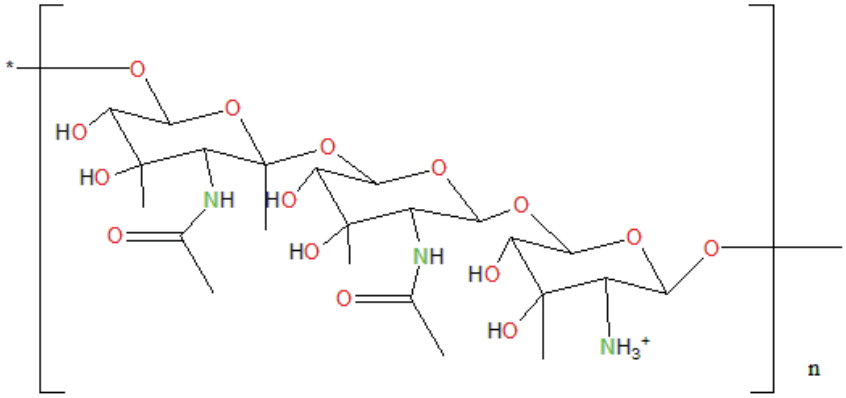

Figure 1.9: Polymeric structure of pGlcNAc [417]

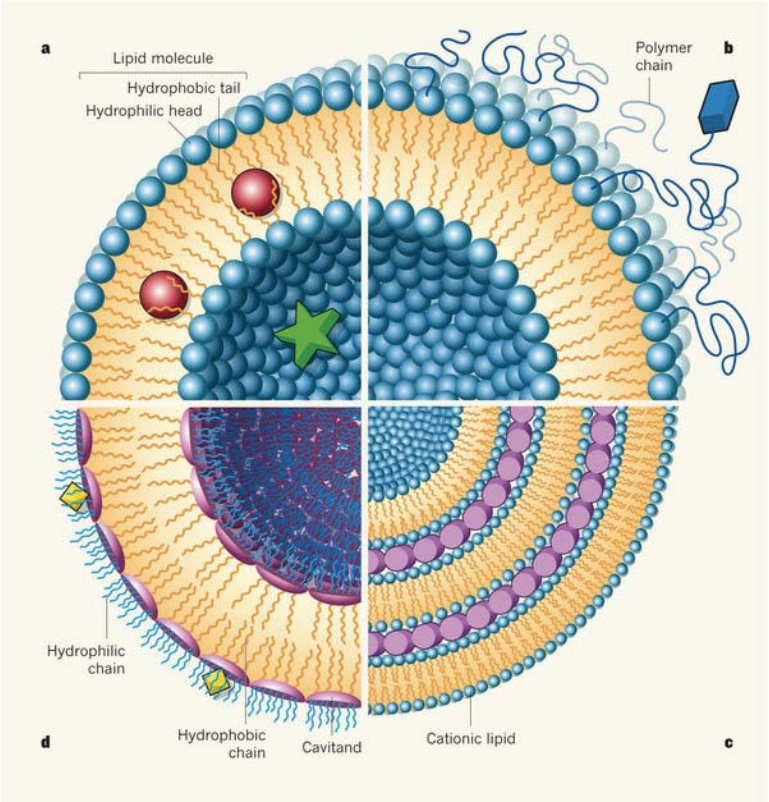

Figure 1.10: Different types of liposomes [418]

(a) Originally, liposomes are vesicles with a lipid bilayer shell. A liposome can carry small (a few nm) hydrophobic functional molecules (red spheres) within the hydrophobic bilayer, and larger (several hundred nm) hydrophilic molecules (green star) in its inner cavity. (**b**) 'Stealth' liposomes are designed for drug-delivery and few polymer lipids are integrated into the lipid bilayer. Targeting peptides (blue rectangle) can also be introduced. (**c**) Liposome–DNA complexes (cationic) most often have a layered structure, with DNA (purple rods) orientated between the cationic membranes. (**d**) Kubitschke et al. [419] describe liposomes with a bilayer made of cavitands (vase-shaped molecules) with attached hydrophobic and hydrophilic chains. The cavitands can trap ångström-sized structures (yellow diamonds) in their hydrophobic cavities.

1.3.3 Nanostructures

More recently, technology based on nanosized structures has become relevant for food science. This is possible because targeting and controlled release delivery systems are linked to size and size distribution [420]: monodisperse populations perform better than polydisperse distributions in controllability of dose and release behaviour, drug encapsulation efficiency and biocompatibility with cells and tissues of the body [420-422]. Generally, nanosized particles have a higher binding capability and accumulation than larger particles at the target sites and trigger less immune response [421, 423].

Membrane emulsification is the preferable technique to produce nanoemulsions [416] as it allows the production of different types of emulsions, solid lipid microcapsules, polymer microspheres and ready microcapsules [424-427].

Prego et al. [428] made chitosan coated particles which adhere to a Caco-2 cell monolayer, after only one hour of incubation. However, the vehicles remained at the apical side. Applied to co-cultured Caco-2/HT29-M6 cells, the particles showed interactions with the cells, whereby nanocapsules were specifically located on the top of the goblet islets, demonstrating mucoadhesive character [429]. Unfortunately, the ability of chitosan to enhance absorption is reduced in mucus-covered cultures [430]. Further, acid-soluble chitosan is prone to precipitation upon reaching the neutral pH in the intestinal region [431]. Precipitation results in reduced swelling, a prerequisite for muco-adhesion [432], which was found to even cause detachment of previously mucin-bound chitosan [433].

A comparison of three nanoparticle constructs with different surface charges and hydrophobicity showed that mucus on IEC in culture has crucial influence on adhesion [434]. Polystyrene (hydrophobic) adheres better to Caco-2 than to HT29-MTX-E12 cultures, whereas chitosan (mucoadhesive) shows inverse behaviour. Poly-lactic acid-poly-ethylene glycol (negative surface charge, hydrophilic) did not adhere well to either cell-type. Reportedly there are indications of stronger interactions of positively charged nanoparticles with bio-membranes

than negative ones. However, positive surface charge seems to increase the transepithelial electric resistance value [435].

1.3.4 Liposomes

Liposomes are spherical structures of one or more phospholipid bilayers enclosing an aqueous core [436, 437]. They can be used for the entrapment and controlled release of hydrophilic and hydrophobic drugs or nutraceuticals or DNA (Figure 1.10) [438]. In addition, other molecules like antibodies or binding proteins can be anchored into liposomes or capsule surfaces, e.g. [439, 440]. However, none of these authors tested liposome targeting of any of the described human intestinal surface layers (Figure 1.6). More recently, liposomes have been appended with surface molecules, for example to allow "stealth" behaviour. Assembling the liposomal surface layer from vase shaped molecules allowed the delivery of functional molecules (Figure 1.10) [418, 419].

In their native state, liposomes are rapidly degraded by bile salts and other GIT secretions, thus they are not suitable for oral delivery. This could be avoided by using polymerised liposomes [147]. Further coating with lectins could facilitate passive targeting of liposomes [441-444].

1.3.5 Anti-adhesive molecules

Molecules that inhibit bacterial adhesion can be considered relevant for the group of intestinal adhesins. In order to prevent bacteria from binding to the GIT surface they must bind either to the bacteria or the GIT surface. In the first case anti-adhesive molecules have the potential to interact with the bacterial biofilm in the human GIT, in the latter the anti-adhesins might be retained by the mucin layer or the epithelial cells themselves.

1.3.5.1 Milk components

Data suggest that human milk oligosaccharides (HMOs) from milk or colostrum are exceptional anti-adhesives for diarrhoeal pathogens [24-29]. In addition, porcine milk contains lipopolysaccharide-binding components: LF, soluble CD14, serum amyloid A [30], α_{S1}-casein, β-casein and κ-casein [31] which might adhere to Gram-negative bacteria [32]. Thus many free

oligosaccharides from (human) milk as well as glycoproteins are considered to be soluble receptor analogues of IEC surface carbohydrates [445]; e.g. *in vitro* attachment to IEC lines of enteropathogenic *E. coli* (EPEC) can be inhibited by the oligosaccharide fraction of human milk, mainly due to fucosyloligosaccharides [33-35], and also by glycosylated proteins like LF or free secretory component. LF may contribute to defence against facultative intracellular bacteria by binding both, target cell membrane glycosaminoglycans and bacterial invasins [446, 447]. Finally, the serine protease activity of LF is considered to inhibit the growth of bacteria, e.g. enteropathogenic *E. coli*, by degrading colonisation proteins [447, 448]; reviewed by Ward et al. [449]. Lactoferricin, a cationic peptide generated by the pepsin digestion of LF, has more potent bactericidal activity than the native protein [447, 450].

1.3.5.2 Glycosides

Sialyloligosaccharides from egg yolk have been shown to inhibit S*taphylococcus enteritidis* (*S. enteritidis*) adherence to Caco-2 cells, presumably due to high density of a lipoprotein fraction that reduces adherence. Those from the water soluble fraction of delipidated egg yolk act as glycomimetics of GM1-oligosaccharide and inhibit toxin adherence [451, 452]. Mannooligosaccharides are a group of oligosaccharides with potential anti-adhesive activity: α-linked mannose (Man) residues are known to inhibit the adhesion of many enterobacterial species, including *Salmonella* and *E. coli* [453, 454].

Cranberry extract appears to contain a multitude of anti-infection and anti-adhesive substances [37-39]. The high concentration of fructose inhibits *in vitro* type 1 fimbriae-mediated *E. coli* adhesion [455]. Proanthocyanidins (flavonoid or condensed tannin) and other high molecular weight compounds were shown to inhibit adherence of uropathogenic *E. coli* [456, 457]. These authors suggest that the cranberry components act as receptor analogues.

Also pectic type and other water soluble oligosaccharides were suggested to have anti-adherence activity [96, 458, 459]. A high-molecular weight extract from tea reduced adherence of *Helicobacter pylori* to a human gastric epithelial cell line and *Staphylococcus aureus* (*S.*

aureus) to fibroblast epithelial cell line. An aqueous extract from carrots blocked enteropathogenic *E. coli* binding to HEp-2 and human mucosal cells [96] with an acidic oligosaccharide containing trigalacturonic acid as the active substance.

1.4 Summary and Conclusions

The human intestinal tract surface layers are diverse with unique characteristics, and able to undergo binding interactions with their environment. This might be cohesion within one layer (e.g. mucin macromolecules form a continuous network), fluidic interaction between layers (liquid mosaic model) or binding of lumen contents like nutrient vehicles. The physiology of each individual layer and even moreso their interplay to form a permeable but protective barrier renders the human gastrointestinal surface layer system complex and demanding to reproduce in a laboratory set-up. Further, the nature of the adherence depends on the individual layer composition. For adherence interactions with the human intestinal surface, three main surface layers need to be considered – bacterial biofilm, mucin layer and IEC.

Most variable are interactions of the bacterial biofilms. These are complex networks of bacteria and their (polymeric) secretions. Two of the most common exopolymeric substances are bacterial cellulose and pGlcNAc which are produced by a variety of bacteria and make up a major components of the biofilm matrices. Their structures make them effective binding partners. Bacterial cellulose is a good carrier for proteins due to high surface density of OH-groups and pGlcNAc is one of the few cationic polymers. Bacterial cells themselves can also provide surface area for adhesins. These interactions are determined by the type of cell wall and exposed receptors. Often receptors are based on lectin mediated binding. Liquid cultures of bacteria with the propensity to form biofilms were used in this thesis as it was beyond the scope of this study to develope a reproducible model of intestinal bacterial biofilms. A fraction of the bacteria in liquid culture might be able to adhere to the culture tube wall and thus initiate the secretion of small amounts of extracellular matrix. The selected bacteria express one of the above biofilm components predominantly.

The mucins secreted from the goblet cells form a large polymer network which can trap or inter-chain with luminal molecules. Further, the functional groups (mostly NeuNAc) in the glycoside chains render the network negatively charged thus generating the option of electrostatic interactions. These can be direct or mediated by Ca^{2+} ions.

Little is reported about adhesive interactions of absorptive IEC themselves. This might be due to their function. More interesting is the glycocalyx, a protective layer adherent to the cells. This is made up of cell-bound mucin molecules and also contains receptors.

Delivery systems for nutrients are necessary to protect, particularly large, molecules from premature degradation. So far, delivery systems are designed to either degrade at a determined site (controlled release) or to adhere to the GIT surface (e.g. muco-adhesion). However, the adhesive molecules are not necessarily food grade and cannot be used in all products (e.g. chitin). For example, in order to have a clean label, only milk derived components are allowed in dairy products. Thus it is desirable to have food-derived adhesive molecules. However, to date little is known about food components which adhere to the three key surface layers of the human GIT. Further, additional time is required to degrade the protective structure in order to release the desired nutrients. No information describing a system combining controlled degradation of the vehicle and adhesion to a specific intestinal layer was found.

Taken together, the different natures of the surface layers open the possibility to target specific parts of the GIT system by choosing the right (food) molecules. Further, nutrient delivery systems can be designed to incorporate molecules into their surfaces, allowing adhesion to the GIT surface.

1.5 Hypothesis and aims

The hypothesis of this dissertation is that various food molecules adhere differently to the models of individual intestinal surface layers (IEC, mucin or bacteria with the propensity to form biofilms) and further, that these differences can be used to target nutrient vehicles

specifically to one intestinal surface layer. Hereby, adhesion is considered as the formation of initial contact between a food molecule and a model of an intestinal suface layer.

It may be possible to develop nutrient delivery systems that (I) get accumulated at the intestinal wall and (II) remain there to give the nutrient vehicle more time to degrade and release its contents at the most effective location (Figure 1.11). Consequently, more of the active ingredient is released close to the site of absorption or the targeted site of function. This would increase the efficacy of the functional food, as often the challenge in functional foods is to deliver sufficient active ingredient to induce an effect.

This thesis aims to develop an adhesion protocol to screen complex food systems for molecules which adhere to one or several layers of the human intestinal surface. Further model systems of the individual layers (cell layer, mucus, bacterial biofilm) are to be identified and prepared. An *in vitro* partial gastric digest protocol will be developed to simulate the varying extents of digestion as it occurs *in vivo*. This digestion protocol will be used to digest the model food. Thus screening for adhering digestion products will be possible.

Figure 1.12 describes the structure of this thesis.

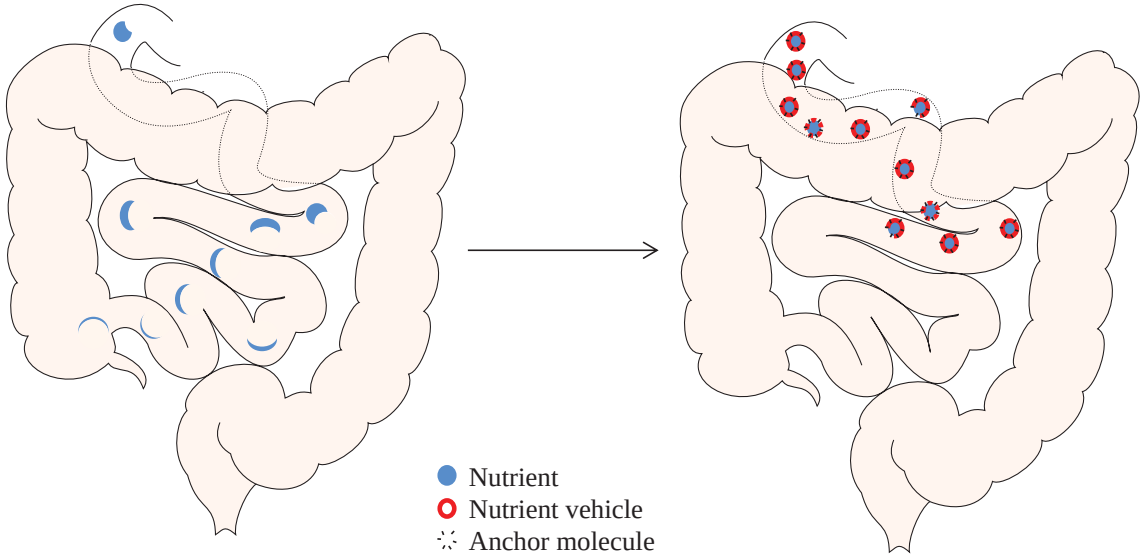

Figure 1.11: Schematic showing the difference in passage of the gastrointestinal tract of unprotected active ingredients (left) and active ingredients delivered through a nutrient vehicle which is retained at the intestinal surface due to the action of anchor proteins (right)

Left: Unprotected nutrients (blue circles) in the human intestinal tract are degraded quickly, have a random localisation regarding the diameter and have a comparably short passage time.

Right: Nutrients protected by a microsphere (red) which is decorated with anchor molecules (black dots) are protected from premature degradation, e.g. in the stomach, accumulate on the intestinal walls and reside longer in the upper intestinal tract where they can be absorbed or function.

	Chapter 1: Review of literature
	Chapter 2: Materials and Methods
Chapter 3	Adhesion assay development • Preparation of MUC2 covered Sepharose beads • Development of an assay to test adhesion of food components to intestinal surface layers using the MUC2 covered beads
Chapter 4	Whey and milk proteins adhering to mucin covered beads • Application of the developed assay and MUC2 beads to screen for mucoadhesive components in milk and whey • Identification of candidate proteins using LC MS/MS and Western blot • Preparation of sediment-free whey from raw milk
Chapter 5	Whey proteins adhering to human IEC in culture • Preparation of human IEC in culture covered by different amounts of mucin • Application of the developed assay and cell cultures to screen for mucoahesive and cytoadhesive components in milk and whey • Identification of candidate proteins using Western blot
Chapter 6	Milk proteins adhering to biofilm producing bacteria *in vitro* • Preparation of liquid cultures of bacteria which produce an extracellular biofilm matrix of mainly one polysaccharide • Application of the developed assay and bacterial cultures to screen for bacterial and extra-cellular matrix binding components in whey • Identification of candidate proteins using LC-MS/MS and Western blot
Chapter 7	Adhesion of isolated proteins to human IEC and bacterial cells • Assessment of the binding of isolated proteins to human IEC and bacterial cells using flow cytometry • Determination of binding progression and saturation levels
	Chapter 8: General discussion

Figure 1.12: Thesis structure

Chapter 2 Materials and Methods

2.1 Introduction

The experimental work in this thesis can be grouped in six blocks. First, model systems for the three intestinal layers (IEC, mucin and bacterial biofilm) were prepared. Test solutions, i.e. skim milk, whey and gastric *in vitro* digests thereof, were also produced. Then a protocol to screen milk and whey for proteins that adhere to these surface layers models was developed using mucin-coated Sepharose beads. The protocol was then adapted for IEC and bacterial cells. Adhering proteins were visualised and identified using a combination of reducing sodium dodecyl sulfate polyacrylamide gel electrophoresis (SDS-PAGE) analysis, Western blot and mass spectroscopy. Also, some bacterial samples were analysed using fluorescent microscopy. Finally, flow cytometry was used to investigate the binding behaviour of isolated proteins to IEC and bacterial cells.

2.1.1 Materials

The following materials were used in the experiments. Suppliers are not indicated for LC-MS/MS analysis which was done by I. Boggs and G. Smolenski (AgResearch, New Zealand).

- α-lactalbumin (Sigma Aldrich, Auckland, New Zealand);
- β-LG (Sigma Aldrich);
- κ-casein (Sigma Aldrich);
- Acetic acid, CH_3COOH (Promega, In Vitro Technologies, Auckland, New Zealand;
- Acetonitrile, C_2H_3N (Merck, Merck Millipore, Auckland, New Zealand);
- Acetonitrile, C_2H_3N, LCMS-grade;
- Alcian blue (Sigma);
- AlexaFluor488 labelled WGA (Sigma Aldrich);

- Ammonium bicarbonate, NH_4HCO_3 (Fluka Biochemika, Sigma Aldrich, Auckland, New Zealand);
- Bovine serum albumin (ICPbio, Auckland, New Zealand);
- Bradford solution (BioRad, Auckland, New Zealand);
- Calcium chloride dihydrate, $CaCl_2 \cdot 2H_2O$ (BDH AnalaR, VWR International Ltd., Auckland, New Zealand);
- Calcium chloride, $CaCl_2$ (BDH Chemicals Ltd.);
- Coomassie blue G-250 (BioRad);
- Crystal Violet (Gibco, Thermo Fisher Scientific, Auckland, New Zealand);
- Dimtheyl sulfoxide, C_2H_6OS (Sigmal Aldrich);
- Dithiohtreitol, $C_4H_{10}O_2S_2$ (ClaBioChem, Merck Millipore);
- Dubelco's Modified Eagle Medium (Invitrogen, Thermo Fisher Scientific, Auckland, New Zealand);
- DyLight594 (Thermo Scientific);
- Epoxy-activated Sepharose (GE Healthcare, Auckland, New Zealand);
- Ethanol amine, C_2H_7NO (Sigma Aldrich);
- Ethanol, C_2H_6O (Sigma Aldrich);
- Fluorescein isothiocyanate (Sigma Aldrich);
- Foetal calf serum (Gibco or Moregate, Bulimba, Australia);
- Formic acid, CH_2O_2;

- Glutaraldehyde, $C_5H_8O_2$ (Sigma Aldrich);
- Glycerol, $C_3H_8O_3$ (BDH AnalaR);
- HPLC-grade water (Fisher Scientific, USA);
- Hydrochloric acid, HCl (Fisher Chemical, Thermo Fisher Scientific, Auckland, New Zealand);
- Hydrogen peroxide, H_2O_2 (Scharlau, Scharlab S.L., VWR International LP, Auckland, New Zealand);
- Hydroxylamine hydrochloride, $HONH_2 \cdot HCl$ (Sigma Aldrich);
- Iodacetamide, C_2H_4INO (Acros Organics, Thermo Fisher Scientific, Auckland, New Zealand);
- Lactose (M&B Laboratory Chemicals);
- Lithium chloride, LiCl (Sigma Aldrich);
- Luminol (Sigma Aldrich);
- Luria broth (Invitrogen);
- Luria broth Lenox L broth (Invitrogen);
- McCoys medium (Gibco);
- Methanol, CH_3OH (Univar, Downers Grove, USA or AnalaR);
- Milk, commercial product (Meadow Fresh, Goodman Fielder, Auckland, New Zealand);
- N-cyclohexyl-3-aminopropanesulfonic acid, CAPS (Sigma Aldrich);

- Non-essential amino acids (Life Technologies, Thermo Fisher Scientific, Auckland, New Zealand);
- Non-fat milk powder (Pams, Foodstuffs, Auckland, New Zealand);
- Ortho-phosphoric acid, H_3PO_4 (Fisher Chemical);
- p-coumaric acid, $C_9H_8O_3$ (Sigma Aldrich);
- Pepsin from porcine gastric mucosa (Sigma Aldrich);
- Pepstatin A (Sigma Aldrich);
- Ponceau S (Sigma Aldrich);
- Porcine MUC2 mucin (Sigma Aldrich);
- Porcine trypsin (Promega, In Vitro Technologies, Auckland, New Zealand);
- Potassium phosphate monobasic, KH_2PO_4 (BDH AnalaR);
- Potassiumchloride, KCl (Sigma Aldrich);
- Propidium iodide (Fluka, Sigma Aldrich, Auckland, New Zealand);
- Raw milk (Kiwi Cross, Tokanui farm, AgResearch, New Zealand);
- Rhodamine (Thermo Fisher Scientific);
- Sodium bicarbonate, $NaHCO_3$ (Sigma Aldrich);
- Sodium chloride, NaCl (LabServ Pronalys, Thermo Fisher Scientific, Auckland, New Zealand);
- Sodium hydroxide, NaOH (Fisher Chemical);
- Sodium phosphate, dibasic, Na_2HPO_4 (Fisher Chemical);

- ß-mercaptoethanol, C_2H_6OS (Sigma);
- Trifluoroacetic acid, $C_2HF_3O_2$ (Merck);
- TriplE Express (Life Technologies);
- Tris-tricine sample loading buffer (BioRad);
- Tris, $C_4H_{11}NO_3$ (Fisher Scientific);
- Tryptic soy broth (BD BactoTM, BD, Auckland, New Zealand);
- Tween20 (BioRad);
- Ultrapure water (MilliQ, Merck Millipore, Auckland, New Zealand);
- XT-running buffer (Bio-Rad).

2.1.2 Experimental work

Bacteria used in this thesis were kindly provided by Dr U. Sonnenborn (*E. coli* Nissle 1917. Ardeypharm GmbH, Germany) and Prof. G. Pier (*S. epidermidis* 1457 and *S. epidermidis* 1457 M10. Harvard Medical School, USA). HT29-MTX cells were kindly provided by Dr R. Anderson (AgResearch, New Zealand). Confocal laser scanning analysis of mucin coated Sepharose beads was done with the support of Dr B. O'Brien (Waikato University, New Zealand). Cy5-labelled sIgA was provided by Dr A. Hodginson and M. Callaghan (AgResearch, New Zealand) and fluorescein isothiocyanate (FITC)-labelled free secretory component and IgG were provided by Dr J. Cakebread (AgResearch, New Zealand). Total combustion (LECO) was done by technical staff of the Riddet Institute (Palmerston North, New Zealand). Mass spectrometric analysis of freeze dried peptides was done by I. Boggs and G. Smolenski (AgResearch, New Zealand). Caco-2 cells and reagents were sourced as indicated, and experiments were conducted by C. Schmidmeier (PhD candidate).

2.2 Intestinal layer components

2.2.1 Mucin

2.2.1.1 Sepharose beads coated with mucin

Porcine MUC2 mucin (Sigma Aldrich, Auckland, New Zealand) was used for the *in vitro* binding assay. The crude mucin was coupled to epoxy-activated Sepharose 6B (GE Healthcare, Auckland, New Zealand) as described by Alvarez et al. [460] and according to manufacturer's instructions. A negative control medium was also prepared (ethanol-amine (EtOH-amine) blocked beads with no mucin).

In brief, MUC2 was hydrated in borate buffer (0.05 M, pH 9.0). pH 9 was chosen as a balance between an increased reactivity of the epoxy groups at higher pH values and a physiological environment for the mucin. Epoxy-Sepharose was swollen in ultrapure (MilliQ) water. Sepharose was washed with at least 200 ml MilliQ water per 1 mg beads. Washed Sepharose and hydrated MUC2 in borate buffer were mixed and incubated over night at 90 revolutions.min^{-1} (rpm) and 25°C. The next day, the beads were washed with coupling buffer to remove unbound mucin and 1 M EtOH-amine (Sigma Aldrich) was added to block yet unbound epoxy groups. Incubation was at 90 rpm and 45°C overnight. Finally, the beads were washed with three cycles of alternating 0.1 M acetate buffer (pH 3.8, 0.5 M sodium chloride (NaCl, LabServ Pronalys, Thermo Fisher Scientific, Auckland, New Zealand)) and 0.1 M Tris-HCl buffer (pH 8.2, 0.5 M NaCl) to ensure that no weakly attached (ionically) ligand remained bound to the immobilised mucin. The ready MUC2 covered beads were stored in borate buffer and 25% ethanol (EtOH, Sigma Aldrich)) at 4°C until use.

The negative control beads were prepared the same way, but without the addition of MUC2. The swollen and washed Sepharose beads were directly incubated with 1 M EtOH-amine, followed by the wash cycle. The beads were stored in MilliQ water and 25% EtOH at 4°C until use.

2.2.1.2 Testing mucin coverage

Confocal Laser Scanning Microscopy

To visualise the mucin covering the Sepharose beads, the MUC2 was labelled using a lectin-flurophore conjugate. Labelled mucins were then evaluated using a confocal laser scanning microscope.

AlexaFluor488 labelled WGA (Sigma Aldrich), a lectin which binds to mucin, was dissolved at 1 $mg.ml^{-1}$ in phosphate buffered saline (PBS) and aliquoted to avoid repeated freeze-thaw-cycles. Unused label was stored at -20°C. Next, 100 µl MUC2 covered beads or negative control beads were transferred into tubes. The beads were washed three times with PBS-T (0.05% Tween20 (BioRad, Auckland, New Zealand) in PBS) to remove the storage buffers. Next the beads were blocked with 1% bovine serum albumin (BSA, ICPbio, Auckland, New Zealand) in PBS for 1 hr at room temperature. Again, the beads were washed three times with PBS-T before adding 100 µl lectin solution at different concentrations (0.1 to 10 $\mu g.ml^{-1}$ lectin) to the beads. This was followed by another 1 hr incubation at room temperature and three washes with PBS-T. Samples were kept in the dark until use. For analysis the beads were transferred onto slides and a coverslip was sealed with nail polish. For visualisation an Olympus Fluoview FV1000 confocal laser scanning microscope and Olympus Fluoview v1.7a software (Olympus America Inc., Center Valley, PA, USA) were used.

PBS was made from a 10-times stock solution. Therefore 80.0 g NaCl, 2.0 g KCl (Sigma Aldrich), 14.4 g Na_2HPO_4 (Fisher Chemical, Thermo Fisher Scientific, Auckland, New Zealand) and 2.4 g KH_2PO_4 (BDH AnalaR, VWR International Ltd., Auckland, New Zealand) were dissolved in 700 ml MilliQ water. After the pH was adjusted to 7.4 with HCl (Fisher Chemical, Thermo Fisher Scientific, Auckland, New Zealand) and sodium hydroxide (NaOH, Fisher Chemical), the volume was topped up to 1000 ml with MilliQ water.

Measurement of mucin using a 2-D Quant Kit

The amount of mucin in the binding buffer before and after coupling to Sepahrose beads was measured with 2-D Quant Kit (GE Healthcare) according to manufacturer's instructions. All regaents and solutions were contained in the kit. In brief, mucin was precipitated with the provided reagents, and re-dissolved in a copper solution. After adding a colour reagent, the amount of protein in the samples was measured against a BSA standard curve by absorption at 480 nm [461].

Total combustion (LECO)

Determination of total nitrogen by total combustion (LECO) was performed at the Riddet Institute (Palmerston North, New Zealand) following the method described in AOAC 968.06. Thereby, nitrogen in the sample was freed through pyrolysis followed by combustion and swept into a nitrometer (with CO_2 as carrier) where residual nitrogen was measured. Total nitrogen was converted to net protein through a conversion factor of 6.25, employing Equation 1.

$$Net\ protein = Total\ nitrogen\ x\ 6.25 \quad \text{(Eq. 1)}$$

Measurement of FITC-WGA binding to mucin using a plate reader

For the colorimetric mucin quantification, AlexaFluor488 labelled WGA (WGA488) was used to indirectly detect the glycoprotein. The labelling was performed as described for confocal laser scanning microscopy. The samples analysed were MUC2 beads with label. Further, controls were prepared: MUC2 beads without label, EtOH-amine blocked beads with label, EtOH-amine blocked beads without label, pure beads with label, pure beads without label.

Alcian Blue (periodic acid Schiff)

Alcian blue (AB, Sigma Aldrich) was used to visualise the mucin before it was coupled to the Sepharose beads and thus allow tracking after coupling. Mucin was hydrated in MilliQ water for at least 5 hr before adding 100 µl AB solution (several grains AB in 3% aq acetic acid (AnalaR)). Double strength borate buffer (0.1 M, pH 9.0) was added (1:1 volume ratio to MilliQ water) to the mix to get a normal strength binding buffer. Epoxy-Sepharose was prepared as

described in Section 3.1.1.1, mixed with the AB-mucin binding-buffer and incubated at 25°C overnight and 90 rpm. Distribution of the blue colour, indicating mucin, was determined visually and used to assess the degree of binding.

2.2.2 Bacteria

Bacterial strains were kindly provided by Dr U. Sonnenborn, Ardeypharm GmbH, Germany (*E. coli* Nissle 1917) and Prof. G. Pier, Harvard Medical School, USA (*S. epidermidis* 1457 and *S. epidermidis* 1457 M10). *S. epidermidis* 1457 M10 is an *ica*ADBC knock-out which does not produce pGlcNAc. The stocks were plated onto Luria broth (Invitrogen, Thermo Fisher Scientific, Auckland, New Zealand) agar plates and incubated at 37°C. Once colonies formed, a single colony each was transferred into liquid culture medium; Luria broth Lenox L broth (Invitrogen) for *E. coli* Nissle 1917 and tryptic soy broth (BD Bacto^{TM}, BD, Auckland, New Zealand) for *S. epidermidis* 1457 and *S. epidermidis* 1457 M10. Cultures were grown overnight at 37°C and 180 rpm in a shaking incubator (Infors HT, Ecotron, Total Lab Systems Ltd. Auckland, New Zealand). To prepare glycerol stocks, 500 µl culture was mixed with 500 µl glycerol (BDH AnalaR) and stored at -80°C until use.

2.2.3 Intestinal epithelial cells

2.2.3.1 Mono cultures

Caco-2 cells were obtained from ATCC HTB-37 and used from passages 56 to 59 and 40 to 43. HT29 cells were obtained from ATCC HTB-38, adapted to 10^{-7}M MTX (Dr R. Anderson, AgResearch Grasslands, New Zealand) and used from passages 14 to 24.

Caco-2 cells were grown in Dubelco's Modified Eagle Medium (DMEM, Invitrogen) with 10% foetal calf serum (FCS, Gibco, Thermo Fisher Scientific, Auckland, New Zealand or Moregate, Bulimba, Australia). HT29-MTX cells were grown in McCoys medium (Gibco) with 10% FCS and 1% non-essential amino acids (Life Technologies, Thermo Fisher Scientific, Auckland, New Zealand). Cells were grown at 37°C in 5% carbon dioxide and culture medium was changed at least every third day. After reaching confluence, cells were detached with TriplE

Express (Life Technologies). After detachment, DMEM was added to neutralise the TriplE and the cells were pelleted by centrifugation (5 min, 10^3 rpm). After re-suspending, 100 µl of the cell suspension was mixed with 900 µl warmed Crystal Violet (Gibco) and counted in a haemocytometer. The remaining cell suspension was re-seeded at 4 x 10^4 cells.cm^{-2}. In preparation for the adhesion assay, cells were grown in 24-well plates (Thermo Scientific Nunc™, Thermo Fisher Scientific, Auckland, New Zealand) for 16 to 18 days. All cell lines were grown on DMEM with 10% FCS and 1% non-essential amino acids to avoid differences in treatment between mono- and co-cultures. HT29 can produce mucin in DMEM with 10% FCS [462, 463].

2.2.3.2 Co-culture

After reaching confluence, mono-cultures were detached and cells counted as described in Section 2.2.3.1. The cells were gently mixed to the desired ratio (e.g. 90% Caco-2 and 10% HT29-MTX) and seeded at 4 x 10^4 cells.cm^{-2} in DMEM with 10% FCS and 1% NEAA. Co-culture medium was changed at least every third day.

2.3 Test solutions

2.3.1 Whey and whey preparations

2.3.1.1 Acid whey

Raw milk was sourced from the local AgResearch farm (Tokanui farm, AgResearch, New Zealand). Whey was produced by acidic precipitation of raw milk. Agitated raw milk was heated to 40°C in a water bath. The milk was acidified with 2 M HCl, decreasing the pH-value to 4.7. Acidification was continuously controlled with a pH-meter to avoid a drop in pH-value under the desired value. After reaching the final pH-value, stirring was stopped and the curd was allowed to set for 1 hr in the water bath. Before filtering the settled curd and whey through a cheese cloth, the pH-value was checked and adjusted to 4.7 if necessary. The separated whey was collected and centrifuged for 30 min at 3 x 10^3 x g. The clarified fractions were pooled and the pH-value adjusted to 6.8 by adding 1 M NaOH. The whey was heated to 40°C in a water

bath and left without stirring for 30 min. To remove any calcium-phosphate precipitate, the whey was again centrifuged for 30 min at 3 x 10^3 x g. The clear fractions were pooled, aliquoted into Falcon tubes (LabServ, Thermo Fisher Scientific, Auckland, New Zealand) and stored at -80°C until use.

2.3.1.2 Whey using centrifugation

Skim milk was centrifuged at 10^5 x g for 60 min at 6°C (Sorvall® Discovery 90SE, Thermo Fisher Scientific, Auckland, New Zealand). The clear whey was removed from the tubes, pooled and aliquoted into Falcon tubes. These were stored at -80°C until use.

From here, "whey" is referred to whey produced by acidification and "whey by centrifugation" refers to whey produced by centrifugation.

2.3.1.3 Protein quantification by Bradford assay

For the Bradford assay, a 7-point BSA-standard (STD) dilution series was prepared, ranging from 0 to 18 µg BSA in 100 µl MilliQ water. Whey was used pure or as 1:10 dilution in MilliQ water in 100 µl aliquots. 900 µl Bradford solution (BioRad) was added to STDs and samples, mixed and allowed to react for 10 min at room temperature. The STDs were measured at 595 nm on a photometer (UV-160A, Shimadzu, Auckland, New Zealand) to generate a STD curve. Next the samples were measured and their protein content calculated. Bradford solution was made from 20x stock solution and stored in the dark at room temperature.

2.3.1.4 Protein quantification with DirectDetect

DirectDetect (Merck Millipore, Auckland, New Zealand) is an alternative method to measure the protein content. It measures the amide bonds and is therefore less susceptible to differences in amino acid sequence or dye binding properties between the calibration protein – routinely BSA – and the sample protein (mix) than colorimetric methods like Bradford. 2 µl samples and one blank (buffer only) were pipetted onto the measurement cards which were then ready for quantification [464].

Protein quantification by Bradford and DirectDetect were compared and are discussed in Section 3.2.1.1.

2.3.1.5 Partially digested whey

To generate a range of whey protein samples, digested to various degrees as needed for the adhesion assay, whey was partially digested with pepsin and adjusted to duodenal conditions (ionic strength and pH-value). The assay was optimised from the US Pharmacopeia standard gastric digestion assay for protein [465]. Testing adhesion properties of a partial *in vitro* gastric digest was initially considered as proteins are hydrolysed in the stomach before reaching the small intestine and thus modified proteins are expected to be available for adhesion. However, this approach was dropped quickly as comprehsive analysis of digestion products was not possible.

Pepsin solution at physiological concentrations was made fresh for every digest; pepsin from porcine gastric mucosa (Sigma Aldrich) was dissolved in simulated gastric fluid (150 mM NaCl, 10 mM HCl, pH 2.0). This was done in two steps: first 45 mg pepsin was dissolved in 20 ml simulated gastric fluid in a shaking water bath (WiseBath®, Wisd. Laboratory Instruments, Witeg Labortechnik GmbH, Wertheim, Germany) at 37°C and 90 rpm. After 30 min 1.86 ml of this solution was added to 18.14 ml simulated gastric fluid and incubated for another 30 min under the same conditions, resulting in 20 ml digest buffer with a final concentration of 0.21 $mg.ml^{-1}$ pepsin. About 15 ml whey was acidified with 1 M HCl to pH 2 and warmed to 37°C in the water bath. To start the digest, 10 ml acidified whey and 5.77 ml digest buffer were mixed; the protein:enzyme ratio was 20:1. After 1 min, the digestion was stopped by mixing 6.86 ml digest, 0.85 ml bicarbonate solution (250 mM $NaHCO_3$ (Sigma Aldrich)), 34.0 µl Pepstatin A (Sigma Aldrich) and 2.29 ml simulated duodenal fluid (60.1 $g.L^{-1}$ NaCl, 4.6 $g.L^{-1}$ KCl, 1.7 $g.L^{-1}$ $CaCl_2 \cdot 2H_2O$ (BDH AnalaR), 0.1 M Tris (Fisher Scientific), pH 7.5). The digest was used immediately for the adhesion assay.

2.3.2 Protein labelling

Throughout the project, different fluorescent tags were used: DyLight594 (DL594, Thermo Scientific), Rhodamine (Rhd, Thermo Fisher Scientific) and FITC (Sigma Aldrich). Rhd and DL594 came as N-hydroxysuccinimide-ester (NHS-ester) and were simply added to the (dialysed) whey and incubated at room temperature. FITC was used for flow cytometry experiments because the instrument was not able to detect the other tags.

2.3.2.1 DyLight594 labelling of whey

DL594 tagging of proteins was done according to manufacturer's instructions. In brief, whey or digest were dialysed against PBS overnight with three buffer exchanges through a 3.5 kDa cut-off membrane (Spectrum Laboratories Inc., Auckland, New Zealand). Then next morning, whey or digest was mixed with fluorophore (1 $mg.ml^{-1}$ in PBS) at 15 µg label per 1 mg protein. The mix was allowed to react for 1 hr in the dark before using it in the adhesion assay.

2.3.2.2 Rhodamine labelling

Rhd-NHS was coupled to protein according to the manufacturer's instructions. Some grains of Rhd were dissolved in 100 µl dimethyl sulfoxide (DMSO, Sigma Aldrich) and this solution was mixed with whey or digest. After incubating for 1 hr in the dark, an equal volume of 1 M Tris, pH 7 was added to block yet unbound NHS-groups. After incubation in the dark for 30 min, it was ready for immediate use.

The Rhd was kept as a powder to avoid premature degradation. Thus fresh Rhd was made up for each labelling. As the amount of Rhd was too small for precise measurement, each experiment can only be compared with itself. For comparison between different experiment days, all values were converted into percentages of whey, which was loaded at 5 µl as reference onto each gel.

2.3.2.3 FITC labelling of proteins for Flow Cytometry

Isolated proteins were dissolved in 0.1 M sodium-bicarbonate, pH 9.0, at concentrations from 3 $mg.ml^{-1}$ to 25 $mg.ml^{-1}$. FITC was made up at 5 $mg.ml^{-1}$ in the same buffer. FITC-label was added in 10-fold molar excess to protein under shaking. The mix was incubated for 2 hr in the

dark. After this, 1.5 M hydroxylamine-HCl (Sigma Aldrich), pH 8.5 was added to block yet unbound FITC (same volume as FITC). To remove unused label from labelled protein, the mix was cleaned over a 10DG desalting column (BioRad; prepacked with Bio-Gel®P-6DG gel). The column was equilibrated with PBS and used according to manufacturer's instructions. However, due to the high protein content, for some proteins a pre-clean with Sephadex G10 (Sigma Aldrich) was necessary. This medium was hydrated in MilliQ water and the slurry transferred into a column. After equilibrating the column with PBS, the sample was loaded. To remove all sample from the column, which binds free label, the column was centrifuged at 2 x 10^3 x g for 2 min. After cleaning, the FITC-labelled protein as aliquoted and stored at -20°C in the dark until use.

The degree of FITC-labelling was calculated by comparing the amount of FITC with the amount of protein in solution. FITC was measured with a plate reader (BioTek, Winooski, USA) against a FITC-STD curve. Protein was measured with DirectDetect. Both values were calculated into moles, allowing the determination of mol FITC.mol^{-1} protein.

2.3.3 Milk

Skim milk was made by centrifugation of raw milk at 2.5 x 10^3 x g and 4°C for 10 min. A commercial product (Meadow Fresh, Goodman Fielder, Auckland, New Zealand) was also used.

2.3.3.1 Digested skim milk

Digestion of skim milk was performed as for the whey digestion. The volume ratio of simulated gastric fluid:milk had to be altered due to the higher protein content in skim milk; 15 ml skim milk were mixed with 18.03 ml pepsin solution. The digestion time was pre-determined from a digestion time course. It was set at 30 min (compare Section 2.2.1.3). To stop the digestion, 1.7 ml bicarbonate solution, 68.0 µl Pepstatin A and 4.58 ml simulated duodenal fluid were added to 13.72 ml digest. The digest was used immediately for the adhesion assay.

2.4 Adhesion assay

2.4.1 Mucin

Affinity chromatography experiments were done in batches using 50 mg MUC2-Sepharose bead-slurry in Eppendorf tubes. MUC2 beads were washed with two cycles of 200 µl acetate buffer (0.1 M, pH 3.8, 0.5M NaCl) followed by 200 µl Tris-HCl buffer (0.1 M, pH 8.2, 0.5M NaCl). Beads and buffer were mixed by gentle vortexing followed by a 1 to 2 sec centrifugation with a table top centrifuge (Eppendorf MiniSpin Plus, Eppendorf, North Ryde, Australia). All beads (MUC2 and EtOH-amine) were washed twice with 200 µl PBS to adjust the beads to the condition during adhesion of digest. One ml digest, whey or milk was added to the beads and the suspension was incubated for 30 min at 37°C in a shaking water bath at 110 rpm. After the incubation was over, the supernatant was removed from the beads. To analyse the protein binding a wash cycle as shown in Figure 2.1 was applied. Thereby all removed solutions were collected as they might contain specifically bound proteins. The sequence consisted of 3 x 200 µl PBS, 3 x 200 µl PBS 5.5 (10 ml PBS + 6 ml MilliQ water, pH 5.5 by 1 M HCl), 3 x 200 µl 20% EtOH (in PBS 5.5) and 3 x 200 µl 2.5 M lithium chloride (LiCl (Sigma Aldrich), in PBS 5.5). A potential last wash with 6 M guanidine HCl (in PBS 5.5) was made redundant after deciding not to use affinity chromatography columns and thus no repeated use of the same beads was required. After the wash with PBS, treatment was stopped for an aliquot of the beads ("bead A"). This was used to analyse generally adhering proteins. The leftover beads underwent the wash cycle including 2.5 M LiCl ("bead B"). The beads were mixed with 70 µl 2 x Tris-tricine sample loading buffer (TT-SLB, BioRad) and boiled for 5 min. The removed wash supernatants were collected. The pooled samples were either precipitated or directly mixed 1:1 with 2 x TT-SLB and boiled for 5 min. Prepared beads and supernatants were stored at -20°C until use in SDS-PAGE analysis.

Controls for this assay were undigested whey or milk, MUC2 beads pure and EtOH-amine beads pure, digest, time 0 control (acidified whey + simulated gastric fluid) and pepsin control (pepsin solution + simulated whey + bicarbonate solution + simulated duodenal fluid) were

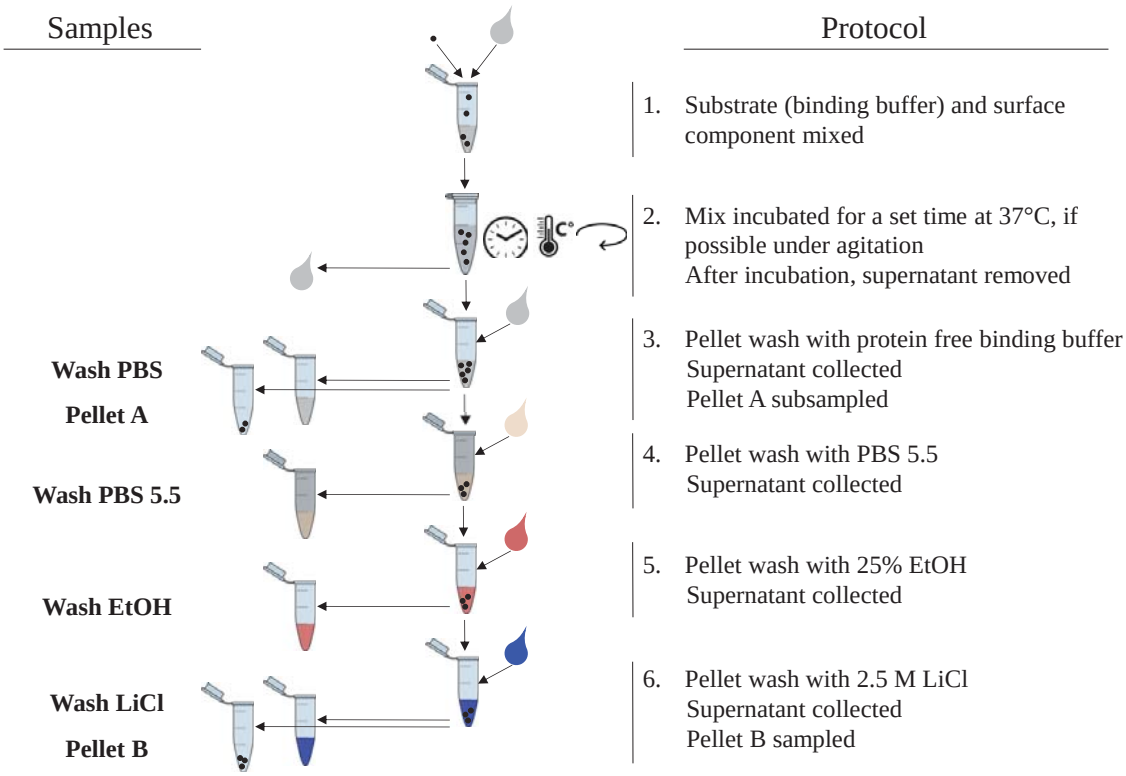

Figure 2.1: Outline of the final adhesion assay

The assay was designed to investigate the adhesion of food component of interest to intestinal surface components followed by a sequential wash to remove adhering molecules according to the nature of their binding. Pellet A and pellet B in the figure will be named “bead A” and “bead B” in samples with mucin coated Sepahorse beads, and “pellet A” and “pellet B” in samples containing bacterial cells or IEC.

included. Simulated protein-free whey was made up of 8.74 g lactose (M&B Laboratory Chemicals), 0.89 g KCl and 0.33 g $CaCl_2$ (BDH Chemicals Ltd.) in 200 ml MillliQ water.

2.4.2 Bacteria

2.4.2.1 Model 1 for bacterial biofilm: isolated biofilm components

GlcNAc was coated onto Sepharose beads similarly as described for mucin. The only differences were the compositions of coupling buffer (0.1 M NaOH) and storage buffer (0.05 M sodium acetate/acetic acid buffer (pH 4.5)).

2.4.2.2 Model 2 for bacterial biofilm: cell pellets from liquid culture

Bacteria stocks were stored at -80°C in 50% glycerol. In preparation for the experiment, aliquots of the stocks were transferred into 2 ml growth medium and incubated overnight at 37°C with agitation at 180 rpm. The next day, the bacteria were diluted 1:100 into 2 ml fresh medium and incubated under the same conditions. After a further 22 to 24 hr incubation, the cultures were used for the adhesion assay. Preparation consisted of gentle centrifugation (10 min, 1.5 x 10^3 x g) and 2 x 200 µl PBS-wash of the bacterial cultures to obtain a cell pellet which can then be used for the adhesion assay. The adhesion assay protocol was the same as for MUC2. The bacterial cell pellets were mixed with tagged whey or digest and incubated for 30 min (37°C, 90 rpm, dark).

After incubation, the pellets were washed with 2 x 200 µl PBS; the pellets and PBS were mixed by gentle pipetting followed by a centrifugation (1 min, 7.5 x 10^3 rpm) to sediment the bacterial cells. At this point "pellet A" was sampled. The wash cycle continued with 2x200 µl washes of each of PBS 5.5, 25% EtOH in PBS 5.5 and 2.5 M LiCl in PBS 5.5. The fully washed pellet, "pellet B", was mixed with 70 µl 2 x TT-SLB, boiled for 5 min and diluted with 140 µl 1x TT-SLB (2 x TT-SLB:MilliQ water / 1:1). The removed wash solutions were collected, and the same solutions were pooled per pellet. The pooled samples were either precipitated or directly diluted 1:1 with 2 x TT-SLB and boiled for 5 min. Prepared pellets and supernatants were stored at -20°C until use for SDS-PAGE analysis.

2.4.2.3 Whey sediment

To identify the composition of the whey sediment, 500 µl aliquots of whey were centrifuged at 7.5 x 10^3 rpm for 1 min (as in the adhesion assay) and supernatant was removed from the tube. The sediment was prepared in 20 µl 2 x TT-SLB and run on SDS-PAGE (gel shown in Figure 4.11).

To remove calcium-phosphate from the whey, the whey was incubated at room temperature or at 45°C and the optical density at 600 nm (OD_{600}), as indicator for turbidity, was measured every 10 min for 1 hr. It was determined that a cycle of six 10 min incubations at 45°C without shaking removed most insoluble calcium-phosphate satisfactorily. After each 10 min-incubation, the whey was centrifuged for 1 min at 7.5 x 10^3 rpm. The supernatant was transferred into a new tube for the next 10 min incubation. The final whey product was free of most calcium-phosphate residue. However, not 100% of the sedimentable material, which also contained low levels of β-LG (compare Figure 4.13), could be removed.

2.4.3 Intestinal epithelial cells

On the day of the experiment (day 16 to 18 post passage), the IEC were washed twice with 500 µl serum free medium. Next, 900 µl serum free medium was transferred to each well and 100 µl Rhd-whey (Figure 2.2) or 100 µl FCS (first sets) or serum free medium (last set) as negative control were added. Cells were then incubated for 15 min, 30 min, 60 min or 120 min in the incubator. After the incubation, the medium was aspirated and the cells were washed twice with 500 µl serum free medium. Half the samples and negative controls were incubated with 100 µl 0.5% dithiothreitol (DTT, ClaBioChem, Merck Millipore, Auckland, New Zealand), a reducing agent that targets disulphide bonds between proteins, in serum free medium in the dark to remove mucin layers by cleaving the "network knots". This was done for all types of cell cultures (i.e. Caco-2, co-cultures, HT29-MTX), although Caco-2 cells do not secrete mucin [161], to obtain comparable cell fractions for analysis. After 10 min, the cells were rinsed with the medium to collect cleaved mucin. The medium containing mucin (more generally: molecules detached by DTT) was then transferred into 100 µl 2 x TT-SLB, samples were

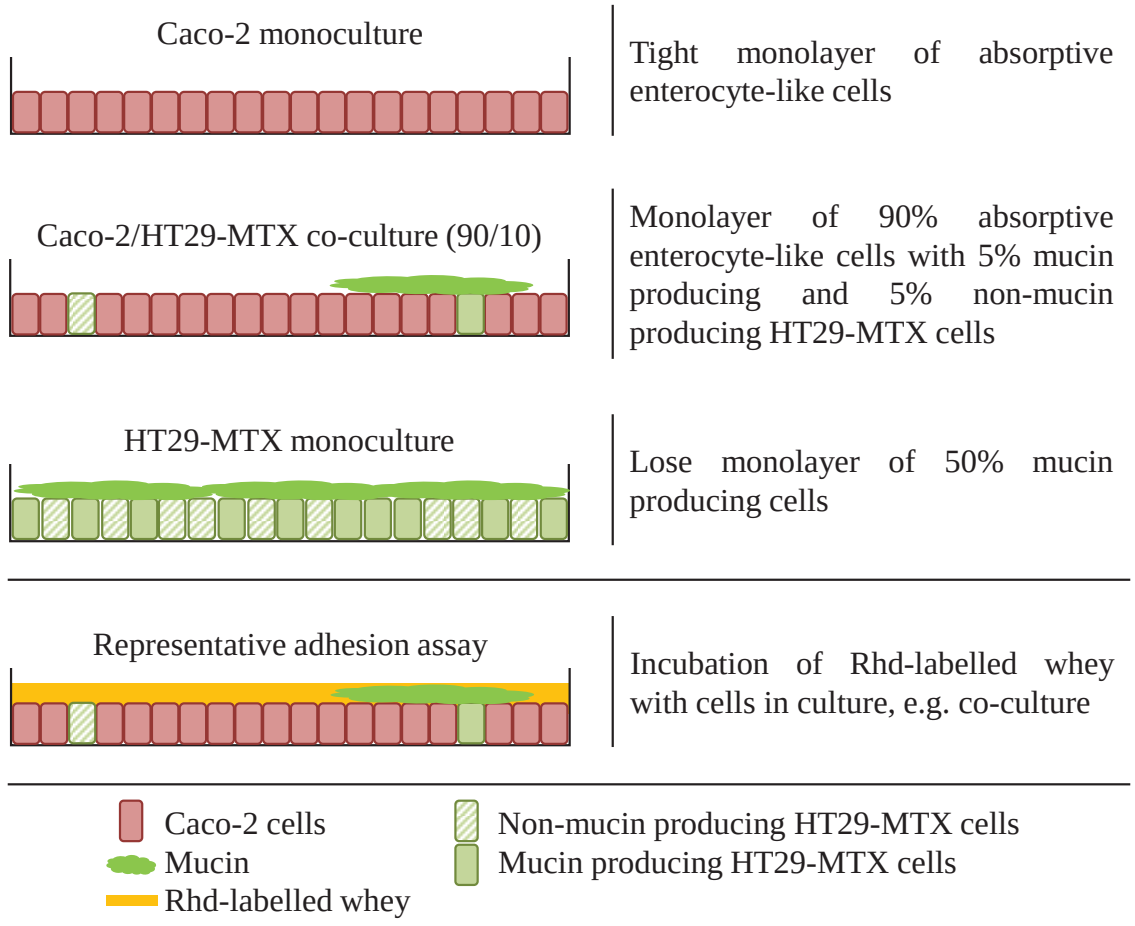

Figure 2.2: Schematic showing different types of epithelial cell cultrueas and adhesionassay set-up

Monocultures (Caco-2 and HT29-MTX) and co-culture (Caco-2/HT29-MTX, 90/10) are grown in 24-well plates, one well each represented in schematic. Cells are adhering to the bottom of the well. For the adhesion assay, Rhodamine (Rhd)-labelled whey is added to the serum free medium (representative for Caco-2/HT29-MTX co-culture).

labelled “mucin”. This nomenclature was decided upon to clearly differentiate between mucin and cell fraction in the cell culture model, although Caco-2 derived samples were not expected to contain mucin.

The cells were then washed once more with 500 µl serum free medium, treated with 150 µl 2 x TT-SLB and transferred into tubes (“cells”). The other half of samples was directly treated with 150 µl 2 x TT-SLB and transferred into tubes (“whole lysate”). All samples were boiled for 5 min and then stored at -20°C until use.

2.5 Analysis of adhering proteins using the adhesion assay

2.5.1 Sodium dodecyl sulfate polyacrylamide gel electrophoresis

2.5.1.1 Chloroform-methanol-precipitation

150 µl of the wash solution was mixed with 600 µl methanol (MeOH, Univar, Downers Grove, USA) and vortexed well before adding 150 µl chloroform followed by another mixing using a vortex. After 450 µl MilliQ water was added, the sample was vortexed then centrifuged for 1 min at 1.4 x 10^4 x g using a bench top centrifuge. The top layer was carefully removed without disturbing the protein containing middle-layer. Another 600 µl MeOH was added and vortexed followed by another centrifugation at 1.4 x 10^4 x g for 2 min. The resulting pellet contained all proteins, and as much MeOH as possible was removed. Left over MeOH was dried off overnight. The pellet was dissolved in 20 µl 2 x TT-SLB and boiled for 5 min. Samples were kept at -20°C until use [466].

2.5.1.2 Mucin beads

Prepared samples were loaded onto the SDS-PAGE gels (10 to 20%, Tris-tricine, BioRad). Routinely 30 µl beads and 30 µl wash supernatants or all precipitate were loaded. Gels were separated at 130 V for 2 to 2.5 hr with XT-running buffer (Bio-Rad). After this, gels were removed from the cassette, fixed in 50% MeOH with 4% ortho-phosphoric acid (Fisher Chemical) for 1.5 hr with one buffer exchange and stained overnight in Coomassie brilliant blue (CBB) stain. The next day, the gels were de-stained with first 10% then 5% MeOH in MilliQ

water until the background was clean and scanned on a GS-800 (BioRad). CBB stain was made up of 0.25% Coomassie blue G-250 (BioRad) in 40% MeOH (AnalaR) and 10% acetic acid.

2.5.1.3 Bacterial pellets

Similar to MUC2 beads, the bacterial cell pellets were separated on SDS-PAGE so that total protein in the samples was visualised. Routinely 20 µl prepared pellet and 150 µl precipitated wash solutions were separated on a gel; first for 10 min at 40 V then for 2.5 to 3 hr at 130 V and protected from light. The gel was then fixed for 30 min and rehydrated for 10 min in MilliQ water. By utilising the fluorescent tag, whey and bacterial proteins were differentiated by fluorescent scanning, using a FX proplus fluorescent scanner (BioRad). QuantityOne software was set up for Texas red wavelengths, low or medium sample intensity and 100 µm cuts. After this the gels were fixed again and stained with CBB to visualise total protein.

2.5.1.4 Intestinal epithelial cells

The same protocol as for bacteria was used. As the FX scanner failed to work reliably, some pictures were taken with an ImageQuant LAS4000 (GE Healthcare). The instrument was set on fluorescent scanning greenRGB as it was equipped with RGB LEDs. The sensitivity was set to ultra or super and pictures were taken in increment mode set at 10 sec with 10 cycles. Picture analysis was done using QuantityOne.

2.5.1.5 Analysis

Band densities obtained with the CBB stain were determined with QuantityOne and data was transferred to and evaluated in a Microsoft Excel spread sheet.

As for CBB, band densities obtained with fluorescent stain were determined and data was evaluated with Microsoft Excel. Further, lane traces and automatic band detection for time course of (co-)cultures of IEC were analysed (one repetition). Automatic band detection was also used, however the bands detected needed to be corrected (add and remove selected bands) to balance the gel background.

2.5.2 Western blot

Gels were separated as described above on Tris-tricine gels. Proteins were transferred onto a nitrocellulose membrane (Pall Corporation, Global Science a VWR Company, Auckland, New Zealand) overnight in CAPS buffer (10<pH<11) at 15 V. Membranes were stained with ponceau to test the success of transfer. The stain was then washed off with MilliQ water, membranes were blocked for 3 hr with 4% non-fat milk (powder (Foodstuffs, Auckland, New Zealand), reconstituted in tris-buffered saline (TBS)-BSA-Tween) or 4% BSA (reconstituted in TBS-BSA-Tween) if antibodies against phospho-proteins were used. Before applying the primary antibody diluted in TBS-BSA-Tween, membranes were washed once with TBS; the primary antibody was incubated for 2 hr at room temperature or overnight at 4°C, for horseradish peroxidase (HRP)-conjugates. Membranes were then washed three times with TBS, followed by 1 hr incubation with the secondary antibody, if required. The antibodies used are listed in Table 2.1. Finally, the membranes were washed five times with TBS and enhanced chemiluminescence (ECL) solution was added for 2 min to start the light reaction. Membranes were transferred into a transparent plastic envelope and into a light-protecting cassette. X-ray films (Kodak, Medi'Ray, Auckland, New Zealand) were exposed to the membrane for defined times (listed in Table 2.1) and developed in a processor (100 Plus, all-ProImage Corp.).

CAPS was made up freshly when needed from 10 x stock solution, 10% MeOH and MilliQ water. The stock solution was a 100 mM CAPS (Sigma Aldrich) solution, adjusted to pH 11 with NaOH. Both solutions were stored at room temperature. Ponceau stain was made up as 0.1% Ponceau S (Sigma Aldrich) in 1% acetic acid. A working solution of TBS was prepared from a 10 x stock solution. This contained 110.9 $g.l^{-1}$ NaCl and 121.9 $g.l^{-1}$ Tris base. After dissolution of the salts in 700 ml MilliQ water, the pH-value was adjusted to pH 7.5 and MilliQ water was added to 1 L total solution. Working and stock solutions were kept in the refrigerator. TBS-BSA-Tween was made up by adding 1% BSA and 1% Tween20 to 1 L TBS. The solution was stored at 4°C until use.

Table 2.1: Antibodies used for the Western blot analysis

GAR: Goat-anti-rabbit antibody. DAS: donkey-anti-sheep antibody. fSC: free secretory component

Biorbyt: Biorbyt, San Francisco, USA. Bethyl: Bethyl, Montgomery, USA

Antibody	Manufacturer	Dilution prim	Dilution sec	exposure
Mucin				
α-LA	Biorbyt	1:250k	GAR 1:10k	2 min
β-LG	In-house	1:25k	GAR 1:10k	2 min
fSC	In-house	1:40k	GAR 1:10k	10 min
LF	In-house	1:10k	GAR 1:10k	2 min
Pseudo-milk	In-house	1:75k	GAR 1:10k	2 min
Bacteria				
LF-HRP	Bethyl	1:75k	---	2 to 3 min
β-LG-HRP	In-house, self conjugated	1:75k	---	10 to 30 sec
fSC-HRP	In-house	1:5k	---	5 min
XOR-HRP	ThermoScientific	1:100k	---	60 min
IgA-HRP	Bethyl, ELISA Kit	1:50k	---	10 to 30 sec
IgM-HRP	Bethyl, ELISA Kit	1:5 to 1:10k	---	1 to 3 min
IgG-hc-HRP	Bethyl, ELISA Kit	1:75k	---	10 to 30 sec
Intestinal epithelial cells				
IgG-hc	Bethyl, ELISA Kit	1:10k	DAS 1:10k	10 min
IgA	Bethyl, ELISA Kit	1:50k	DAS1:10k	30 min
IgM	Bethyl, ELISA Kit	1:5k	DAS1:10k	2 min
BSA	ThermoScientific	1:10k	GAR 1:10k	2 min
β-LG	In-house	1:25k	GAR 1:10k	2 min
α-LA	Biorbyt	1:50k	GAR 1:10k	2 min
LF-HRP	Bethyl	1:75k	---	2 to 3 min after 30 min
XOR-HRP	ThermoScientific	1:100k (3 days at 4°C)	---	2 min
IgM-HRP	Bethyl, ELISA Kit	1:5 to 1:10k (3 days at 4°C)	---	1 to 3 min after 30 min
IgA-HRP	Bethyl, ELISA Kit	1:50k (3 days at 4°C)	---	10 to 30 sec

ECL solution was kept in three components. Component A was 5.5 mg luminol (Sigma Aldrich) in 60 µl DMSO; component B was 2.8 mg p-coumaric acid (Sigma Aldrich) in 100 µl DMSO (Sigma Aldrich) and 30% peroxide (Scharlau, Scharlab S.L., VWR International LP, Auckland, New Zealand). One working aliquot each was kept at -20°C. Further aliquots of component A and B were kept at -80°C, 30% peroxide was kept at 4°C, all in the dark. A working ECL solution was made by mixing 10 ml 0.1 M Tris-HCl, pH 8.6, (made up from 1 M stock solution), with 24 µl component A, 4 µl component B and 3 µl peroxide. After adding each component, the solution was mixed briefly.

2.5.3 Mass spectrometry analysis (ESI LC-MS/MS)

All analyses were done with carefully cleaned equipment and low-bind tubes to avoid contamination or loss of peptides. Bands of interest were cut out from the gel and gel plugs were de-stained with 50% acetonitrile (Merck) and 50% 50 mM NH_4HCO_3 (pH 8.1, Fluka Biochemika, Sigma Aldrich, Auckland, New Zealand) overnight at 4°C. The stained solution was removed and the plugs were washed with further 50% acetonitrile / 50% 50 mM NH_4HCO_3 for 1 hr. The gel pieces were then incubated in 25 mM DTT for 30 min at 60°C and cooled to room temperature, followed by incubation with 100 mM iodacetamide (Acros Organics, Thermo Fisher Scientific, Auckland, New Zealand) for 1 hr in the dark. This was followed by two washes with de-stain solution for 30 min each and dehydration with acetonitrile. Finally, the gel pieces were dried by a vacuum concentrator. For the digestion, 5 µl porcine trypsin in 50 mM CH_3COOH (both Promega, In Vitro Technologies, Auckland, New Zealand) and 5 µl 50 mM NH_4HCO_3 / 10% acetonitrile were added to the dried gel pieces and plugs were rehydrated on ice for 1 hr. Additional NH_4HCO_3 / 10% acetonitrile was added to each tube to cover the gel pieces. Tubes were incubated at 37°C overnight. Next morning, tubes were centrifuged, sonicated for 10 min and the supernatant was transferred into clean tubes. More peptides were recovered by twice incubating the gel pieces in 50% (v/v) acetonitrile / 0.1% (v/v) trifluoroacetic acid (Merck) for 10 min with sonication. Each time the supernatant was removed

with the same pipette tip and the supernatants were pooled. Finally the plugs were dehydrated with acetonitrile. Collected supernatants were frozen and dried in a vacuum concentrator.

In preparation for electrospray ionisation (ESI), the dried peptides were re-dissolved in 50 µl of 0.2% (v/v) CH_3COOH / 2% (v/v) acetonitrile. A 10 µl portion of each of the peptide extracts was loaded onto a C18 pre-column (300 µm i.d., 5 µm particles, 300 ångstrom pore size, Varian Microsorb, Agilent, Mulgrave, Australia) at a flow rate of 8 $\mu l.min^{-1}$. The pre-column was then switched in line with the analytical column (Microsorb C18, 20 cm, 75 µm i.d., 5 µm particles, 300 Å pore size), and eluted at a flow rate of 150 $nl.min^{-1}$, with a gradient from 2% to 55% solvent B in 50 min. The column outlet was directly connected by a nanoelectrospray source to a Q-STAR Pulsar *i* mass spectrometer (Applied Biosystems, Foster City, USA) which was programmed to acquire tandem mass spectrometry (MS/MS) traces of 1+, 2+, 3+, 4+ and 5+ ions. The data was used to query the NCBI non-redundant database (release date, Jan 2012), restricted to *Bos taurus* taxonomy using MASCOT. Search parameters for peptide mass tolerances were set to 0.3 Da, with allowance made for one missed tryptic cleavage. Modification of cysteine through carbamidomethylation, was selected as a fixed modification, while oxidation on methionine, deamination of asparagine and glutamine, and phosphorylation of serine and tyrosine were selected as variable modifications. A significance threshold of less than 0.05 was selected within ProteinScape. This produced an average false discovery rate of 1.4%.

Solvent A was made up from high performance liquid chromatography (HPLC)-grade water (Fisher Scientific, USA) with 0.2% (v/v) formic acid. Solvent B was made up from LCMS-grade acetonitrile containing 0.2% (v/v) formic acid.

2.6 Microscopy

2.6.1 Bacteria

For microscopy, a shortened version of the adhesion assay was used. Basically the protocol was stopped after producing pellet A. The bacteria were then fixed in 4% glutaraldehyde (Sigma

Aldrich) for 30 min at room temperature and 10 µl sample was transferred onto a microscopy slide and sealed under a cover slip. For visualisation a DMI 6000 B (Leica Camera AG; Wetzlar) microscope with a DFC 300 FX (Leica) camera was used.

2.7 Flow cytometry

2.7.1 Bacterial cell number and OD_{600}

Figure 2.3 shows the increase of OD_{600} with increasing bacterial cell number with equations and correlation coefficients. Data was gained by measuring optical density at 600 nm (OD_{600}, BioPhotometer, Eppendorf) and plating corresponding samples on Luria Broth agar plates (Invitrogen), followed by colony counting. This data allowed repeatable preparation of samples with constant cell number.

2.7.2 Titrating proteins onto bacteria

Bacteria were grown as described for the adhesion assay (Chapter 2.4.2). Once ready, the bacteria were diluted with PBS to 2 x 10^7 colony forming units (cfu).ml^{-1} by adjusting the OD_{600}. Then 10^6 bacteria in 50 µl were transferred into Eppendorf tubes and centrifuged for 1 min at 7.5 x 10^3 rpm before removing the supernatant. Between 0 to 1 µmol labelled protein (endpoint differs between proteins because of availability and molecular weight) were added to 10^6 cfu bacteria and the total volume was filled up to 80 µl with PBS. Because of limited stocks not all proteins were titrated completely. Protein and bacteria were then incubated for 2 hr at 37°C and 90 rpm in the dark. After this, the supernatant was removed and the cells were washed with 2 x 200 µl PBS. Bacteria were pelleted by centrifugation for 10 min at 1.5x10^3 rpm. Finally the bacteria were fixed for 30 min in 50 µl 4% glutaraldehyde, then diluted with 900 µl filtered PBS before analysing them on a FacsFlow (BD, Auckland, New Zealand). If necessary, flow cytometer samples were further diluted with filtered PBS to obtain an event rate of 150 to 200 cells.sec^{-1}. Forward scatter and side scatter were adjusted to centre the displayed events. Propidium iodide (Fluka, Sigma Aldrich, Auckland, New Zealand) was added to pure cells without protein to gate on bacteria. Thus only bacterial events were counted and analysed.

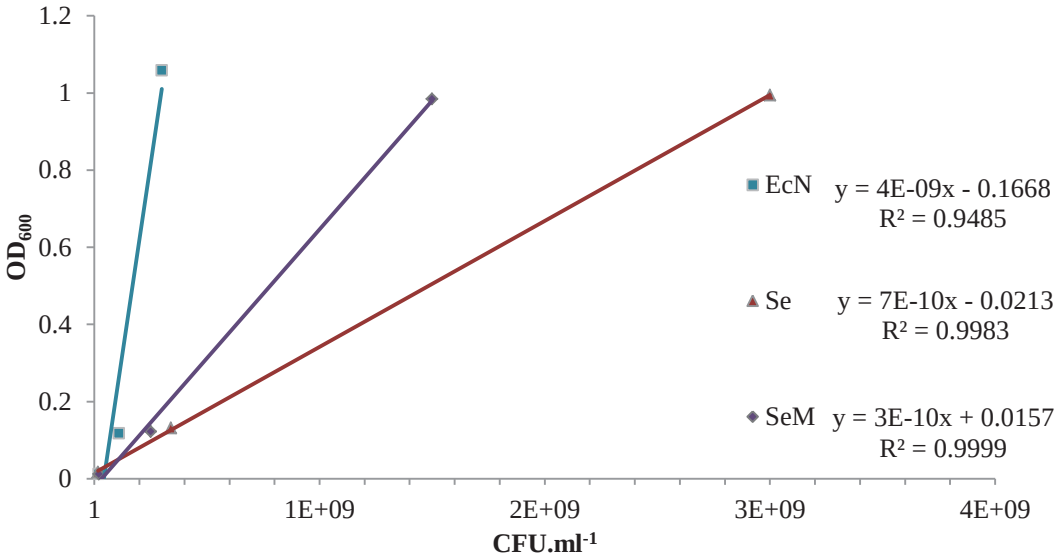

Figure 2.3: Relation between CFU.ml^{-1} and OD_{600} for three strains of bacteria

The graphs show linear trend lines with equation and R^2. One repetition was analysed. EcN: *E. coli* Nissle 1917. Se: *S. epidermidis* 1457. SeM: *S. epidermidis* 1457 M10

Next, a graph showing FITC emission on the X-axsis was set up and auto-fluorescence was gated out by introducing a (vertical) gate on the FITC detection, including 1% of parental population as FITC-positive. Thus an increase in FITC emission, i.e. protein adhesion, was detected as right shift of the FITC peak or an increase in peak hight. Calibration of the instrument was done with calibration beads (BD Calibrate, BD), allowing inter-day comparison.

2.7.3 Titrating proteins onto intestinal epithelial cells

Cells were grown as described for the adhesion assay. At confluence, the cells were detached with TriplE and counted. 5 x 10^5 (HT29-MTX) or 2 x 10^5 (Caco-2) cells were transferred into 1.5 ml tubes, supernatants aspirated and the cells mixed with 0.005 to 4 µmol (LF, IgG and BSA) or 0.02 to 15 µmol (β-LG, α-lactalbumin (α-LA) and κ-casein, all Sigma Aldrich) FITC-labelled proteins. Volumes were adjusted to 200 µl with PBS. Negative controls were mixed with 10% FCS in PBS. Proteins and cells were then incubated for 90 min in the incubator after which the supernatant was removed, the cells were washed once with PBS and re-suspended in 1 ml (HT29-MTX) or 500 µl (Caco-2) filtered PBS; 100 µl of the suspensions was then added to 1 ml filtered PBS before injection into the FacsFlow. Event rates were under 300 cells.sec^{-1}. Samples were analysed as described above for bacterial cells. The data obtained was analysed using flow cytometer software (FacsSuite, BD) and Microsoft Excel.

2.8 Statistics

For statistical analysis Microsoft Excel was used. For the figures, the data were averaged and the standard deviation (STDEV.P) was determined. For significance levels, the Student's T-test was performed using a two-tailed distribution and two-sample equal variance (homoscedastic).

Chapter 3 Development of the adhesion protocol and preparation of the input materials

3.1 Introduction

In order for a functional nutrient to be effective, it needs to be in close proximity with its designated site of utilisation. This could be any of the human intestinal surface layers, i.e. the bacterial biofilm, the mucin layer, or the IEC. The nutrient may also be beneficial after absorption by the IEC. In either situation, it would be an advantage if the vehicle carrying the nutrient bound to the applicable surface layer. Several researchers have explored the interactions between food molecules or products thereof and IEC, their brush border membranes or bacteria. The studies focussed on allergic or immunogenic effects [467-469] and inhibition of bacterial adhesion [26, 470-473]. However, only selected isolated molecules were investigated or details about adhesion of food molecules to the GIT layer components were not directly addressed.

Furthermore, no *in vitro* protocol has yet been described to simultaneously screen for specific adhesive properties of different foods, and the binding potential of individual food components (e.g. proteins) to components of the intestinal surface layers. Such an *in vitro* approach will allow greater control and manipulation of parameters at low cost compared to more complex systems such as animal models.

3.1.1 Hypothesis and aims

The main hypothesis tested in this chapter is that foods and partially digested foods contain components which differ in their adhesive properties. Further, that it is possible to screen for such components which adhere to one specific layer of the human intestinal surface using an appropriate adhesion assay.

The aim of this chapter was to prepare and characterise MUC2-covered Sepharose beads for use in an *in vitro* adhesion assay to model the binding of food proteins to the human intestinal surface. In addition, an *in vitro* partial gastric digest of milk and whey was developed to simulate the digestive processes before the food reaches the small intestine. The partial digestion protocol produced a digest which contained a mix of proteins and peptides, similar to digestion products in the stomach (partial digest). This is supported by findings of Heyman et al.

[128] who demonstrated that a small proportion of ingested proteins reaches the circulation in an antigenically intact state. Further, Davidson and Lonnerdal [474] showed that intact human IgA and LF were found in faecal samples of breast-fed children.

In addition, a method to inhibit pepsin activity before all food proteins were hydrolysed was implemented. This should not involve heat inactivation of the enzyme. Elevated temperature would have the undesirable effect of denaturing other components in the digest solution. Finally, the partial digest was adjusted to conditions as they occur in the early digestion phase in the duodenum (pH 6.8 to 7.0 and ionic strength). This partial digest was then used for the adhesion assay.

3.2 Results

3.2.1 Preparation of test solutions

3.2.1.1 Whey samples

Figure 3.1 compares the protein profiles of whey samples produced by acidification of skim milk or centrifugation of skim milk. Samples were separated using reducing SDS-PAGE analysis. Overall, both whey preparations showed the same protein profile. However, in the whey prepared by centrifugation, the 25 kDa fraction (marked with a black box, labelled "Ig light chain, casein residues") was more abundant whereas the 55 kDa band (labelled "Ig heavy chain") was less intense. A second band under the 18 kDa band (labelled "β-lactoglobulin") was also detectable in the whey prepared by centrifugation.

Acidification resulted in a protein concentration of 2.3 to 2.4 $mg.ml^{-1}$ in the whey, as measured by the Bradford method, and a volume yield of different whey batches was between 54 to 77%. Protein quantification for the last batch of acidified whey was also done by DirectDetect (MerckMillipore) and was determined to be 4.9 $mg.ml^{-1}$. This discrepancy was likely due to the different principles of the two methods. Bradford is based on dye binding to the protein and thus relies on the accessibility of the protein backbone and also the amino acid sequence [475],

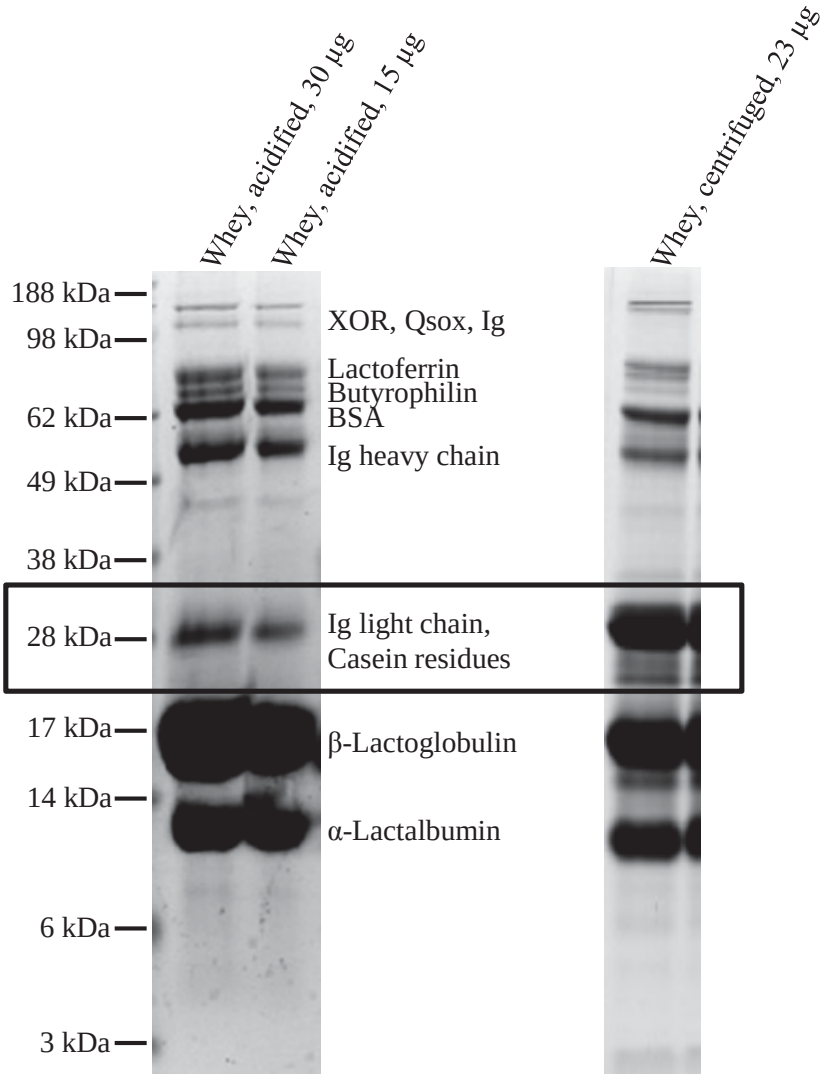

Figure 3.1: Protein band patterns of whey samples from different preparation methods

Reducing SDS-PAGE gel of whey produced by acidification and centrifugation (10^5 x g for 60 min). Gel separated at 130 V for 2 hr and stained with CBB R250 overnight. Whey proteins are putative identifications based on the molecular weights of known whey components. Box highlights the difference in casein content in the two differently prepared whey samples. XOR: Xanthine oxidoreductase. Qsox: Quiescin sulfhydryl oxidase. Ig: Immunoglobulin. BSA: Bovine serum albumin.

whereas the DirectDetect measures infrared (IR) waves emitted from the amide bonds. For consistency, all calculations were based on the Bradford results. In comparison, whey had 5.4 $mg.ml^{-1}$ protein by the Bradford method after the first centrifugation, and 4.7 $mg.ml^{-1}$ after the second centrifugation. Two times centrifuged whey was used for the experiments as it contained less residual casein compared to the whey obtained after one centrifugation. The volume yield for this method was in the same range as the acidification method.

3.2.1.2 Optimisation of in vitro gastric digestion

This study aimed to mimic the interactions of food materials in the GIT. Therefore, it was important to include assessments of whole as well as partially digested samples. The standard gastric digestion, as described in the US Pharmacopeia [465], needed adjustment for optimal protein:enzyme ratio. A method to stop the digestion without compromising the proteins also needed to be implemented. Finally, a digestion time was chosen to mirror a partial digest and generate an array of digestion peptides as might be found during normal food intake.

Optimisation of the digest started with adjustment of protein:enzyme ratio and digestion time to achieve a suitable partial digest, as close to physiological conditions as possible. The template assay was designed for milk with 15 $mg.ml^{-1}$ protein but the whey (acid precipitation or centrifugation) had only 2.3 $mg.ml^{-1}$ or 4.7 $mg.ml^{-1}$ protein, respectively, and consequently demanded lower pepsin concentration in the simulated gastric fluid. To have better control over the pepsin concentration, the pepsin solution was made in two steps. First, a high pepsin concentration solution was prepared which was then diluted with simulated gastric fluid to fit with the substrate requirements. Protein:enzyme ratios from 5:1 to 200:1 were tested over a time course from 0.5 to 60 min digestion time. Figure 3.2 shows the time course of an *in vitro* gastric whey digestion. The degradation of whey proteins increased with increasing digestion time. After 30 sec, there was little intact α-LA (14.2 kDa) and higher molecular weight fractions remained but a variety of peptides were observed. After 10 min of digestion, the only intact proteins with molecular weight over 5 kDa were pepsin (35 kDa) and monomeric β-LG (18 kDa). β-LG was resistant to pepsin digestion up to 60 min. It was decided to use a

protein:enzyme ratio of 20:1, which is close to the physiological conditions. The optimal digestion time was set at 30 sec. Under these conditions whey is partially digested, resulting in fractions of molecular weight less than 10 kDa whilst some full-sized proteins were retained. To stop the digestion process, Pepstatin A (a pepsin inhibitor) was introduced and sodium bicarbonate (stop solution) was added to raise the pH-value. Samples were stored on ice until further use. Figure 3.3 shows that this combination of treatments effectively inhibited pepsin activity and maintained the degree of digestion for up to 24 hr. It was decided to use Pepstatin A in 1:1 ratio with pepsin to increase the probability of complete inactivation. At this ratio, statistically, the active centre of each pepsin molecule was blocked with one Pepstatin A molecule.

When the digestion was transferred from whey to skim milk, the milk:simulated gastric fluid-ratio was altered to achieve physiological protein:enzyme ratio. A calculation error resulted in a low protein:enzyme ratio of 176:1. In order to obtain a comparable partial digest, digestion of skim milk was allowed for 30 min instead of 30 sec to 1 min as for the whey (Figure 3.4). This agrees with data from Mahe et al. [476] who found that the half-life of skim milk in the human stomach is about 25 min. As for whey, Pepstatin A and sodium bicarbonate were used to inhibit further enzyme activity (data not shown).

A simulated duodenal fluid was developed to generate a binding environment more representative of the duodenal conditions. The simulated duodenal fluid changes the ionic milieu in the digest from a gastric to a duodenal state, without introducing further enzymes. Adding the necessary salts in the right composition initially led to precipitation, most likely of insoluble phosphates or carbonates. The phosphate or carbonate based buffer systems used are known to form complexes with the calcium ions, both in the digest and in the simulated duodenal fluid. This resulted in uncontrollable alterations of the digest mix. Therefore, the simulated duodenal fluid was changed to a Tris-HCl buffer which is still close to the model proposed by the US Pharmacopeia [465] (Dr A. Sarkar, Nestle, Vevey, Switzerland, November 2011). Table 3.1 lists all tested simulated duodenal fluid systems. Adding this final solution

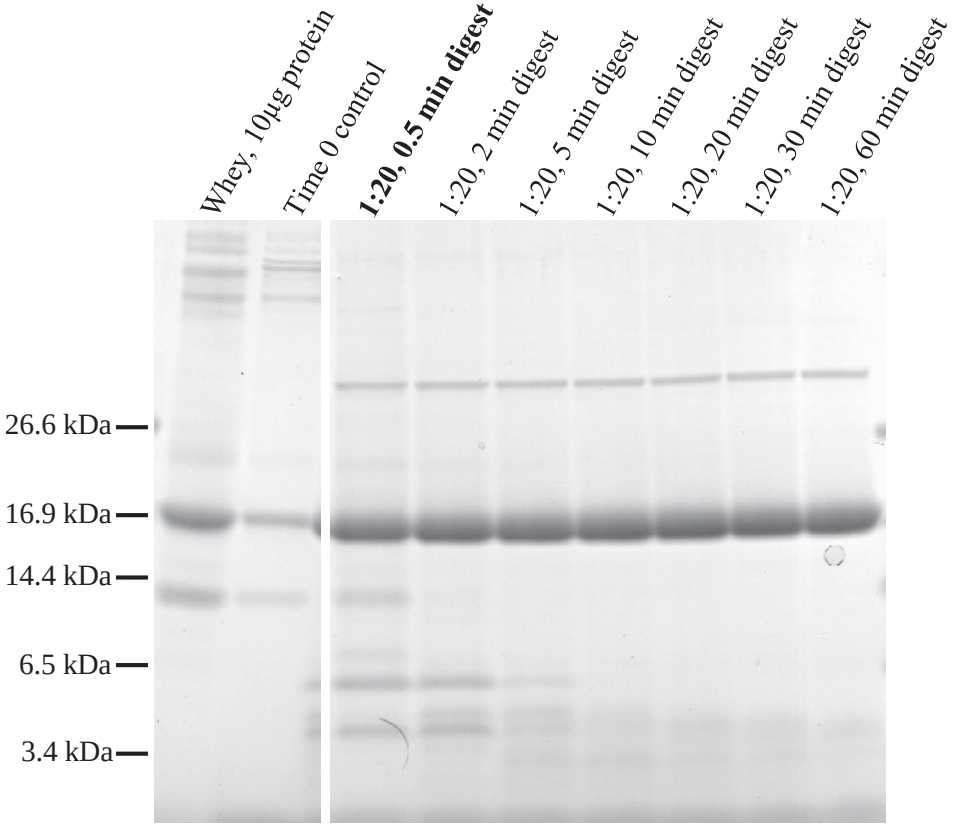

Figure 3.2: Pepsin digestion time course of whey

Reducing SDS-PAGE gel of digestion time course of pepsin digested whey prepared by acidification of skim milk. Protein:enzyme ratio was 20:1. Gel separated at 130 V for 2 hr and stained with CBB G250 overnight. Bold font indicates digest conditions used for further experiments.

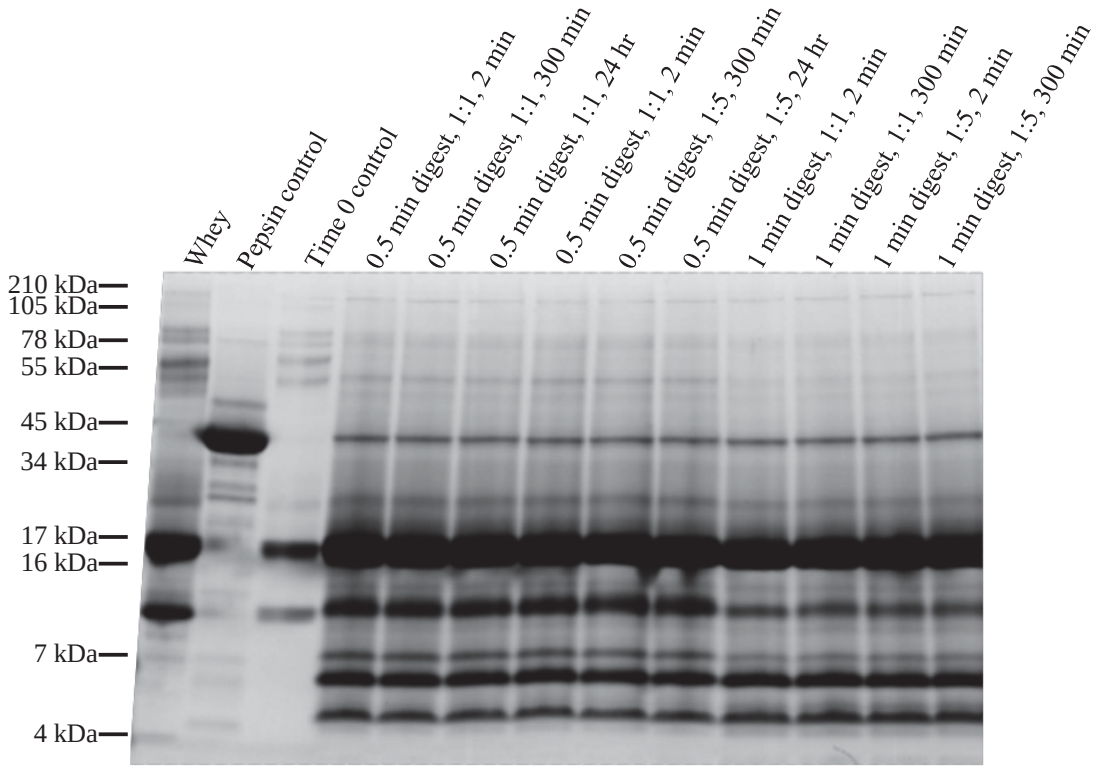

Figure 3.3: Efficiency of pepsin inhibition by bicarbonate and Pepstatin A

Reducing SDS-PAGE gel of partially pepsin digested whey, digestion stopped with bicarbonate solution and varying concentrations of Pepstatin A. Digest mix with inhibited pepsin was allowed to stand for 2 min to 24 hr to test the extent of enzyme inhibition. Gel separated at 130 V for 2 hr and stained with CBB G250 overnight.

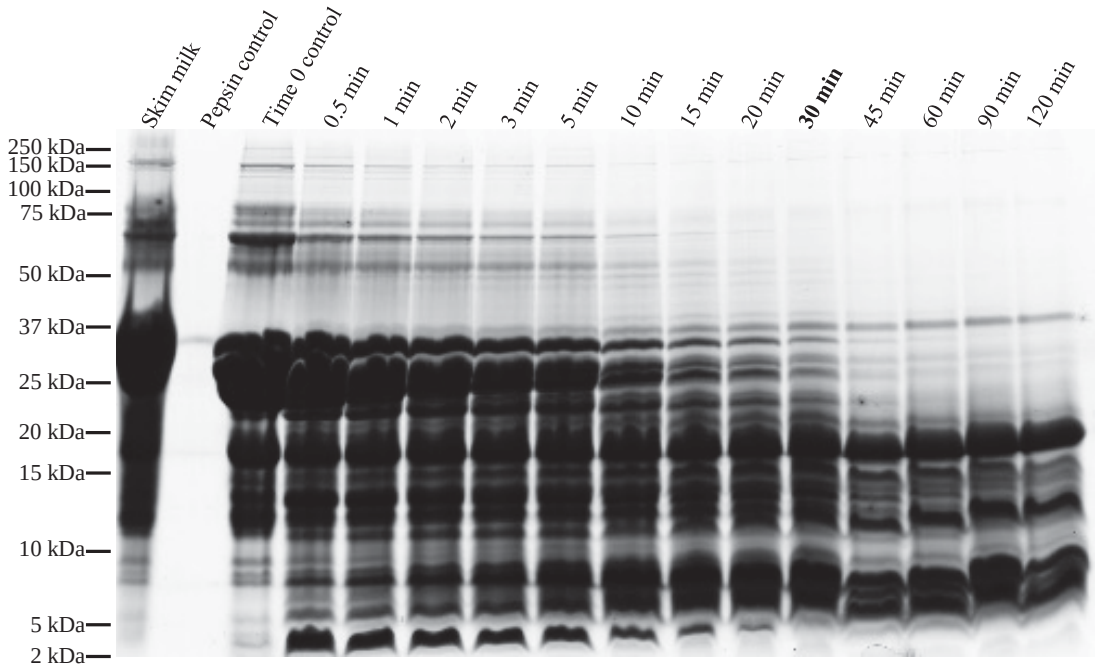

Figure 3.4: Pepsin digestion time course of skim milk

Reducing SDS-PAGE gel of digestion time course of pepsin digested skim milk (commercial). Protein:enzyme ration 176:1. Gel separated at 130 V for 2 hr and stained with CBB G250 overnight. Bold font indicates digest conditions used for further experiments.

Table 3.1: Development of a simulated duodenal fluid

Tested systems for the simulated duodenal fluid (SDF) added to digest mix with inhibited pepsin in order to change milieu to human duodenal conditions

#	Buffer / composition	Observation	Comment
1	Modified stop solution: 250 mM $NaHCO_3$, 100 mM $CaCl_2$, 100 mM NaCl	Precipitate	Initial idea was to combine sodium-bicarbonate and SDF in one solution
2	Phosphate buffer pH 7.5 35 mM, 30 mM CaCl2, 150 mM NaCl	Precipitate	Tried phosphate instead of carbonate
3	Hur et al. [477] 100 ml: 0.08 g KH_2PO_4, 6.65 g NaCl, 0.02 g $CaCl_2 \cdot 2H_2O$, 3.21 g $NaCO_3$, 0.54 gKCl, 170.62 µl 37% HCl, pH 8.1±0.2	Precipitate	Without $MgCl_2$, urea, BSA, pancreatin or lipase
4	Singh and Sarkar [111] 100 ml: 0.68 g K_2HPO_4, 0.88 g NaCl, 0.33 g $CaCl_2$, 0.2 N NaOH, pH 7.5	Precipitate	Filtered after precipitate formation with 0.22 µm filter; addition of whey caused new precipitate formation
5	Tris-HCl buffer as described in 2.2.1.5	Stable	Used for experiments

changed the ionic milieu to that in the human duodenum. The mix was then added to mucin covered Sepharose beads.

3.2.1.3 Effects of pepsin on mucin used to cover Sepharose beads

It was also tested if mucin was degraded by pepsin. Incubation of hydrated mucin with pepsin, at a higher concentration than used in the experiment, for up to 120 min did not result in any visible digestion products on SDS-PAGE gels (data not shown). It was concluded that the MUC2 used in the assay was not subjected to pepsin activity under the assay conditions used.

3.2.2 Coupling mucin onto Sepharose beads

As outlined in Figure 1.12, the experimental plan for this thesis was to begin with *in vitro* systems for the screening of adhering food components and gradually move to more realistic models. Thus the first step was to prepare affinity chromatography medium coated with isolated components of the human intestinal surface layers. Of these, mucin was the most available and was chosen as a starting material. Crude porcine MUC2 mucin was coated onto epoxy-activated Sepharose beads. The initial idea of preparing chromatography columns was reconsidered and a batch approach, using Eppendorf tubes, was chosen. This had the advantage that the mucin coated beads themselves could be analysed for adhering proteins (direct proof), whereas the use of affinity chromatography columns was restricted to the analysis of eluents (indirect proof). Additional to the mucin covered beads, negative control beads were prepared by blocking the activated epoxy groups with EtOH-amine. Similarity in protein band pattern on SDS-PAGE gels between EtOH-amine beads and MUC2 beads (e.g. compare Figure 3.15) implied that the beads were not fully covered with mucin. To estimate the degree of mucin coverage of the Sepharose beads, several methods were employed.

3.2.2.1 Confocal laser scanning microscopy

Mucin covered beads and EtOH-amine blocked beads were tagged with AlexaFluor488 via WGA. Beads were then visualised under a confocal laser scanning microscope and fluorescence

was associated with MUC2 as the lectin specifically binds to mucin. No reports of WGA binding to Sepharose were found.

Figure 3.5 shows a "cut" through a MUC2 covered bead with yellow-green emission in front of a more black background. Emission of mucin covered beads (circle 1, red line) and background (circle 4, orange line) was measured from 500 to 600 nm. The beads show a peak emission at 512 to 517 nm. Background emission was consistently low. Figure 3.6 shows a comparable micrograph for EtOH-amine blocked beads from the same experiment. The beads were less bright than the MUC2 covered beads. The emission spectra for EtOH-amine blocked bead (circle1, red line) and background (circle 2, green line) show a similar topography with a peak at 512 nm. The background emission was comparable with the one in Figure 3.5 (ca. 60 units) whereas the emission coming from the EtOH-amine blocked bead was about half the intensity of the MUC2 bead emission (ca. 90 units for EtOH-amine compared to ca. 160 units for MUC2). Independent of the type of bead coverage, the beads seem to emit light in a circular shape, which corresponded to their projection area.

3.2.2.2 2-D QuantKit

Protein quantification of mucin in binding buffer before and after coupling to Sepharose beads was made against a MUC2-calibration curve. Calibration was done for mucin concentrations from 0 to 50 $\mu g.ml^{-1}$ and resulted in absorption between 0.963 to 0.95 units at 480 nm. The measured values were approximated with a linear regression (Figure 3.7). Samples measured were mucin in 20 µl binding buffer before binding and mucin in 50 µl binding buffer after 200 min and 400 min coupling (Figure 3.8). The values for absorption at 480 nm were averaged per sample (n=3) before calculating the average mucin quantity per sample with the linear regression of the calibration (Figure 3.7). To obtain the average mucin concentration for each sample, the different sample volumes were considered. Concentration values show that there was a significant (p-value 0.015 after 200 min; p-value 0.001 after 400 min) decrease in free soluble mucin concentration during binding.

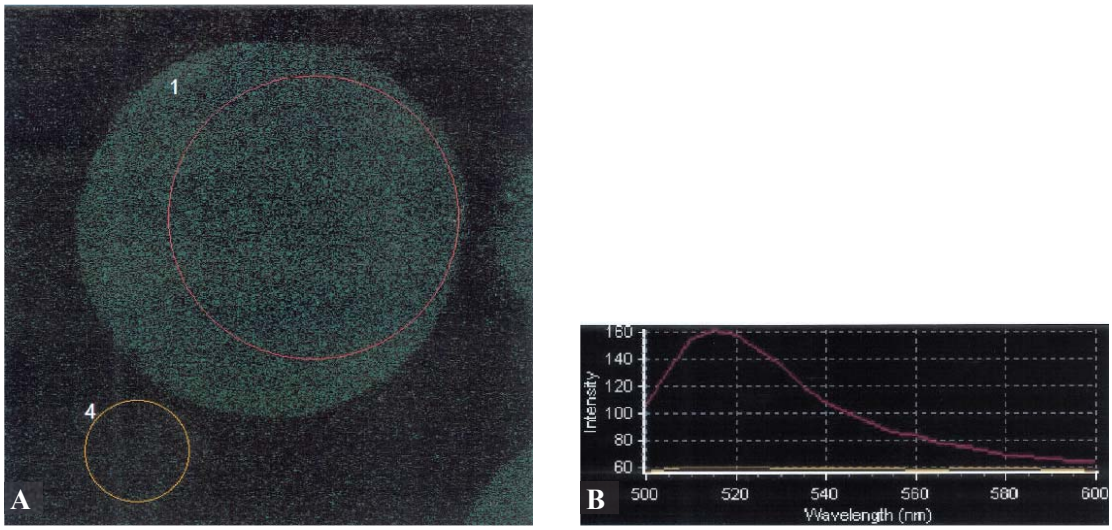

Figure 3.5: Micrograph of mucin covered beads and fluorescence signal

(A) Confocal laser scanning micrograph of WGA488 tagged MUC2 covered Sepharose beads (1) and background (4). (B) Intensity graph for emission wavelength from 500 to 600 nm. Micrographs were from the same experiment as those in Figure 3.6.

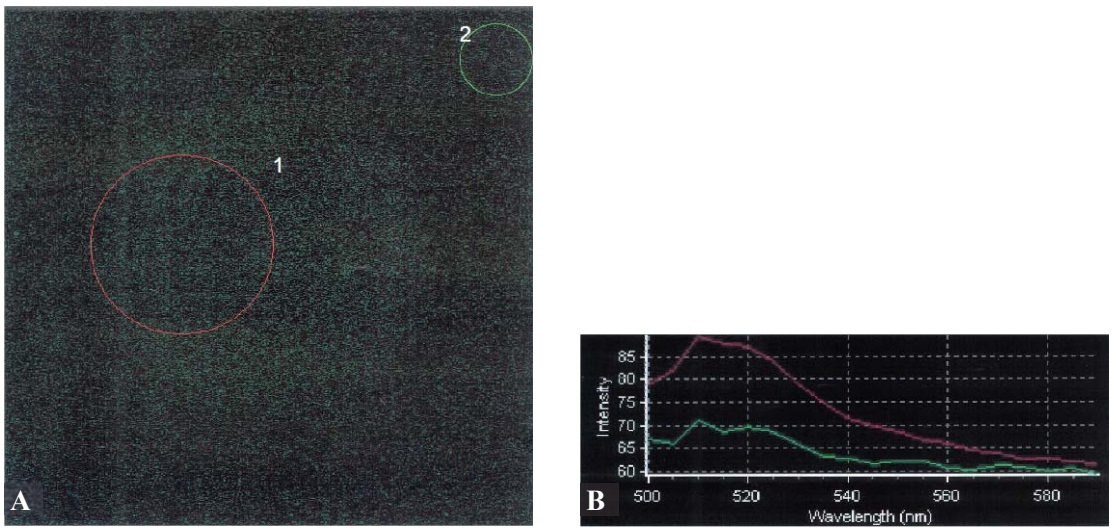

Figure 3.6: Micrograph of EtOH-amine blocked beads and fluorescence signal

(A): Confocal laser scanning micrograph of WGA488 tagged EtOH-amine blocked Sepharose beads (1) and background (2). (B) Intensity graph for emission wavelength from 500 to 590 nm. Micrographs were from the same experiment as those in Figure 3.5.

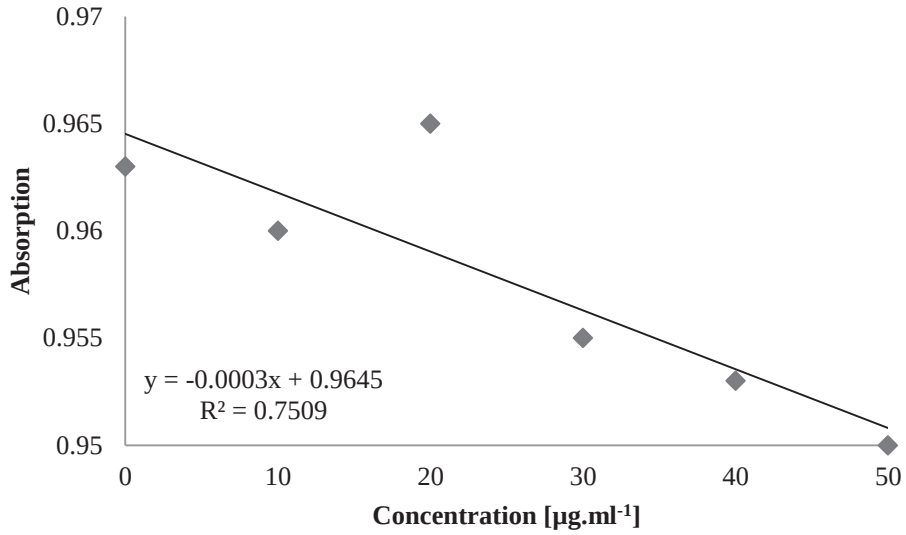

Figure 3.7: 2D-Quantkit calibration curve

2D-QuantKit protein quantification calibration curve for MUC2 concentrations from 0 to 50 µg.ml^{-1} against absorption at 480 nm, including linear regression with equation and R^2.

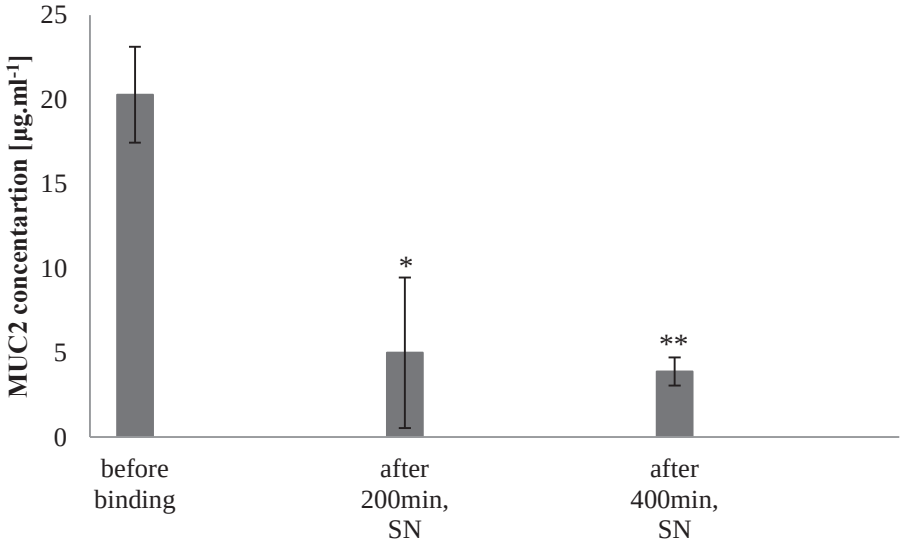

Figure 3.8: Calculated mucin concentration in coupling solutions

Mucin in samples analysed with 2D-QuantKit. Samples (n=3) are analysed for absorption at 480 nm, and average mucin concentrations were calculated. Average mucin concentrations, standard deviations and significance levels compared to "before binding" are indicated * (significant 0.05>p> 0.01) and ** (highly significant, p<0.01). SN: Supernatant.

3.2.2.3 Nitrogen quantification by total combustion (LECO)

Total combustion of MUC2 covered and EtOH-amine blocked beads allowed determination of total nitrogen and consequently crude protein by applying the conversion factor 6.25. This method detected 0.05% total nitrogen in MUC2 covered beads and 0.04% total nitrogen in EtOH-amine blocked beads. Both measurements result in 0.3% protein after multiplying with the conversion factor of 6.25 (data not shown).

3.2.2.4 Wheat germ agglutinin tagging of mucin

This approach used the same labelling of beads as described for confocal laser scanning microscopy. However, emission was detected by a plate reader at only one wavelength (528 nm). A 7-point calibration with WGA488 concentrations from 0 to 10 $\mu g.ml^{-1}$ was performed; the values shown in Figure 3.9 were averages of 4-fold measurements.

Six wells per sample were prepared, measured and emission at 528 nm was recorded and averaged. WGA488 levels in the samples were calculated employing the linear regression derived from the calibration curve (Figure 3.9) and values for plain, EtOH-amine and MUC2 beads with and without WGA488-tag are shown in Figure 3.10. Generally, WGA488 labelled beads showed higher emission levels than their unlabelled comparison. Highest levels of WGA488 were found in EtOH-amine beads, followed by MUC2 covered beads. Both showed a highly significant (p-values 0.000) difference in WGA488 concentration compared to their respective pure (unlabelled) beads.

3.2.2.5 Alcian blue (periodic acid Schiff)

For this experiment, visual examination but no colorimetric measurements were taken. After mixing with alcian blue, the MUC2 solution became blue. The blue colour was associated with alcian blue binding specifically to mucin. After mixing the tagged mucin with Sepharose beads in the binding buffer, the blue distributed through the whole volume of the suspension. After incubation overnight, the beads were allowed to settle by gravity. Once this was completed, the only blue colour observed was in the supernatant. There was no blue colour among the beads.

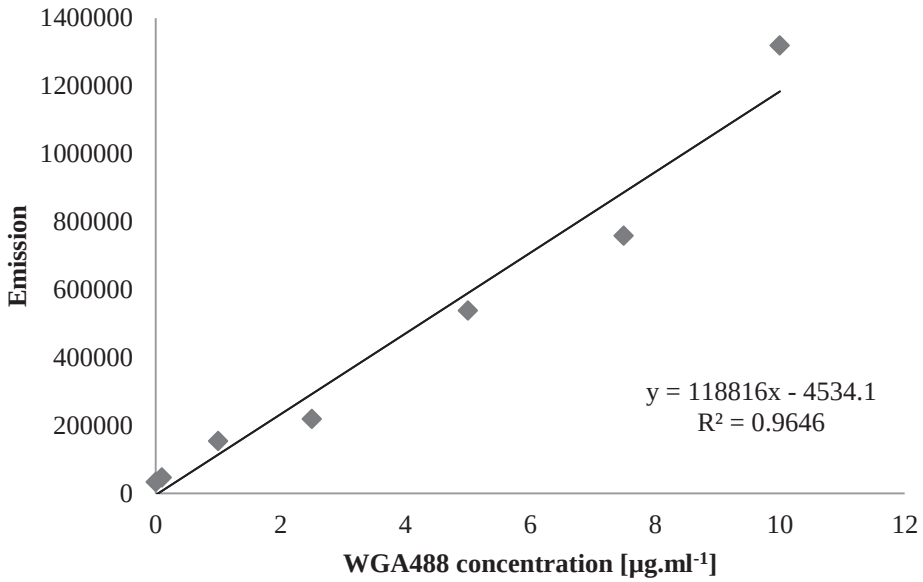

Figure 3.9: Calibration curve for AlexaFluor488-WGA measurements using a plate reader

Plate reader (485/528) calibration curve for WGA-AlexaFluor488 concentrations from 0 to 10 µg.ml^{-1}; including linear regression with equation and R^2.

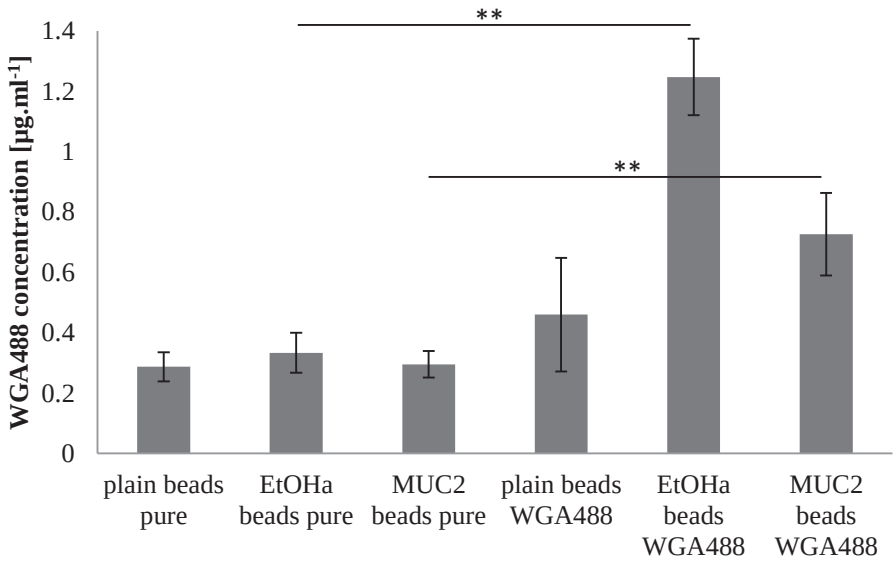

Figure 3.10: Mucin concentration in different bead preparations

Mucin in samples analysed by WGA488 and Plate Reader. Samples (n=6) are analysed for average emission at 528 nm and average quantities of WGA488 in samples referring to the calibration curve are calculated and shown. STD deviations and significance levels are indicated * (significant 0.05>p> 0.01) and ** (highly significant, p<0.01) for significant differences. WGA: wheat germ agglutinin. EtOHa: Ethanol amine.

Also further incubation for up to one week did not change this result.

The only assay which showed that mucin was covering the Sepharose beads was the confocal laser scanning microscopy after WGA tagging of the mucin. However, this did not allow quantification. Measuring mucin in solution before and after coupling using the 2-D Quant kit indirectly showed that mucin has been passed onto the beads. The other assay did not show mucin binding to the beads. Taken together this shows that mucin was bound, but only to a limited degree and quantification was not possible.

3.2.3 Design of the mucin bead adhesion assay

Once the input materials were defined, the actual adhesion assay was designed. Figure 3.11 outlines the basic protocol for the mucin bead experiments. The mucin covered beads were mixed with a defined volume of protein solution and incubated for a defined time under physiological conditions, i.e. agitation, temperature and pH value. This adherence phase was followed by a wash sequence to first remove unbound protein and then adhering proteins step by step depending on the nature of the formed interactions. The composition of wash solutions to address different types of interactions, and the wash process were assessed. At two points during the wash cycle, samples were taken to analyse for total binding protein (bead A) or strongly bound proteins (bead B), respectively.

3.2.4 Optimisation and evaluation of the assay

Conducting the adhesion assay in batch mode, as opposed to affinity chromatography columns, had the advantage that the MUC2 medium could be prepared for SDS-PAGE gels. This assisted the development of the adhesion assay protocol as visualisation of the proteins adhering to the MUC2 beads was possible and thus, the beads could be evaluated regarding efficiency of wash steps.

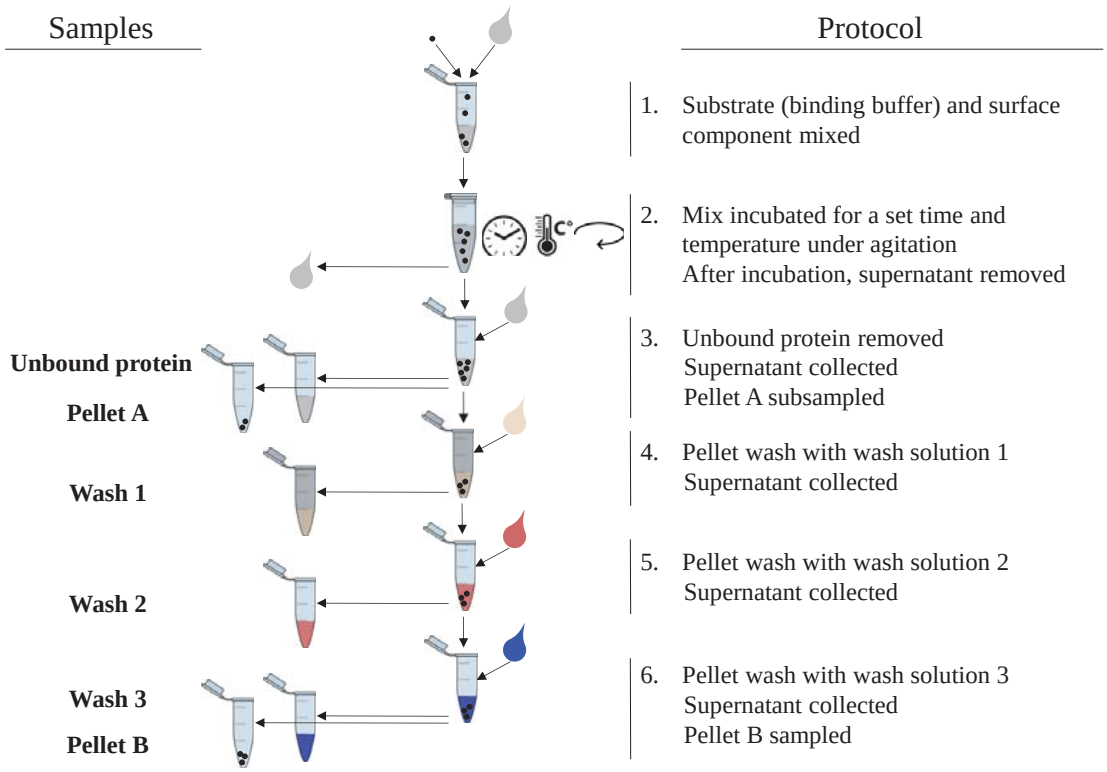

Figure 3.11: Outline of adhesion assay protocol

Pellet A and pellet B in the figure are named “bead A” and “bead B” in samples with mucin coated Sepahorse beads, and “pellet A” and “pellet B” in samples containing bacterial cells or IEC.

3.2.4.1 Washing sequence and solutions

The developed adhesion assay consisted of two phases; initially an incubation to allow adhesion followed by a wash cycle to sequentially remove bound molecules. The first wash step was the removal of all unbound material with a buffer that had the same composition as the binding buffer but did not contain any proteins. For this early stage wash solution, PBS was used. Preliminary experiments (not shown) showed that PBS had the same effects as a tailored solution mimicking the binding buffer. After this step, the first beads were removed for SDS-PAGE analysis (bead A) to visualise all adhering proteins.

The late phase digest wash solution (PBS 5.5) was made from the early phase solution by dilution and a decrease of the pH-value. This mimicked an increasing volume of food and saliva entering the duodenum which causes a dilution of digest secretions. These changes also allowed a first differentiation of strength and type of interaction. In the last phase of the wash cycle, the beads were treated to remove ligands according to other possible types of interaction forces; 25% EtOH (hydrophobic interactions) and 2.5 M LiCl (electrostatic interactions), both in the post-prandial (state after food intake) washing buffer (PBS 5.5). A second aliquot of beads was then removed for SDS-PAGE analysis (bead B). The last wash step was done with 6 M guanidine HCl to remove all remaining adherents and to prepare the media for the next run if it was used in chromatography columns. In the end, this last wash step was dropped when the decision was made not to use affinity chromatography columns. Further, high concentrations of 6 M guanidine HCl might also impair the MUC2 network integrity [478]. Each wash step (PBS 5.5, 25% EtOH and 2.5 M LiCl) consisted of three washes with the same wash solution. The first wash solution of each step was collected separately, while solutions from the second and third wash were pooled to reduce carry-over from one wash to the next wash. This way, cleaner protein profiles of the individual wash steps were obtained.

3.2.4.2 Sample resolution on SDS-PAGE

Figure 3.1 shows an initial SDS-PAGE gel of samples from the adhesion assay between mucin coated Sepharose beads and partially *in vitro* gastric digested whey. Control samples ("Whey,

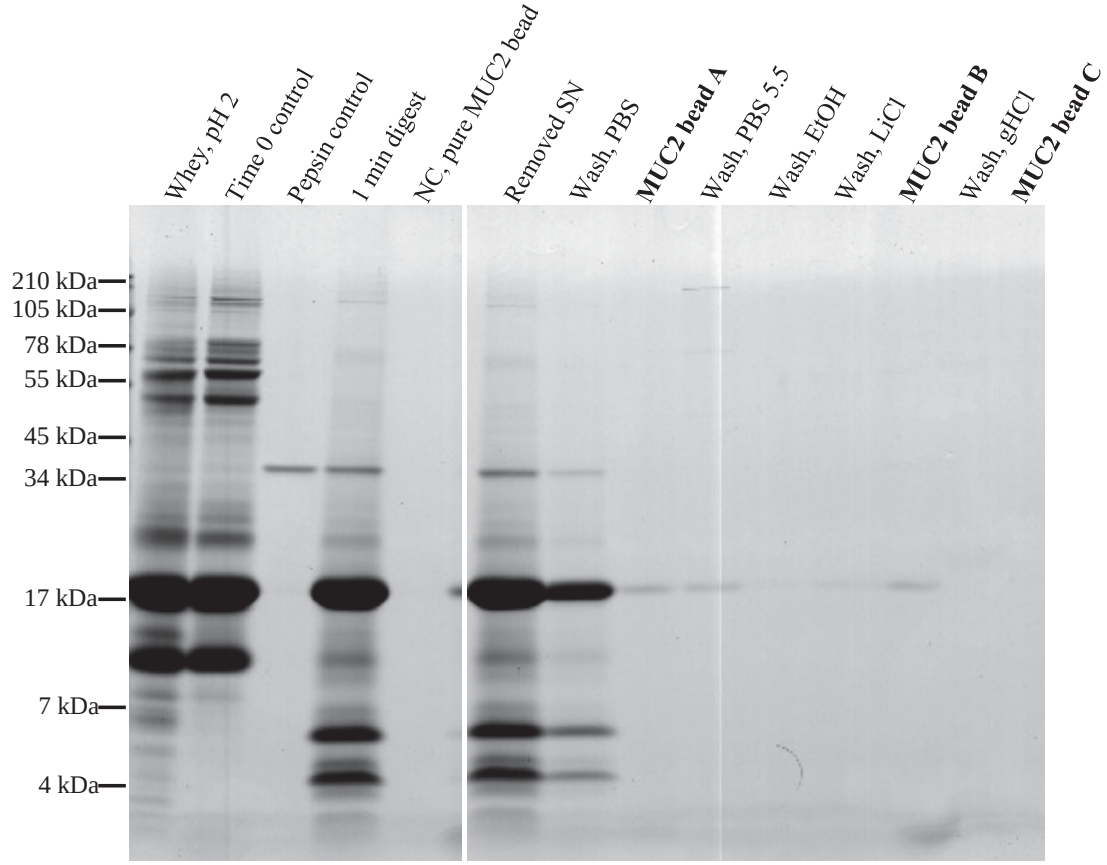

Figure 3.12: Adhesion assay between mucin-beads and digested whey

Reducing SDS-PAGE gel of MUC2 covered Sepharose beads after incubation with digest mix (acidified whey); EtOH and LiCl wash solutions prepared with PBS 5.5. Gel separated at 130 V for 2 hr and stained with CBB G250 overnight. Bold font indicates samples that contain Sepharose beads (i.e. shows adhering proteins). NC: Negative control.

pH 2" to "NC, pure MUC2 bead") show good protein band resolution. Protein profiles in "Whey, pH 2" and "Time 0 control" are comparable to the profile of whey observed in Figure 3.1. Control sample "1 min digest" shows that most proteines were hydrolysed and only bands for pepsin (35 kDa), monomeric β-LG (18 kDa), little α-LA (14 kDa) and peptides (<10 kDa) can be observed. Samples from the adhesion assay show that no protein or peptide fraction bound completely to the mucin coated beads ("Removed SN") and that most proteins and peptides were washed off the mucin coated beads during the first wash with PBS. Only a faint band of β-LG was observed from "MUC2 bead A", suggesting that protein adhesion to the beads was very limited. Further, no protein bands could be observed in the collected wash supernatants. To resolve this issue, the volume loaded onto the gels was increased. 12% and 15% acrylamide SDS-PAGE gels (1 mm width) were cast instead of using precast gels. This allowed doubling the sample volume from 30 µl to 60 µl. Figure 3.13 shows a representative 12% acrylamide gel. Overall, this SDS-PAGE gel is comparable to the one in Figure 3.12 with regards to band pattern. In particular, the band intensity in the wash solutions was comparable with the one in pre-cast gels (e.g. Figure 3.12). However, the resolution, especially in the higher molecular weight region, was very poor. To get a better quality gel for this part, 15% acrylamide gels were prepared. These resulted in a poor resolution for the lower molecular weight proteins (data not shown). Overall the qualities of self-cast gels did not meet the requirements for clear band correlation between samples throughout the whole molecular weight range of interest (10 to 150 kDa) and these gels were discontinued. As the increase of sample volume did not result in stronger bands, an attempt was made to increase the protein concentration within the samples by precipitating and re-dissolving in less volume. EtOH precipitation and chloroform-MeOH precipitation were assayed and chloroform-MeOH precipitation was determined best suited for the samples as it resulted in gels with more distinct bands (Figure 3.14 and Figure 3.15). Figure 3.14 shows removed whey and wash solutions. Figure 3.15 has the same gel layout as previous SDS-PAGE gels (e.g. Figure 3.12). In both gels, protein and peptide fractions are enriched due to precipitation which increased the load onto SDS-PAGE gels from 30 µl untreated wash solution up to 2 x 150 µl solution precipitate, a 10-

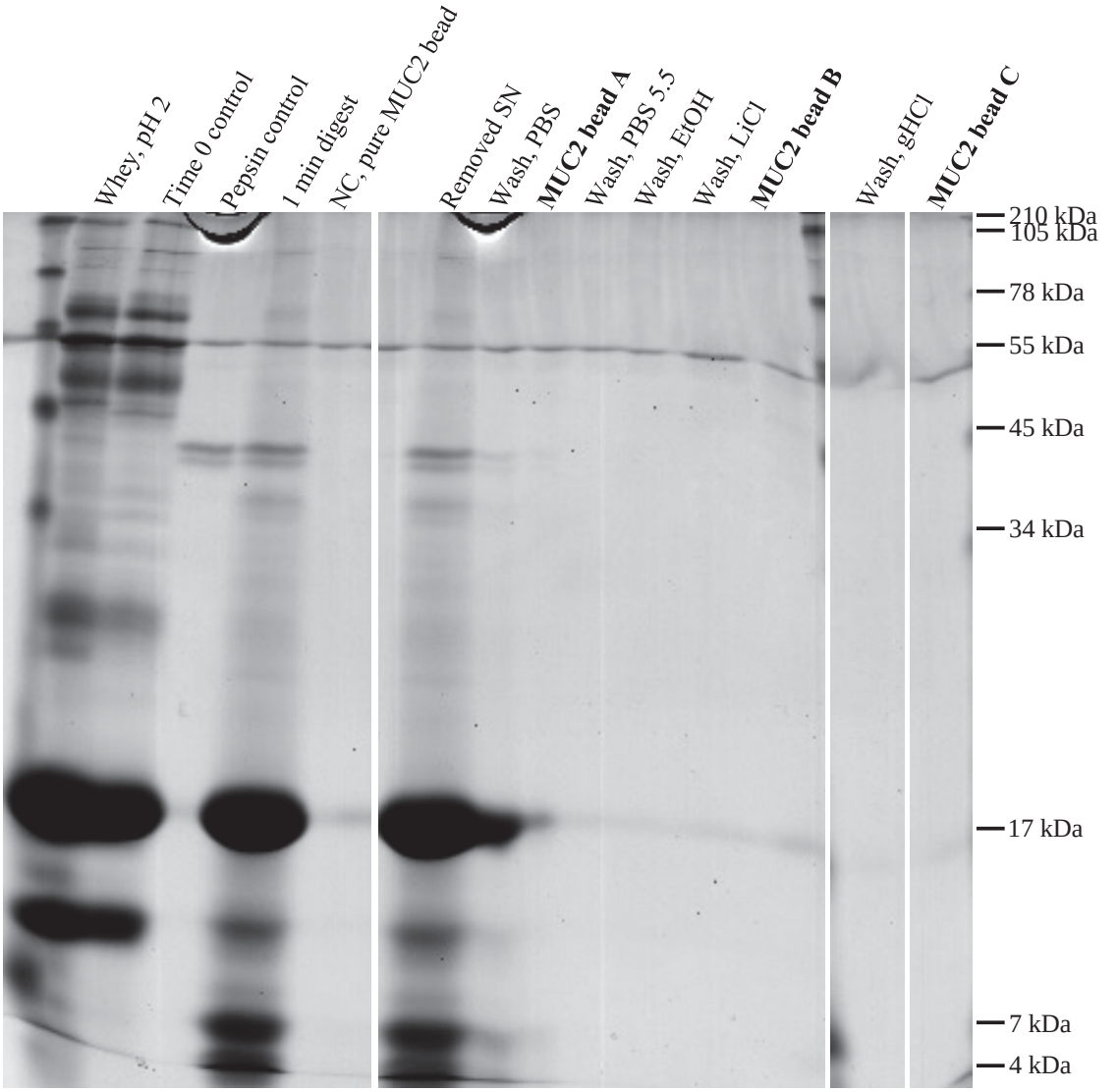

Figure 3.13: Adhesion assay between mucin-beads and digested whey; 12% acrylamide SDS-PAGE gel

Reducing SDS-PAGE gel, 12% acrylamide, of MUC2 covered Sepharose beads after incubation with 1 min digested whey. No EtOH-amine controls for beads A, B and C. Double volume of sample compared with pre-cast gels loaded onto gels in order to increase band intensities in wash solutions. Gel separated at 25 V overnight and stained with CBB G250 overnight. Bold font indicates samples that contain Sepharose beads (i.e. shows adhering proteins). NC: Negative control.

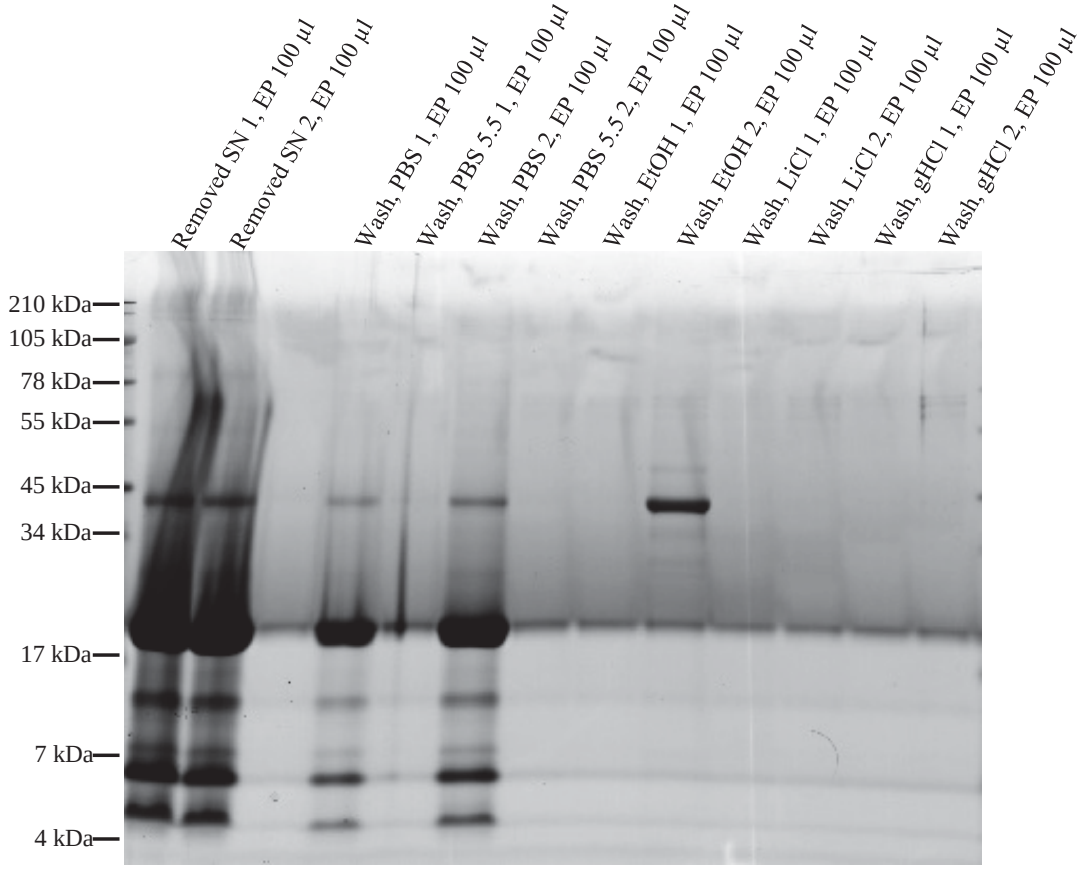

Figure 3.14: Adhesion assay between mucin-beads and digested whey, concentrated by EtOH-precipitation

Reducing SDS-PAGE gel of complete adhesion assay with EP of 100 µl wash solutions. Gel separated at 130 V for 2 hr and stained with CBB G250 overnight. NC: Negative control. EP: Ethanol precipitation.

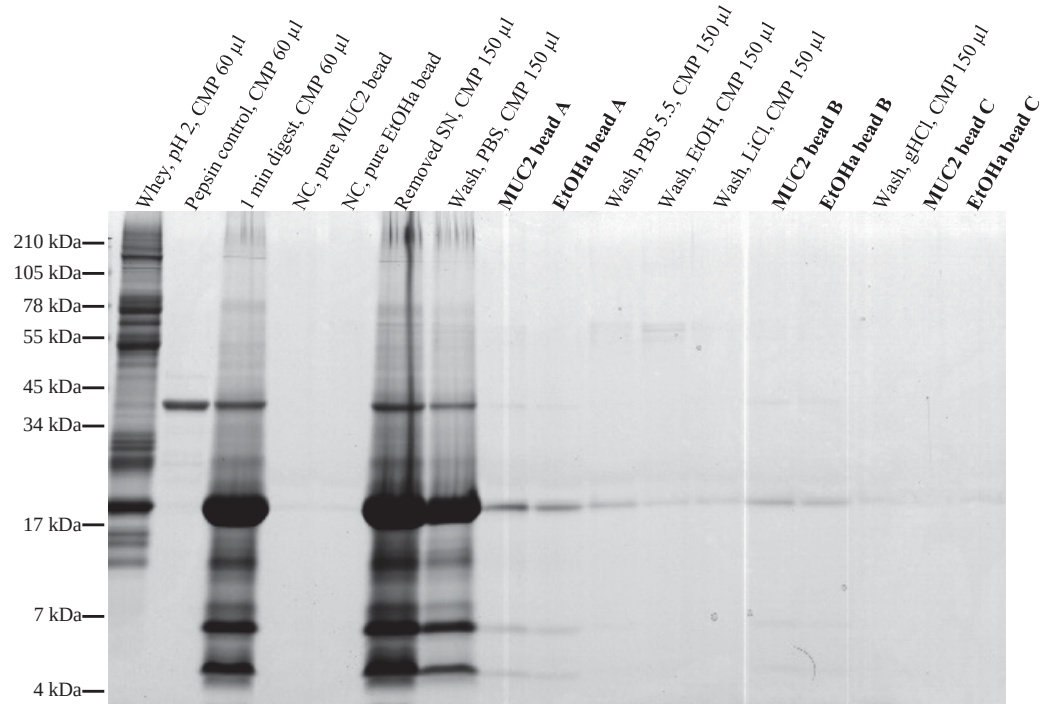

Figure 3.15: Adhesion assay between mucin-beads and digested whey, concentrated by CMP

Reducing SDS-PAGE gel of MUC2 covered Sepharose beads after incubation with digest mix (whey); Full adhesion assay with CMP of 100 µl wash solutions. Gel separated at 130 V for 2 hr and stained with CBB G250 overnight. Bold font indicates samples that contain Sepharose beads (i.e. shows adhering proteins). NC: Negative control. CMP: chloroform-MeOH precipitation.

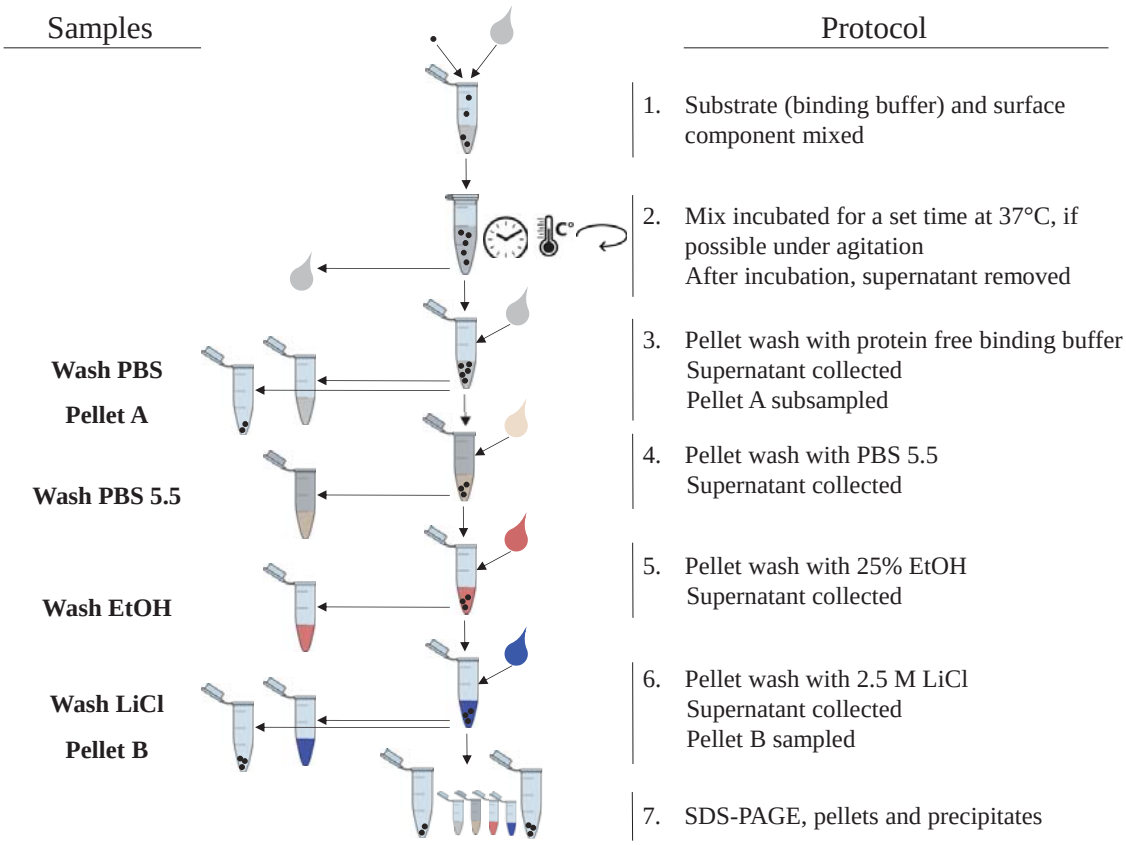

Figure 3.16: Scheme of the final adhesion protocol including sample preparation

Pellet A and pellet B in the figure are named “bead A” and “bead B” in samples with mucin coated Sepahorse beads, and “pellet A” and “pellet B” in samples containing bacterial cells or IEC. CMP: chloroform-MeOH precipitation. Precipitated samples are indicated by smaller tubes in the figure.

fold increase of protein load onto pre-cast gels. EtOH precipitation caused more streaking and also appeared to interfere with the EtOH wash (Figure 3.14 “Wash, EtOH2, EP 100 µl”). Thus CMP was considerd the more practicable method for further assays. Despite precipitation, only few bands at 18 kDa were observed in the wash solutions (Figure 3.15).

3.2.5 Final assay

The optimised adhesion assay protocol is presented as a flow chart in Figure 3.16.

3.3 Discussion

3.3.1 Whey and partial digestion

Comparing whey and whey by centrifugation shows differences in protein binding pattern (Figure 3.1). Most outstanding was the intense band at approximately 25 to 28 kDa in the whey by centrifugation which were casein residues that could not be removed by centrifugation. This band was weaker in whey made by acidification. The larger amount of casein in whey by centrifugation led to a decrease in band density of some other proteins. Overall the relative band intensities of whey proteins (all bands except casein) to each other appeared to be similar. Only

the bands between 65 and 80 kDa, but not LF, seemed to be weaker in whey by centrifugation. These bands represent milk fat globule membrane (MFGM) proteins and might have been removed from the whey more efficiently through repeated centrifugation. The initial decision to use whey was based on the aim to also explore the binding properties of minor whey proteins like Ig fractions or LF without predominant binding of caseins. Therefore, work was focused on whey which contained less casein.

The developed partial *in vitro* gastric digestion generated an array of proteins with various degrees of digestion as it might occur *in vivo*. This digest-mix was used for initial screening experiments (Chapter 4). The protein-to-enzyme ratio during whey digestion was 20:1. This is high, even considering an underestimation of whey protein concentration (comparison of Bradford analysis and DirectDetect results), compared with summarised data from Moreno et al.

[479] which calculates 0.13 mg pepsin per 1 g dietary protein (0.27 to 0.4 U per mg protein). This was balanced by the short incubation time of 30 sec to 1 min to achieve a mix of different degrees of digestion. During digestion, porcine pepsin, a product common for *in vitro* digestion experiments, as opposed to a human derived product (which is very difficult to obtain) was used. Despite being the same enzyme there could be a discrepancy in cleaving specificity between the two species. No information on bovine whey could be found, but Eriksen et al. [480] showed that no differences could be observed on SDS-PAGE gels between caprine whey digested by porcine pepsin and human gastric juices.

It was not determined whether this had an effect on the findings in this thesis, mostly because only early experiments were conducted with partially digested proteins. Later in the project, a shift in focus to only undigested whey took place which was mostly due to the fact that Western blot is more reliable using whole proteins as the fragments might be missing the recognising domain. Further, peptides could not be easily identified on SDS-PAGE gels because of reduced molecular weight (sometimes below the resolution of SDS-PAGE gels), and mass spectrometry analysis becomes less precise with decreasing length of the primary sequence. In addition, isolation of peptides would have started an extended block of experiments whereas whole proteins can be purchased readily purified; this was relevant for the flow cytometry studies. Taken together the greater knowledge about structure and adherence behaviour of undigested proteins made them the more suitable candidates. This decision has no detrimental effect on the next step of the thesis, which was the incorporation of adhering proteins into nutrient vehicle surfaces. Anchors can be protected from proteolytic attacks by an additional outer layer which is designed to dissolve quickly at the site of absorption only. Besides, assaying partially digested proteins under the assumption that the proteolysis generates new adhesion sites does not take into account that incorporation of the proteins into the vehicles might block the appropriate sites for enzyme activity and force new hydrolysis patterns.

3.3.2 Sepharose beads with mucin

Several attempts to quantify the mucin bound to the Sepharose beads were undertaken. The combined tests could not demonstrate that there was sufficient mucin layered on the surface of the beads. Some assays indicated that mucin was deposited onto the beads (2-D Quant Kit and confocal laser scanning microscopy). However, confocal laser scanning microscopy did not show the expected corona of mucin around the beads. This might be caused by the beads themselves and their potential opaqueness to the laser (Dr B. O'Brien, Waikato University, Hamilton, New Zealand, October 2012). Other assays did not detect any difference (LECO, alcian blue stain and WGA488 detection by plate reader). The Bradford assay was not used for mucin quantification as the glycoside side chains prevent the dye from accessing the protein backbone. Removing bound mucin from the beads for chromatographic analysis was also not feasible as complete stripping of the mucin was not likely to be achievable. Taken together, this suggests that some mucin was bound to the Sepharose beads, but no full coverage was achieved. An attempt to precipitate mucin and thereby increasing its density before coupling it onto the Sepharose beads was unsuccessful because precipitation is based on the pH-value. As the pH-value of the coupling buffer cannot be altered, the previously achieved increase in mucin density would be reversed with the start of the coupling procedure.

Another cause of concern was the degree of glycosylation of the Sigma commercial mucin preparation, which was only about 5% of the molecular weight (Prof. G. Jameson, Riddet Institute, Palmerston North, New Zealand, February 2015) with about 1% bound NeuNAc [481], and the mucin exists as stiff monomers (reviewed by Bansil and Turner [482]). Native mucin is about 95% glycosylated, with small intestine mucin being particularly high in NeuNAc residues [264, 483] – a functional group high in hydroxyl-endings. It has been shown before that the purification procedure from Sigma alters mucin properties like network formation [484]. Decreased glycosylation, as described by Glenister et al. [485], means that the PTS-domains (glycosylation sites) are bare and less primary amines or OH-groups are available for binding. This results in limited binding partners for the epoxy-groups from the Sepharose-beads. In

combination with “stiff” monomers (reduced network), which might cause steric shielding of epoxy-groups, this results in a reduced number of mucin molecules binding to the Sepharose-beads. Consequently, a complete coverage of the beads’ surfaces by mucin was difficult to achieve. This causes a problem as milk proteins like LF and IgM are known to bind to Sepharose [32, 445], which can create false positive results. To avoid these, two new concepts for conducting the adhesion assay were attempted. Sepharose-bead free approaches using well-plates (96 wells, maxisorb, Nunc™, Sigma Aldrich) and a liquid assay using high cut-off dialysis membranes (data not shown) were explored. Unfortunately, both assays had their own difficulties, namely the inability to fix the mucin to the wells and insufficient separation of unbound proteins. Due to time restrictions these assays were not continued.

For future investigation of muco-adhesion, a mucin particle adhesion assay or BIACORE [308, 486] is of interest. These methods still need to be tested and compared with cell culture experiments. BIACORE delivers indirect results based on surface plasmon resonance, and the output of the mucin particle adhesion assay is a change in zeta-potential. These are indirect results and further, the evaluation of only one type of protein is possible at a time as neither method can identify what type of molecule caused the change in signal. The BIACORE assay could be adapted to other coatings by preparing respective chips; however this would come at a cost. One of its advantages is that the BIACORE allows the measurement of binding affinities [487]. In contrast, and as the name suggests, the mucin particle adhesion assay is based on mucin, specifically its physicochemical properties in solution, and it is not easily transferable to other (macro)molecules. Coated Sepharose beads are still the method of choice if the coating molecules bind well to the beads, cover the whole surface, and if the expected ligand shows little or no adherence to Sepharose beads. The advantage of coated beads over the other two methods (mentioned above) is that the beads could be prepared for SDS-PAGE analysis and thus allows direct results and identification (using Western blot or mass spectrometry) of binding molecules.

3.3.3 Adhesion assay

The developed adhesion assay consists of two phases; initially an incubation to allow adhesion followed by a wash cycle to sequentially remove bound molecules. The first wash step is the removal of all unbound material with a buffer which has the same composition as the binding buffer but does not contain any proteins. This is followed by a wash buffer simulating a small intestinal environment with decreased pH and decreased ionic strength. The last phase of the wash cycle is made up by a wash with 20% EtOH followed by 2.5 M LiCl, both in the post-prandial washing buffer. These are of analytical nature and target specific types of interactions. The EtOH removes molecules adhering through hydrophobic interactions and the LiCl weakens ionic interactions between food molecules and the small intestinal layer component. Using a batch type experimental set up, for example using Eppendorf tubes or well plates, samples can be taken at any time for analysis. Technically, an assay was developed which contains a number of steps to replicate aspects of the digestion process. However, it will take testing of the assay in further experiments (such as subsequent chapters) to demonstrate its performance.

The protocol was optimised for liquid whey and milk and will need to be adapted to the food and its composition (e.g. calcium content [41]) or types (e.g. meat, grains). These changes will also affect the composition of the binding buffer which needs to take into account demands from the surface model and the food while maintaining the small intestinal binding environment. While the binding buffer initially used in this thesis resembled a small intestinal environment (Table 3.1), the results with PBS as binding buffer were comparable (data not shown). Thus PBS was used in the subsequent experiments. The whey and milk used here introduced ions such as Ca^{2+} (mucin-binding [41]) into the binding buffer. However, other foods may not provide respective binding mediators (e.g. Ca^{2+}) and researchers should determine these factors and decide whether they need to be supplemented. Finally, the effect of the wash solutions on the integrity of intestinal surface layer components needs to be considered. For example, surface proteins can be denaturated by EtOH or extracted by LiCl. As a consequence,

and if it appears reasonable one should focus on generally adhering proteins (bead / pellet A), as opposed to proteins that might be removed by specific wash solutions, like in Chapters 5 and 6.

3.4 Conclusion

This chapter describes the development of a partial gastric *in vitro* digest of liquid protein preparations and a subsequent adhesion assay. Both, the digest and adhesion assay were optimised and can be used as guidelines for further adaptations, e.g. for meat or grain products. Further, mucin covered Sepharose beads were prepared, however the degree of mucin coverage could not be determined.

The developed assay provided a tool to screen for food components which adhere to one specific layer of the human intestinal surface.

Chapter 4 Interactions between whey or milk proteins and mucin-coated beads

Whey and milk proteins adhering to mucin covered beads

4.1 Introduction

The mucus in the intestinal tract consists of approximately 95% water. Approximately 1 to 10% of the remaining 5% (matter) comprises mucin polymers (molecular weight up to 10 MDa [263]). Electrolytes, proteins, trefoil-peptides, antibodies and nucleic acids are other components contained in the mucin network [88, 262]. Lafitte et al. showed that the barrier efficiency of this network and also the diffusion rate is determined by size, charge, and physicochemical properties of the nutrient molecule [488]. Mucins are highly sialated, gel forming glycoproteins which are crucial for the viscoelasticity of the mucus layer throughout the intestinal tract [160, 173, 200, 265, 266] (Figure 4.1 (A)). The mucin concentration in pig duodenum is about 30 $mg.ml^{-1}$ (2 to 3% w/w) [478]. The strong negative charges of glycoside termini, due to NeuNAc and ester sulphate, [157, 304, 489] influence the overall interaction characteristics of mucin (Figure 4.1 (B)). NeuNAc is often the terminal monosaccharide in the oligosaccharide chain attached to the protein backbone. It is a relatively strong acid (pK_s=2.6) and completely deprotonated at physiological pH-value [304, 305]. Thus it generates an acidic micro-environment around mucin-glycoside tips.

Mucin has been the subject of food interaction studies for over 30 years. Muco-adhesive properties *in vitro* were shown for polymers, e.g. chitosan, using a BIACORE device [308, 309] or in oral delivery studies [310]. Further, lectins, like wheat germ agglutinin or soy bean agglutinin, can be used as mucin adhesives [311, 312]. The pectin-polymer group [313] and some chatechins, tea polyphenols, were also found to bind to different mucins or act as cross-linking agent [40]. Most likely, the presence of a gallyol ring plays a vital role in the latter interaction as epigallocatechin gallate but not epicatechin seems to show this behaviour [314].

However, there have been only few studies describing the adherence interactions between food components and mucin in the intestinal tract. None of them have investigated milk derived proteins. It is desirable to gain this information, especially as it was shown recently that the mucin layer is thicker *in vivo* than predicted from *in vitro* experiments [91, 267]. This makes the mucin layer a more important player when it comes to adhesion of targeted delivery vehicles in

A

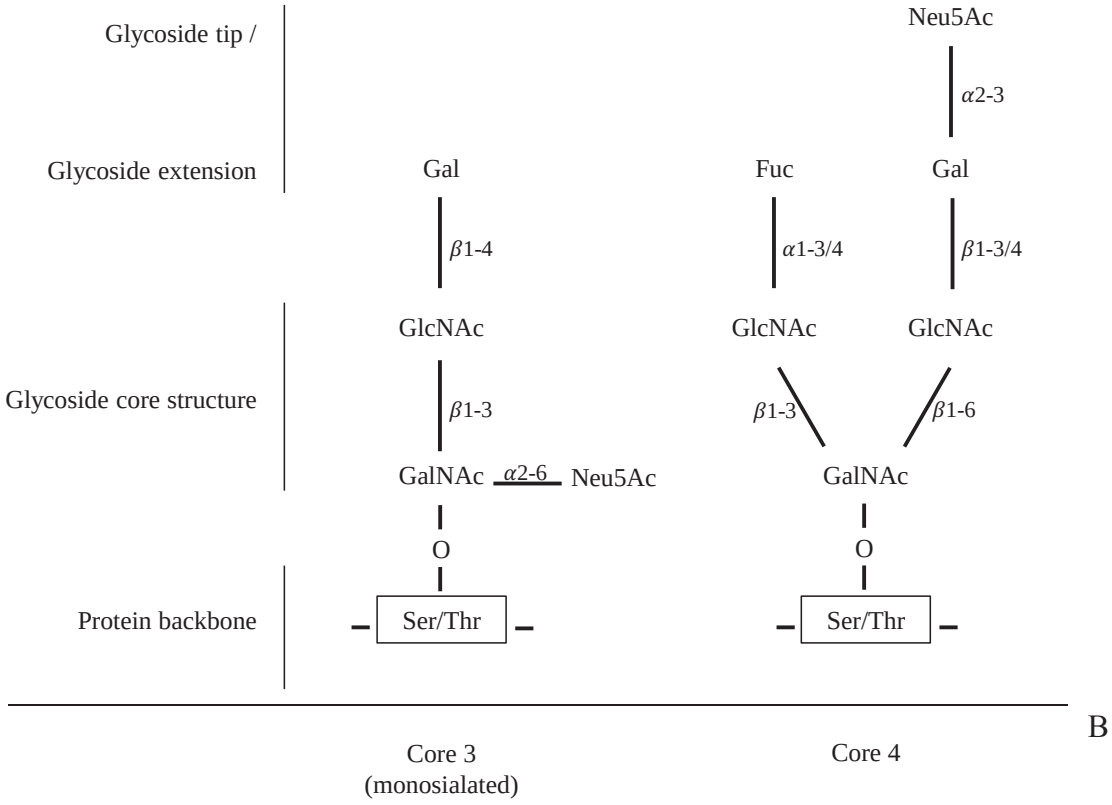

B

Figure 4.1 A and B: Representative models of the mucin network and glycoside side chain composition

(A) Model of the mucin glycoprotein network, showing the potential to form three disulphide-bridges at the N-terminus (left and right edge of the schematic) and one disulphide-bridge at the C-terminus (center of the schematic). The protein backbone is shown in red, the glycoside side chains attached to the central PTS-domains in green [490]. (B) Representative structure of mucin glycoside side chains. Core 3 typically occurs in the human small intestine, while the mucins in the colon are of type 3 or 4. Here, core 3 is monosilated. Extenstions are attached to the core structure and can be Galactose (Gal), GlcNAc, GalNAc, Fucose (Fuc) and sialic acid (NeuNAc). Fuc and NeuNAc typically are terminal groups. The glycoside chains are modelled after Tailford et al. [491]. Structures are representative and do not show all described structures.

the intestinal tract. Dairy proteins are of particular interest as functional food delivery system components because they are food grade molecules which have a healthy image and are readily available.

4.1.1 Hypothesis and aims

The main research hypothesis of this chapter is that milk proteins differ in their adhesive properties and that some of them adhere to small intestinal mucin. Therefore, this chapter aims to screen milk and whey for muco-adhesive proteins as described in Chapter 2, Section 2.4.1. Proteins of interest will then be identified by liquid chromatography tandem mass spectrometry (LC-MS/MS) and results validated by Western blot analysis as described in Chapter 2, Section 2.5.

4.2 Results

4.2.1 Milk

4.2.1.1 Skim milk

Once all individual parts of the assay were optimised (duodenal conditions, adhesion period, wash cycle, and chloroform-MeOH precipitation of wash solutions), a complete adhesion assay with partially digested skim milk was conducted and a complete sample set was analysed on reducing SDS-PAGE gels (Figure 4.2). In parallel, an assay with undigested skim milk was conducted (Figure 4.3). Samples loaded onto the gels were wash solutions and beads from assays with MUC2 covered beads and EtOH-amine beads which served as negative control.

A direct comparison between respective samples from MUC2 beads and EtOH-amine beads showed that some proteins from skim milk bound differently to the two types of beads (different band densities for corresponding bands in Figure 4.3). More affinity for the mucin beads was observed for the bands at 80 kDa, 70 kDa and 50 kDa. Proteins with molecular weight under 40 kDa showed decreased binding to mucin-covered beads compared with the negative control (e.g. 29 kDa, 25 kDa or 18 kDa). Some bands were analysed with LC-MS/MS, these were marked with black boxes. A comparison of the protein bands in the wash solutions suggests that

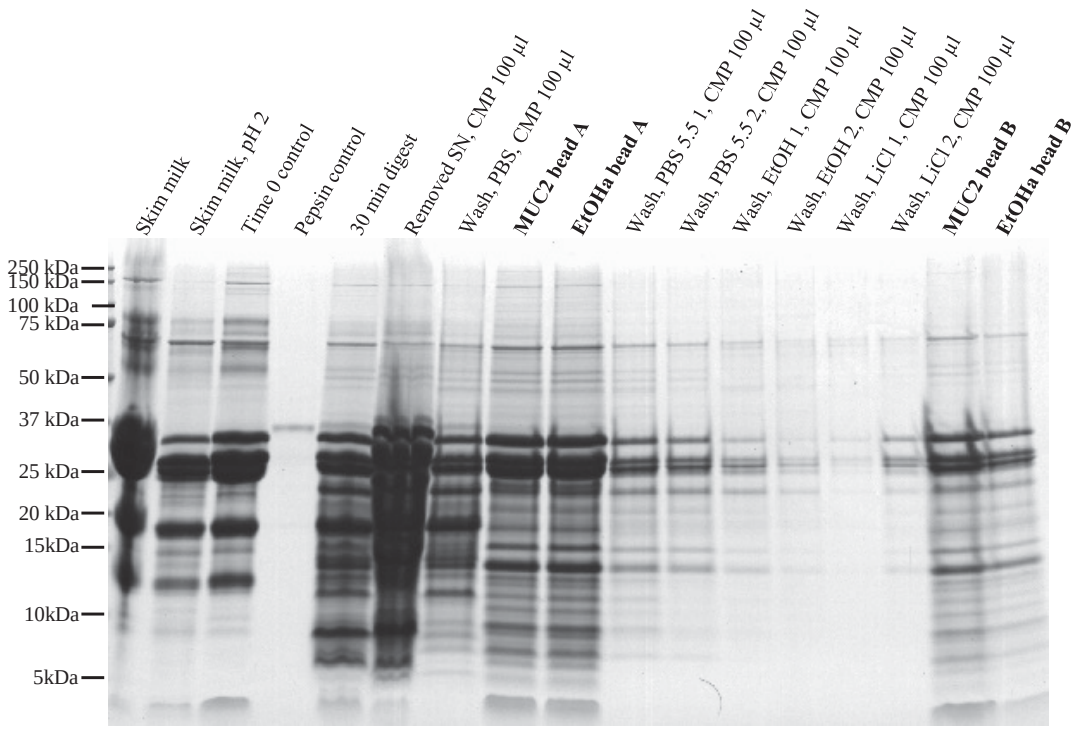

Figure 4.2: Adhesion assay between mucin-beads and digested skim milk

Reducing SDS-PAGE gel of MUC2 covered Sepharose beads after incubation with digested skim milk. Full adhesion assay with CMP of 100 µl wash solutions. Gel separated at 130 V for 2 hr and stained with CBB G250 overnight. Bold font indicates samples that contain Sepharose beads (i.e. shows adhering proteins). CMP: chloroform-MeOH precipitation.

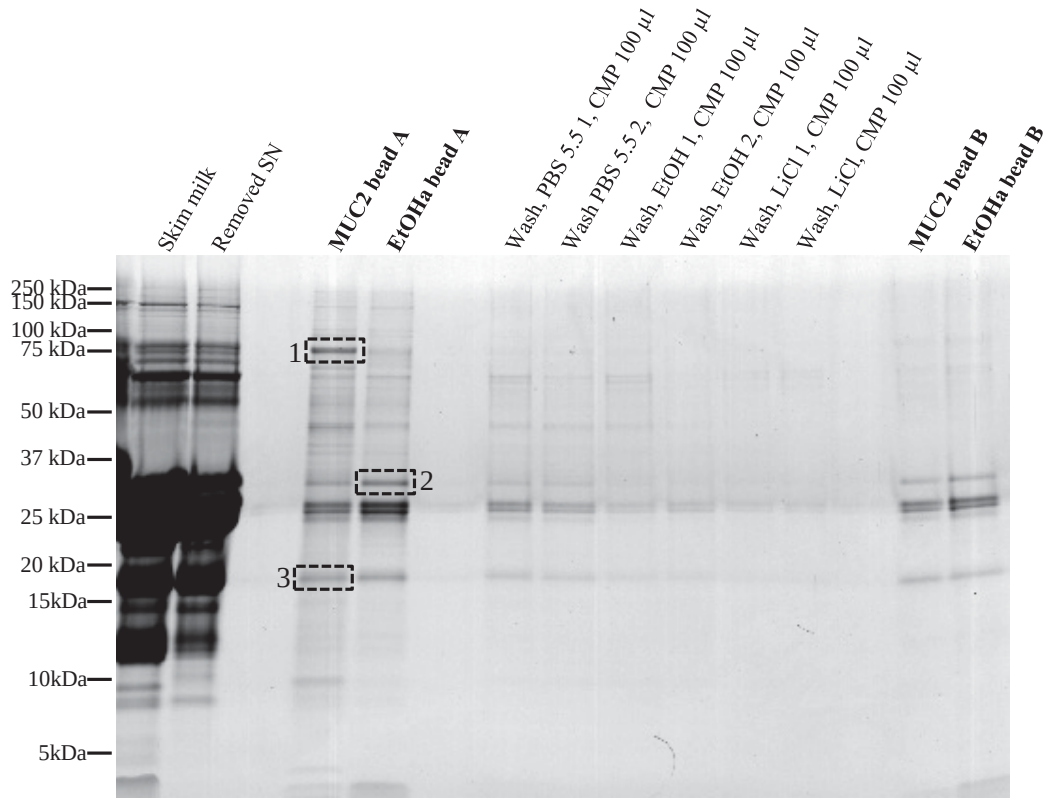

Figure 4.3: Adhesion assay between mucin-beads and skim milk

Reducing SDS-PAGE gel of MUC2 covered Sepharose beads after incubation with skim milk. Full adhesion assay with CMP of 100 µl wash solutions. Gel separated at 130 V for 2 hr and stained with CBB G250 overnight. Dashed black boxes represent bands which have been cut out for LC-MS/MS analysis. Bold font indicates samples that contain Sepharose beads (i.e. shows adhering proteins). CMP: chloroform-MeOH precipitation.

the dominant effect was of a more physical than chemical nature as no change in band pattern was observed. Proteins that remained on the mucin coated and also negative control beads after the wash cycle had molecular weights between 29 kDa and 14 kDa and probably represent caseins and major whey proteins. Band patterns in bead B samples showed no differences. Also no differences in band pattern or relative intensity of adhering proteins were observed for digested skim milk (Figure 4.2). Generally, the protein band pattern observed in the input material was comparable to that found in beads A and B. Thereby, no difference was observed between respective mucin coated and negative control beads. The only difference observed between input material and proteins adhering to beads was the band at 18 kDa (possibly β-LG). This observation will be discussed in more detail in Section 4.2.1.4. All experiments indicated that there was a considerable amount of protein being washed away with PBS 5.5. This was more likely to be due to the process of washing the beads rather than the reduced pH-value and ionic strength compared with PBS. This was parallel to observations in wash-solution gradients (data not shown).

For skim milk several assays were conducted and a SDS-PAGE gel was prepared to assess the reproducibility between experimental days (Figure 4.4). Some proteins, especially molecular weight of 50 kDa and 18 kDa and under, were enriched on the MUC2. These results are in contrast to those observed in Figure 4.3. A possible reason is that a new batch of mucin coated beads was used, further emphasising the difficulties experienced to obtain reproducible results for muco-adhesion using the mucin coated Sepharose beads.

4.2.1.2 Whole milk

The band patterns of whole milk proteins binding to mucin covered and negative control beads were almost identical (shown in Figure 4.5). Major bands were observed at 24 kDa to 29 kDa (possibly caseins) and at 18 kDa (possibly β-LG) and five faint bands between 40 kDa and 80 kDa, while no band at 14 kDa (α-LA) was detected on the beads. The only observable difference was three to four faint bands in the high molecular weight region (ca. 150 kDa to 250 kDa) which appeared to be more intense in the mucin covered beads. Corresponding proteins

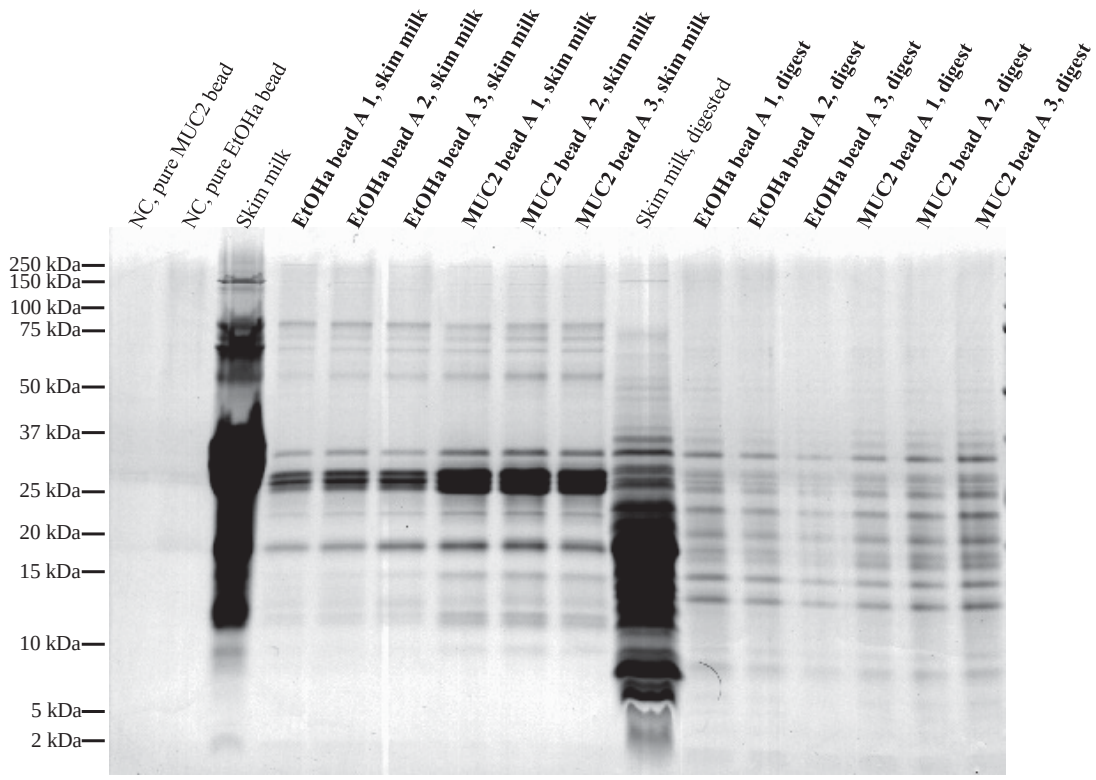

Figure 4.4: Reproducibility of the adhesion assay between mucin-beads and digested or undigested skim milk

Reducing SDS-PAGE gel of MUC2 covered Sepharose beads after incubation with skim milk and digested skim milk. Only beads A and B to test reproducibility. Gel separated at 130 V for 2 hr and stained with CBB G250 overnight. Bold font indicates samples that contain Sepharose beads (i.e. shows adhering proteins).

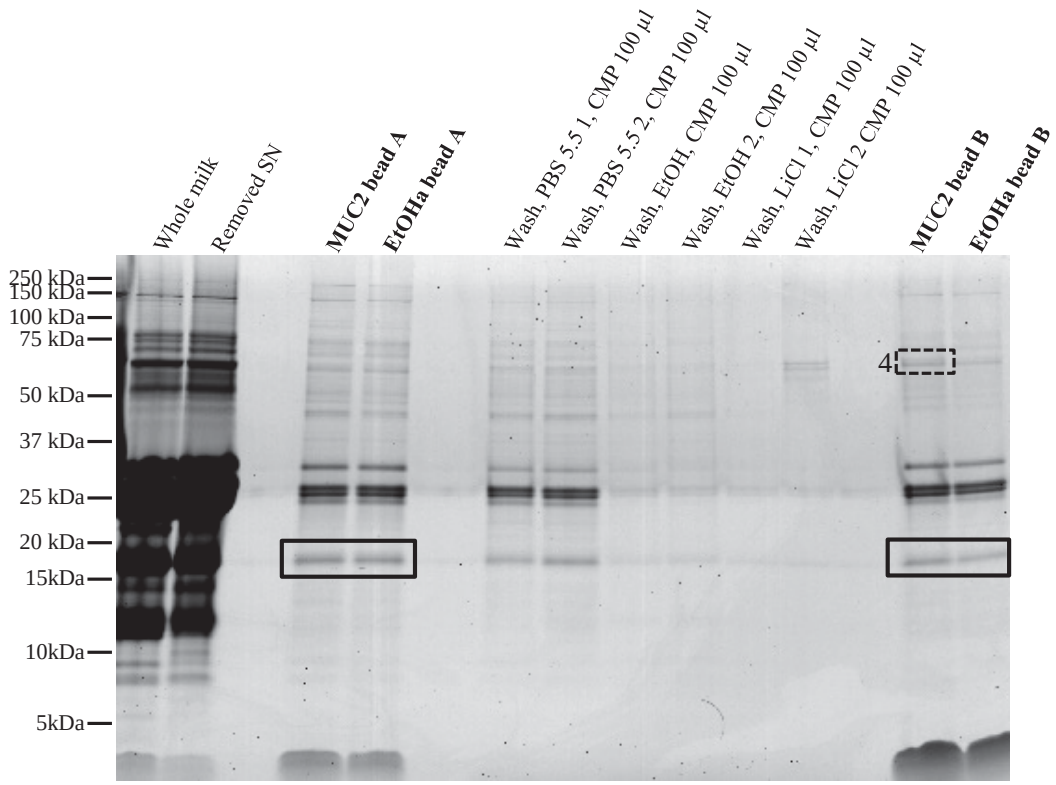

Figure 4.5: Adhesion assay between mucin-beads and whole milk

Reducing SDS-PAGE gel of MUC2 covered Sepharose beads after incubation with whole milk. Full adhesion assay with CMP of 100 µl wash solutions. Gel separated at 130 V for 2 hr and stained with CBB G250 overnight. Dashed black boxes represent bands which have been cut out for LC-MS/MS analysis. Solid black box indicates β-LG bands Bold font indicates samples that contain Sepharose beads (i.e. shows adhering proteins).

Table 4.1: Mass spectrometric identification of selected adhering milk proteins

Bands are indicated in Figure 4.4Figure 4.3 and Figure 4.5.

MW: Molecular weight. Peptide hits: Peptide identifications per MS/MS spectrum [492].

#	MW excised	Protein identified as	Peptide hits	MW theoretical	Substrate
1	75 kDa	---	---	---	Skim milk
2	37 kDa	α_{S1}-casein	3	23.6	Skim milk
3	18 kDa	β-lactoglobulin S100 A9	5 3	18.3 16.4	Skim milk
4	75 kDa	β-lactoglobulin Ca-binding L1 complex	8 4	18.3 13.7	Whole milk

from skim milk showed limited adherence (Figure 4.3) or were less abundant in skim milk. This suggests that these proteins had a higher binding potential when they were derived from whole milk. However, one cannot exclude that the whole milk milieu, e.g. phospholipids, supported adherence of proteins, especially more hydrophobic ones. On the other hand, proteins that were observed to bind from skim milk to mucin (e.g. 80 kDa or 50 kDa) did not show adherence from whole milk. The difference in binding might be due to changes in total protein composition (i.e. MFGM proteins), the protein conformation or charges during separation, or the change in milk composition through removal of low density components. The latter might imply an adherence mediating effect of these low density fractions, like fat or phospholipids. This question could be addressed through experimental set-ups with cream or other MFGM enriched fractions.

4.2.1.3 Mass spectrometric identification of adhering milk proteins

LC-MS/MS analysis was performed to identify proteins of interest from skim milk (Figure 4.3) and whole milk (Figure 4.5). Bands were excised from SDS-PAGE gels of MUC2 covered beads and EtOH-amine beads. The latter were selected if the band of interest was more dominant in these samples than in the respective MUC2 samples. The results are listed in Table 4.1. Proteins with the highest peptide hits were α_{S1}-casein and β-LG. The band excised at 75 kDa from skim milk could not be identified. The identification of band #4 (75 kDa) as β-LG might be wrong as β-LG appeared to have a tendency to stick to the column (observation) and thus bias the following sample.

4.2.1.4 Western blot analysis

Western blot analyses were performed to validate the LC-MS/MS results. The antibodies used represented the proteins which had the highest peptide scores. The results for β-LG are shown in Figure 4.6. In whole milk derived samples, the protein band was stronger in samples from MUC2 beads than in those from EtOH-amine (negative control). This suggests binding of β-LG from whole milk to MUC2. However, this data needs to be considered carefully as the Western blot analysis was performed only once (insufficient mucin coverage of the Sepharose beads).

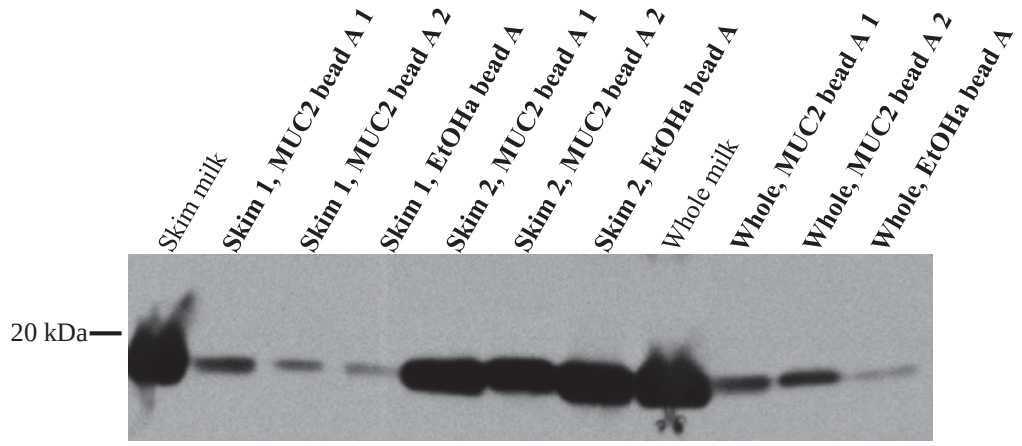

Figure 4.6: Western blot for β-LG on beads A after incubation of mucin-beads with skim and whole milk

Western blot for β-LG of MUC2 covered Sepharose beads after incubation with skim milk (two experiments) and whole milk (one experiment). One or two repetition(s) of bead A only (MUC2 bead A 1 and A 2 indicate two repetitions of the same experiment). Gel separated at 130 V for 2 hr, transfer overnight at 15 V, 3 hr block with 4% NFM, 2 hr primary antibody, 1 hr secondary antibody (GAR) and 2 min exposure after ECL. Bold font indicates samples that contain Sepharose beads (i.e. shows adhering proteins).

Also, the described difference was not observed in the corresponding SDS-PAGE gel (Figure 4.5) where β-LG from whole milk gave equally strong signals in MUC2 and negative control beads (relevant bands are highlighted in a solid box). Results from skim milk samples were ambiguous and did not show any consistent difference between the two types of beads. While the bands from "skim 1" samples were more intense for MUC2 beads than for the negative control, the opposite was the case for "skim 2".

A Western blot probing for α_{S1}-casein did not show any bands in the samples (data not shown). Probing skim milk derived samples with pseudo-milk antibodies (raised against a mix of purified α-LA, β-LG, κ-casein, β-casein, α-casein) and LF antibodies showed what appeared to be binding of the casein-fraction (25 to 34 kDa, undigested and digested skim milk) and β-LG (18 kDa, undigested skim milk) to the beads (Figure 4.7). α-LA did not show any signal, even in the positive control (skim milk). LF gave a signal (ca. 80 kDa) in skim milk (positive control) and faint corresponding bands were observed in some of the of the MUC2 bead samples indicating that LF showed low degree binding to the beads. Further, the intact protein was not present after digestion with pepsin. The proteins from undigested skim milk (left part of the blot) with molecular weight 29 kDa and 18 kDa (strong bands), likely α_{S1}- and β-caseins and β-LG, did show slightly more intense bands in the mucin-beads than in the negative controls, indicating binding. Further, two weak bands at about 34 kDa and 25 kDa were observed only in the mucin bead derived samples. These were also likely to be caseins.

A fragment of about 37 kDa was produced during partial pepsin digestion of skim milk (right part of the blot). It showed binding to mucin covered beads but not to the negative control (relevant bands are highlighted in a solid box). The other proteins or fragments (ca. 34 kDa, 29 kDa and 25 kDa) from partially digested skim milk showed binding to mucin covered and negative control beads, but no difference could be quantified (data not shown). The three adhering proteins or fragments had the same molecular weight as proteins, probably caseins, that showed binding from undigested skim milk. This suggests that the bands represent proteins with a low level of digestion or remaining undigested caseins. However, the proteins from the

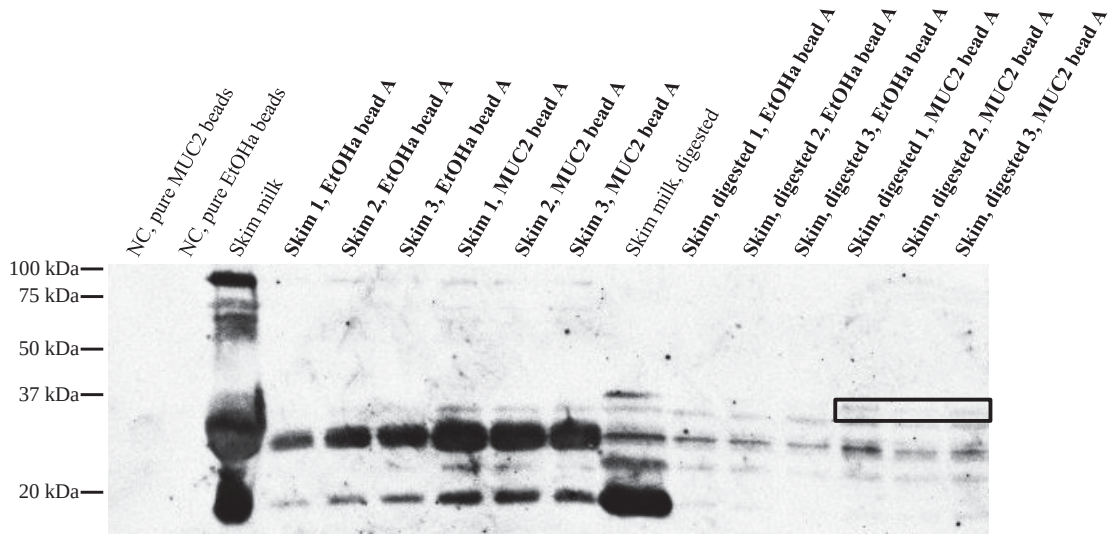

Figure 4.7: Western blot for LF and pseudo milk (α-LA, β-LG, κ-CN, β-CN, α-CN) on beads A after incubation with skim and digested skim milk

Western blot for LF and pseudo-milk of MUC2 covered Sepharose beads after incubation with skim milk and digested skim milk. Three repetitions of beads A are shown. Gel separated at 130 V for 2 hr, transfer overnight at 15 V, 3 hr block with 4% NFM, 2 hr primary antibody, 1 hr secondary antibody (GAR) and 2 min exposure after ECL. Solid black box indicates ca. 37 kDa fragment binding only to MUC2 covered beads. Bold font indicates samples that contain Sepharose beads (i.e. shows adhering proteins).NC: Negative control.

undigested skim milk bound only (34 kDa and 25 kDa) or better (29 kDa) to mucin covered beads but not to the negative control, indicating muco-adhesion. Thus it is likely that the partial digestion with pepsin decreased the binding potential of those three proteins. β-LG was notaffected by pepsin digestion (strong 18 kDa band in digested skim milk). However, β-LG in milk after pepsin treatment did not bind to the mucin covered or negative control beads. A possible reason for this could be blocking of binding sites (on the beads and the β-LG molecule) by peptides of other proteins. This would allow intact β-LG to be detected in the input material (digested skim milk) but β-LG could not adhere to the beads and was washed off before the samples were prepared in SDS-PAGE sample loading buffer. It is further possible that binding site(s) on the β-LG molecule are compromised through digestion. However, the exact mechanism is yet to be determined, involving isolated β-LG and partial gastric digest thereof.

4.2.2 Isolated protein solutions

After LC-MS/MS identification of proteins of interest from skim milk and whole milk, candidate proteins and further available milk proteins were applied as solutions of isolated proteins to test specifically for their adhesive properties: LF digested; β-LG heat denaturated and β-LG digested; quiescin sulfhydryl oxidase digested and quiescin sulfhydryl oxidase undigested; free secretory component digested and free secretory component undigested; α-LA undigested as potential negative control protein; and α-LA and β-LG undigested combined (introduced later). These experiments showed that proteins adhered better as isolates than in mixture, maybe due to the lack of competition (β-LG and α-LA shown as examples in Figure 4.8). α-LA and β-LG seemed to bind equally to the mucin covered beads from a mixture of pure α-LA and β-LG (Figure 4.9), further both proteins showed adhesion to mucin and negative control beads. Most likely, β-LG was not a competitor to α-LA binding as α-LA binding in this experiment was better than in experiments with milk (Figure 4.4 or Figure 4.5). Thus, in order to have a realistic competitive environment as it might occur after ingestion of food, adhesion of individual proteins was tested by conducting adhesion tests with complex mixes (whey, milk or digests thereof) followed by analysis with Western blot for specific proteins of interest.

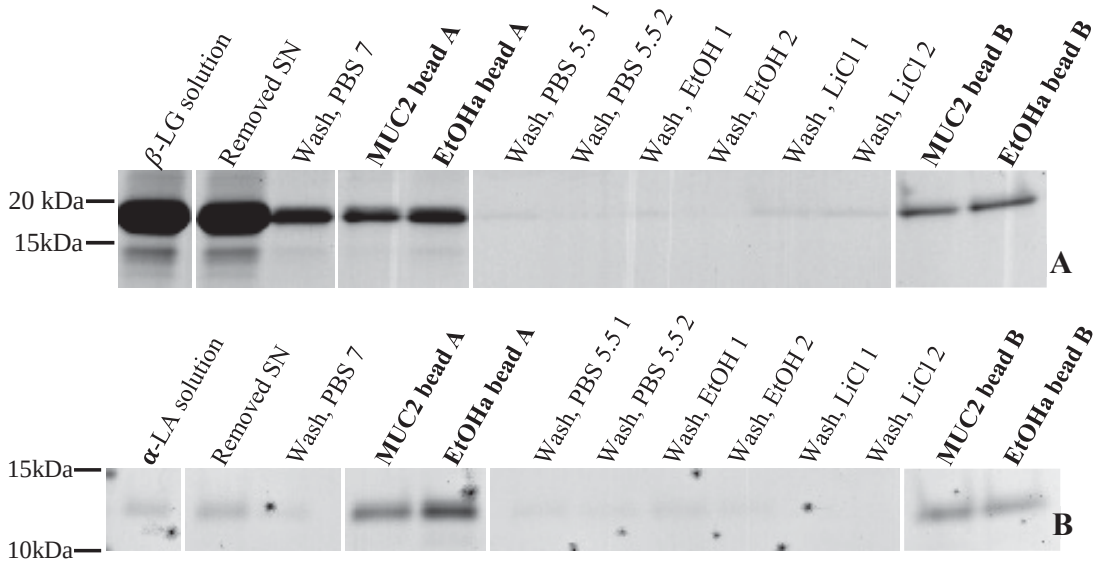

Figure 4.8: **Western blot for (A) β-LG and (B) α-LA on beads A after incubation with isolated β-LG and α-LA**

Reducing SDS-PAGE gel of MUC2 covered Sepharose beads after incubation with purified (A) β-LG or (B) α-LA. Full adhesion assay with CMP of 100 µl wash solutions. Bands assembled from the same gel, respectively. Gel separated at 130 V for 2 hr and stained with CBB G250 overnight. Bold font indicates samples that contain Sepharose beads (i.e. shows adhering proteins). Dots in (B) are artefacts as gel could not be scanned immediately.

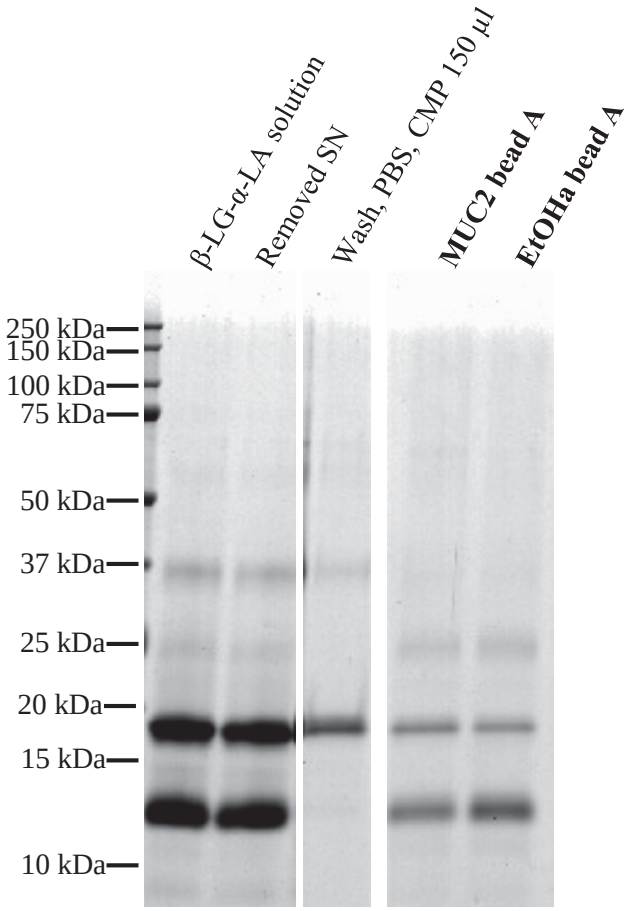

Figure 4.9: Adhesion assay between mucin-beads and a β-LG and α-LA mix solution

Reducing SDS-PAGE gel of MUC2 covered Sepharose beads after incubation with β-LG and α-LA mix solution (5 $mg.ml^{-1}$ each). Bands assembled from the same gel of an adhesion assay. Where indicated, CMP of 150 µl was loaded; other samples were 1:1 diluted with SLB. Gel separated at 130 V for 2 hr and stained with CBB G250 overnight. Bold font indicates samples that contain Sepharose beads (i.e. shows adhering proteins). CMP: chloroform-MeOH precipitation.

4.2.3 Whey and whey sediment

The whey used in the adhesion test was produced by acidification of skim milk. Therefore skim milk was acidified with HCl and filtered through a cheese cloth to separate the curd from whey. Then the whey was clarified by centrifugation to remove casein fines and the pH of the clear whey was adjusted to pH 6.8. The whey was centrifuged again to remove calcium phosphate that became insoluble through the change in pH. The whey was frozen until it was used for the adhesion assay.

After the initial experiments (Chapter 3), a whey only control (whey in a tube without beads) was included in the adhesion test to monitor what happens to the whey alone during the test. After the first centrifugation step it became apparent that the whey contained a considerable amount of sedimentable products which co-purified with the binding proteins during the wash cycle. To test if those sediments were responsible for the protein bands in SDS-PAGE gels of MUC2- and EtOH-amine beads A, the assay with whey was repeated. Figure 4.10 shows that the bands which were thought to represent adhering whey proteins in some initial optimisation experiments (Figure 3.12) were insoluble material which sedimented in the tube (also Figure 3.13 to Figure 3.15 were potentially affected). Protein bands in the sediment had molecular weights of 14kDa, 18 kDa, 24 to 29 kDa and several bands between50 kDa and 80 kDa and around 150 kDa. Thus in order to obtain unbiased adhesion results from whey proteins, the sediment needed to be removed from the whey.

4.2.3.1 Description of whey sediment

The sediment in whey showed as a white pellet in the bottom of the tube after centrifugation. It was insoluble in PBS and its protein composition is illustrated by SDS-PAGE analysis in Figure 4.11. The protein bands from the original whey and in the sediment were similar in the higher molecular weight region (>50 kDa), especially after the PBS washes (wash, PBS 1 and 2). Corresponding bands could be observed, but in different intensities; the two bands around 75 kDa were comparably strong in the sediment, whereas the band at approximately 60 kDa was more intense in the original whey. Three to four bands between 20 kDa and 30 kDa were

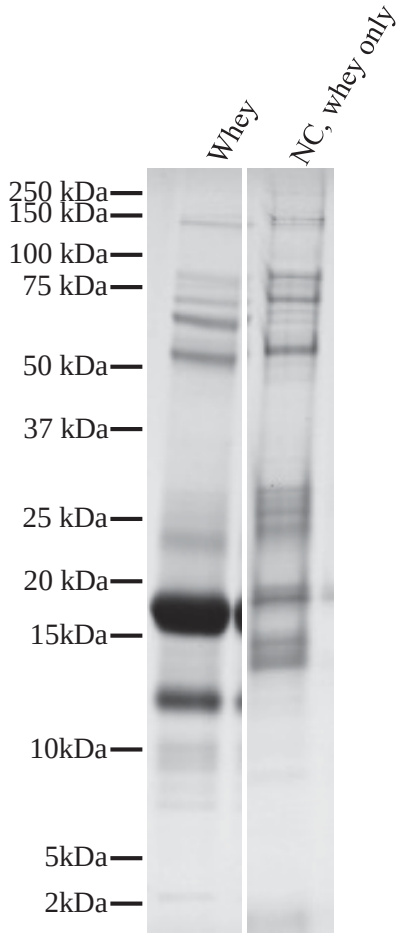

Figure 4.10: Comparison whey or whey sediment observed during the adhesion assay

Reducing SDS-PAGE gel of whey and the negative control (NC) tube for bead A to test if proteins detected in previous samples are actually adhering proteins or only sedimented residues which have not been removed completely. Bands assembled from the same gel. Gel separated at 130 V for 2 hr and stained with CBB G250 overnight. NC tube: Tube contained only whey, no beads, but was treated like bead containing samples during the adhesion test, i.e. incubation at 37°C, centrifugation and removal of supernatant. Protein bands observed in this negative control are contained in the pellet that formed during centrifugation.

observable in the sediment. The same bands were visible in the whey, but less intense. The dominant band at 18 kDa in the whey was less dominant in the sediment and its intensity was comparable to that of other bands in the sediment. The most notable observation was the absence of α-LA in the sediment. Finally, bands for proteins or fragments with molecular weights under 14 kDa did not show common bands in the whey and the sediment.

4.2.3.2 Analysis of whey sediment

Sedimentation was further observed to occur upon mixing with PBS and also after previous freezing and thawing treatment (observation). In order to determine if any of the PBS components (Figure 4.12) or wash solutions (EtOH and LiCl, Figure 4.11) caused sediment formation, whey was incubated with the individual salts or solutions. Figure 4.12 shows that adding NaCl to whey reduced the amount of sediment (Figure 4.12, lane 5). The other salts (Na_2HPO_4, KH_2PO_4 and KCl, lanes 3, 4 and 6) also reduced sediment formation but less efficiently than NaCl. In contrast, the addition of phosphate buffer (pH 7.4, lane 7) increased the amount of sediment compared to the sediment formed in untreated whey (Figure 4.12, lane 1). This suggested that sediment formation was pH dependent and accelerated at higher pH values. The effect of the wash solutions on sediment formation was less pronounced, and only LiCl appeared to reduce sediment formation (Figure 4.11). It was hypothesised that the sediment consisted of calcium phosphate ($Ca_3(PO_4)_2$), which slowly started to precipitate after re-adjusting of the pH value of the whey to pH 6.8.

4.2.3.4 Treatments to remove the sediment from whey

To eliminate the sediment from whey, either the sediment needed to be re-solubilised or removed. Calcium phosphate is insoluble under the conditions (i.e. pH, temperature or ionic strength) of this study. Thus removing the sediment from the initial whey was considered a more feasible approach. This was supported by the observation that the clear supernatant (Figure 4.12, lane 2) has the typical band pattern for whey proteins (e.g. Figure 3.1). Thus the removal of the sediment from the whey did not alter the protein composition.

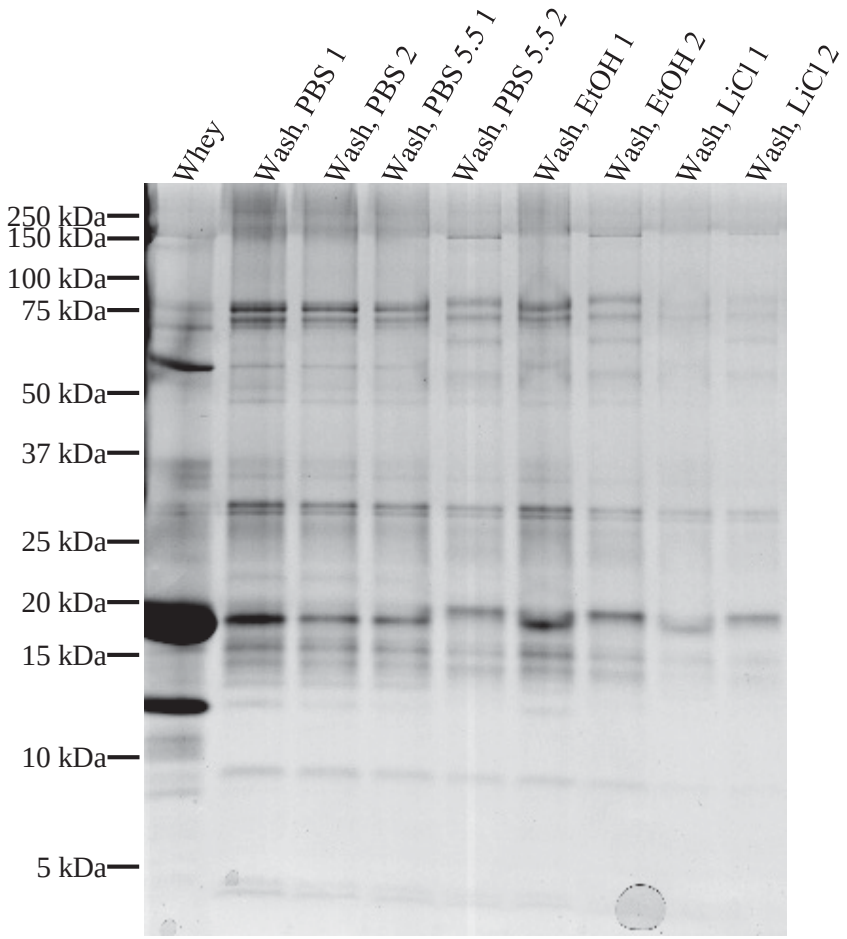

Figure 4.11: Whey sediment after each step of the wash cycle

Reducing SDS-PAGE gel of sedimentable material after centrifugation of whey as done in the adhesion assay during wash cycle. Gel separated at 130 V for 2 hr and stained with CBB G250 overnight.

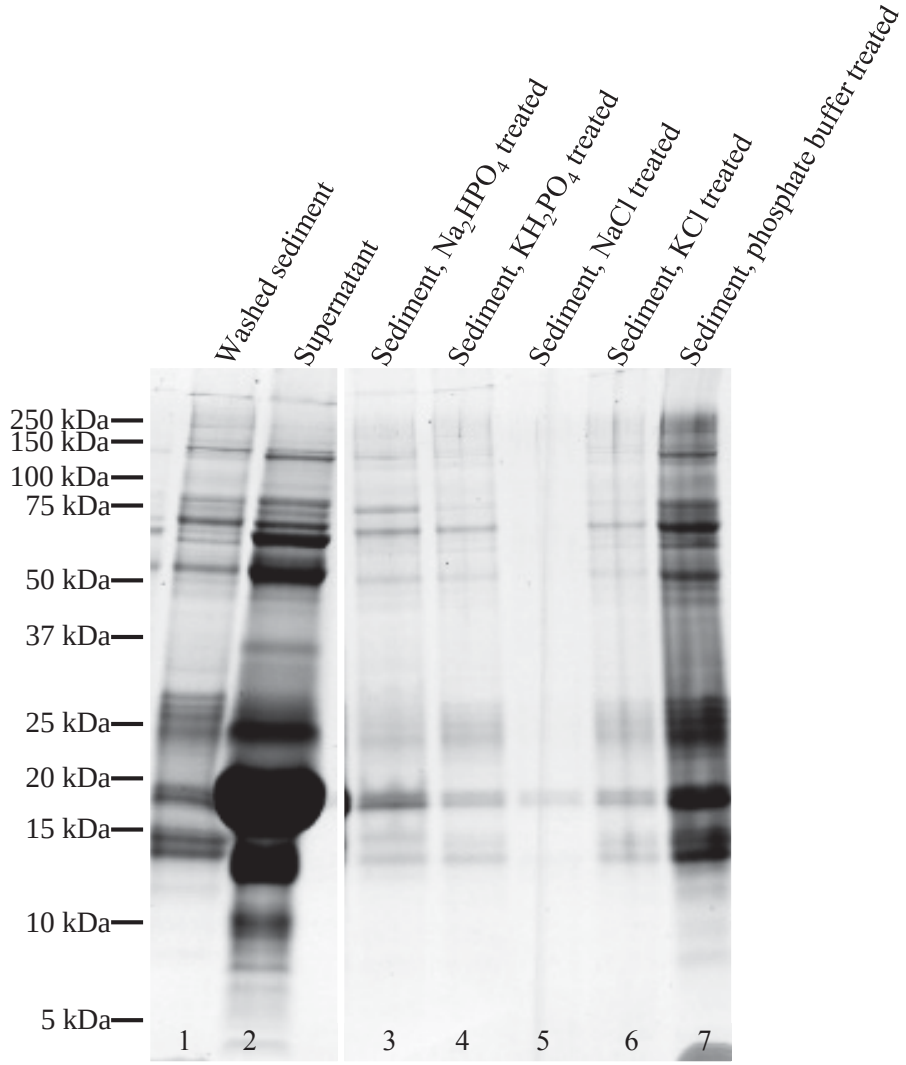

Figure 4.12: Whey sediment after adding PBS salts individually

Reducing SDS-PAGE gel of sediment and clear supernatant (SN) in whey (lanes 1 and 2); sedimented material after mixing whey with single PBS components and subjected to centrifugation as per the adhesion assay (lanes 3-7). Bands assembled form the same gel. Gel separated at 130 V for 2 hr and stained with CBB G250 overnight. Sediment, Na_2HPO_4 / KH_2PO_4 / NaCl / KCl / Phosphate buffer treated: Whey was mixed with respective salts (concentration like in PBS), centrifuged and the sediment analysed.

The influence of temperature (RT, 45°C, and 48°C) on the formation of the precipitate was determined (data not shown). The aim was to favour the formation of precipitate and quantitatively remove all of the insoluble materials. Further it was tested whether one long incubation (60 min) or repeated 10 min incubations (to encourage precipitate formation in the case of an equilibrium reaction) were more effective in removing sediment. After each of the 10 min incubation intervals, the whey was centrifuged and only clear supernatant was used for the next 10 min incubation.

Results indicated that 6 x 10 min at 45°C without shaking was sufficient to remove most detectable levels of sediment bound proteins with the exception of β-LG (Figure 4.13). Figure 4.13 shows that the greatest reduction in the amount of sediment happened between lanes 2 (sediment of untreated whey) and 3 (sediment of whey incubated once for 10 min at 45°C). Every further 10 min-incubation had a smaller effect. β-LG was used as indicator for the reduction in sediment as it was the only protein with a detectable band in every sediment sample. The band density appeared to stabilise after 6 x 10 min incubations. Based on these results, all stored whey was thawed, pooled and incubated for 5 x 10 min at 45°C. The samples were centrifuged to remove the sediment and the clear whey was then aliquoted and stored at -20°C until further use. Before its use for the adhesion assay, the whey was incubated for 10 min at 45°C to remove precipitate which formed during storage.

A Western blot probing for LF shows the effect of removing the sediment from the input material (Figure 4.14). The signal detected for LF in the untreated whey is strong while no comparable signal was detected in sediment free whey. The adhesion assay was then repeated with sediment-free whey and whey only controls were included (Figure 4.15). This confirmed that the removal of sediment did not impact the protein profile of whey ("whey" and "sediment free whey" have the same band pattern), and that the removal of whey protein containing sediment was mostly successful and only residues of β-LG (18 kDa band) and a faint 50 kDa band could be observed in the whey only control ("NC, sediment free whey"). Samples from the sediment free whey showed that few whey proteins bound to the beads (50 to 75 kDa, 18 kDa

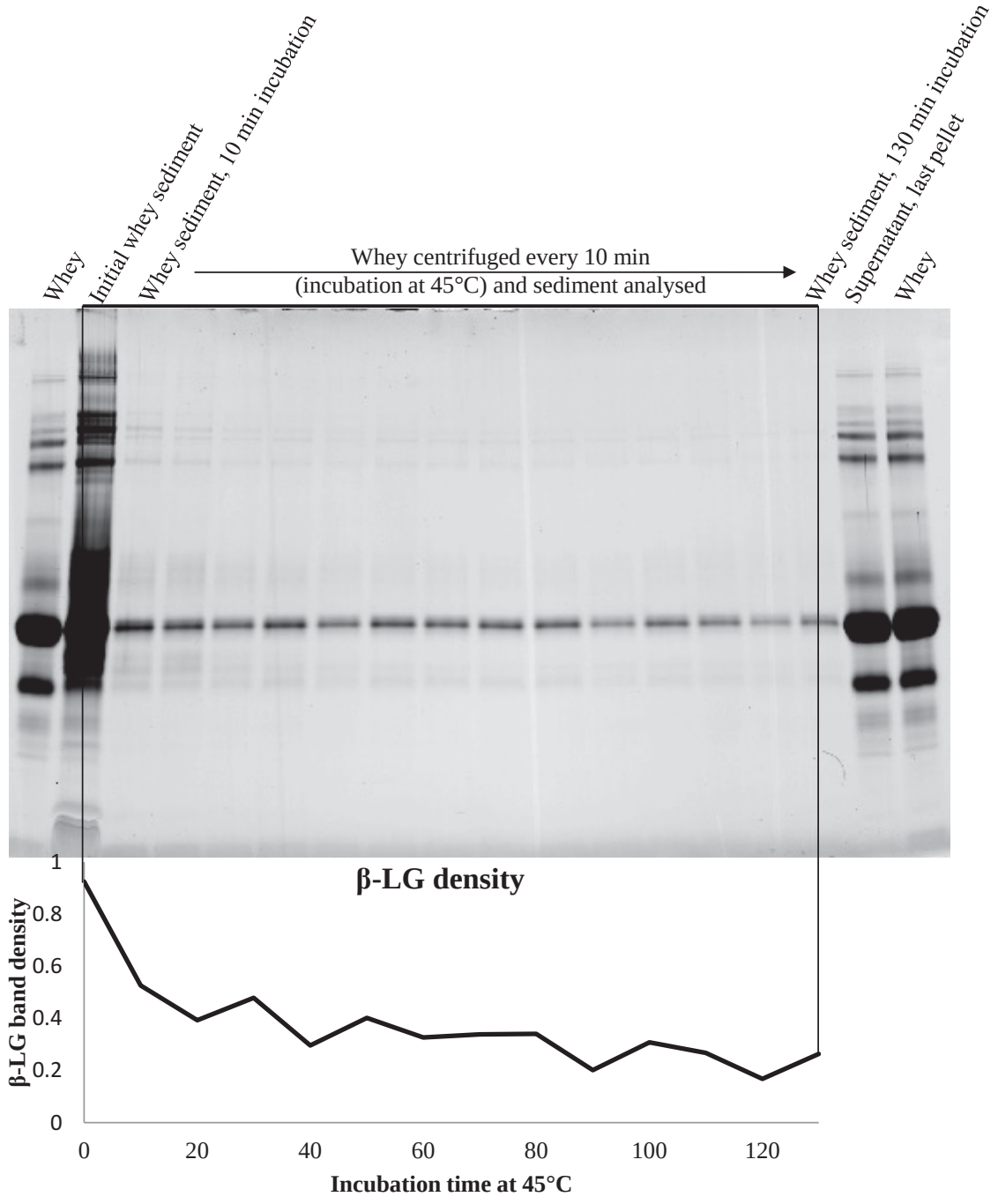

Figure 4.13: Decrease in whey sediment through incubation at 45°C

Reducing SDS-PAGE gel of sedimented material in whey after 0 to140 min incubation at 45°C and supernatant after 140 min incubation in comparison with pure whey. β-LG band in sediments was analysed with QuantityOne and density is blotted below the gel. Most changes seem to appear within the first 60 min of incubation. Gel separated at 130 V for 2 hr and stained with CBB G250 overnight.

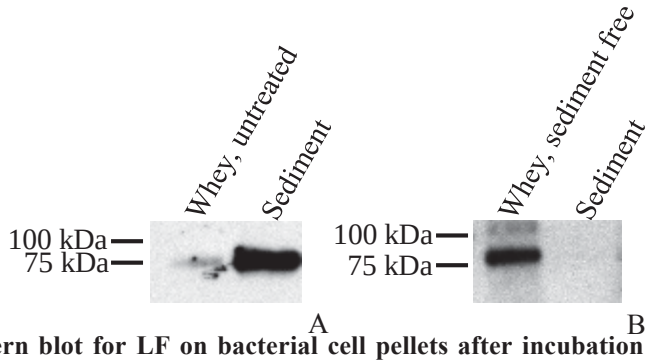

Figure 4.14: Western blot for LF on bacterial cell pellets after incubation with (A) whey and (B) sediment-free whey

Western blot for LF on bacterial cell pellets after incubation with whey and sediment-free whey. Gel separated at 130 V for 2 hr, transfer overnight at 15 V, 3 hr block with 4% NFM, 2 hr antibody-HRP and 30 sec (whey) and 1 min (sediment-free whey) exposure after ECL.

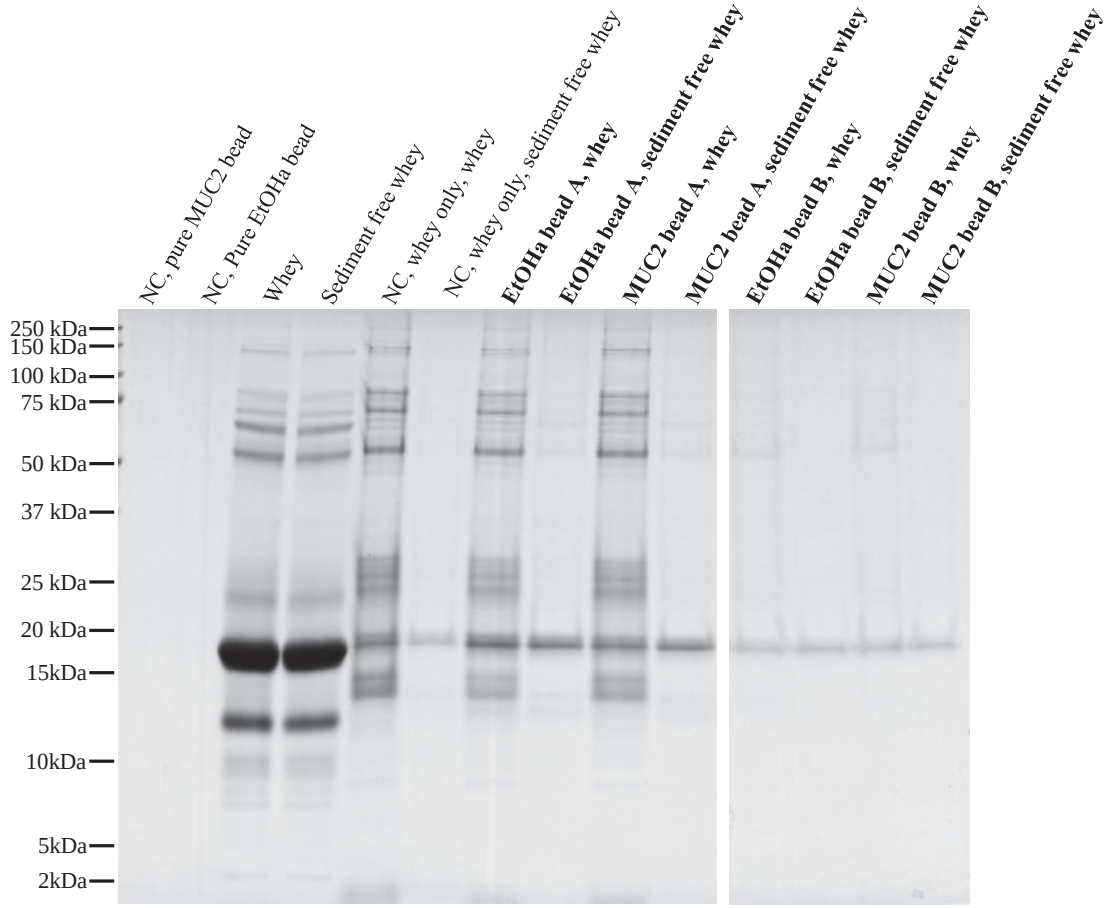

Figure 4.15: Comparison of the adhesion assay (beads A) between mucin-beads and whey or sediment-free whey

Reducing SDS-PAGE gel of MUC2 covered Sepharose beads after incubation with whey and sediment-free whey (SF); beads A and B only to test if proteins detected in samples are actually adhering proteins or only sedimented material that has not been removed completely. Bands assembled from the same gel. Gel separated at 130 V for 2 hr and stained with CBB G250 overnight. Bold font indicates samples that contain Sepharose beads (i.e. shows adhering proteins). SF: Sediment-free. NC: Negative control.

bands in “EtOHa bead A, sediment free whey” and “MUC2 bead A, sediment free whey”). However, no difference in protein binding between negative control and mucin covered beads was observed. This suggests that proteins bound to the Sepharose beads and not to the mucin on the beads. On beads B (MUC2 and EtOH-amine, sediment free whey samples) only residues of β-LG could be observed (18 kDa band). It is likely that this again was sediment as the band intensity is similar to that in the whey only control.

Sediment formation in milk was also investigated to exclude the possibility of sediment based bias. Figure 4.16 shows that the sediment from 500 µl milk, after centrifugation and one to three washes with PBS, was lower than in 1.5 µl milk. The sediment is mostly protein of about 25 kDa molecular weight and was not visually observable in the tube or detectable by DirectDetect. It is possible that the residues were proteins which adhered to the tube itself. Thus it was not considered necessary to pre-treat milk in order to remove sediment. This also agrees with the hypothesis that the sediment formation is caused by the acidification step during whey production (see Section 4.3). Milk was skimmed before using it in the adhesion experiments, but no other pre-treatment took place.

4.3 Discussion

The results from the application of the adhesion assay itself were only evaluated to a limited extent due to the incomplete MUC2 coating of the Sepharose beads.

4.3.1 Adhering milk proteins

In the experiments with skim milk and whole milk (Figure 4.3 and Figure 4.5), differences in relative band intensity were observed between the input material and beads A in both, mucin coated and negative control beads. This indicated selective binding of milk proteins from the input material to mucin or Sepharose. The bands representing α_{S1}- and β-caseins were stronger than those for α_{S2}- and κ-casein. However, these differences merely represent the concentration differences in the input material (Table 4.2). A comparison of the ratios of binding caseins (normalised to α_{S2}-casein) with their 1:3:3:1-ratio (α_{S2}-casein:β-casein:α_{S1}-casein:κ-casein) in

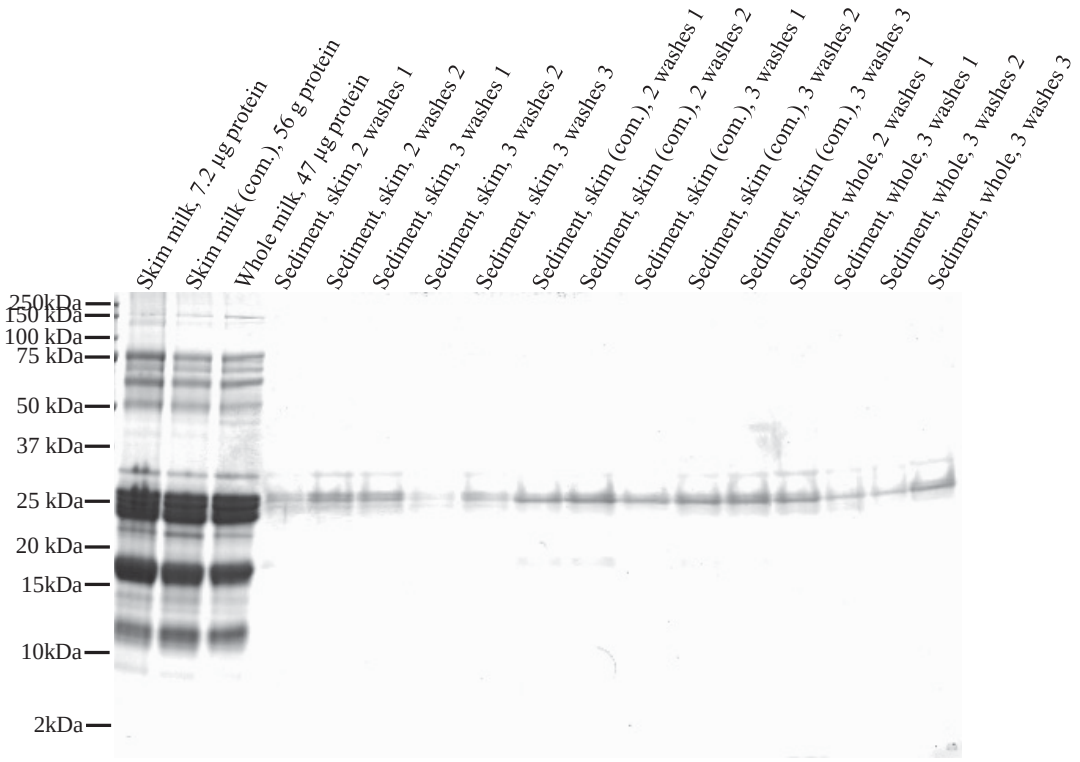

Figure 4.16: Sediment in milks of different fat contents and degrees of processing

SDS-PAGE gel showing 1.5 µl skim milk or commercial skim and whole milk and sediment of 500 µl milk after treatment like in the adhesion assay (30 min at 37°C and 2 or 3 PBS washes). Gel separated at 130 V for 2 hr and stained with CBB G250 overnight.

the casein micelle [493] suggests that α_{S2}- and κ-casein actually showed preferential binding to the beads with exception of the combination of skim milk and EtOH-amine beads.

κ-Casein has only few phosphorylation sites and does not precipitate even at high Ca^{2+}-concentrations [494], indicating low calcium binding. However, a fraction of the κ-casein molecules can be glycosylated [495] and the side chains might introduce functional groups (e.g. hydroxy groups) which can mediate binding. With their phosphoserine (and carboxyl) residues, α_{S1}-, α_{S2}- and β-caseins are able to bind Ca^{2+} ions. Mucins can also bind positively charged ions [496], such as calcium [497]. It is possible that these ions act as bridges between milk proteins and mucins and thus are an important factor in muco-ahesion.

Results from Western blot analysis (Figure 4.6 and Figure 4.7) indicate that the binding affinity of caseins is reduced through pepsin hydrolysis. Some of the undigested samples show a difference in band intensity between mucin-coated and negative control beads (more signal on mucin coated beads). After digestion all bands were generally weaker but also the difference in intensity was reduced. This implies a stronger reduction in binding potential of caseins to the mucin beads compared to the negative control beads. However, the effect of gastric digestion on the binding potential of caseins requires further research. A key question here would be whether the partial *in vitro* gastric digestion decreased the binding potential of casein molecules to mucin coated Sepharose beads or the size of the adhesive molecule decreased; i.e. were binding sites reduced or were non-binding parts cleaved off? Further, the effect of entropically-driven interactions, e.g. hydrophobic interactions, was not addressed extensively in this study. Although the EtOH wash was included to remove hydrophobically bound molecules, results here are inconclusive. This could be due to the changes in temperature, i.e. adhesion was allowed at 37°C while the washes took place at room temperature. An interesting experimental design could combine hydrophobic interactions and the MFGM-rich fractions.

Further, some proteins showed stronger affinity for one of the two types of beads. These occurred more often in skim milk than in whole milk. For example, the 75 kDa band was

Table 4.2: Comparison of casein fraction ratios from Figure 4.3 (skim milk; n=1) and Figure 4.5 (whole milk; n=1) and those found in the casein micelle.

25 kDa: α_{S2}-casein. ca. 24 kDa: β-casein. ca. 23 kDa: α_{S1}-casein. 19 kDa: κ-casein. EtOHa: ethanol amine

	Band density ratio (normalised to 25 kDa band)				
	Skim milk MUC2 beads	Skim milk EtOHa beads	Whole milk MUC2 beads	Whole milk EtOHa beads	Casein micelle [493]
25 kDa	1.0	1.0	1.0	1.0	1
ca. 24 kDa	2.3	2.7	1.9	2.1	3
ca. 23 kDa	2.2	2.9	1.8	2.2	3
19 kDa	1.2	0.9	0.9	0.9	1

stronger on the MUC2 beads than on the negative control beads after incubation with skim milk; this might show actual binding of the milk protein to MUC2. The molecular weight and position of the band indicate that this protein could be LF (compare Figure 3.1). The binding also showed in the Western blot analysis where a faint band for LF was observed in the mucin-coated beads (Figure 4.7). LF has been shown to bind to mucin glycoproteins (e.g. Soares et al. showed binding to MG2 [498]) but no information specifically to MUC2 binding was found.

Other skim milk proteins with different affinities for mucin and negative control beads were found at 45 kDa and approximately 30 kDa (Figure 4.3). In the case of whole milk, only little difference was observed between the mucin covered and negative control beads. These proteins had molecular weights over 150 kDa which corresponds to multimeric Igs and some MFGM proteins. This agrees with the observation that these proteins showed reduced binding from skim milk which has a considerably reduced content of milk fat. MFGM proteins contain Muc1 (58 kDa protein backbone [499] with glycosylation which was found to separate at approximately 200 kDa on SDS-PAGE gels [500, 501]). Muc1 is a secretory mucin and likely to interact with other mucins because of the similar nature. Xanthine oxidoreductase (146 kDa) was shown in preliminary SDS-PAGE experiments to bind to mucin beads, the experiments were done with sediment in the whey and results also could not be confirmed by Western blot (data not shown). Both of these proteins need further research to confirm their binding potential.

Generally, binding seemed to be dominated by caseins. This could be due to the phosphoproteins sticking to the tube. Figure 4.16 shows that several proteins with molecular weights between 20 kDa and 30 kDa remain in the tubes (tubes contained skim or whole milk but no beads) after up to three washes with PBS. This molecular weight agrees with that of caseins. Further, caseins have been shown to bind to hydrophobic surfaces [502]. However, no specific information about binding to polypropylene, the tube material, could be found. It is also possible that casein micelles cause a thicker binding layer due to micelle clustering [503] and thus show a self-enhancing binding behavior while excluding other proteins from adhering.

Despite showing indications of specific binding of proteins to MUC2, these results need to be considered with reservation as the bands were weak and sample repetitions were limited. It appeared that proteins bound to the Sepharose beads are what caused high background levels and false positive results. Thus, in the interest of time and the cost of the Sepharose beads, it was decided to continue the investigation of muco-adhesion with mucin producing IEC in culture (Chapter 5). Considering LC-MS/MS results and Western blot, β-LG and caseins were the adherent proteins. Both proteins have been suggested to show oral muco-adhesion before [504]. However, the 75 kDa protein from skim milk, which was analysed but not identified by LC-MS/MS (Table 4.1), showed the greatest accumulation potential at MUC2. Based on its molecular weight this protein could be LF or an Ig-fragment, e.g. secretory component.

4.3.2 Isolated proteins

It was shown that competitive binding of proteins played a role in the binding behaviour of the proteins tested here. All proteins bound better when they were applied as isolated solutions (Figure 4.8) than from the complex systems, i.e. milk or whey. The multi-protein environment of skim milk, especially the presence of casein, reduced the binding ability of some proteins, e.g. α-LA. Strong casein bands were observed in skim and whole milk derived samples and also casein residues that remained in whey bound on mucin and negative control beads. The strong affinity of caseins for this human intestinal surface layer component might inhibit adhesion of proteins with lower affinity by blocking binding sites. Also, the purification process could have caused changes in the proteins. Alterations could include limited proteolysis, removal of side chains or accessories or changes in conformation [505].

These results demonstrated that binding studies, especially screening of candidate proteins, should be conducted in physiological relevant environments where possible; however experiments with isolated proteins are useful when the behaviour or mechanism of one specific protein is of interest (compare Chapter 7). Relevant environmental conditions also include a relevant concentration of ions in the mix. In the case of mucin binding, especially calcium, as discussed before for caseins. Calcium ions (for example in the milk) are already known for their

role in mucin packaging before being secreted from goblet cells [506] and also in NeuNAc based interactions, e.g. [507].

4.3.3 Whey

Sediment was observed in the acid whey after centrifugation during the adhesion test. It was hypothesised that the sediment was calcium phosphate which started to precipitate after the pH of the whey was raised again. It is well known that the acidification of milk releases calcium phosphate from the casein micelles, resulting in whey that is calcium-enriched [508-510]. The acidification method was used to produce the whey for this study, so it is likely that the whey had increased calcium content. It was further documented that calcium and phosphate co-precipitate when whey is heat-treated (inverse solubility of calcium phosphate [511]) or the pH is increased [512]. Both these steps happen during the processing of whey, before storage (elevating pH to 6.8) and during the adhesion assay (incubation at 37°C). Further, the addition of NaCl (Figure 4.12) appears to reduce the precipitate formation. This ties in with the theory of Mekmene et al. [513] who have developed a model to predict salt equilibria in milk solutions and calculated that after adding 300 mM NaCl to milk, 2.85 mM NaOH are needed to maintain pH 6.75. The authors hypothesise a reduction in ion activity (ionic strength multiplied with the activity coefficient to account for interactions between ions, and ions and water molecules resulting in the concentration that is effectively available for reactions [514]), as consequence of the increased ionic strength, followed by an increase in the dissociation of calcium phosphate. The observations also indicate a slightly acidifying effect of NaCl on milk solutions. A drop in pH could cause re-solubilisation of calcium-phosphate-whey protein co-precipitates [515] and explain the reduced precipitate under these conditions. Taken together, the tests carried out here and the results obtained support the hypothesis that the sediment in whey was calcium-phosphate which was subsequently removed from the whey by incubation at elevated temperature and subsequent centrifugation.

Findings by Saulnier et al. [516] are the only reports found describing the formation of mineral precipitate from acid whey (concentrated to 30% total solids). They showed that whey obtained

by acidification of milk was richer in phosphate (factor 1.4), calcium (factor 2.3), calcium citrate (factor 3.3) and calcium phosphate (factor 2.8) than sweet whey. The authors also suggested the presence of protein impurities, a phosphorylated β-casein fragment, in the precipitate. This agrees with results by Tercinier et al. [517] who found that hydroxy-apatite particles showed preferential binding to β-casein compared to other caseins after incubation with a sodium caseinate solution. For whey proteins, β-LG was preferred over α-LA. This agrees with observations in this thesis that α-LA was absent in the sediment (Figure 4.15). Further, the little casein residues contained in the whey were accumulated in the sediment, suggesting preferential binding of caseins. However, results from Terciener et al. [518] can only serve as indicators as they used inorganic hydroxy apatite particles in a MilliQ or simulated milk ultrafiltrate system.

Figure 4.15 suggests that calcium phosphate had precipitated onto the beads or the bottom of the tubes. The protein bands observed in the samples containing beads and untreated whey (samples labelled with "EtOHa bead A, whey" or "MUC2 bead A, whey") was the same as the protein band pattern in the control containing only whey but no beads (sample labelled "NC, whey"). In contrast, in samples from sediment free whey, the bands observed for β-LG (18 kDa) and protein with 50 kDa and 75 kDa appeared to be more intense in the bead containing samples (samples labelled with "EtOHa bead A, sediment free whey" or "MUC2 bead A, sediment free whey") than in the respective control (sample labelled "NC, sediment free whey"). This indicates that β-LG and the 50 kDa and 75 kDa (possible LF or Ig fragments) proteins are of interest as proteins targeting the mucus layer.

4.4 Conclusions

The experiments conducted in this chapter identified β-LG and caseins as muco-adhesive milk proteins. Further LF and high molecular weight proteins from whole milk, likely MFGM proteins, showed indications of muco-adhesive behaviour. After successfully removing the sediment from whey, β-LG was shown to be a protein with potential muco-adhesive properties. The differences in binding potential of the same proteins between input materials (e.g. β-LG

from milk and whey) showed that the binding environment and protein pre-treatment were crucial for binding and need to be considered for adhesion studies. Further, it was demonstrated that protein binding was increased in isolated solutions. This showed that the adhesion assay developed and used in this thesis is able to screen for food proteins which have superior binding in complex mixtures. However, due to being unable to quantify the extent of mucin coverage on the beads and the low peptide scores in LC-MS/MS, these results require further validation. This was done using human epithelial cells in culture in subsequent chapters.

Whey and milk proteins adhering to mucin covered beads

Chapter 5 Adaption of the adhesion assay to cell culture conditions and investigation of the interactions between whey proteins and human intestinal cells in culture

5.1 Introduction

The cell culture model described in this chapter was used to validate the results of the *in vitro* mucin assay in a more realistic environment. Due to the intermediate complexity of these systems, the cell-based models provide a bridge between animal experiments and *in vitro* systems like cell membrane fractions [164]. Bolte et al. [468] found that food proteins (β-LG, gliadin peptides and ovalbumin) bound to brush border membranes of early-confluent Caco-2 and T84 cells. Binding was specific and the more differentiated Caco-2 cell membranes had higher binding capacities for β-LG and gliadin peptides. Introducing a mucin layer into the cell-culture system, i.e. HT29-MTX cells, adds complexity. Laparra et al. [519] noted the mucin layer produced by HT29-MTX cells could cover potential recognition sites in the plasma membrane of Caco-2 cells making them inaccessible for adhesion. Thus having a cell culture model that closely resembles the human intestinal epithelial surface is desirable to focus on protein binding as it might occur *in vivo*.

The appropriate cell culture model should reflect both the physical and the biochemical nature of the barrier [164]. Therefore, in this thesis, with a focus on adhesion as opposed to absorption of proteins (compare Section 1.5), neither of the commonly used human intestinal cell lines – Caco-2 and HT29-MTX – by itself was sufficient. However, together they complement each other with regard to cell variety as they can be found in the human small intestine and mucin layer (refer to Table 1.2). Caco-2 cells differentiate into enterocyte like absorptive cells (no mucus secretion [161]), while the HT29-MTX cells used here contain 50% mucus secreting goblet cells (Dr A. Barnett, AgResearch, Palmerston North, New Zealand, February 2015).

Thus the decision was made to use a co-culture model of Caco-2 and HT29-MTX cells whereby the ratio of cells was adjusted to resemble a goblet cell percentage, mucus layer thickness and continuity similar to that in the upper small intestine.

5.1.1 Hypothesis and aims

The main hypothesis of this chapter was that whey proteins differ in their adhesive properties and that some of them adhere to small intestinal mucin and to human IEC. Therefore, this chapter aimed to prepare cultures of Caco-2 and HT29-MTX cells and co-cultures thereof to obtain a series of cell cultures with increasing mucin coverage. This mucin gradient allowed the screening of whey for muco-adhesive proteins as described in Chapter 2, Section 2.4.3. Cyto-adhesive proteins could also be screened. Proteins of interest were then confirmed by Western blot as described in Chapter 2, Section 2.5.2.

5.2 Results

5.2.1 Adhesion assays

The cells used for the experiments were Caco-2, un-modified from ATCC HTB-37, and HT29 cells which were stably adapted to 10^{-7} mol MTX by Dr R. Anderson (AgResearch, Palmerston North, New Zealand). This resulted in HT29-MTX cells with 50% mucin secreting goblet cells.

5.2.1.1 Band pattern and reproducibility

In the first adhesion experiments, incubation times from 15 to 120 min were tested for the adhesion phase between whey and a series of cell cultures with increasing amount of mucin (0 to 50% mucus secreting cells). Cell cultures included pure Caco-2, Caco-2/HT29MTX co-cultures (90/10, 75/25 and 50/50) and pure HT29-MTX. For the adhesion test, cells were grown until post-confluence (16 to 18 days), washed with serum free medium, and Rhd-tagged whey (10% in serum free medium) was added. At the end of incubation with Rhd-whey, unbound whey proteins were removed, and one part of the cells was briefly incubated with 0.05% DTT to detach the mucin layer; also non-mucin secreting Caco-2 cells were treated this way to obtain comparable cell fractions. The “mucin” fraction generally contained molecules that were detached through the reducing agent DTT, but was called “mucin” to differentiate from the “cell” fraction, in alignment with the intestinal surface layers defined for this thesis (compare Section 2.3.3). After the “mucin” fraction was collected, all cells were treated with 2 x SDS-PAGE TT-SLB to solubilise the entire cell culture in preparation for SDS-PAGE analysis.

Protein adhesion was visualised using SDS-PAGE gels and fluorescence scanning to differentiate Rhd-tagged whey proteins from unlabelled endogenous cell proteins.

As an example, Figure 5.1 shows an SDS-PAGE analysis of samples from a 90/10 co-culture. In the cell fractions (cells only, mucin only, whole lysate) which have not been incubated with whey (NC) some shadows were observed, particularly at 18 kDa and above. This was likely the result of a combination of density differences in the gradient-gel itself and background signal from endogenous cell proteins (Figure 6.3; a comparable SDS-PAGE gel with bacteria in Chapter 6, shows a similar pattern in NC samples containing only bacterial cells, but less shadow in an empty lane). After the incubation with Rhd-whey, more (66 kDa and ca. 16 kDa) and stronger (150 kDa, 75 kDa, 70 kDa, 60 kDa, 23 to 25 kDa and 18 kDa) bands corresponding to whey proteins were observed in the samples containing mammalian cells (cells and whole lysate) than in the mucin fractions. This indicated that whey proteins bound better to the cells than the mucin. Due to the differences in band intensities between the SDS-PAGE gels (high background and shadows in the gels themselves), after background subtraction, there were no differences between the four incubation times or cell types in the fluorescent scans of cell-culture samples analysed with SDS-PAGE (data not shown). Therefore, experiments were focussed on one incubation time to allow three replicates per samples on the same SDS-PAGE gel. Incubation time of choice was 30 min as it was the incubation interval determined for the adhesion assay with mucin beads (Chapter 4). Analysis for 30 min samples of the 90/10 co-culture are shown in Figure 5.2.

Reproducibility of experiments with Caco-2, 90/10 co-culture and HT29-MTX cells after 30 min incubation with whey (sediment-free) was also determined (represented by Figure 5.2). It appears that there was a slight upward shift of protein bands in cell containing samples. This could be due to the large amount of cell proteins present in the sample which separated at the same molecular weights as whey proteins and thus competed for pockets in the gel. In total, eight proteins were quantified with QuantityOne in the Caco-2 and HT29-MTX cells, whereas

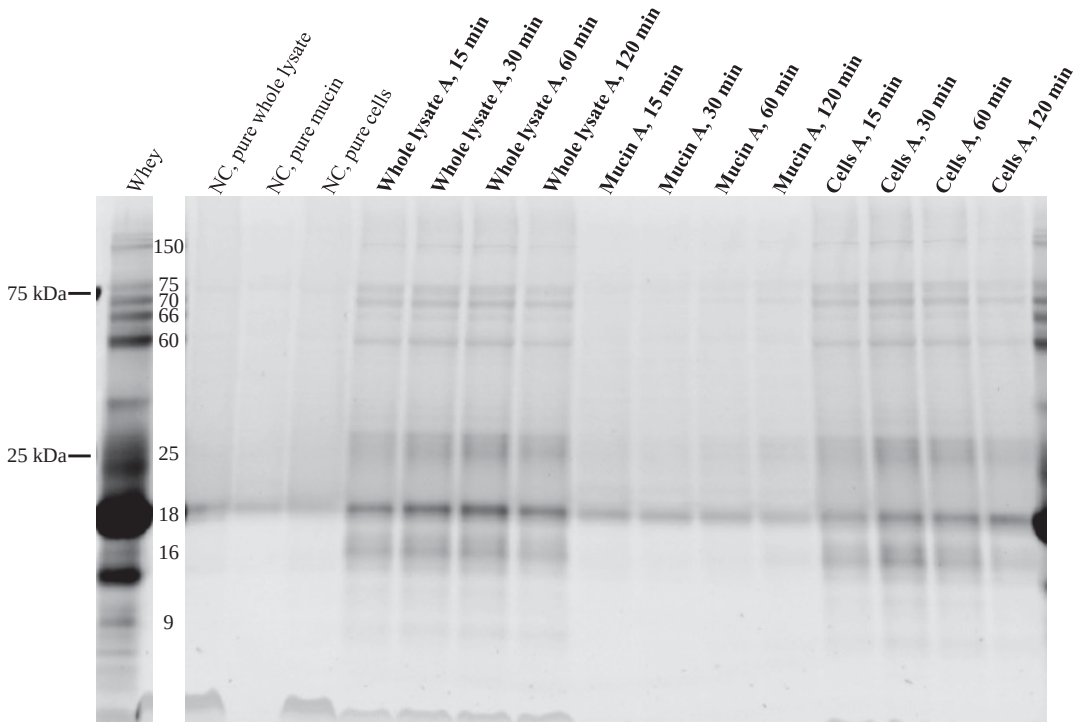

Figure 5.1: Time course adhesion assay between 90/10 co-culture and Rhd-whey (fluorescent scan)

Reducing SDS-PAGE gel of 90/10 co-culture fractions, pellets A, after incubation with Rhd labelled whey or with serum free medium (NC) for 15 to 120 min. Pellets prepared in 150 µl SLB. Gel separated at 130 V for 2 hr and scanned with FX proplus fluorescent scanner at low sample intensity. NC: Negative control. WL: Whole lysate. Bold font indicates samples that contain cell culture fractions (i.e. shows adhering proteins).

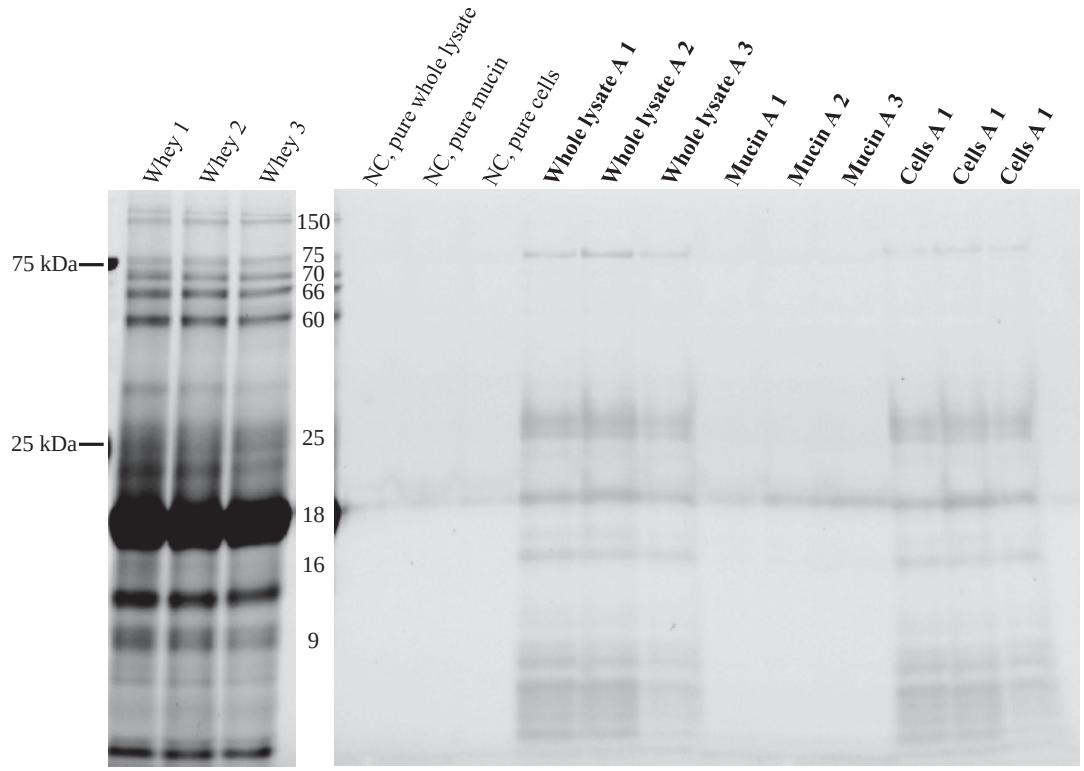

Figure 5.2: 30 min adhesion assay between 90/10 co-culture and Rhd-whey (fluorescent scan), triplicate sample

Reducing SDS-PAGE gel of 90/10 co-culture fractions, pellets A, after incubation with Rhd labelled sediment-free whey or with serum free medium (NC) for 30 min. Pellets prepared in 150 µl SLB. Gel separated at 130 V for 2 hr and scanned with FX proplus fluorescent scanner at low sample intensity. NC: Negative control. WL: Whole lysate. Bold font indicates samples that contain cell culture fractions (i.e. shows adhering proteins).

an additional band was analysed from the 90/10 co-culture (66 kDa; data not shown as there were no significant results). The quantified protein was calculated as percentage input material to allow comparison between SDS-PAGE gels (quantification not shown as high background increased standard deviation and no significant differences were found). Some of the bands detected in the samples on SDS-PAGE gels could not be aligned clearly with a whey protein band. For example, it could not be determined if the 16 kDa band corresponded to α-LA (14 kDa) in the input material or represented a different whey protein that strongly accumulated on the cells. The latter would suggest preferential binding and make this protein an interesting candidate for targeting IEC. Broad bands in the lower molecular weight range (whole lysate and cell fraction after incubation with whey) could be the products of proteolytic activity at the IEC brush borders [520]. As there were no corresponding bands in the input material, these bands could not be quantified.

Generally, the patterns of binding proteins in the whole lysate and cell fractions were very similar to each other, which in turn was similar to the input material. However, some proteins did not bind (e.g. 40 kDa) and others bound weaker (e.g. 18 kDa) or stronger (potentially 16 kDa) compared to the majority of proteins. This indicated selective and preferential binding of proteins from whey to IEC in culture. A comparison of the two SDS-PAGE gels also showed the difference between normal (Figure 5.1) and sediment-free whey (Figure 5.2) in the assay, as well as the variation in band density between different SDS-PAGE-gels. Band densities, particularly that of β-LG (18 kDa), were less intense in Figure 5.2, suggesting that some sediment deposited onto the cells in the time course experiments (Figure 5.1). Sediment-free whey was used for following cell culture experiments.

5.2.1.2 Quantification of SDS-PAGE gels using lane traces

When SDS-PAGE gels from the time course experiments (represented by Figure 5.1) were analysed using lane traces, it became apparent that SDS-PAGE is not an appropriate method to analyse these samples (Figure 5.3). Possible reasons are the high level of background signal in the SDS-PAGE gels, weak signals from proteins of interest and variation between repetitions of

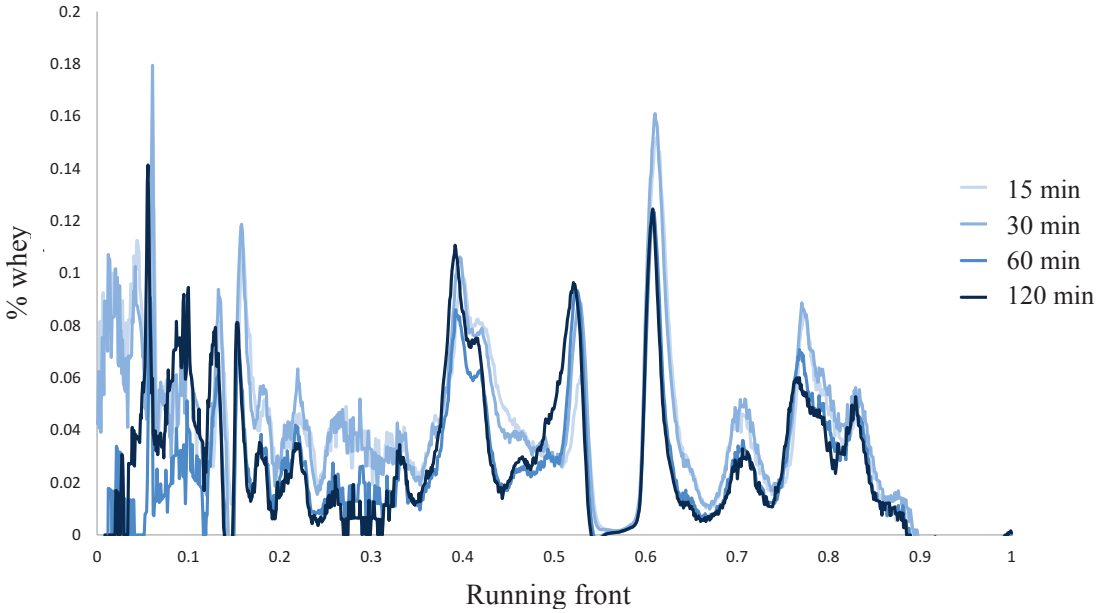

Figure 5.3: Lane traces from SDS-PAGE analysis of HT29-MTX whole lysate after different incubation times with Rhd-whey

Lane trace analysis of fluorescent scans of SDS-PAGE gels for samples after 15 to 120 min incubation with Rhd-whey. Data shown expresses band intensity as % of whey after background subtraction. Data shown is extracted from HT29-MTX cell cultures, whole lysate (WL) fraction.

the same SDS-PAGE gels. The differences between the individual lane traces (different incubation times) in Figure 5.3 are small and do not allow any conclusions on time depenedcy of protein adhesion to epithelial cells in culture.

Taken together, the SDS-PAGE analysis showed high variability between gels and thus the ability to generate statistically significant (T-test) results was limited. Western blot analysis was done for quantitative analysis of individual, clearly identified, binding proteins.

5.2.2 Cell-adhesion of individual proteins analysed by Western blot

For this set of experiments, comparable samples (with and without fluorescence tag) were loaded on the same SDS-PAGE-gel for Western blot analysis (Figure 5.4 to Figure 5.6). First Western blot analysis was done with primary antibody-HRP conjugates. This resulted in high background levels for some protein-culture fraction combinations. A further set of Western blot analysis, using a primary-secondary antibody system, aimed to reduce the background levels. For Figure 5.4 to Figure 5.6 the cleaner blot each was chosen.

Band density analysis was performed for the proteins depicted in Figure 5.4 to Figure 5.6 (Figure 5.7). Most of the samples, especially those from whole lysate and cells only, show signal in the whey free controls at similar levels to that observed in the corresponding whey treated samples. This implies that most of the signal in the whey treated samples was underlying signal from the cells themselves. Only IgM and β-LG were detected above background (Figure 5.7). IgM was found in whole lysate and cell fraction but not in the mucin (surface molecules removed with DTT) of the Caco-2 cells and to a lesser degree in the co-culture. On the contrary, in HT29-MTX, IgM showed a strong signal in the mucin fraction, indicating muco-adhesion of IgM in these cells. Similarly, higher levels of β-LG were present in the whole lysate and mucin fraction of the co-culture and in the whole lysate of Caco-2 cells. These results indicate binding of the respective protein to the mucin layer. Further, β-LG was found in the whole lysate of Caco-2 cell cultures; however no whey protein was detected in either the mucin (components removed with DTT from the cell culture surface) or the cell fraction alone.

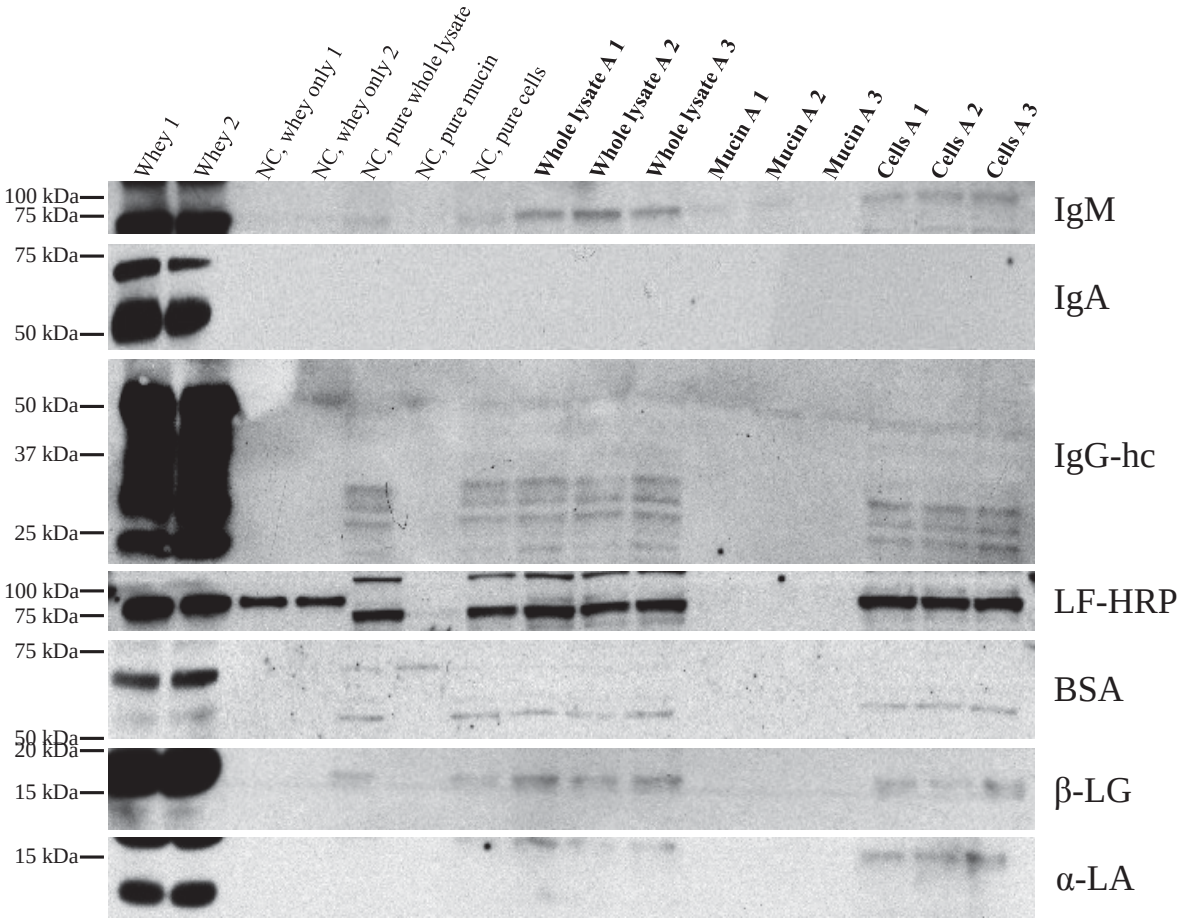

Figure 5.4: Overview of Western blot analysis of Caco-2 cell fractions

Western blot for selected proteins adhering to Caco-2 fractions after incubation with Rhd-whey; three repetitions per fraction. Gels separated at 130 V for 2 hr, transferred overnight at 15 V, 3 hr block with 4% NFM, overnight incubated with antibody-HRP conjugate or 3 hr with primary and 2 hr with secondary antibodies, and 2 min exposure after ECL. Bold font indicates samples that contain cell culture fractions (i.e. shows adhering proteins).

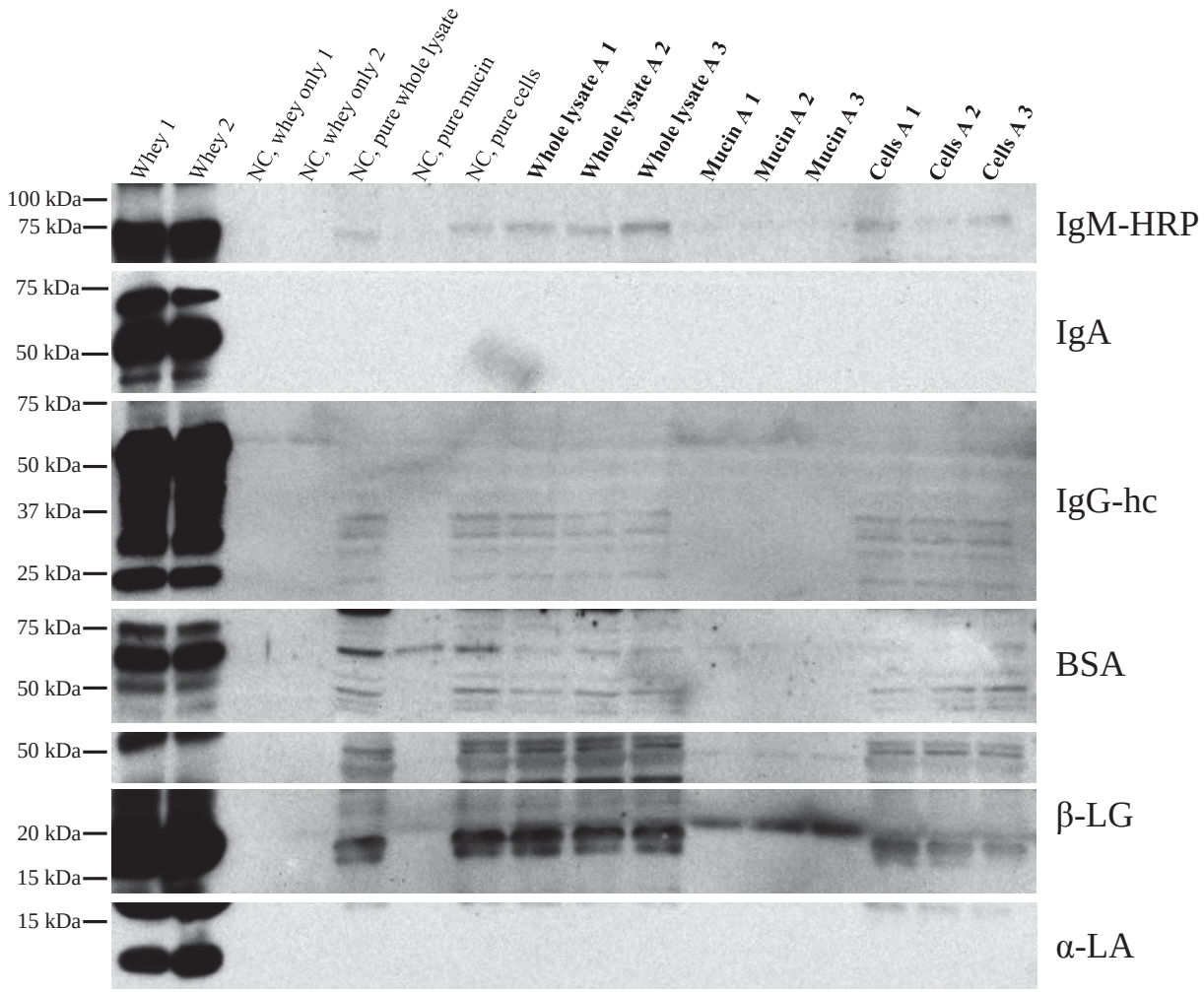

Figure 5.5: Overview of Western blot analysis of 90/10 co-culture cell fractions

Western blot for selected proteins adhering to 90/10 co-culture fractions after incubation with Rhd-whey; three repetitions per fraction. Gels separated at 130 V for 2 hr, transferred overnight at 15 V, 3 hr block with 4% NFM, overnight incubated with antibody-HRP conjugate or 3 hr with primary and 2 hr with secondary antibodies, and 2 min exposure after ECL. Bold font indicates samples that contain cell culture fractions (i.e. shows adhering proteins).

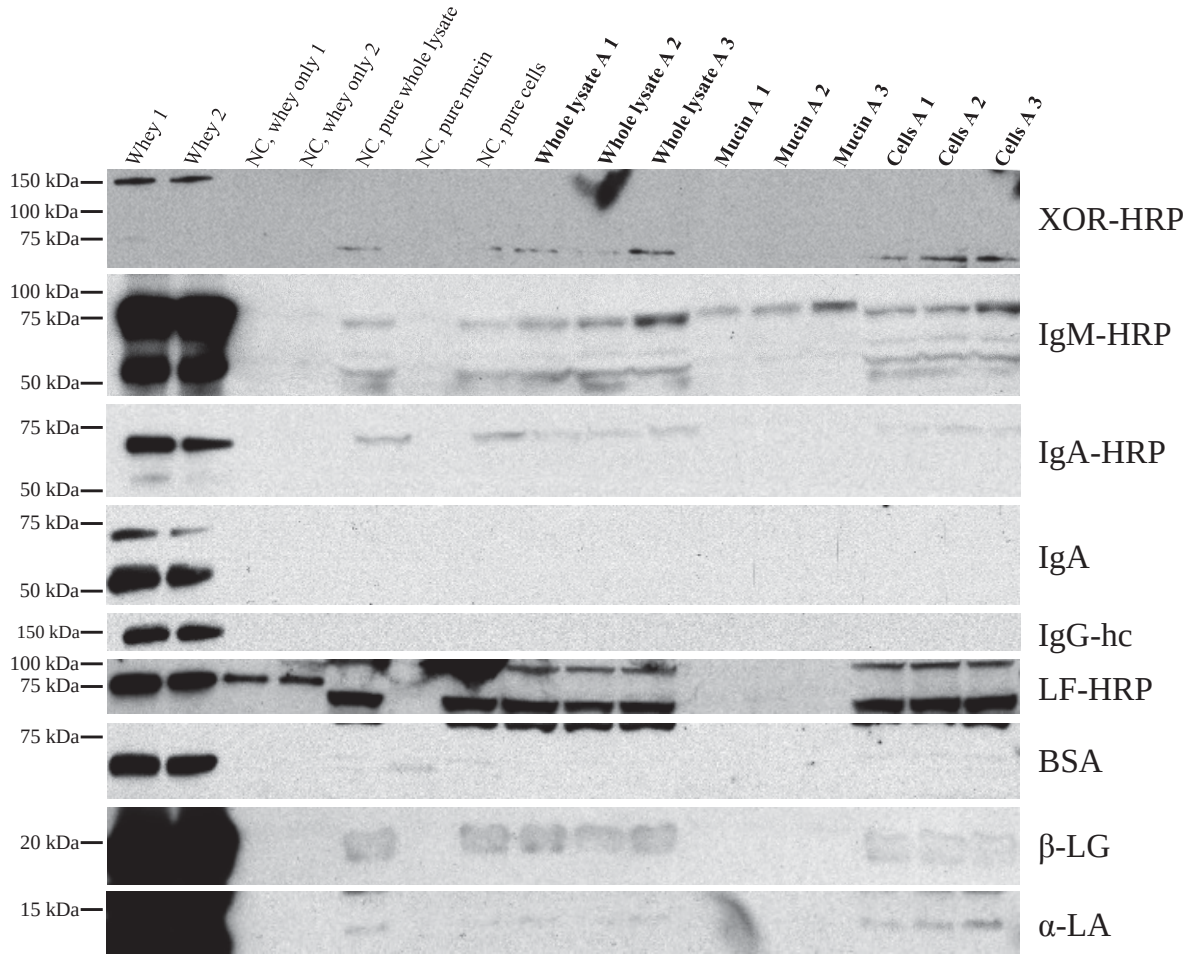

Figure 5.6: Overview of Western blot analysis of HT29-MTX cell fractions

Western blot for selected proteins adhering to HT29-MTX fractions after incubation with Rhd-whey; three repetitions per fraction. Gels separated at 130 V for 2 hr, transferred overnight at 15 V, 3 hr block with 4% NFM, overnight incubated with antibody-HRP conjugate or 3 hr with primary and 2 hr with secondary antibodies, and 2 min exposure after ECL. Bold font indicates samples that contain cell culture fractions (i.e. shows adhering proteins).

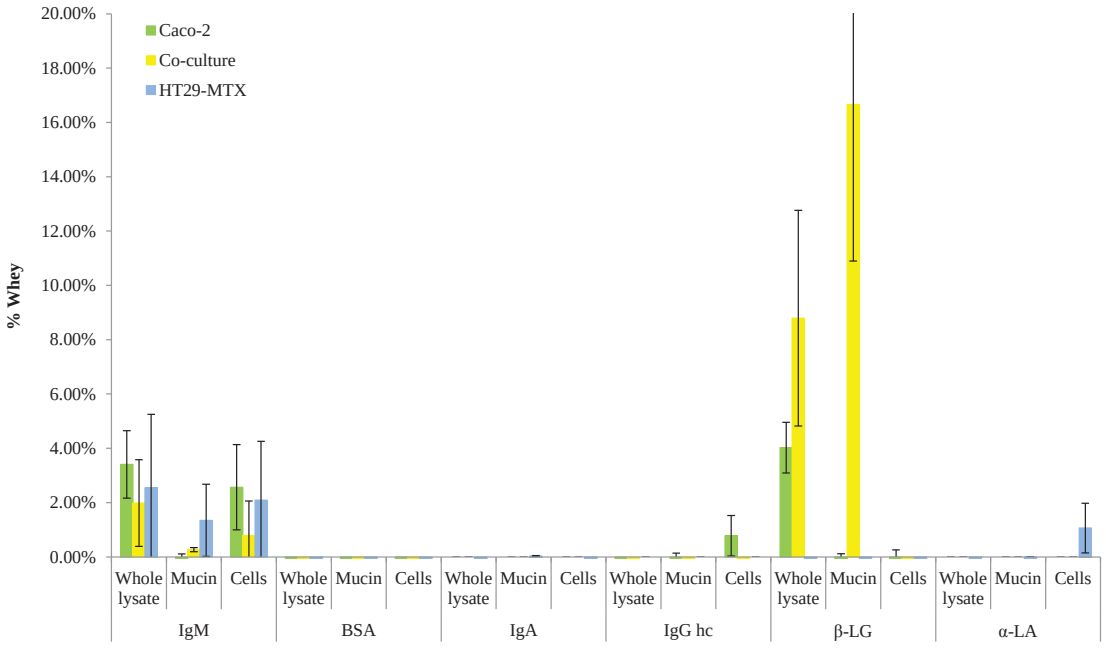

Figure 5.7: Band density analysis of Figure 5.4 to Figure 5.6

Bar graphs for bands from Figure 5.4 to Figure 5.6 analysed with QuantityOne. Band densities are expressed as percentage input whey band density (using the loading material as reference) after background (whey sediment and pure cell culture fractions) subtraction. Thus sample values could not be compared with a control and no T-test was possible. Where there is no bar, no protein band was detectable above background. Results are averaged of three experiments. Error bars indicate STD deviation.

LF was the only protein that bound to the wells without cells ("NC, Whey only"). Further it appeared that the LF band was located between the two bands (70 kDa and 100 kDa) that were observed in the whole lysate and cells only without whey. Thus it was decided that the band in the cell fraction of Caco-2 cultures (Figure 5.4) was likely not LF but the result of an upward shift of the lower protein band (70 kDa) as discussed before for β-LG. For xanthine oxidoreductase (Figure 5.6), BSA and α-LA, the bands in the positive control and the samples did not have the same molecular weight.

5.3 Discussion

5.3.1 Cell culture conditions

Studies have shown that absorptive and goblet cells form monolayers with tight junctions when they were grown together [226, 521]. After seeding, the two cell types of the co-culture grew in patches but at time of confluence, cells were homogenously distributed with small clusters of HT29-MTX embedded between Caco-2 cells. The HT29-MTX type used for the experiments here was generated by stably adaption to 10^{-7} mol MTX. This resulted in a cell line with only 50% goblet cells, lower mucus secretion and consequently a thin mucus layer. This means that the co-cultures used had only half the number of mucin-producing cells than expected. As the mucus layer distributes evenly over the whole cell layer independent of the initial seeding ratios [226, 463], this was not considered a problem. The amount of mucin in the co-culture used here was sufficient to show different results between Caco-2 cells and the co-culture (e.g. Western blot results for β-LG). With about 5% goblet cells in the 90/10 co-culture, this represented the lower ratio of the goblet cells in the human small intestine (Table 1.2). Although the optimal mucin secretion in culture was observed after 21 days [224, 225], cells used in the experiments were grown for only 16 to 18 days, when the cells were post-confluent. This was sufficient as differences in protein binding between mucin producers and non-producers were observed, e.g. β-LG (Figure 5.7).

Preliminary trials did not indicate that replacing FCS with whey for the time of the adhesion period causes increased cell death (data not shown). Further, wash steps were conducted as quicky as possible to avoid cell lysis at any stage during the assay. However, it was not feasible to do a live cell count on every well tested as this would have interfered with the handling and incubation times foreseen in the adhesion protocol.

5.3.2 Adhesion assay

The SDS-PAGE gels show that some bands were only detectable (e.g. 16 kDa) or more intense (e.g. 75 kDa) in the cell culture samples compared to the input material. This could indicate accumulation of proteins on the cells. Accumulation could have been caused by adherence or through retention or slow diffusion of proteins into the mucin layer. Binding of a 66 kDa protein which was only observed in co-cultures could show synergistic adhesion mediation of absorptive IEC and mucin. The molecular weight dependent diffusion rate of proteins described in Figure 5.3 agreed with results from Matthes et al. (1992). These authors found that the mucin network can be considered a molecular filter with a cut-off of about 600 to 700 $g.mol^{-1}$ (600 to 700 kDa). Above this size, absorption occurs at low level [522].

The lack of significance in the results was due to the variability between results and also the set up of analysis (wide range of parameters but only three repetitions). A comparison between SDS-PAGE gels was not feasible, although sample band densities were normalised to band densities of input material. This approach might have been successful with more repetitions. However, more repetitions would have reduced the range of parameters that were screened. These variations were done to explore a wide range of mucin coverage and incubation time. In order to reduce sample numbers and thus increase repetitions to generate statistically significant results, a next step could be to focus on the adhesion assay on most physiologically relevant parameters. This could be done by using only a 90/10 (Caco-2/HT29-MTX^{-6}) co-culture, which most closely resembles the small intestine S-layer, and incubate with sediment-free whey for 30 to 60 min. The analysis of individual bands on SDS-PAGE gels was more precise than lane traces. Lane traces were hard to align exactly and already little shifts had an impact on the

profile of the average lane trace. Thus, densitometry on individual bands was the preferred analysis method. For future work, this could be combined with mass spectrometry identification of proteins of interest to confirm that the correct proteins are compared.

5.3.3 Western blot analysis

Contrary to what was suggested for SDS-PAGE analysis, the second block of Western blot analysis showed that there was no difference between the samples from normal and sediment-free whey with regard to detectable whey protein residues in the whey only controls. Thus, evaluation of the first block of Western blot (normal whey) was not based on artefacts. This was confirmed by the lack of signal in the whey only controls for most proteins. Analysis showed that two proteins bound to mucin. These were β-LG which bound to the co-culture and IgM which had a binding rate that increased with increasing percentage of mucin secreting cells, i.e. there was an increase in signal from Caco-2 to HT29-MTX cells. Results show that β-LG binding to mucin was favoured in co-cultures containing enterocyte-like Caco-2 cells and mucin producing HT29-MTX cells (Figure 5.5). This suggests that β-LG might have bound preferentially at the interface between cells and mucin or that the protein has been modified by brush border membrane enzymes in a way that increases muco-adhesion of β-LG. As also pure HT29-MTX cultures provide an interface between mucin and cells, it is more likely that brush border enzymes were involved.

An hypothesis for the observed binding of β-LG to the mucin of the co-culture is that β-LG was slightly hydrolysed. For example, if internal disulphide bonds were cleaved, previously shielded or occupied regions could have been exposed and new binding sites such as hydrophobic regions (inside the β-barrel) or cysteines were made accessible. These changes have no effect on the molecular weight of β-LG and thus would not change the SDS-PAGE band pattern. Potential enzymatic cleavage sites in β-LG were predicted using an online-tool. The Protease Specificity Prediction Server (PROSPER) was developed by Song et al. [523] and uses the primary and secondary structure to predicted solvent accessibility, and native disorder features to predict enzymatic cleavage of proteins based on FASTA sequences (Table 5.1). Protein

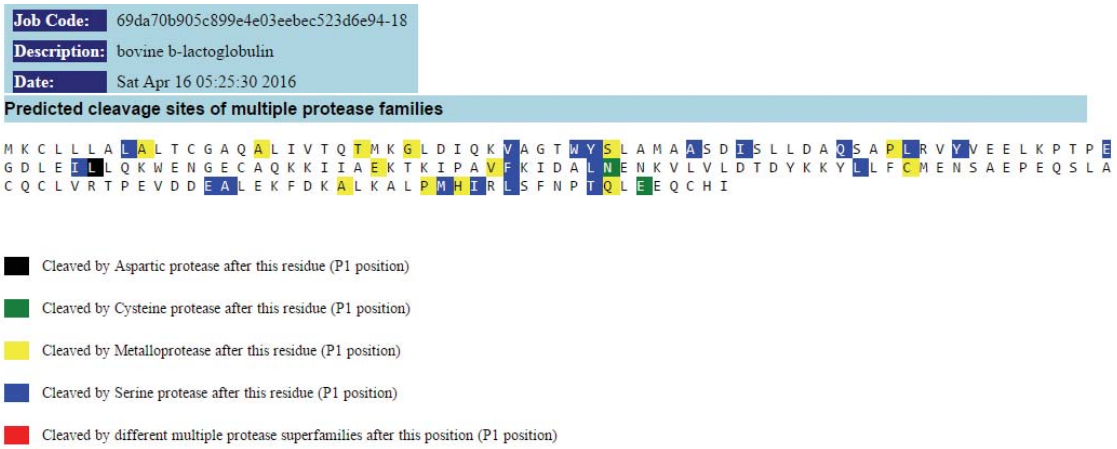

Figure 5.8: Screenshot (assembled sections) of the PROSPER analysis, showing all determined potential enzymatic cleavage sites of β-LG [523].

structures and solvent accessibility are integrated to distinguish more complex cleavage sites than detectable by using only the primary sequence. PROSPER analysis of β-LG (Job Code: 69da70b905c899e4e03eebec523d6e94-18, Figure 5.8) showed possible sites for cleavage byseveral enzymes. Most of the proteases in the database can be found in the human body, and some proteases have been described for Caco-2 or HT29-MTX cell lines (Table 5.1). Thus it can be assumed that protease activity on β-LG predicted in the online-tool could take place *in vivo*. Further proteins belonging to the serine protease super familiy are trypsin and dipeptidyl peptidase which can be found in the human body [524] and Caco-2 cells [525-527]. In HT29 cells only dipeptidyl peptidase IV was found [526, 527]. Although these enzymes are not considered in the database, their activity is simlar to that of other proteins in the same superfamiliy. Howell et al. [526] described a set of eight membrane peptidases in Caco-2 cells (aminopeptidase N, aminopeptidase P, aminopeptidase W, dipeptidyl peptidase IV, endopeptidase-24.11, γ-glutamyl transpeptidase, microsomal dipeptidase and peptidyl dipeptidase), and three in HT29 cells (aminopeptidase W, carboxypeptidase M and dipeptidyl peptidase IV).

Another hypothesis for the increase in muco-adhesion of β-LG through brush border enzymes is that glycosides were transferred onto the proteins (e.g. GlcNAc transferase [528]), forming glycoproteins. The new side groups can then facilitate binding to e.g. lectins or receptors. Glycosyl transferases have been shown to be present in glycocalyx (dense apical extracellular layer embedding brush border; Section 1.2.1) of confluent or differentiated Caco-2 monolayers [529]. The enzymes catalyse the transfer of glycosyl groups from a donor to an acceptor molecule [454, 530]. During a glycosylation reaction, the donor typically is a sugar molecule that needs to be activated (e.g. by cleavage) to be an electrophile. Acceptor molecules can be of various natures, including proteins or peptides [531, 532]. The glycosylation of dietary proteins such as β-LG on the intestinal brush border has not been described to date. Yet, potential receptor sites are present in the β-LG molecule: linkages to proteins can be formed [532] through O-glycosylation of tyrosine, serine or threonine, or N-glycosylation of asparagine

Table 5.1: Comparison of enzymes in the PROSPER database and those found in the human body and Caco-2 and HT29-MTX cells

---: No information was found if the enzyme is present in the human body or the respective cell line. n/a: non-human enzyme. Cys: Cysteine. Ser: Serine.

Super-family	Protease	Merops ID	Human enzyme [524]	Caco-2 enzyme	HT29-MTX enzyme
Aspartic protease	HIV-1 retropepsin	A02.001	---	---	---
Cys protease	Cathepsin K	C01.036	CTSK	---	---
	Calpain-1	C02.001	CAPN1	---	---
	Caspase-1	C14.001	CASP1	---	---
	Caspase-3	C14.003	CASP3	---	---
	Caspase-7	C14.004	CASP7	---	---
	Caspase-6	C14.005	CASP6	---	---
	Caspase-8	C14.009	CASP8	---	---
Metallo protease	Matrix metallopeptidase-2	M10.003	MMP2	---	---
	Matrix metallopeptidase-9	M10.004	MMP9	---	---
	Matrix metallopeptidase-3	M10.005	MMP3	---	---
	Matrix metallopeptidase-7	M10.008	MMP7	---	---
Ser protease	Chymotrypsin A (cattle-type)	S01.001	n/a	α-chymotrypsin [525]	---
	Granzyme B (Homo sapiens-type)	S01.010	GZMB	---	---
	Elastase-2	S01.131	---	No [525]	---
	Cathepsin G	S01.133	CTSG	---	---
	Granzyme B (rodent-type)	S01.136	n/a	---	---
	Thrombin	S01.217	F2	---	---
	Plasmin	S01.233	PLG	---	---
	Glutamyl peptidase I	S01.269	---	γ-Glutamyl transpeptidase [526]	No [526]
	Furin	S08.071	FURIN	---	---
	Signal peptidase I	S26.001	---	---	---
	Thylakoidal processing peptidase	S26.008	---	---	---
	Signalase (animal)	S26.010	SEC11C	---	---

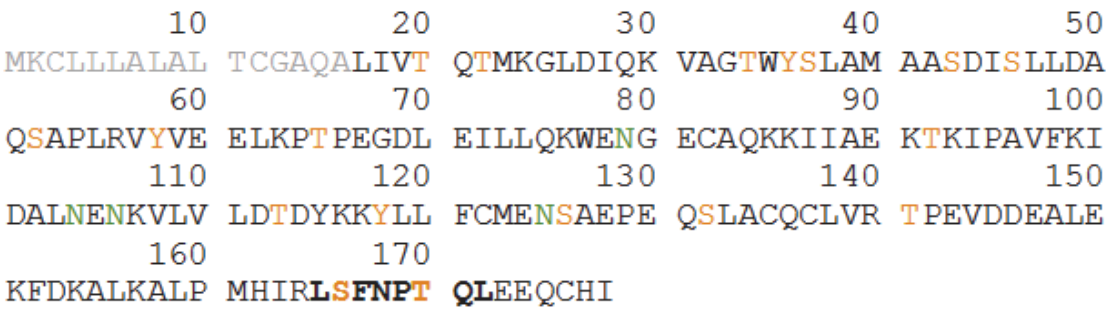

Figure 5.9: Primary sequence of β-LG [533].

Grey font indicates signal peptide. Orange font indicates O-glycosylation sites: Tyrosine (Y), Serine (S), or Threonine (T). Green font indicates N-glycosylation site: Asparagine (N). Bold font indicates candidate region for the formation of an O-glycosidic link [534].

(summarised by Spiro [534]). These amino acids are found throughout the β-LG primary sequence [533] (Figure 5.9). Although it could not be determined if all of these sites are actually accessible by the enzyme, the abundance of reaction sites should provide access to some of them. In Figure 5.9, amino acids 165-172 (bold font) show a region with serine and threonine close to a proline residue with little or no charged amino acids - these conditions were described as favourable for the formation of an O-glycosidic linkage [535]. Although the region here is not a β-turn (another favourable factor for glycosylation), the α-helical configuration in this part of β-LG provides a similar spherical relation of the amino acids [533]. Finally, this loop appears to be accessible for enzymes [536] as it lies at the outside of the globular protein. Taken together, this makes β-LG a target for glycosylation at the intestinal brush border which in turn can increase muco-adhesion of β-LG. For further investigation of this hypothesis, an experimental design could include traceable sugars, for example through radioactive markers.

IgM appeared to interact with mucin and IEC (Figure 5.7). Mucin was reported to be "impregnated" with secreted Igs like secretory IgA (sIgA) [537]. As the IgM molecule is considerably larger than the IgA molecule, diffusion might take longer, resulting in a temporary enrichment of IgM molecules in the mucin layer. This could explain why IgM was detected in the mucin fraction of HT29-MTX cells. Although most proteins appeared to have background signal from the cell culture fractions, some of the most interesting candidates, e.g. 75 kDa IgM fraction in the mucin of HT29-MTX cells (Figure 5.6), did not have a corresponding background signal in the control. This suggests that all protein detected came from whey. To verify this, further methods such as mass spectrometry can be used. Binding of IgM to the cell containing fractions of cell cultures were observed for all three types of cell culture in this thesis, indicating that IgM adheres to IEC, independent of the degree of mucin coverage. This makes IgM a good candidate for targeting IEC. Binding of IgM will be discussed further in Chapter 8.

5.4 Conclusion

The experiments in this chapter showed that the adhesion assay can be adapted to a cell culture set up. With regards to the hypothesis of this chapter, that whey proteins differ in their adhesive properties and that some of them adhere to small intestinal mucin and to human IEC. Western blot analysis showed that β-LG and, to a lesser degree, IgM bind to mucin or the underlying cells, respectively. SDS-PAGE analysis suggested that proteins with molecular weights of 16 kDa, 66 kDa, and 75 kDa could adhere to IEC. However, these results need further validation, e.g. using flow cytometry, due to background signal on the gels and also to identify the proteins.

Chapter 6 Adaption of the adhesion assay and investigation of the interactions between whey and milk proteins and representative bacteria with the propensity to form biofilms *in vitro*

6.1 Introduction

Despite variations in species and function (Figure 1.3), all bacteria in the human GIT have one important characteristic in common: they all possess various surface structures which enable them to interact with the GIT surface [538-540]. Bacterial adhesins behave as lectins, recognising oligosaccharide residues of glycoproteins or glycolipids [541-548]. The adhesins are located at the tip of bacterial filaments and at a few sites along the filaments [541-544, 549, 550]. Besides targeting host structures, bacterial adhesins are involved in biofilm development, and even distantly related bacterial species make use of the same elements to produce biofilms [354, 395, 551-554]. Two of the most common exopolysaccharides produced by a range of different bacteria are cellulose and pGlcNAc [555, 556]. Other extracellular matrix components like curli and colanic acid are not relevant in the context of the human intestinal tract [557-560]. Also antigen 43 (Ag43) appears to play no role in a nutrient-rich environment [561]. In comparison to plant cellulose, enterobacterial cellulose is a good carrier (especially for proteins) with a large specific surface area of 50 to 150 $m^2.g^{-1}$ [389]. pGlcNAc is also made up of glucose monomers, however with a combination of deacetylation [398] (Figure 1.9) and O-succinate substituents [334, 391, 397]. This leads to the introduction of simultaneously positive and negative charges on the polysaccharide. Deacetylation is an uncommon feature for extracellular polymeric substances and the resulting cationic character of pGlcNAc presumably is essential for biofilm formation and attachment (theoretical pK 6.9). Thus, by expressing pGlcNAc (called PIA if secreted by *S. epidermidis* 1457), bacteria can efficiently change the electrostatic properties of their cell surface [374, 375].

Sialyloligosaccharides from egg yolk have been shown to inhibit bacterial adherence to Caco-2 cells (*S. enteritidis* and *E. coli*) and mice GIT (*S. enteritidis*) [451] [562]. α-linked Man residues (as they appear in mannooligosaccharides) are also known to inhibit enterobacterial adhesion, including *Salmonella* and *E. coli* [453, 454]. Further, pectic-type and other water-soluble oligosaccharides are suggested to have anti-adherence activity [96, 458, 459]. A high-molecular weight extract from tea reduced adherence of *H. pylori* to a human gastric epithelial cell line

and *S. aureus* to fibroblast epithelial cell line [459] while an aqueous extract from carrots blocked enteropathogenic *E. coli* binding to HEp-2 and human mucosal cells [96] with an acidic oligosaccharide containing trigalacturonic acid as active substance. Cranberry extract contains a multitude of anti-infection and anti-adhesive substances [37-39]. The high concentration of fructose inhibits *in vitro* type 1 fimbriae-mediated *E. coli* adhesion [455]. Proanthocyanidins and other high molecular weight compounds were shown to inhibit adherence of uropathogenic *E. coli*. The authors suggest that the cranberry components act as receptor analogues [457]. Free oligosaccharides and glycoproteins from (human) milk or colostrum are considered to be soluble receptor analogues of epithelial cell-surface carbohydrates [445] and act as anti-adhesives for diarrheal pathogens [24-29]; e.g. *in vitro* attachment of enteropathogenic *E. coli* to intestinal cell lines can be inhibited mainly due to fucosyloligosaccharides [33-35]. Further proteins from (porcine) milk have been shown to bind to lipopolysaccharide of Gram-negative bacteria [32] (e.g. LF, serum amyloid A [30], caseins [31]). Thereby LF may bind to target cell membrane glycosaminoglycans and bacterial invasins [446, 447]. Although the above summarised food derived molecules have been investigated from an anti-adhesin point of view, they are also relevant in the context of of this thesis. In order to prevent adhesion, the molecules need to either bind to a surface or to the bacteria, i.e. bacterial adhesion was investigated indirectly.

To date, a range of food derived molecules has been shown to interact with bacteria. Studies combining bacterial adhesion, the human intestinal tract and effects of isolated food molecules normally focus on anti-adhesive effects. Often the question regarding the mechanism, i.e. what the molecules with anti-adhesive effect bind to, remains unanswered.

6.1.1 Hypothesis and aims

The main hypothesis of this chapter is that whey proteins differ in their adhesive properties and that some of them adhere to components of the human small intestinal biofilm. Therefore this chapter aims to prepare monocultures of selected bacteria with the propensity to form biofilms and to use them for the adhesion assay to screen for adhesive whey proteins as described in

Chapter 2, Section 2.4.2. The reductionist approach taken here employs liquid cultures of selected bacteria which carry genes encoding the production and secretion of different types of biofilm polymers which together represent a great proportion of extracellular matrix found in biofilms *in vivo*. However, it was not the aim of this chapter to develop realistic and reproducible multi-species biofim as it might occur in the human GIT.

6.2 Results

6.2.1 Development of the adhesion assay

The adhesion protocol was transferred from the assay developed using mucin coated Sepharose beads (Chapter 2, Section 2.4). The protocol needed to be adapted to experiments with bacteria. Assay optimisation included the selection of a bacterial affinity method (biofilm model), the addition of a fluorescent label to differentiate proteins of different origins and the effects of the wash-cycle (data not shown). The individual optimisation steps are presented in the first part of this chapter.

6.2.1.1 Selection of model for bacterial biofilm components

Initial experiments investigated the use of isolated bacterial biofilm components (specifically monomeric GlcNAc) attached to Sepharose beads, in a similar manner to mucin bead experiments described in Chapter 4. Here, again, there was no observed difference between GlcNAc covered beads and NC beads (Figure 6.1), likely due to insufficient coverage of the Sepharose beads with GlcNAc monomers. Another cause of concern was that both, Sepharose and GlcNAc, are saccharides and thus have structural similarities. Thus it was likely that proteins would also bind to the beads instead of the GlcNAc monomers. Finally, GlcNAc in bacterial biofilms exists as polymers and its purification and size reduction into monomers was likely to change its binding behaviour. The experimental approach was altered and cell pellets were used for all further bacterial experiments. Bacteria may provide an adequate method for isolating adherent proteins as they can be separated from suspension by centrifugation. Although bacterial pellets contain several surface and extracellular structures which all can

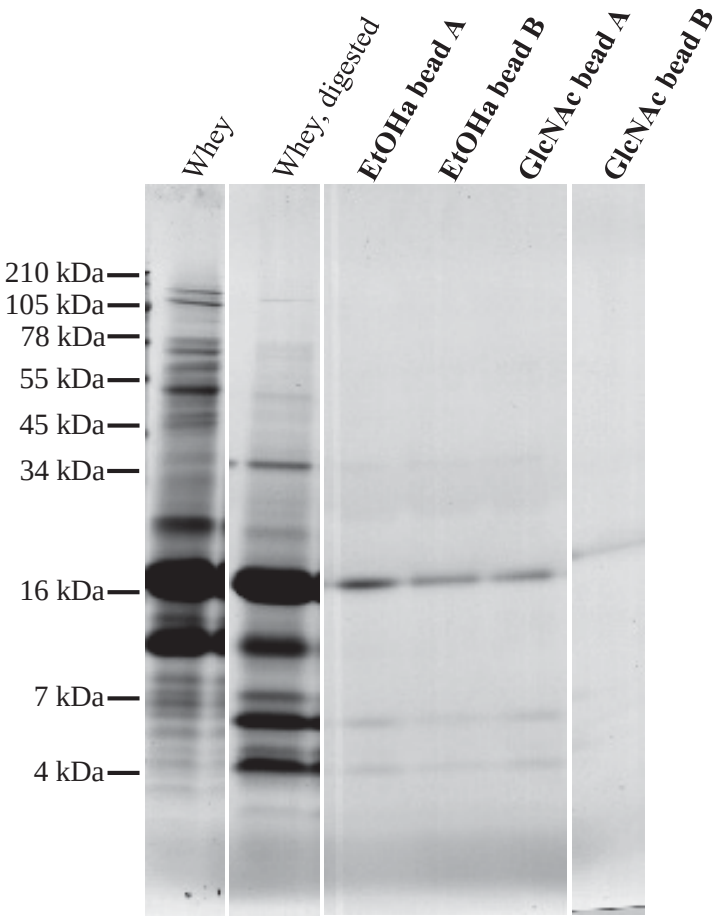

Figure 6.1: Binding of whey proteins to GlcNAc covered Sepharose and negative control beads
Reducing SDS-PAGE of GlcNAc covered Sepharose beads after incubation with whey. Beads A showing all adhering proteins, beads B showing proteins adhering after wash cycle (Figure 3.16). Washed beads prepared in 70 µl SLB. Bands assembled form the same gel of an adhesion assay. Gel separated at 130 V for 2 hr and stained with CBB G250 overnight. Bold font indicates samples that contain Sepharose beads (i.e. shows adhering proteins). GlcNAc: N-acetyl-glucosamine.

influence binding of proteins, this was considered a more realistic approach. To reduce the influence of components other than the biofilm component of interest, bacteria with the propensity to produce biofilms with one main component, i.e. pGlcNAc (*S. epidermidis* 1457) or bacterial cellulose (*E. coli* Nissle 1917), were chosen.

The approach taken here, using pellets of bacterial cells grown in liquid cultures, was not expected to result in large quantities of secreted biofilm matrices. In order to change their methabolism from planktonic to sessile, bacteria need to adhere to a surface (compare Section 1.2.3.1), e.g. liquid-solid. In a liquid culture, only a minor proportion of bacterial cells might adhere to the culture tube wall which could resulst in the secretion of low levels of extracellular matrix components. However, these quantities do not suffiently cover all bacterial cells and have limited effect on the adhesion properties of the cell pellets. Thus, most of the binding observed, is expected to be dependent on the nature of the bacterial cell surfaces.

For the first experiments with bacterial cell pellets, the adhesion assay was adapted from the mucin bead assay. The bacterial cell pellets were mixed with whey or digested whey, incubated for 30 min, washed, solubilised in SLB and then separated on a SDS-PAGE gel. Regular CBB stained SDS-PAGE gels did not allow bacterial and digested whey proteins to be differentiated (Figure 6.2) as the Coomassie binds equally to all proteins in the gel (despite its low quality, this SDS-PAGE gel was included in this thesis to demonstrate that the use a fluorescent label was necessary for the screening of whey proteins adhering to bacterial celsl or IEC). Thus samples with bacterial cell pellets contained too much protein and the whole lane was strongly stained. An appropriate dilution of bacterial pellets to provide separation of distinct protein bands would most likely decrease the whey protein content below the detection limit. Although samples from wash solutions contained less protein overall and individual bands were observed, it was still impossible to confidently identify whey protein bands. More protein bands were observed in the wash solutions with 20% EtOH and 2.5M LiCl than in the input material. This was a strong indication that bacterial surface structures were also removed during the wash cycle; mostly

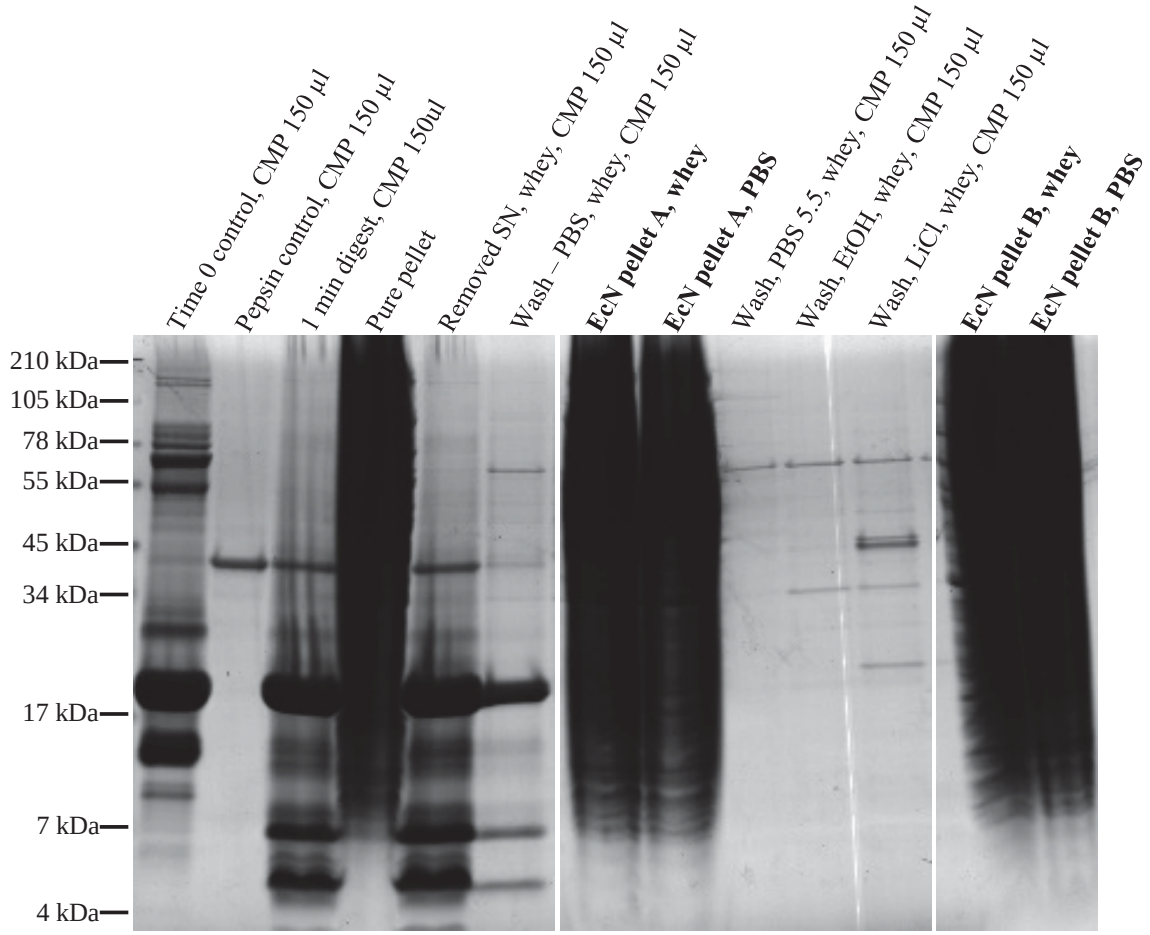

Figure 6.2: Adhesion assay between *E. coli* Nissle and whey

Reducing SDS-PAGE gel of *E. coli* Nissle 1917 pellets after incubation with whey. Supernatants 150 µl CMP, pellets prepared in 70 µl SLB. Gel separated at 130 V for 2 hr and stained with CBB G250 overnight. Bold font indicates samples that contain bacterial cell pellets (i.e. shows adhering proteins). CMP: chloroform-MeOH precipitation.

during the LiCl wash. Also, as all proteins were stained equally, one band could represent both, bacterial and whey proteins, if the proteins had the same molecular weight.

Further investigations to resolve these issues were conducted before the feasibility of using bacterial pellets for direct purification of adherent proteins could be determined.

6.2.1.2 Inclusion of fluorescent label

To enable bacterial and whey derived proteins to be distinguished, whey and digested whey were tagged with a relatively small fluorescent label; first DL594 (1.1 kDa), later Rhd (0.48 kDa). This allowed the bacterial and milk proteins to be differentiated by fluorescent scanning (Figure 6.3). Only two of the molecular weight marker bands were visible in the fluorescent scan. Thus only these two bands (25 kDa and 75 kDa) were labelled in figures with fluorescent scans. Other molecular weights referred to are based on comparison with Coomassie stained SDS-PAGE gels of whey (Figure 3.1) and experience.

Figure 6.3 shows samples from an adhesion assay, including whey (lane 1 to 3), whey sediment (lane 4 to 6), pure bacterial pellets (lane 7 to 9) and bacterial pellets after incubation with whey (lane 10 to 15). The experiment was done in triplicate and all three replicates are shown in the figure (numbers 1, 2, and 3 after sample descriptions), bacterial pellets were loaded twice per replicate (numbers 1 and 2 after replicate numbers in sample descriptions in lanes 10 to 15).

The scan shows that the labelling of whey proteins was successful as the observed band patterns in the fluorescently labelled whey (lanes 1 to 3) corresponded to the one of whey after CBB staining (e.g. shown in Figure 3.1). Although the whey used for the experiment was sediment free whey, there were some protein residues remaining in the Eppendorf tubes when the assay was done with only whey in the tubes. These residues are shown in lanes 4 to 6. In their molecular weight the residues corresponded to β-LG (18 kDa) and caseins (25 kDa) which were shown before to not be completely removable (compare Figure 3.1 and Figure 4.13). Lanes 7 to 9 contain only the bacterial cell pellets of the respective microorganisms (A: *E. coli* Nissle 1917. B: *S. epidermidis* 1457. C: *S. epidermidis* 1457 M10). Thus these lanes show the auto-

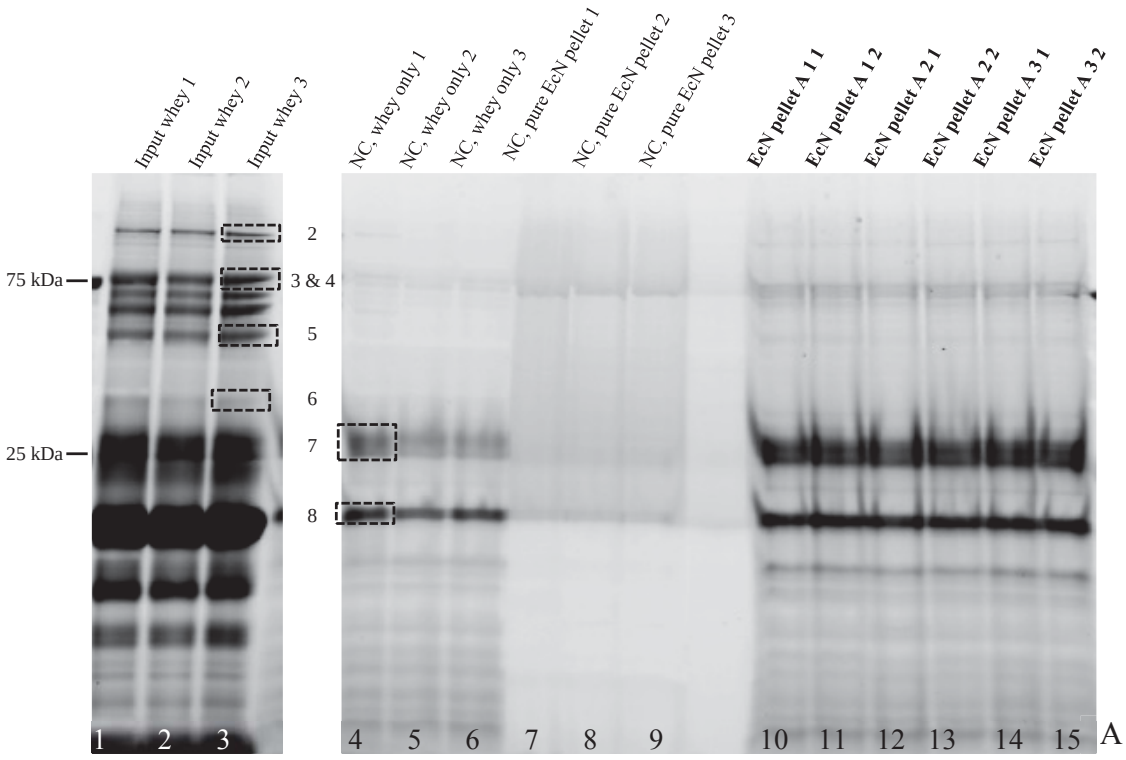

Figure 6.3 A: Adhesion assay between bacterial cell pellets and Rhd-labelled whey

Reducing SDS-PAGE gel of (A) *E. coli* Nissle 1917 pellets A, 2 x 10^8 cfu, after incubation with Rhd labelled sediment-free whey or with PBS (NC). Pellets prepared in 60 µl SLB. Gel separated at 130 V for 2 hr and scanned with FX proplus fluorescent scanner at low sample intensity. Mass spectrometry spots indicated with black boxes (A) and density of selected bands (molecular weight indicated in B and C) was analysed in Figure 6.4. Bold font indicates samples that contain bacterial cell pellets (i.e. shows adhering proteins).

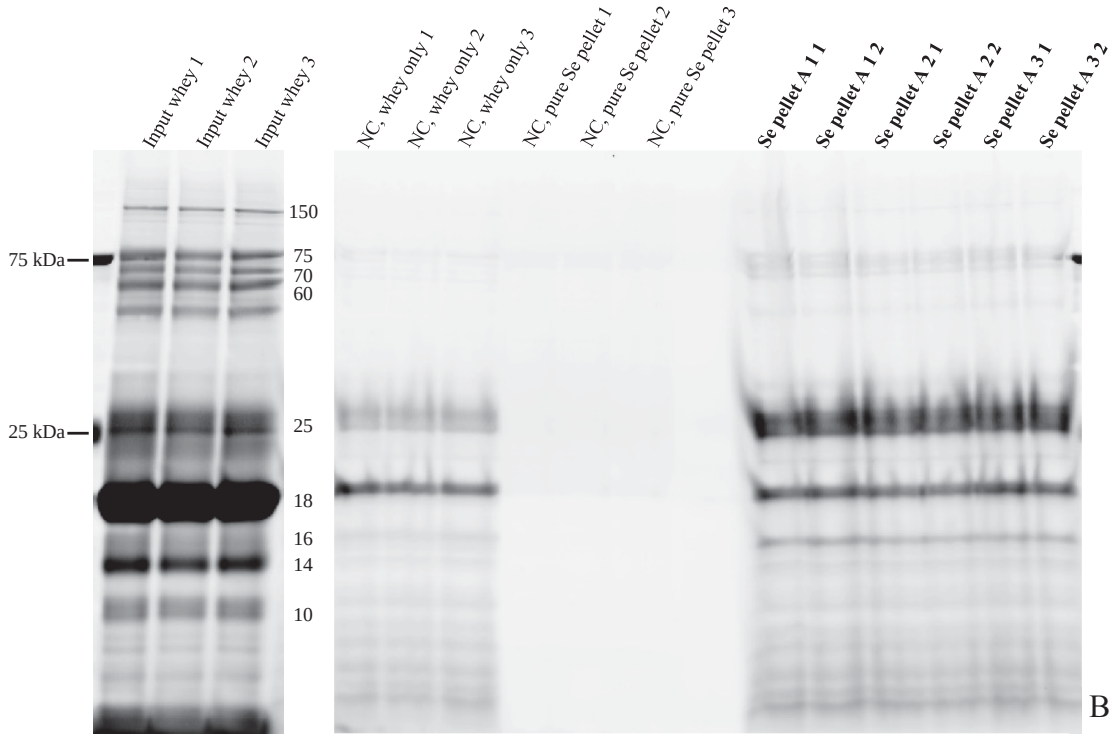

Figure 6.3 B (continued): Adhesion assay between bacterial cell pellets and Rhd-labelled whey

Reducing SDS-PAGE gel of (B) *S. epidermidis* 1457 pellets A, 2 x 10^8 cfu, after incubation with Rhd labelled sediment-free whey or with PBS (NC).

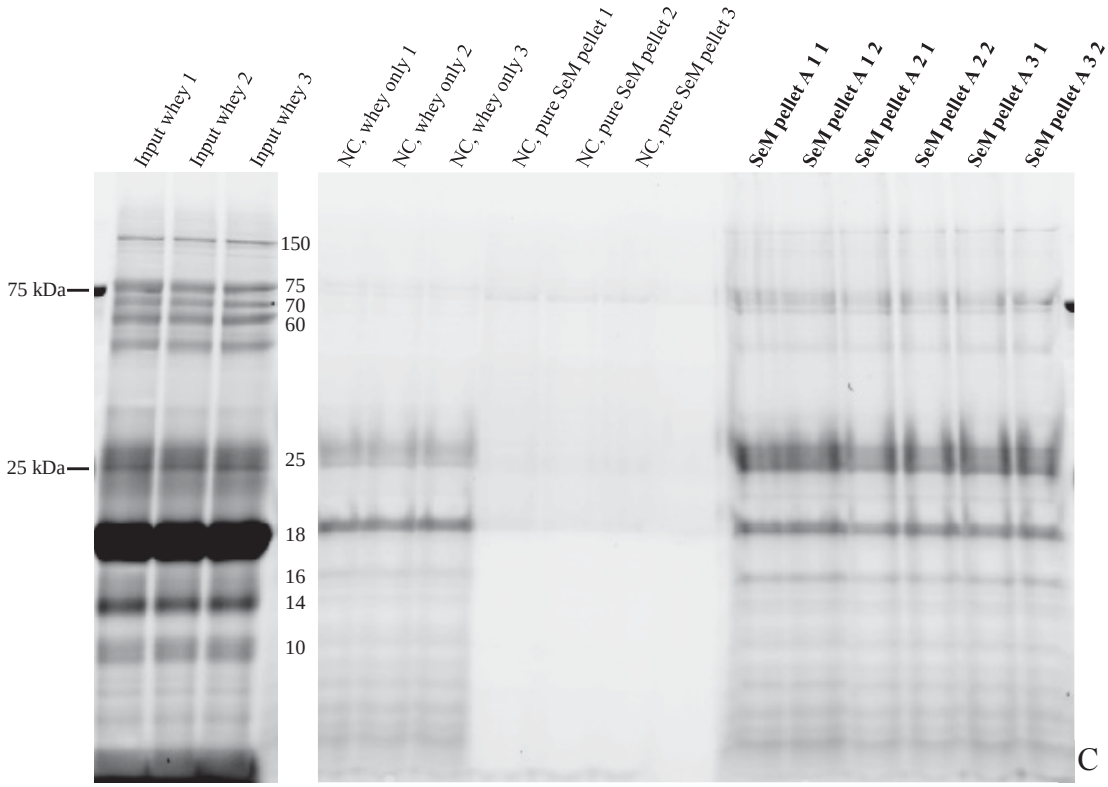

Figure 6.3 C (continued): Adhesion assay between bacterial cell pellets and Rhd-labelled whey

Reducing SDS-PAGE gel of (C) *S. epidermidis* 1457 M10 pellets A, 2 x 10^8 cfu, after incubation with Rhd labelled sediment-free whey or with PBS (NC).

fluorescence of the bacteria at the excitation and emission wavelengths used in this assay. The faint bands were most likely carry-over from neighbouring lanes or shadows in the gradient gel itself. Finally, lanes 10 to 15 show whey proteins adhering to bacterial cell pellets. The bacterial pellets were incubated with the fluorescently labelled whey for 30 min and unbound protein was washed off with PBS. Bands representing adhering proteins were observed at 150 kDa, between 60 kDa and 70 kDa, 25 kDa, 18 kDa and 14 kDa for all three bacteria. Further, a 10 kDa band was quantified for *E. coli* Nissle 1917 (Figure 6.3 A). For quantification of binding proteins (Figure 6.4), individual bands were quantified (binding proteins in lanes 10 to 15, pure bacterial pellets in lanes 7 to 9) using QuantityOne and corresponding background signal from whey sediment (lanes 4 to 6) was subtracted.

6.2.3 Use of the adhesion assay to identify bacterial adherent whey proteins

Density analysis was done for up to nine bands (150 kDa, 75 kDa, 70 kDa, 60 kDa, 25 kDa, 18 kDa, 16 kDa, 14 kDa and 10 kDa) which were identified as whey proteins binding to bacteria (indicated for *S. epidermidis* 1457 and *S. epidermidis* 1457 M10 in Figure 6.3 (B) and (C)). Density analysis is shown in Figure 6.4. This shows that most of the analysed proteins bound well to the bacteria, showing stronger band intensity than the pure bacterial pellets. Only the 150 kDa protein did not bind to *E. coli* Nissle 1917, whereas this was the only bacterium with binding of the 18 kDa band. The 10 kDa band which has only been analysed for *E. coli* Nissle 1917 showed no significant binding. The higher molecular weight proteins (60 to 150 kDa) gave the strongest signal when binding to *S. epidermidis* 1457 M10. On the contrary, the lower molecular weight bands were strongest for *E. coli* Nissle 1917 (18 kDa) or *S. epidermidis* 1457 (25, 16 and 14 kDa), respectively. The strongest signal overall was observed in the 25 kDa bands, the lowest in the 18kD bands. The latter is surprising as the bands appear strong in lanes 10 to 15 (adhering proteins) of Figure 6.3. However, a comparison with lanes 4 to 6 (background signal from whey sediment) showed that most of this signal was caused by protein sedimenting and remaining in the tube but not by binding to the bacterial pellets.

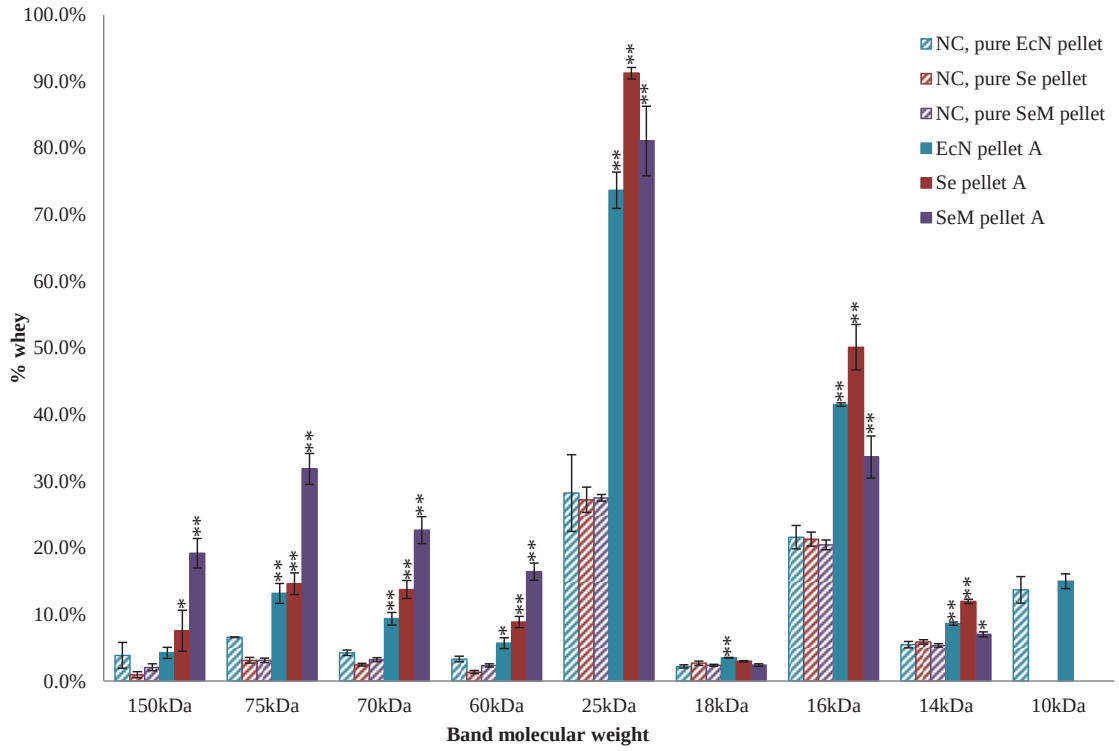

Figure 6.4: Density analysis of bands from Figure 6.

Bar graphs for bands indicated in Figure 6.3 analysed with QuantityOne. Band densities are expressed as percentage of input whey band density. Where there is no bar, no protein band was detectable above background. Results are averaged of three repetitions. NC: Negative control. EcN: *E. coli* Nissle 1917. Se: *S. epidermidis* 1457. SeM: *S. epidermidis* 1457 M10. STD deviation is indicated by error bars and significance levels to NC pellet are shown (*significant, **highly significant).

6.2.4 Identification of adhering milk proteins by mass spectrometry

Bands of interest were analysed by LC-MS/MS. Spots are indicated by black boxes in Figure 6.3 A. Results are shown in Table 6.1. Proteins detected were LF and Ig-components; both are associated with innate immunity and were expected to interact with bacteria. Further, two MFGM proteins, component PP3 and xanthine oxidoreductase, were identified. A possible explanation for the binding of these proteins to bacteria is that the MFGM is partially derived from the surface of secreting mammary cells and thus it carries properties of epithelial cell surfaces [563]. Bacteria are targeting epithelial surfaces to adhere to and thus MFGM proteins might trigger adhesion. The band excised at 18 kDa was identified as β-LG, the major whey protein. Some hydrolysis products of BSA were also identified as bacterial adhesins.

6.2.5 Validation of adhering proteins using Western blot analysis

To confirm whether the bands with greater abundance (Figure 6.3) were the proteins identified by mass spectrometry (Table 6.1), Western blot analysis was conducted. Figure 6.5 and Figure 6.6 show the results for LF, IgA, IgG heavy chain, IgM, xanthine oxidoreductase and β-LG after probing with primary antibody-horse radish peroxidase conjugates. Similar to Figure 6.3, experiments were done in triplicate. However, to allow a comparison between the three bacteria, samples from all three strains were analysed on the same blot. Thus, only two whey samples (lane 1 and 2), and one bacterial pellet without whey per microorganism (lane 6 (*E coli* Nissle 1917), lane 10 (*S. epidermidis* 1457), and lane 14 (*S. epidermidis* 1457 M10)) could be accommodated on the blot. Lanes 1 and 2 show the signal from whey (positive control) and lanes 3 to 5 show signal from whey sediment. As before in the SDS-PAGE gels, β-LG was observed in the whey sediment (whey only controls). The other proteins gave no, or very faint (LF, IgM) signals. Samples from bacteria incubated with whey were analysed in triplicate: lanes 7 to 9 (*E coli* Nissle 1917), lanes 11 to 13 (*S. epidermidis* 1457), and lanes 15 to 17 (*S. epidermidis* 1457 M10). LF, IgM and IgG heavy chain (50 kDa) showed signals for all three bacteria incubated with whey, but not in the respective bacterial pellets alone, indicating binding of these three proteins. Probing with IgG heavy chain or IgM antibodies further resulted in

Table 6.1: Bacterial binding proteins identified by LC-MS/MS

Bands are indicated in Figure 6.3 (A). Bands 1, 9 and 10 are not shown in Figure 6.3 (A).

MW: molecular weight. Digested: *In vitro* gastric digest of whey. Whole: Undigested whey. LF: lactoferrin. Ig: Immunoglobulin. β-LG: β-lactoglobulin.

#	MW excised	Protein identified as	Peptide hits	MW theor.	Substrate (whey)
1	150	Component PP3	2	15	digested
2	150	Xanthine oxidoredutase	12	147	whole
3	75	LF IgM (hc, const region)	15 5	75 76 to 92	whole
4	75	LF	7	75	whole
5	52	Ig (hc, const. region)	4	36 to 51	whole
6	35	Not identified	---	---	whole
7	25	Ig (light chain, various loci)	14	25	whole
8	18	β-LG	11	18	whole
9	5	Albumin	20	66	digested
10	3	Albumin	11	66	digested

signals indicating binding for a ca. 22 kDa band in *S. epidermidis* 1457 M10, IgM also showed a 50 kDa band for *S. epidermidis* 1457 M10. Due to excess signal over *S. epidermidis* 1457 M10 which could not be reduced, IgA and xanthine oxidoreductase could not be evaluated precisely. Although fractions of IgA appeared to bind better to the two *S. epidermidis* 1457 strains than to *E. coli* Nissle 1917.

Blots were evaluated by measuring the density of individual bands with QuantityOne (Figure 6.5 and Figure 6.6). Results of the quantification are shown in Figure 6.7. All tested proteins or their fractions with exception of β-LG showed significant binding to *S. epidermidis* 1457 M10. Binding to the other two bacteria was lower and only significant for the 75 kDa IgM fraction, and LF also bound to *E. coli* Nissle 1917.

The data for β-LG is not significant due to the residual protein in the negative controls. This suggests that β-LG does not bind well to bacteria in a competitive environment. Results by Petschow et al. [564] support this observation. The authors showed in competitive binding studies that adhesion of β-LG was inhibited by LF. However, β-LG should still be considered for further experiments as it is a major whey protein and could be added in high concentrations to favour its adhesion. Thus binding can be increased despite low binding affinity. Signals for IgA (2) and xanthine oxidoreductase in *S. epidermidis 1457* M10 could not be analysed due to the high background signal. It was suggested that this signal was caused by the binding of antibody-HRP conjugate to components of the unprotect cell surface of the mutant. Attempts were made to control the signal by including a peroxide blocking step or using a more specific primary-secondary antibody system, but both were unsuccessful.

6.2.6 Direct visualisation of adhering proteins with fluorescent microscopy

Fluorescent microscopy was used to visualise adherence of fluorescently tagged proteins from whey and skim milk to bacteria. Both whey and skim milk were readily available and used for initial fluorescent microscopy experiments. Skim milk was chosen over whole milk to focus on

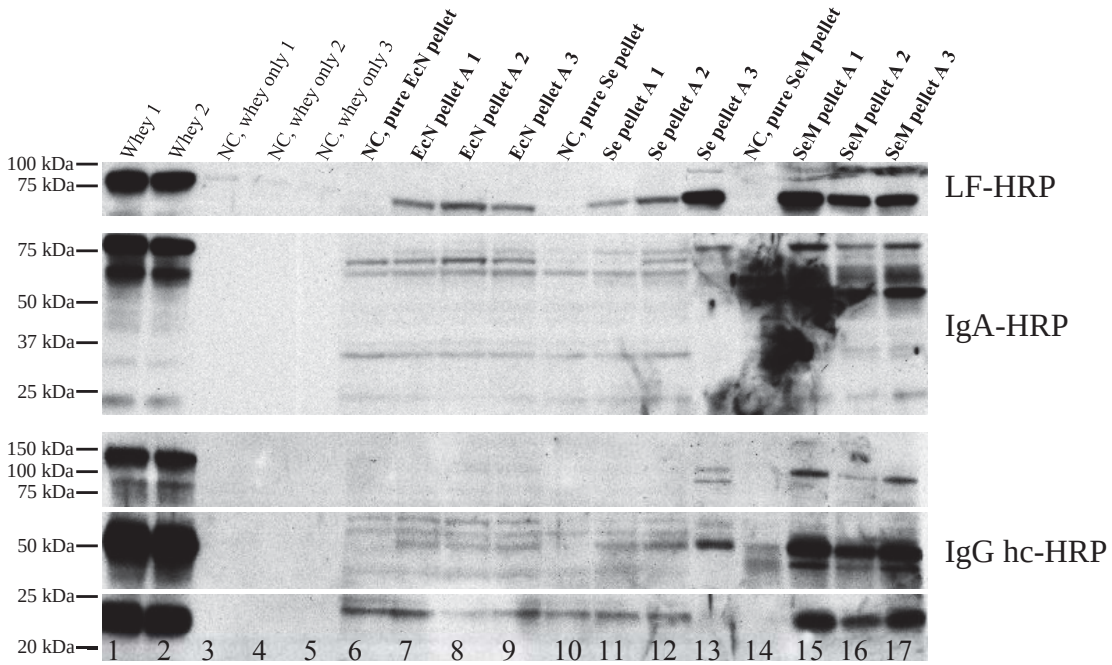

Figure 6.5: Western blot analysis of all bacteria for LF, IgA and IgG heavy chain

Western blot for different proteins I of all three bacterial pellets A after incubation with sediment-free whey (3-fold samples) and PBS (NC, 1 sample each). Gels separated at 130 V for 2 hr, transferred overnight at 15 V, 3 hr block with 4% NFM, overnight incubated with HRP-conjugated antibodies and exposure after ECL. Bold font indicates samples that contain bacterial cell pellets (i.e. shows adhering proteins).

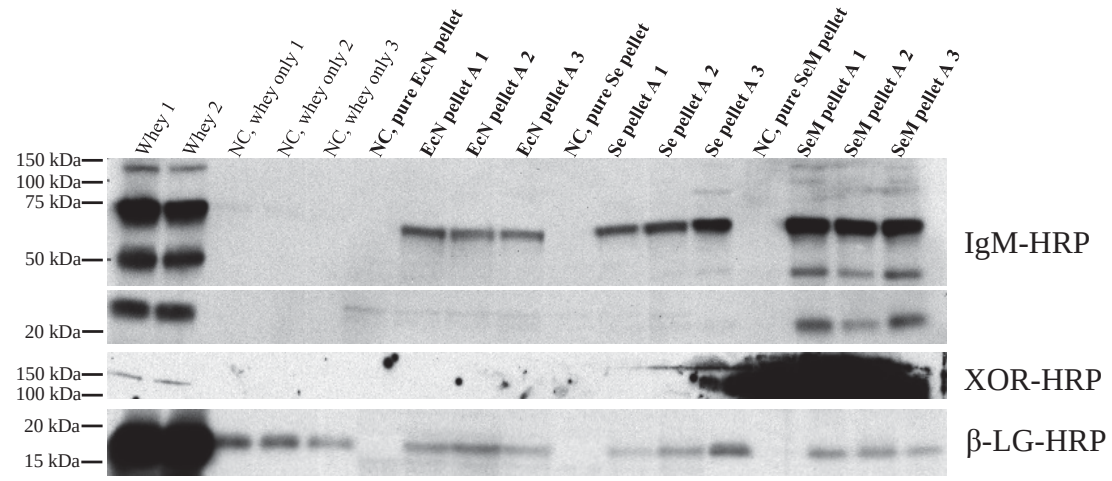

Figure 6.6: Western blot analysis of all bacteria for IgM, XOR and β-LG

Western blot for different proteins II of all three bacterial pellets A after incubation with sediment-free whey (3-fold samples) and PBS (NC, 1 sample each). Gels separated at 130 V for 2 hr, transferred overnight at 15 V, 3 hr block with 4% NFM, overnight incubated with HRP-conjugated antibodies and exposure after ECL. Bold font indicates samples that contain bacterial cell pellets (i.e. shows adhering proteins).

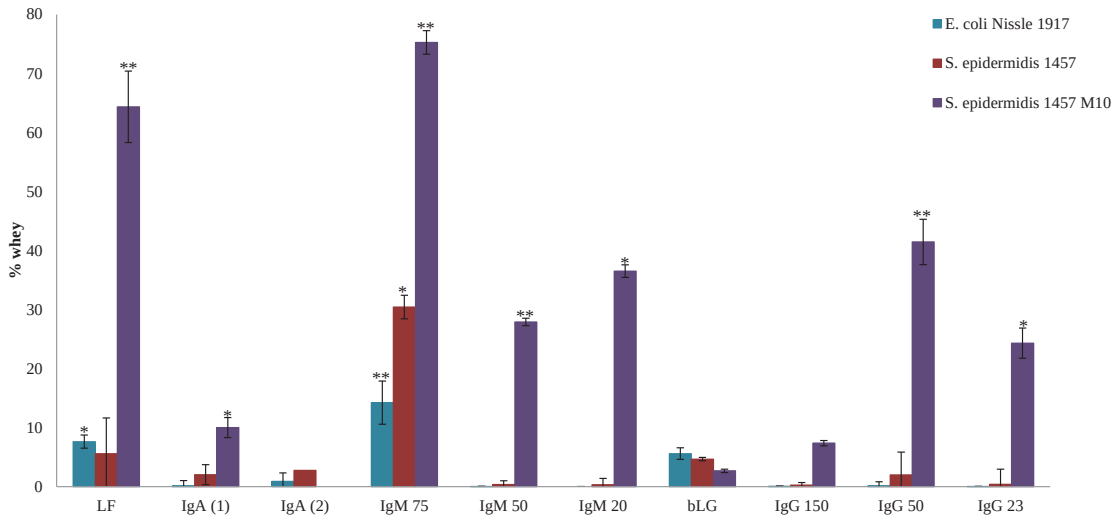

Figure 6.7: Density analysis of bands from Figure 6.5 and Figure 6.6

Bar graphs for proteinbands from Figure 6.5 and Figure 6.6 analysed with QuantityOne. Band densities are expressed as % of input whey band density. IgA was analysed twice, from two samples. STD deviation is indicated by error bars and significance levels to NC pellet are shown (*significant, **highly significant). No bars for NC tubes are shown as they were close to 0% input whey apart from β-LG where their value was 7.4% input whey.

protein-adherence and reduce effects from fats and phospoholipids contained in whole milk. Rhd-tagged whey and skim milk was mixed with bacteria and unbound material washed off with PBS. Bacteria were then prepared for microscopy. For labelling, the same flurophore-to-protein ratio was used for skim milk and whey, but labelling efficiency was not determined. Figure 6.8 shows composite pictures of phase contrast and fluorescent images of all three bacteria after incubation with whey or skim milk. As expected, no fluorescence was observed in the PBS samples (left column). This shows that there was no auto fluorescence at the selected excitation and emission wavelengths. When comparing bacteria incubated with whey and skim milk, the skim milk treated bacteria showed more fluorescence (as a proxy for binding proteins) than the corresponding whey treated sample. The difference between whey and skim milk is the presence of caseins in skim milk. Thus it is possible that the increased fluorescence was caused by caseins, suggesting that caseins bind well to bacteria. Further, most fluorescence was observed in *S. epidermidis* 1457 M10 samples whereas *S. epidermidis* 1457 showed no fluorescence. *E. coli* Nissle 1917 lies in the middle; however it seems to be more similar to *S. epidermidis* 1457 than to *S. epidermidis* 1457 M10. This suggests that more skim milk and whey protein molecules bound to the mutant which is unable to produce or secrete pGlcNAc and thus has no biofilm. Similar to the isogenic *ica*-mutant *S. epidermidis* 1457 M11 which does not produce a capsule, also the M 10 strain used here is likely to have no capsule [565].

In the *E. coli* Nissle 1917 cultures, fibrous strands can be observed. To exclude a contamination, the culture was plated onto LB agar and incubated for 7 days at 37°C. The plates were checked every day and no secondary culture was observed. It was further excluded tha the fibers were introduced through handling errors as they were only apparent in the *E coli* Nissle 1917 but not in either of the *S. epidermidis* 1457 cultures. Thus it is suggested that the fibrous structures could be bacterial cellulose secreted by few cells adhering to the culture tube wall (polystyrene). This is supported by the protein binding properties of the fibers (micorpgraph labelled “EcM, Rhd-skim milk”) which agrees with data summarised in Section 1.2.2.5).

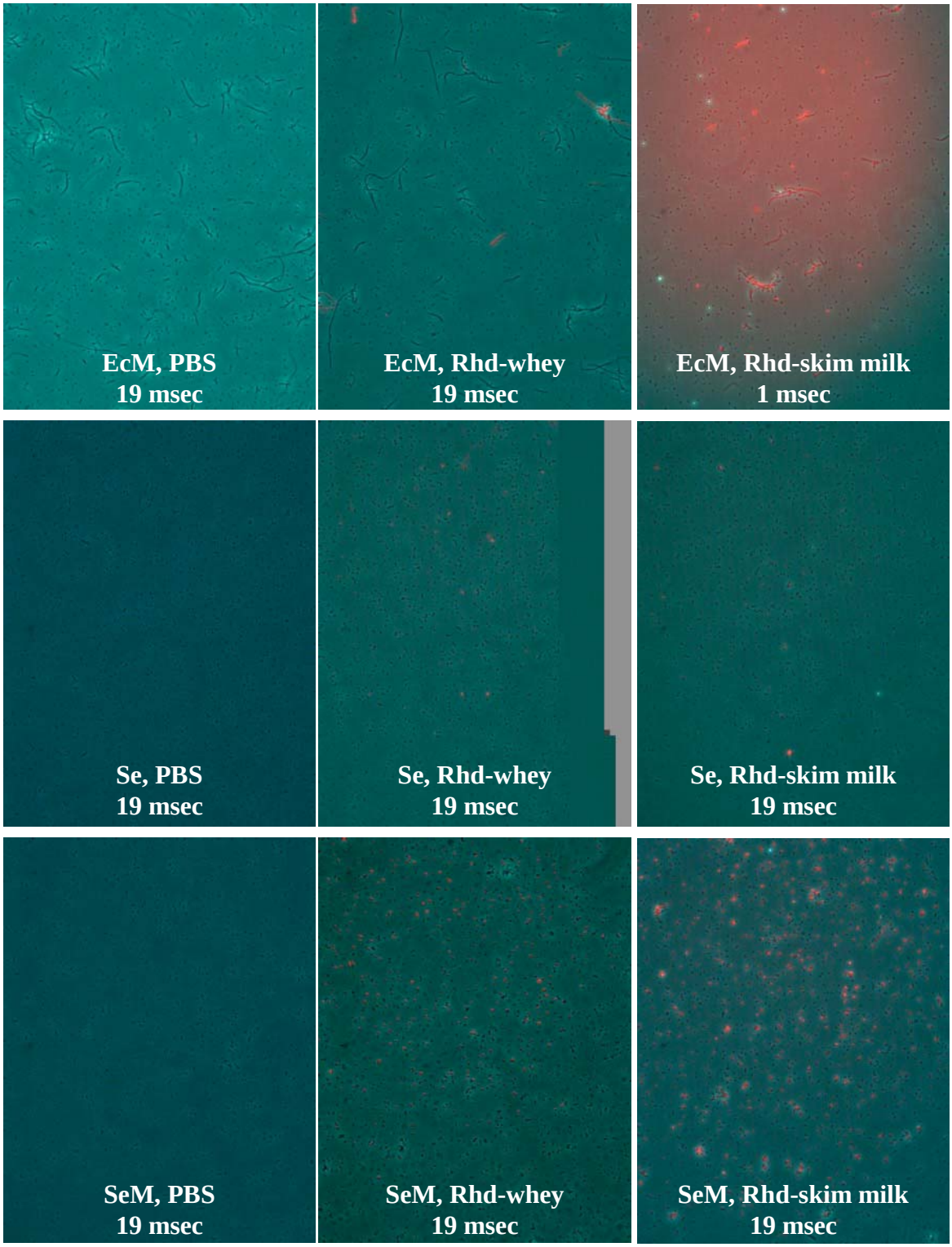

Figure 6.8: Micrographs of Rhd-skim milk or Rhd-whey binding to bacteria

Overlay micrographs of phase contrast and fluorescent images from all three bacteria after incubation with PBS NC (left column), whey (middle column) or skim milk (right column). Bacteria were incubated for 30 min, washed with PBS and fixed in 4% glutaraldehyde. 10 µl suspension per microscope slide and sealed under cover slip.

6.3 Discussion

6.3.1 Adhesion assay

The adhesion assay could be transferred from mucin-covered beads (Chapter 4) to bacterial cells with some adaptions. Like for IEC in culture (Chapter 5), the milk proteins needed to be labelled with a flurophore to differentiate between bacterial and milk derived proteins on the SDS-PAGE gels. Also, the wash sequence with 20% EtOH and 2.5 M LiCl had to be excluded from the assay as the exact site of protein removal through the wash could not be determined (data not shown). Thus, the analysis focussed on pellets A (cell pellets containing all adhering milk proteins) to gain information on all adhering proteins; however the mechanism of binding was not investigated.

The two representative microorganisms are both *Enterobacteriaceae*. This decision is supported by the fact that the properties of cellulose from this family are more suitable for a microorganism to adhere to surfaces, as it occurs in biofilms in the human GIT, than those of *Gluconacetobacter ssp*. (compare Section 1.2.3.5).

6.3.1.1 Impact of bacterial surface structures on the wash cycle

Treatment of the pure bacterial cell pellets with 2.5 M LiCl confirmed that this wash solution extracts bacterial cell surface proteins for up to 11 treatment cycles (data not shown). The observation agreed with results of Sanchez et al. [566], although the authors used 5 M LiCl, and Tiong et al. [567]. As bacterial proteins were removed during the wash cycle it was not possible, using SDS-PAGE analysis, to determine if the whey proteins were removed alone or as complexes with bacterial surface proteins. Determining this might be possible using native PAGE and appropriate mass spectrometry analysis to detect bonds between different proteins [568].

The effect of the EtOH wash step was also questionable as EtOH can change the protein structure [569-571]. Thus the bacterial surface proteins could change their conformation and

consequently binding potential. Because of these unknown effects the focus was shifted to pellets A.

6.3.1.2 Adhesion assay

The binding of proteins from whey (not isolated whey proteins) to *E. coli* Nissle 1917, *S. epidermidis* 1457 and *S. epidermidis* 1457 M10 cell pellets was described for the first time. Adhering proteins represented a subset of the input whey (Figure 6.3). This indicates selective binding under competitive conditions. Competitors here were other whey proteins but *in vivo* could also be proteins from different food components in the digesta. The binding pattern between the three bacteria was very similar (Figure 6.3), e.g. bands at 60 to 75 kDa, 25 to 30 kDa and 18 kDa which were further analysed and identified by mass spectrometry (Section 6.3.2). Unfortunately, the nature of binding could not be evaluated, as described above. From what is known about the biofilm structures, expected interactions with proteins are hydrogen bonding (cellulose [383, 387]) or electrostatic interactions (PIA [397]); but not covalent bonds. Further physical trapping of molecules might also occur. Contrary, interactions with bacterial adhesins on the cell surface are characteristically lectin-based [541-544].

6.3.2 Mass spectrometry and Western blot analysis

Mass spectrometry analysis of proteins and peptides of interest led to the identification of four different adhering proteins (counting Igs and specific regions thereof as one protein) from undigested whey and further fragments of component PP3 and BSA (Table 6.1). Three of these proteins (LF [572-574], Igs [575-577], and xanthine oxidoreductase [578, 579]) are known to interact with bacteria. Xanthine oxidoreductase is a MFGM protein associated with innate immunity [580, 581]. Further β-LG was detected. It is a well-studied major whey protein [582] with yet unclear biological function [583-585]. Hydrolysis products (component PP3 and BSA) will not be discussed due to low peptide scores and because validation of the fragments with Western blot was difficult. All mass spectrometry analysis was done on samples containing whey sediment, so these results are only an indicator for candidate adhering proteins. Final validation was done by Western blot with sediment-free whey.

Western blot shows that the IgM heavy chain (75 kDa) binds well to the bacterial surface (strong signal from *S. epidermidis* 1457 M10) and less to the bacteria with the propensity to form a biofilm (less signal from wild types; Figure 6.5 to Figure 6.7). This might be explained by the function of the biofilm to protect and hide bacteria from harmful immune components (e.g. reviewed by Costerton et al. [317]). IgM light chain (22 kDa) and F(ab)' or Fc fragment (50 kDa) bound only to *S. epidermidis* 1457 M10, indicating binding to the cell surface directly. Although extracellular matrix is characteristic for biofilms, not all bacterial cells in a biofilm are covered by the matrix. It was demonstrated that the bottom layer of a biofilm becomes more and more rich in dead bacteria [586]. This suggests that the percentage of extracellular matrix in this area of the biofilm reduces over time. Despite the compaction taking place at the same time [587, 588], the biofilm architecture does not collapse and voids and channels remain open [588]. Thus it becomes more likely that bacterial cells surfaces are not masked by extracellular matrix and are accessible for solutes. It was further shown that mature biofilms are more susceptible to eradication by chemical agents such as N-chlorotaurine [589]. Taken together this suggests that biofilms with a comparably high percentage of free bacterial cell surfaces are more likely to be available for binding of proteins, e.g. Igs. Thus introducing non-biofilm producing bacteria, e.g. the PIA-depleted *S. epidermidis* 1457 M10, into biofilms could be beneficial for targeting nutrient vehicles to intestinal biofilms. However, the introduced bacteria must be safe and may not present substitute virulence-factors as a result of the extracellular matrix-depletion.

Further, during the early stages of biofilm development, initial sessile bacteria are not yet protected by a biofilm matrix (Figure 1.7). Thus it is likely that bacteria in an immature biofilm are not protected from the immune system and are more easily to detect and eradicate.

Of the IgG fractions, only the heavy chain (50 kDa) bound to all three bacteria, best to *S. epidermidis* 1457 M10. This agrees with the mass spectrometry results which showed that a constant region in the heavy chain but also the light chain of Igs bind to bacterial pellets. Analysis of Ig-binding in this study showed all of the tested Igs (IgG, IgM and IgA; Figure 6.7) adhered with one or several fractions to the bacteria. Binding to the biofilm-free *S. epidermidis*

1457 M10 was consistent throughout all tested Igs. This agrees with the theory that Igs can bind with the proteins expressed by bacteria, especially pathogens. These proteins for example are protein A (pI 5.1) or protein G (pI 3.5) [590-594]. These molecules are charged at physiological pH and are able to undergo electrostatic interactions. sIgA also was found to bind to *E. coli* in a fimbriae and capsule independent manner [595].

Xanthine oxidoreductase did not bind to the bacteria with the propensity to form biofilms. Analysis of *S. epidermidis 1457* M10 was not possible due to excess signal. Whether the signal came from bound xanthine oxidoreductase or antibody binding to the bacterial cells or a mixture of both could not be determined. Xanthine oxidoreductase does have an affinity for acidic polysaccharides, which occur in bacterial capsules [596, 597] and was identified as binding protein by mass spectrometry. Despite these indications that it could be a sticky protein, xanthine oxidoreductase might not be suitable for targeting nutrients to intestinal bacteria. Hypoxic conditions in the intestinal tract are detrimental to bacteria due to the formation of antimicrobial superoxide, hydrogen peroxide or peroxynitrite from bacterial metabolites [579].

The Western blot shows good binding for LF, with the strongest bands detected for *S. epidermidis* 1457 M10 (Figure 6.5 and Figure 6.7). LF is a glycoprotein [598] with a high isoelectric point and is positively charged at physiological pH. Consequently, LF interacts with negatively charged bacterial surface structures [599], like lipopolysaccharide [600] but also receptors [601-603]. It has been shown to inhibit adhesion of several bacteria, including *S. epidermidis* [573, 602, 604], even at low concentrations [605] and independent of colonisation form [606]. The findings of this study agree with the literature regarding the ability of LF to bind to bacteria. Like binding of Igs, this information is not new, but it shows that the assay is able to produce valid data.

Two glycosides are contained in several of the above proteins, Man and NeuNAc. NeuNAc is also an element in the glycoside side chains of mucins which protect the intestinal S-layer from bacteria (microorganisms are trapped and in and removed with the fast eroding mucin). This

suggests that NeuNAc acts as bacterial adhesin, most likely due to the negative net charge it displays at physiological pH, and that glycoproteins which carry accessible NeuNAc show superior bacterial binding. Thus, coupling NeuNAc (or other binding groups) to proteins could improve their binding potential. The function of Man could be based on lectin-mediated binding [607]. This hypothesis of glycoside-mediated binding will be discussed in more detail in Chapter 8.

Under competitive conditions α-LA was not able to bind to bacteria (14 kDa band from the input whey does not appear on pellets A in Figure 6.3). This agrees with findings by De Araujo et al. [605] who demonstrated that even isolated α-LA has no *E. coli* (EPEC) adhesion. Barman et al. [12] described a minor (heterogeneous) fraction of α-LA, glyco-α-LA, which contains 11 to 12 sugar residues (GalNAc, Man, Gal, GlcNAc and NeuNAc). The molecular weight of this fraction was about 16.8 kDa which corresponds to the yet unidentified SDS-PAGE band at 16 kDa (Figure 6.3). Shida et al. [608] also found a 16 kDa whey protein with N-terminal sequence similarity to α-LA and glycoside appendices in the proteose peptone fraction which bound to *E. coli* heat-labile enterotoxins. However, the authors concluded that the fraction was not glyco-α-LA but a Maillard-product which develops during the preparation of the proteose peptone fraction. The 16 kDa binding protein described here could be a naturally occurring glycoprotein fraction of α-LA that is able to adhere to bacterial surfaces via its sugar moieties. This hypothesis however needs confirmation by mass spectrometry. It is further possible that α-LA, glyco-α-LA and glycosylated α-LA (e.g. through *Maillard*-reaction) show increased binding through proteolysis. This was described by Brück et al. [609] who report that α-LA inhibits *E. coli* (EPEC) and *Salmonella* binding to Caco-2 cells. The effect was enhanced by using pepsin- or pepsin-pancreatin hydrolysates.

Bands for β-LG were observed for all three bacteria after incubation with whey but not in their respective untreated pellets, indicating adhesion. However, quantitative analysis suggested that most of this signal was the result of β-LG residues that could not be removed from the whey

sediment. Thus it was concluded that binding β-LG to bacteria in this thesis was weak compared to other proteins such as LF or IgM.

Most literature data describing an anti-adhesive effect of BSA to surfaces are based on BSA binding to the abiotic (e.g. plastic polymer) surface and not to the microorganisms themselves [610-613]. However, human serum albumin was shown to bind to S*taphylococcus* protein G [614-616]. Caseins (κ-casein [617]; caseinate, glycomacropeptide, and caseinphosphopeptides [618]) were shown to reduce bacterial adhesion. Despite this, caseins were not analysed here as they were only contained as residues in whey (25 kDa band in Figure 6.3).

Taken together the findings suggest that there were different types of interactions established between immune-related and other whey proteins and bacteria, including receptor based, electrostatic and glycoside binding. As pellets of bacterial liquid cultures were used, it is likely that the described adhesion occurs between ingested whey proteins and planktonic bacteria in the lumen as well as bacteria in biofilms. In the first case, it is also possible that a whey protein that is already adhering to an insteinal surface layer shows secondary binding to plactonic bacteria.

6.3.3 Fluorescent Microscopy

The overlay images in Figure 6.8 show more binding of proteins from skim milk than from whey to all three bacteria. Thereby binding to *E. coli* Nissle 1917 and *S. epidermidis* 1457 was relatively low compared to *S. epidermidis* 1457 M10. This indicates that proteins bind better directly to the bacterial cell surface than to the extra-cellular matrix. A comparison between whey and skim milk was not possible due to different protein loads in the samples. However, one could expect binding of caseins to bacteria. In line with this consideration, Brück et al. [609] hypothesise that κ-casein derived glyco-macropeptide inhibits bacterial adhesion to Caco-2 cells by a decoy effect.

Even though a centrifugation step was included in the preparation of the samples and sediment containing whey was used, it was unlikely that the fluorescence comes from sedimented

residues. The samples visualised were bacteria in suspension. If there was sediment, it should appear as background. It is unlikely that all sediment overlaid with bacteria. Further there was no sediment in the skim milk used in this experiment (Figure 4.16). Thus it was concluded that the observed fluorescence represented binding of food proteins to bacteria. However, this approach was not used with isolated proteins. It was demonstrated before that isolated proteins have increased binding compared to proteins in mixture. Isolated proteins can be used to generate titration curves and determine saturation levels. This demands high numbers of individual samples. Therefore flow cytometry would be the method of choice because it allows quick analysis of a high number of cells (10^5 cells in 2 min) and delivers quantitative data.

6.4 Conclusion

The experiments in this chapter showed that the adhesion assay can be adapted to using pellets of bacterial liquid cultures. In agreement with the hypothesis of this chapter, that whey proteins differ in their adhesive properties and that some of them adhere to components of the human small intestinal biofilm, SDS-PAGE analysis of fluorophore labelled whey proteins showed selective binding of whey proteins to bacterial cell pellets. Several adhesive proteins were identified. Western blot data showed that most tested proteins (LF and several Ig-fractions) bound to the unprotected bacterial cells, whereas only the 75 kDa fraction of IgM bound to all three bacteria and LF also bound to *E. coli* Nissle 1917. As mentioned above, LF and Igs have been identified as bacterial binding proteins before and thus confirm the validity of the assay.

On the contrary, data on the binding of major whey proteins is limited (BSA and α-LA) and no bacterial binding has been reported for β-LG yet. The binding of β-LG could not be confirmed nor ruled out due to residues of β-LG in the whey sediment. However, SDS-PAGE analysis suggested binding of a ca. 70 kDa protein (possibly BSA) and also a ca. 16 kDa fraction that could be a version of α-LA. This demands further confirmation and was addressed in Chapter 7 of this thesis.

Chapter 7 Binding behaviour of isolated proteins to human epithelial cells in culture and representative bacterial cells with the propensity to form biofilms observed by flow cytometry

7.1 Introduction

After the identification of proteins of interest which showed increased binding from whey or milk systems to IEC or bacterial cells, these proteins were subjected to further investigation. Flow cytometry experiments were conducted to explore the progressive binding pattern (increasing concentration) of isolated candidate proteins to human IEC in culture and bacterial cells. Flow cytometry allowed the detection of weak and additional bacterium-cell interactions compared to solid-phase experiments [619]. This might be transferable to interactions between human or bacterial cells and proteins. Furthermore, flow cytometry is based on the detection of single events (i.e. cells) and thus could give information about the amount of protein binding to one cell instead of showing all proteins in question in the sample as it is the case on SDS-PAGE gels, Western blot or mass spectrometry. The software also allows the analysis of sub-populations, for example only cells with binding proteins. Observing individual populations and the development of sub-populations might support the understanding of binding processes.

7.1.1 Hypothesis and aims

The hypothesis of this chapter was that the proteins identified as adhering to the different intestinal surface layers in previous chapters differ in their binding behaviour and also that binding to human IEC in culture differs from binding to bacterial cells. Therefore, this chapter aimed to investigate binding of selected isolated proteins to each of the human IEC and bacterial cell types individually. Flow cytometry was used as described in Chapter 2, Section 2.7. Binding was observed as intensity of FITC emission whereby an increase in peak hight or a right shift of the peak represented an increase in emission, i.e. in bound protein. The proteins were added at increasing concentrations to generate binding curves. Proteins also needed to be equipped with a fluorescent tag which can then be used to differentiate between cell auto-fluorescence and increased fluorescence due to ligands.

7.2 Results

7.2.1 Degree of FITC labelling of isolated proteins

The flow cytometer did not have the appropriate detectors for Rhd, thus proteins needed to be tagged with an alternative label. The choice was made to use FITC, as preliminary experiments showed that bacterial auto-fluorescent could be gated out and the labelling procedure for proteins was relatively simple. For the flow cytometry analysis, six proteins were labelled with FITC: β-LG, α-LA, LF, IgG, free secretory component and BSA. A seventh protein, sIgA, was labelled with Cy5 (it was prepared in this manner by another researcher). Cy5 is a brighter label than FITC (e.g. compare Life Technologies [620] and [621]); this is of relevance for analysis of the observed shift in fluorescence (Δgeometric mean) as the stronger signal could also be interpreted as a more sensitive detection of sIgA. The degrees of FITC or Cy5 labelling are shown in Table 7.1 and Table 7.2. Some proteins were provided by other researchers (IgG, free secretory component, and sIgA) and the degree of fluorophore labelling was not determined to save sample. These proteins were stored in a sodium azide-supplemented solution.

7.2.2 Binding of isolated proteins to human epithelial cells in culture

Instead of measuring cell-adhesion of proteins at a single concentration, proteins were titrated onto the cells to follow the binding process (e.g. in layers or more random) and to determine the maximum binding capacity per cell and protein. Representative graphs are shown in Figure 7.1 to Figure 7.4. Titrations reached from 0 to 15 μmol.5 x 10^5 $cells^{-1}$ for HT29-MTX cells and 0 to 15 μmol.2 x 10^5 $cells^{-1}$ for Caco-2 cells. However, not all proteins were titrated to the maximum endpoint due to limited availability of protein stocks. Molarity was used to allow a better comparison between proteins. All concentrations referred to in this chapter are based on molarity, e.g. “higher concentration” means a greater number of protein molecules per volume. As the proteins investigated have very different molecular weights (14.2 kDa for α-LA to 385 kDa for sIgA), using a weight based concentration, i.e. $mg.ml^{-1}$, would result in different titration end points regarding the actual number of bound protein molecules per cell. In contrast, the molarity based concentration, i.e. $mol.ml^{-1}$, delivers exactly that comparison. However, the

Table 7.1: Degree of FITC or Cy5 label at proteins for flow cytometry analysis (bacteria)

fSC: free secretory component. Na-azide: sodium azide. n.d.: not determined

Protein	Mol FITC / Mol protein	Storage
β-lactoglobulin	4.10	PBS
α-lactalbumin	0.91	PBS
Lactoferrin	0.15	PBS
IgG	n.d.	0.1% Na-azide
fSC	n.d.	0.1% Na-azide
Bovine serum albumin	1.10	PBS
Mol Cy5 / Mol protein		
sIgA	n.d.	0.1% Na-azide

Table 7.2: Degree of FITC label at proteins for flow cytometry analysis (cell culture)

Na-bicarbonate: sodium-bicarbonate

Protein	Mol FITC / Mol protein	Storage
β-lactoglobulin	0.66	Na-bicarbonate buffer
α-lactalbumin	0.72	Na-bicarbonate buffer
Lactoferrin	0.75	PBS
IgG	4.67	PBS
κ-casein	0.73	PBS
Bovine serum albumin	1.10	PBS

different protein sizes and the degrees of labelling can affect the results, as larger proteins might cause steric blocking.

7.2.2.1 Titration curves

The increase in FITC positive cells was traced using the flow cytometry software. Accumulation of bound protein on the IEC happened in two ways. Either more cells were detected positive for FITC (increase in peak height) or the amount of FITC per cell increased (right shift), representing protein binding to a greater proportion of cells and binding of more protein molecules per cell, respectively. A representative set of titration curves is shown in Figure 7.1. In all tested combinations, both effects happened in parallel. The tailing of the peak increased with increasing protein concentration until an almost triangular shape was reached. Increasing the protein concentration further resulted in the formation of a bimodal distribution for some of the β-LG experiments in both cell types (Figure 7.2). LF and IgG also showed this behaviour (Figure 7.3 and Figure 7.4). The effect was less intense for IgG than for the other two proteins. A possible cause for the change in shape of titration curves and development of a bimodal distribution is self-organisation of the proteins and the formation of clusters around the cells, but also different types of binding (i.e. non-specific and receptor-based) and protein polymerisation [622] should be considered. On the contrary, the triangular shape (tailing) could be indicative of a more random binding (statistical distribution bound molecules) of proteins around the cell surface. This was also observed for BSA which is known for non-specific binding [623]. Like BSA, increasing the concentration of α-LA resulted in the development of the triangular shape of titration curves.

7.2.2.2 Analysis of area under the curve-progression: binding curves

Figure 7.5 shows the graphs of proteins bound to HT29-MTX or Caco-2 cells. The graphs show the complete area under one titration curve (e.g. the yellow titration curve representing 0.2 µmol α-LA in Figure 7.1), whereby the area under one titration curve is one data point in Figure 7.5 (e.g. Figure 7.5 B, α-LA at 0.2 µmol). Therefore, the graphs in Figure 7.5 represent all cells

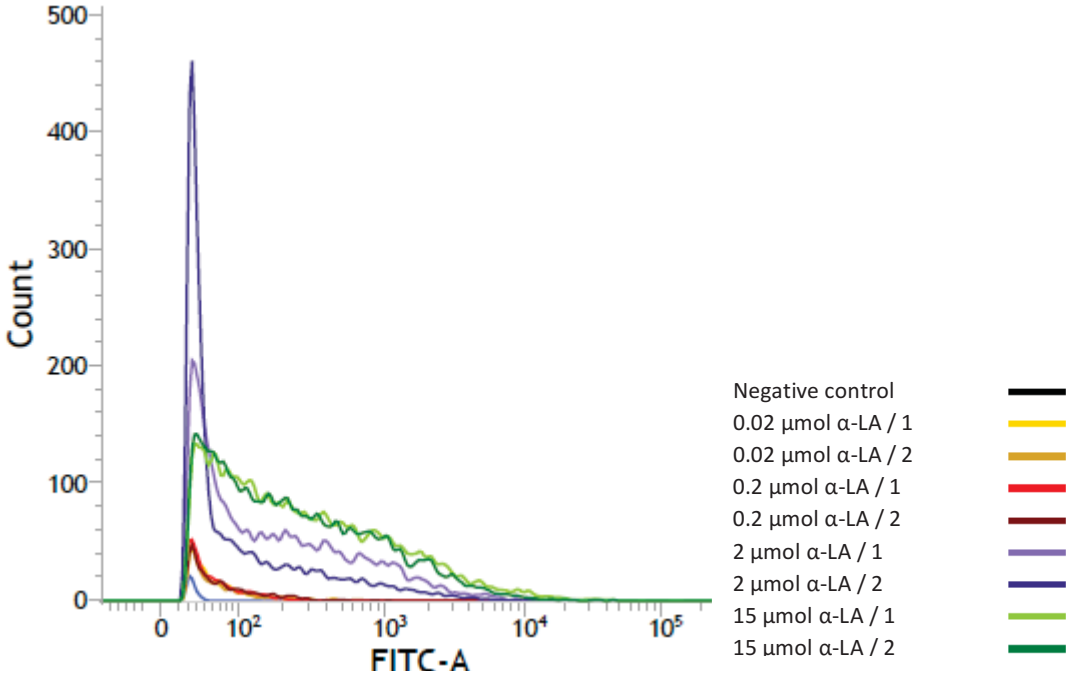

Figure 7.1: Flow cytometry titration curves for α-LA binding to HT29-MTX cells.

Titration curves of α-LA titration onto HT29-MTX cells. Only FITC positive cells are shown.

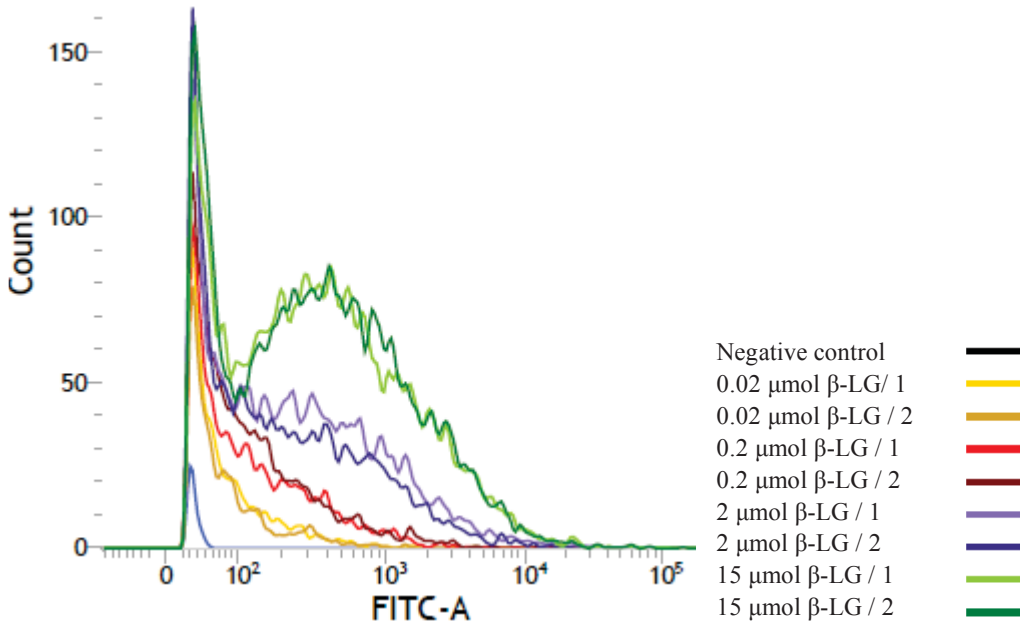

Figure 7.2: Flow cytometry titration curves for β-LG binding to Caco-2 cells.

Titration curves of β-LG titration onto Caco-2 cells. Only FITC positive cells are shown.

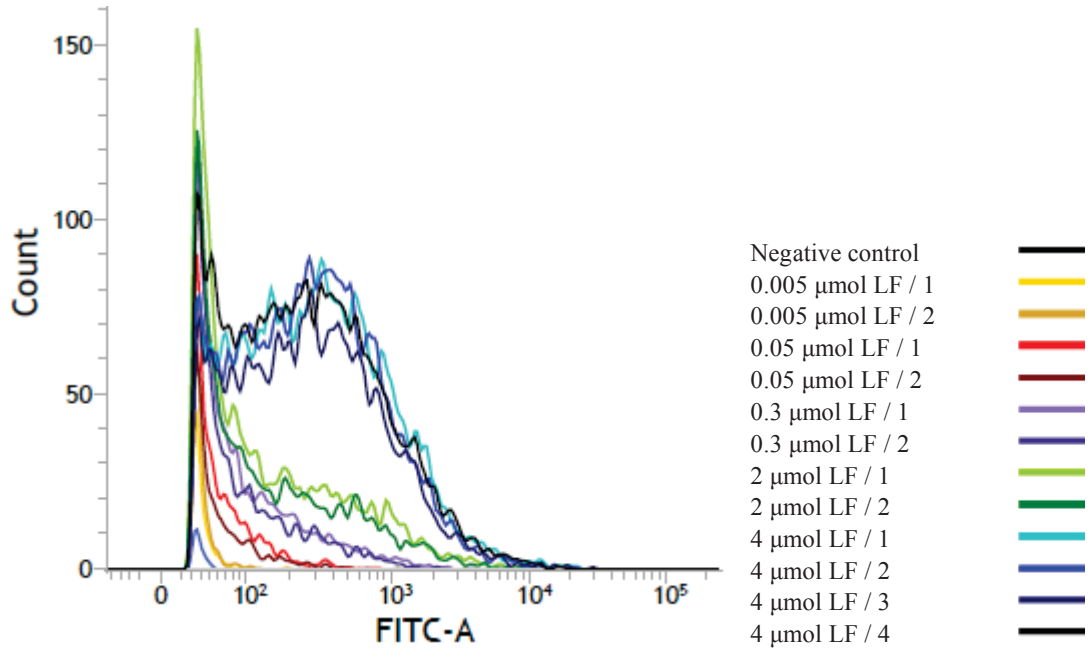

Figure 7.3: Flow cytometry titration curves for LF binding to Caco-2 cells

Titration curves of LF titration onto Caco-2 cells. Only FITC positive cells are shown.

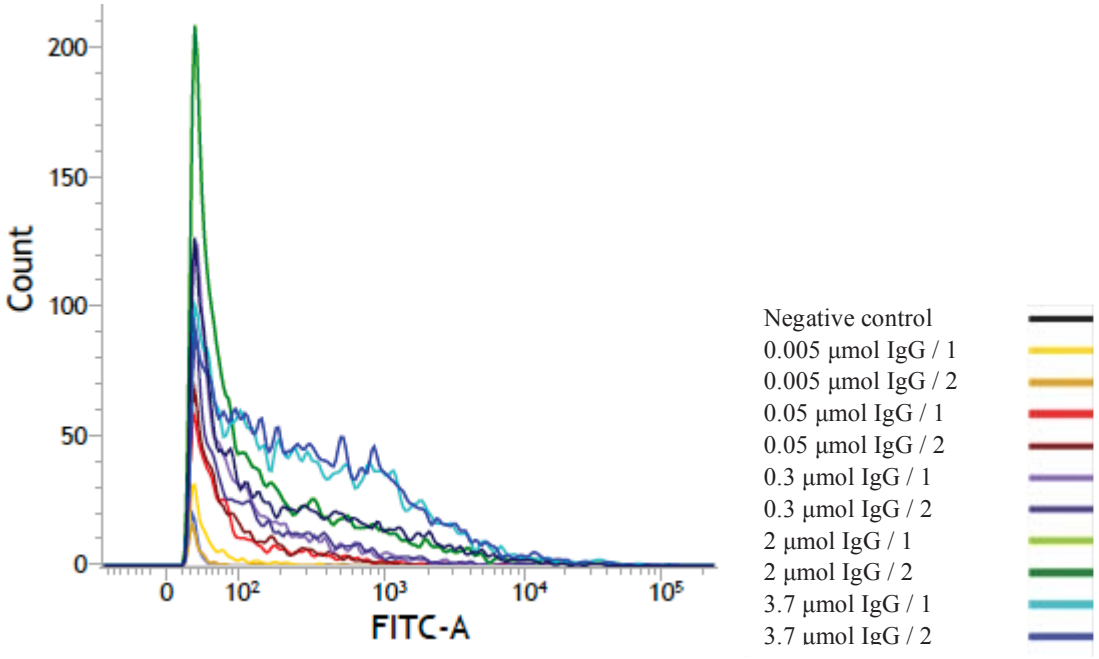

Figure 7.4: Flow cytometry titration curves for IgG binding to HT29-MTX cells

Titration curves of IgG titration onto HT29-MTX cells. Only FITC positive cells are shown.

which were detected positive for FITC after incubation at a given protein concentration. Consequently, the graphs do not carry information about the number of proteins bound per cell.

At comparable concentrations, all proteins showed more binding (a greater proportion of the cells have protein bound, but the amount of protein was not determined here) to HT29-MTX cells than to Caco-2 cells. The binding curves of LF and IgG to Caco-2 cells showed a plateau at medium protein concentration followed by a second increase in FITC positive cells at higher protein concentrations. LF might also have shown a plateau for HT29-MTX cells, but there were not enough data points to confirm this (Figure 7.5 D). The binding curve for IgG to HT29-MTX cells appeared to be less steep in the same concentration range but did not show a plateau. The plateau could be associated with different types of binding (discussed in Section 7.3.1). However, this behaviour was not observed for β-LG which also showed bimodal distributions (Figure 7.2).

Generally all proteins showed a smaller slope at low concentrations for binding to Caco-2 cells (Figure 7.5). This suggests that more protein was needed to achieve the same percentage proportion of labelled cells as for HT29-MTX. A possible reason is that the Caco-2 cells had a larger cell surface area than the HT29-MTX cells and thus more available binding area for the proteins. Another possibility is that Caco-2 cells had a slight fluorescence quenching effect on the FITC. Finally, it is also possible that the mucin secreted by HT29-MTX cells retained proteins.

Of all proteins titrated onto the cells, κ-casein had the lowest and most steady maximum binding level for both cell types (approximately 30% of cells). α-LA showed the highest plateau level, followed by β-LG. The data did not allow determining whether saturation levels of α-LA or β-LG were reached. The titration endpoint for the other three proteins (LF, IgG, and BSA) was not reached and no conclusions about the saturation levels could be drawn.

Figure 7.6 gives a comparison of the percentage of FITC-positive cells after incubation with 0.4 to 1 μmol (0.06 to 0.15 μmol for BSA) per 10^5 cells. Due to the variations in protein

concentrations, no absolute comparison between the proteins could be drawn. However, all protein-cell combinations resulted in significant ratios of cells with adhering proteins. Further, it appeared that for the proteins with lower molecular weights (α-LA, β-LG and κ-casein) there was no difference in percentage FITC positive cells between the two cell types, although HT29-MTX cells were incubated with lower protein concentrations. This confirms earlier observations, that the binding curves from Caco-2 have a smaller slope at low protein concentrations. In contrast, and despite the incubation with more similar protein concentrations, LF and IgG appeared to bind to a greater proportion of HT29-MTX cells. This could be due to more efficient binding to HT29-MTX cells.

As observed before (Section 4.2.2), when applied as isolate solutions, whey proteins appear to always show binding; although proteins might not bind well in competitive situations. Thus it was expected that all proteins in this chapter would bind to bacterial cells or IEC, i.e. no negative control protein could be included. The experiments in this chapter were desigened to get a better insight into how binding happens and potential changes at higer protein concentrations. This is useful inormation as proteins, when they are incorporated into nutrient delivery vehicle surfaces, are enriched in a competitive environment.

7.2.2.3 Analysis of peak-progression along the X-axis: changes in signal intensity per cell

Analysing the peak position in the titration curves relative to the X-axis provided information on the increase in protein bound per cell. The further right a peak was the more fluorescent labels per cell were detected. As the cell auto-fluorescence was gated out at the beginning of each run (a new "zero" position was determined), not the absolute position of the peak was measured but the difference between the new "zero" value and the final peak. The results were expressed as shift in geometric mean or Δgeometric mean. Figure 7.7 shows the right shift along the X-axis as an indicator for the change in amount of protein per cell (values shown are

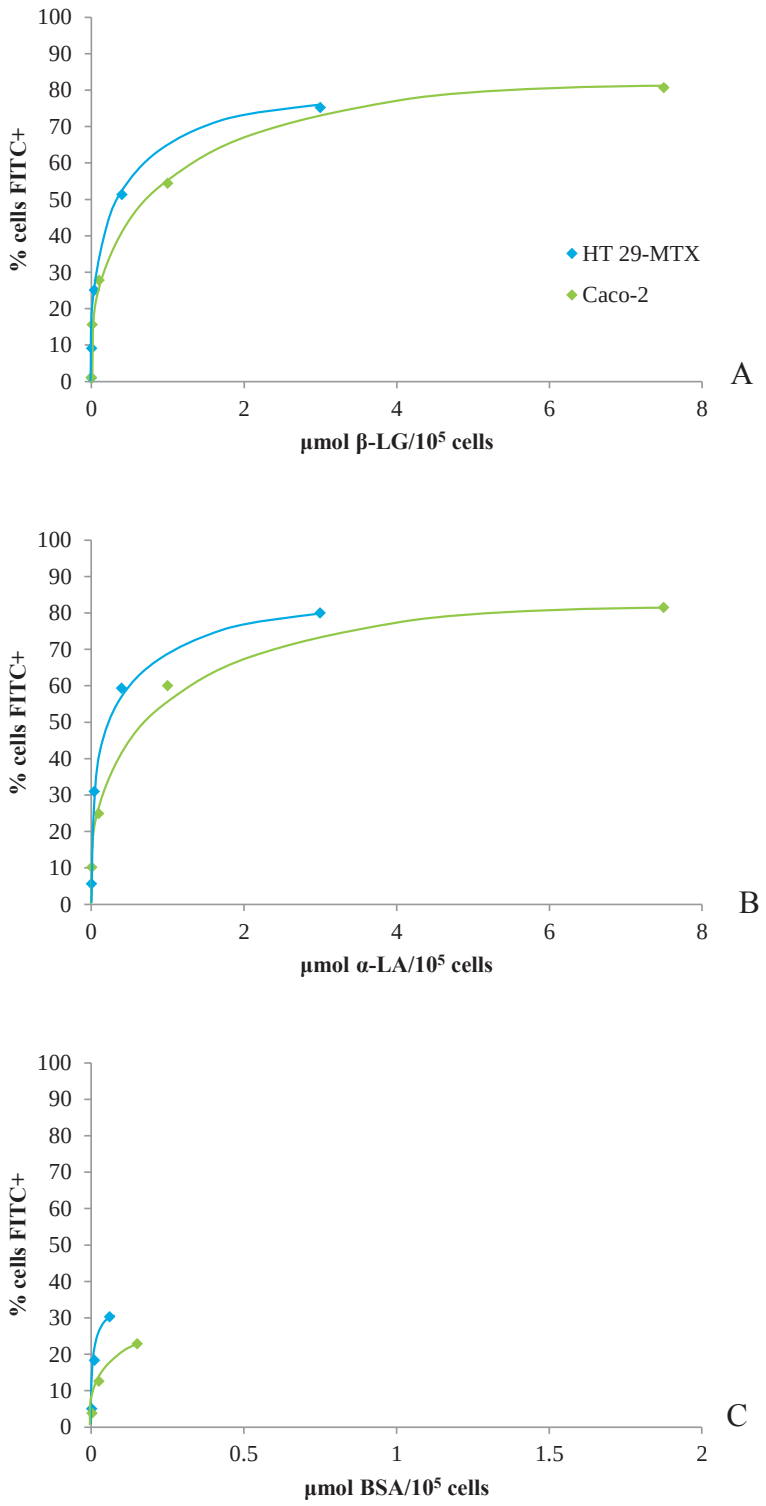

Figure 7.5 A-C: Flow cytometry binding curves for all tested proteins and both cell types

Binding of isolated proteins to cell types as analysed by flow cytometry. Graphs show average percentage of FITC-positive bacteria (n=6). Lines connecting data points were approximated by hand. (A) β-LG, (B) α-LA, (C) BSA.

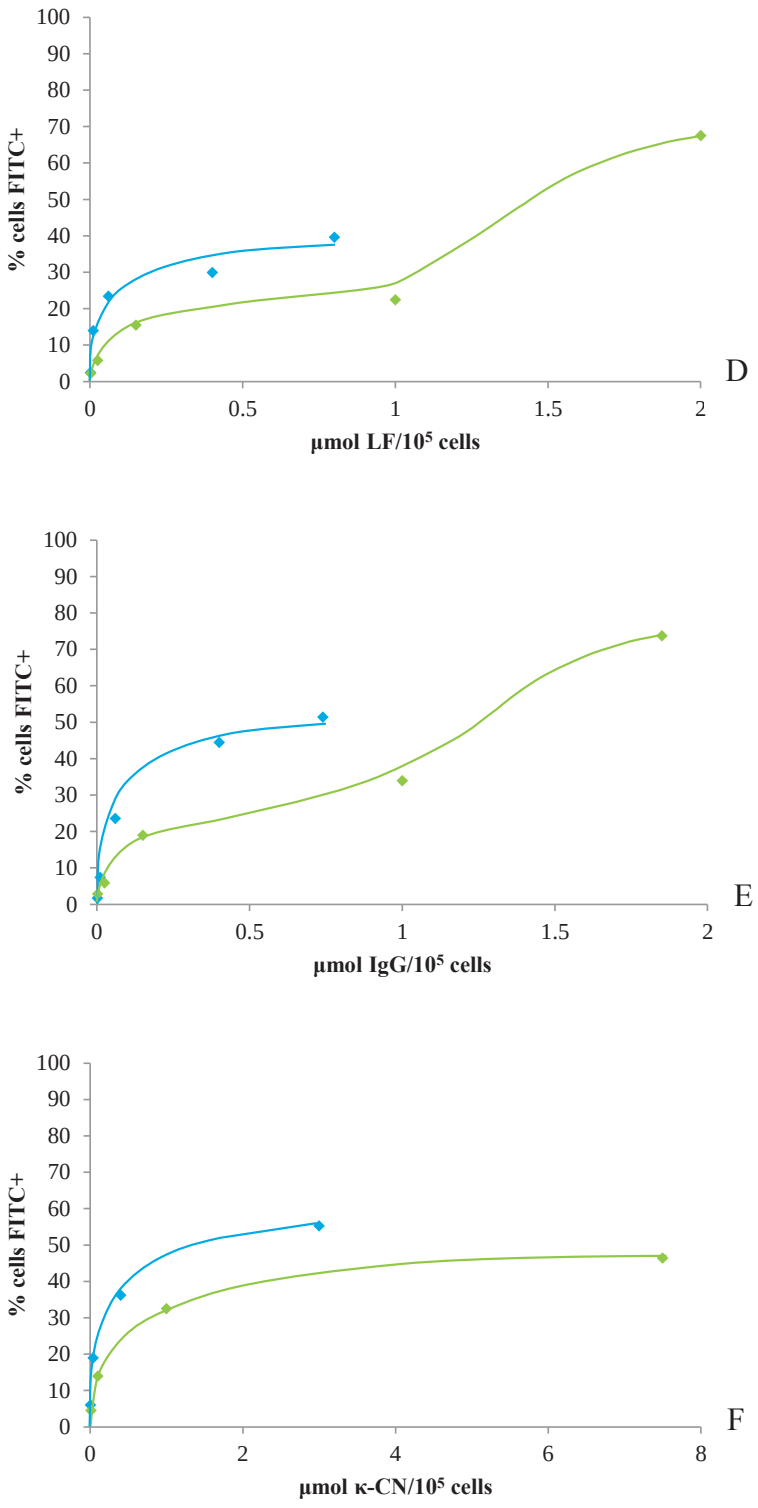

Figure 7.5 D-F (continued): Flow cytometry binding curves for all tested proteins and both cell types

Binding of isolated proteins to cell types as analysed by flow cytometry. Graphs show average percentage of FITC-positive bacteria (n=6). Lines connecting data points were approximated by hand. (D) LF, (E) IgG, (F) κ-CN.

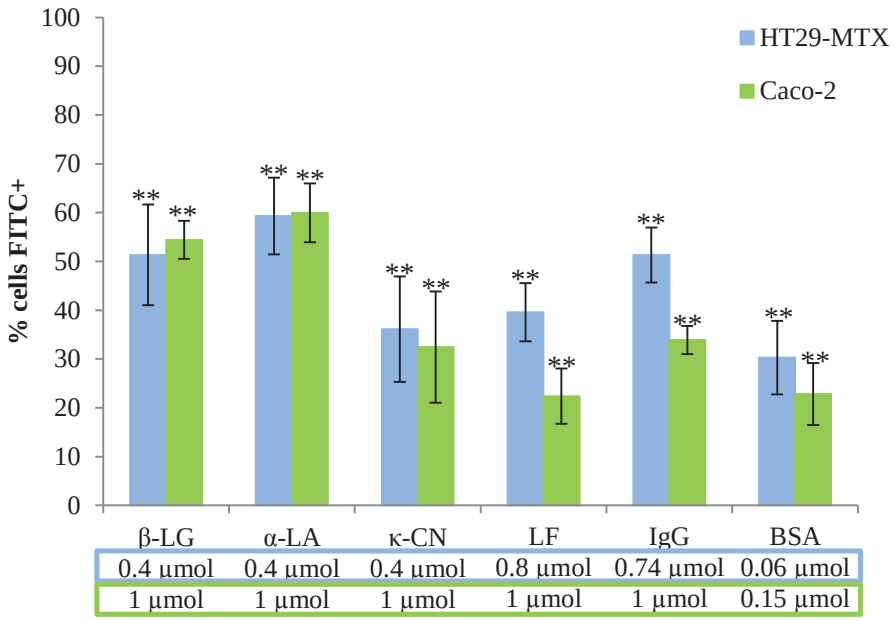

Figure 7.6: Overview of binding of tested proteins (0.04 to 1 µmol) to both cell types, as % total cells.

Bar graphs summarising the FITC positive cells as % of all cells (parent population) after titration of 0.04 to 1 µmol (0.006 and 0.15 µmol for BSA) protein onto 10^5 cells. The lower concentration (marked in blue) per protein relates to HT29-MTX cells while the higher concentration (marked in green) relates to Caco-2 cells. STD deviation and significance to untreated cells ($^+$trend ($0.1 \geq p > 0.05$), *high ($0.05 \geq p > 0.01$), **very high ($0.01 \geq p$)) shown.

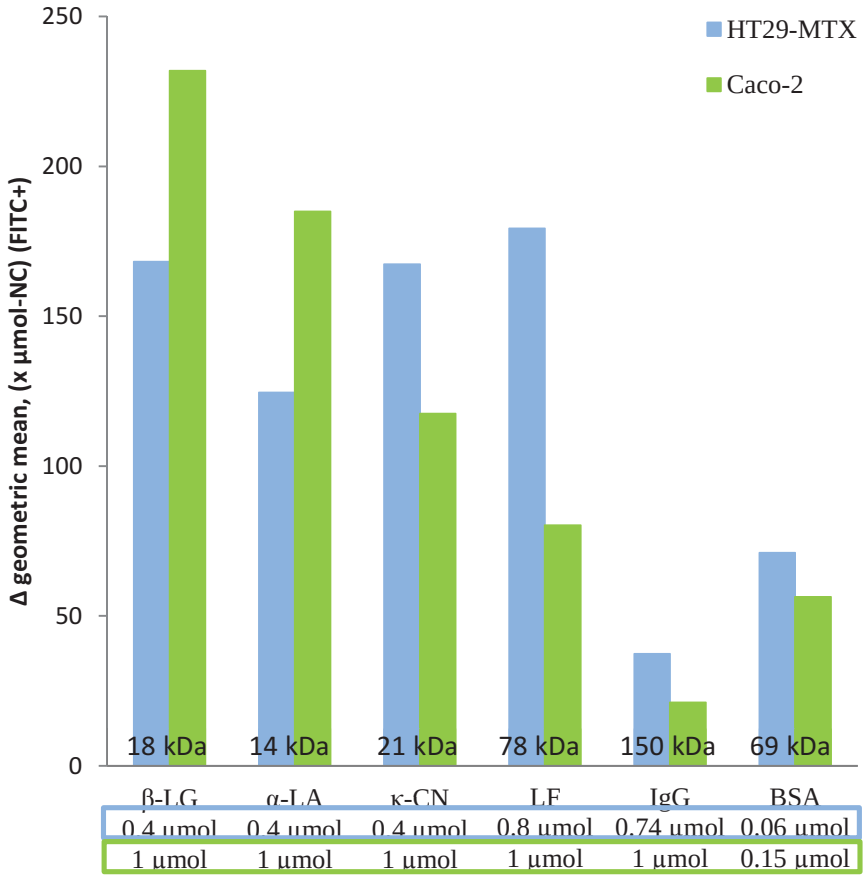

Figure 7.7: Overview of binding of tested proteins (indicated concentrations) to both cell types, as Δgeometric mean

Summary of the difference in geometric mean of FITC positive bacteria after titration of 0.04 to 1 µmol (0.06 and 0.15 µmol for BSA) protein onto 10^5 cells and the NC (untreated bacteria). The lower concentration (marked in blue) per protein relates to HT29-MTX cells while the higher concentration (marked in green) relates to Caco-2 cells. Data has been corrected for the degree of FITC-labelling.

corrected for degree of FITC labelling). With the exception of BSA and α-LA, a trend could be observed for Caco-2 cells that the larger the protein the smaller was the shift in geomean. As the values were corrected for degree of FITC labelling they can be compared directly. The non-conforming behaviour of α-LA and BSA suggests a lower binding affinity to the cells. Amongst the latter two again, more molecules of the smaller protein (α-LA) bound per cell. For HT29-MTX cells no clear trend was observed.

7.2.3 Binding of isolated proteins to bacterial cells

In a similar manner to the epithelial cells, proteins were titrated onto bacteria to follow the binding process and to determine the level of maximum protein load per cell (i.e. maximum binding capacity per bacterial cell and protein). Titrations reached from 0 to 1 μmol.10^6cfu^{-1}.

7.2.3.1 Initial titration curves

The increase in FITC positive cells was traced using the flow cytometry software (Figure 7.8 to Figure 7.10). Figure 7.8 (α-LA binding to *S. epidermidis* 1457 M10) shows that increased FITC counts either occurred by more FITC signal detected per cell (right shift) or by more cells being FITC positive (higher peak). Here, both processes happened at the same time, suggesting that all cells showed the same binding behaviour and protein concentrations did not reach maximum binding capacities or trigger alternative interaction types. However, some other combinations of proteins and bacteria showed different behaviours.

β-LG binding to *S. epidermidis* 1457 M10 showed an increase in FITC load per cell with small variations in peak height (Figure 7.9). This indicated that the amount of FITC per cell increased while the number of cells that bound FITC did not increase, i.e. all cells that could bind β-LG were carrying protein molecules after adding the lowest protein concentration. This agreed with the binding curve (Figure 7.11 B) which described the onset of a plateau at about 97% of all cells after titration of 0.2 μmol β-LG. This suggested good binding of β-LG to *S. epidermidis* 1457 M10. As *S. epidermidis* 1457 M10 has (I) the smallest cell surface area of all cells studied and is (II) not protected by an extracellular matrix, this could mean that: (I) its surface is

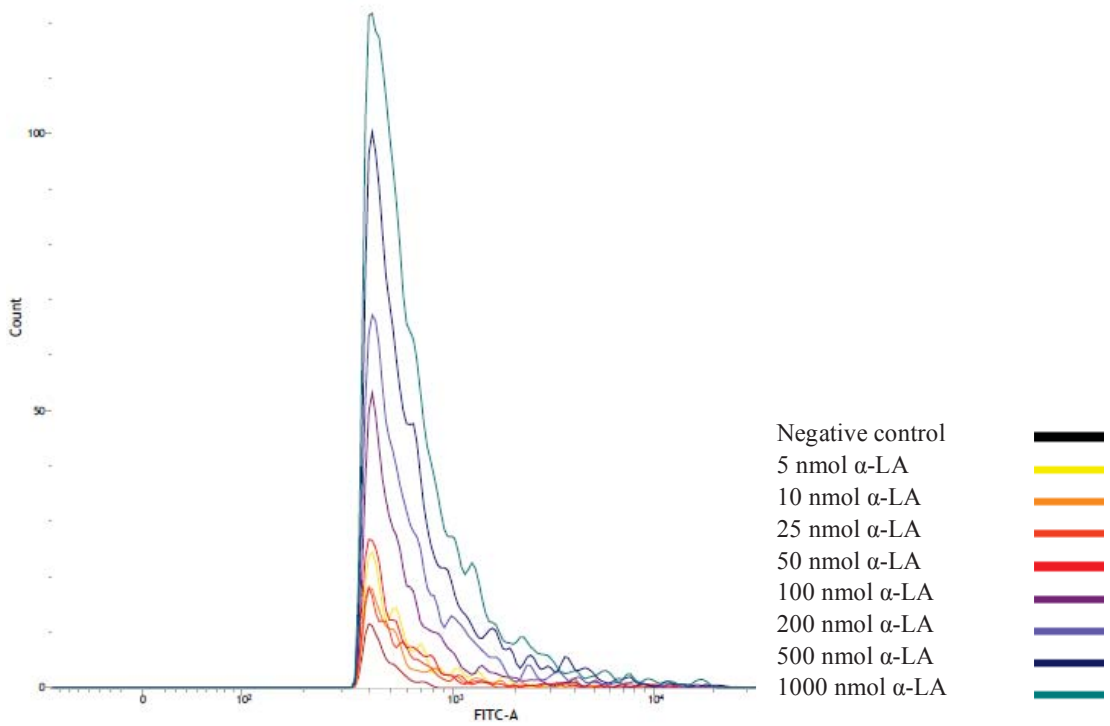

Figure 7.8: Flow cytometry titration curves for α-LA binding to *S. epidermidis* 1457 M10

Titration curves of α-LA titration onto *S. epidermidis* 1457 M10; only FITC positive cells are shown.

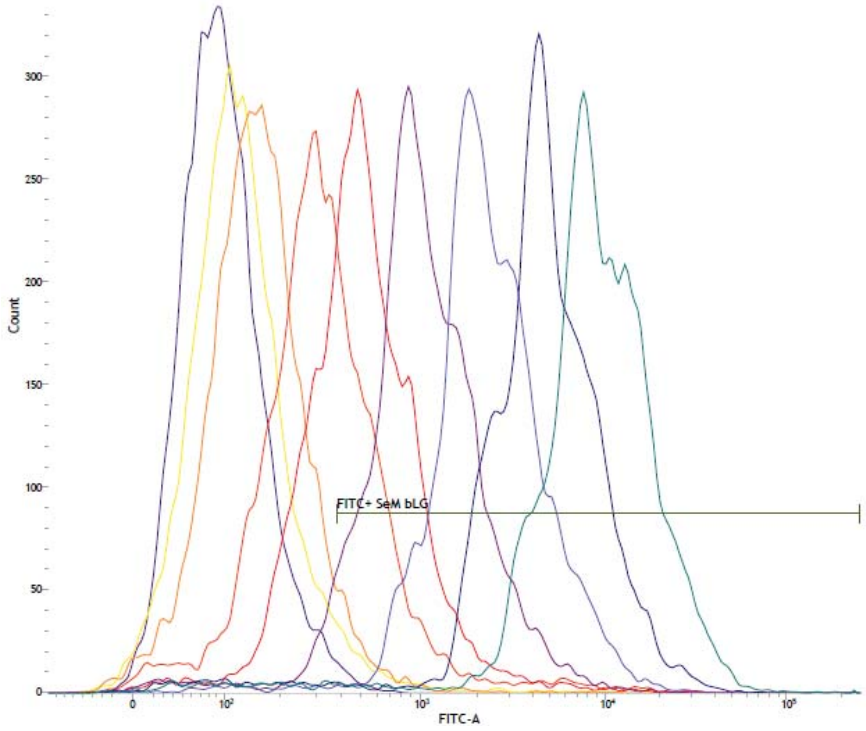

Figure 7.9: Flow cytometry titration curves for β-LG binding to *S. epidermidis* 1457 M10

Titration curves of β-LG titration onto *S. epidermidis* 1457 M10; all events are shown. Horizontal bar indicates cells defined as FITC+. Key from Figure 7.8applies.

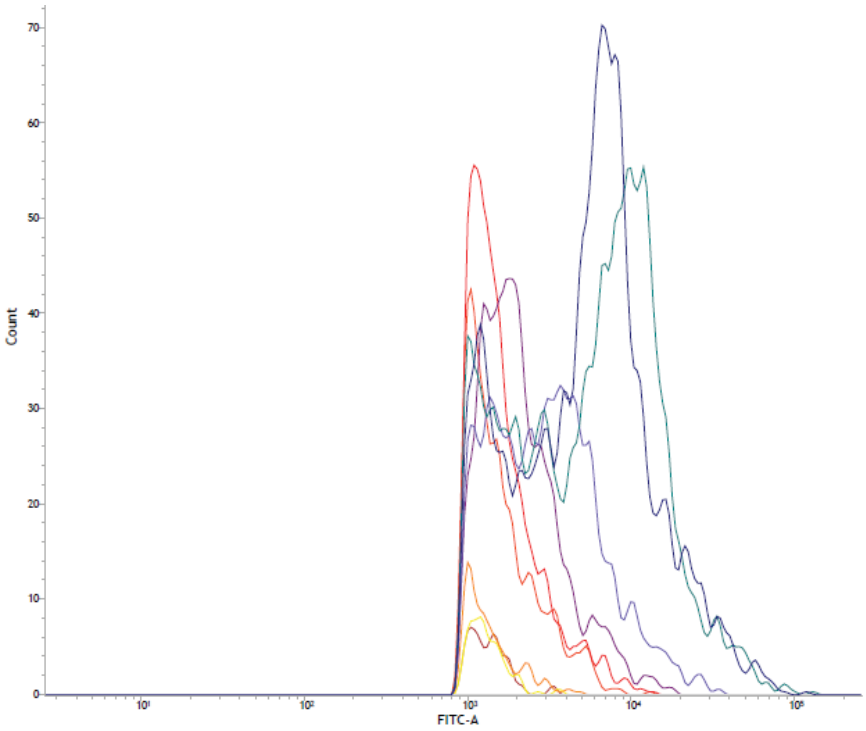

Figure 7.10: Flow cytometry titration curves for β-LG binding to *E. coli* Nissle

Titration curves of β-LG titration onto *E. coli* Nissle; only FITC positive cells are shown. Key from Figure 7.8 applies.

quickly occupied by the milk protein and that this leaves more milk protein for secondary binding, possibly in protein clusters. Adhesion could also have been enhanced by the lack of biofilm leading to a higher number of exposed receptors (II). When binding to *E. coli* Nissle 1917 or S. epidermidis 1457, β-LG showed the tendency to first increase the number of FITC positive cells followed by a right shift under the development of a bimodal distribution (Figure 7.10 shows the changes in distribution). The left peak in the titration curves appeared to have reached a maximum height before a second (right) peak developed. This observation was similar to the behaviour β-LG showed on IEC. However, the titration curves of *E. coli* Nissle 1917 did show the development of the second peak more clearly than it was observed before (i.e. the triangular shape slowly rises into a second peak). Other proteins, including LF and IgG, did not show a bimodal distribution and their histograms were similar to that of α-LA in Figure 7.8. A possible reason is the fact that both those proteins are related to the immune system and are designed to interact with bacteria in a more receptor-based manner [572-575].

7.2.3.2 Analysis of area under the curve-progression: Binding curves

Figure 7.11 shows the graphs of proteins binding to bacteria. The proteins were divided in two groups: those which bound better to *S. epidermidis* 1457 M10 (β-LG, α-LA , LF and sIgA) and those which bound better to *E. coli* Nissle 1917 (free secretory component, IgG and BSA). Binding to *S. epidermidis* 1457 was lower than that to *S. epidermidis* 1457 M10. Figure 7.12 summarises the binding curve data at a comparable protein concentration (0.05 μmol).

In agreement with observations from Figure 7.9, the binding curve for β-LG and *S. epidermidis* 1457 M10 showed saturation with an onset point between 0.1 and 0.2 μmol protein (Figure 7.11 A). The saturation level was about 97% bacterial cells. No other protein-bacterium combination showed a comparable behaviour. Generally, all binding curves showed a plateau after an initial increase. The only exception was the binding curve for α-LA binding to *S. epidermidis* 1457, which did not reach a plateau, indicating that the cells were not saturated with protein.

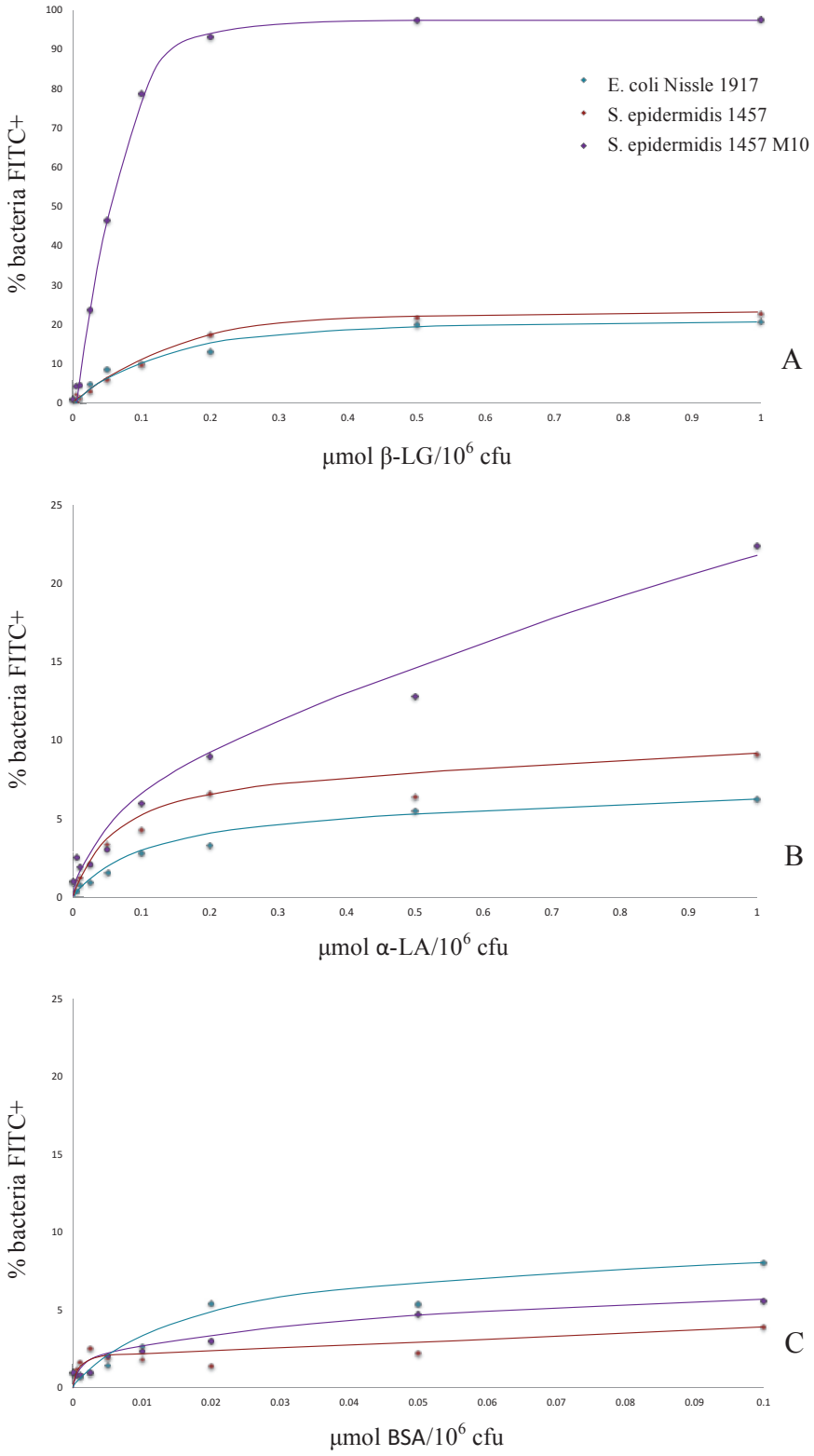

Figure 7.11 A-C: Flow cytometry binding curves for all tested proteins and bacteria

Binding of isolated proteins to all three bacteria as analysed by flow cytometry. Graphs show average percentage of FITC-positive bacteria (n=3). Lines connecting data points were approximated by hand. (A) β-LG, (B) α-LA, (C) BSA.

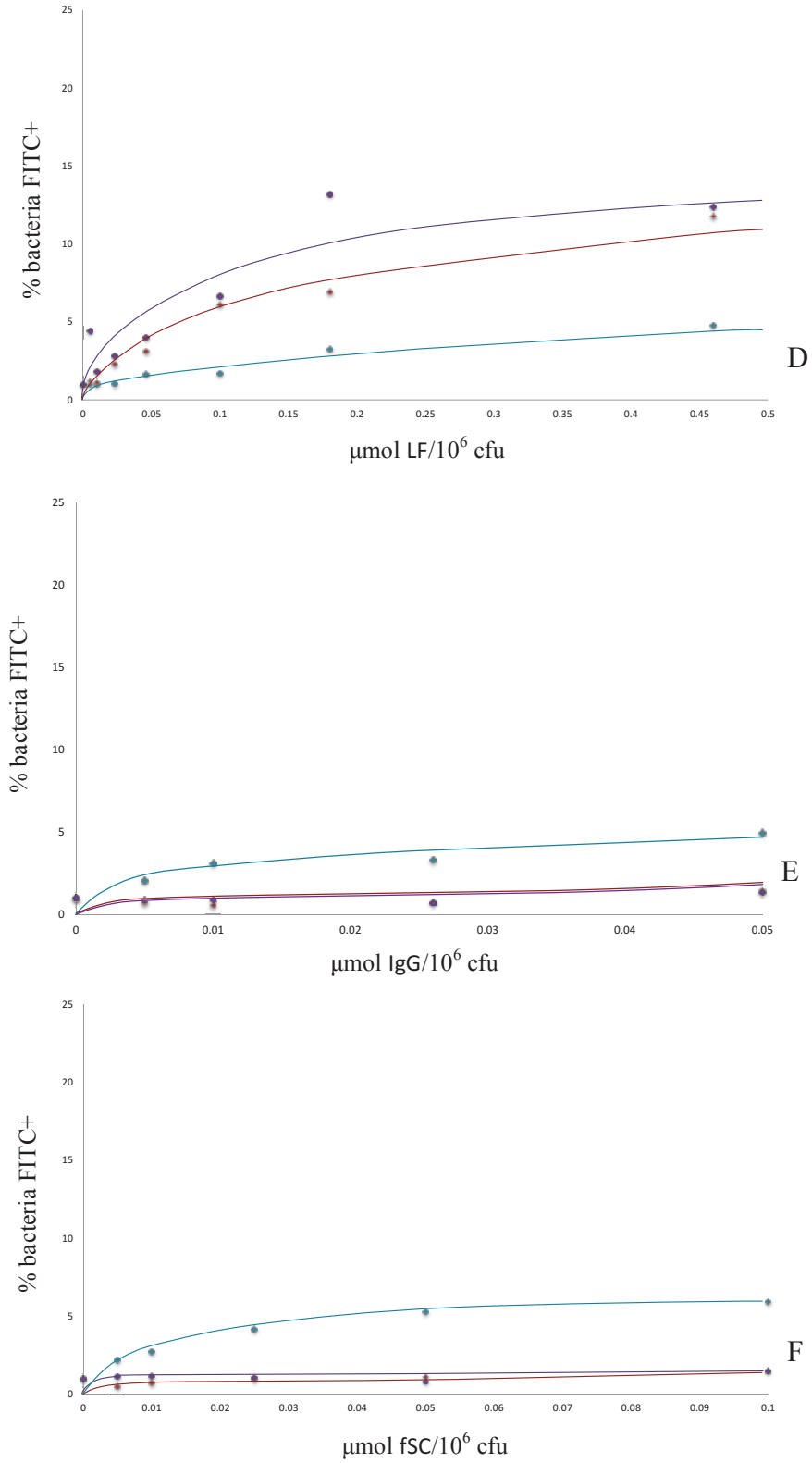

Figure 7.11 D-F (continued): Flow cytometry binding curves for all tested proteins and bacteria

Binding of isolated proteins to all three bacteria as analysed by flow cytometry. Graphs show average percentage of FITC-positive bacteria (n=3). Lines connecting data points were approximated by hand. (D) LF, (E) IgG, (F) fSC: free secretory component.

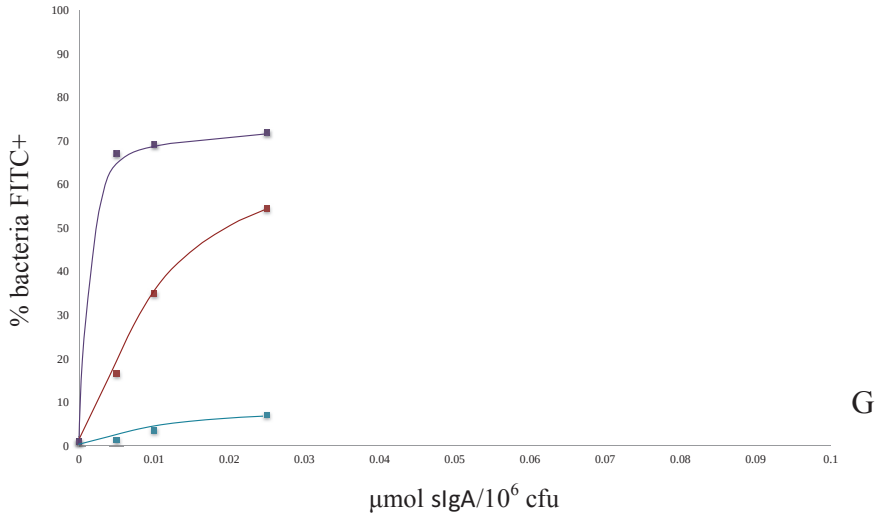

Figure 7.11 G (continued): Flow cytometry binding curves for all tested proteins and bacteria

Binding of isolated proteins to all three bacteria as analysed by flow cytometry. Graphs show average percentage of FITC-positive bacteria (n=3). Lines connecting data points were approximated by hand. (G) sIgA.

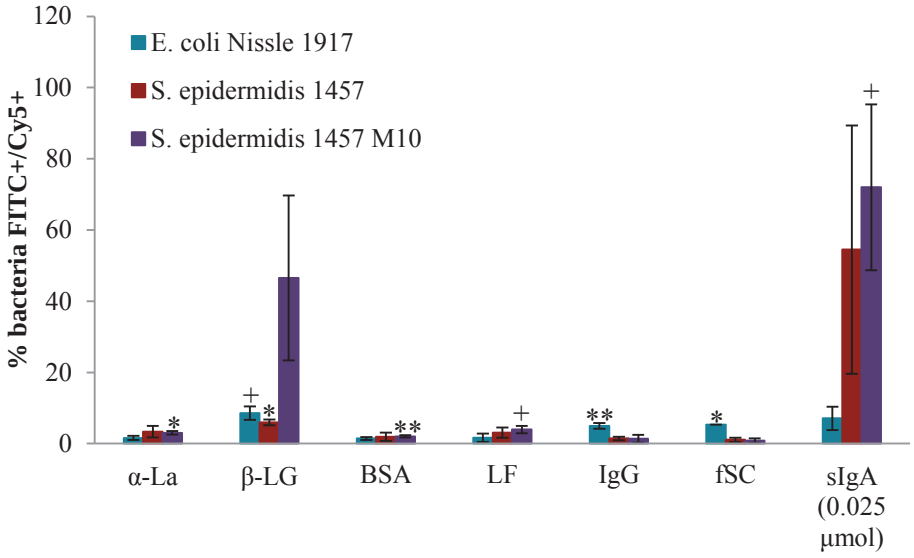

Figure 7.12: Overview of binding of tested proteins (0.05 µmol) to all bacteria, as % total bacteria.

Bar graphs summarising the FITC positive bacteria as % of all bacteria (parent population) after titration of 0.05 µmol (0.025 µmol for sIgA) protein onto bacteria. STD deviation and significance to untreated bacteria ($^{+}$trend (0.1≥p>0.05), *high (0.05≥p>0.01), **very high (0.01≥p)) shown.

A comparison of all binding curves is shown in Figure 7.12 for bacteria after incubation with 0.05 µmol proteins. sIgA was only titrated to 0.025 µmol and cannot be directly compared with the other proteins. However, a comparison of the binding patterns (i.e. what percentages of the three different bacteria the protein adheres to) is possible. Comparing the binding patterns of sIgA and free secretory component (a component of sIgA) suggests that free secretory component is responsible for sIgA binding to *E. coli* Nissle 1917, while another part of sIgA adheres to the pathogens. Figure 7.12 indicates that some proteins bound to significant numbers of bacterial cells. These are α-La and BSA for *S. epidermidis* 1457 M10, β-LG for *S. epidermidis* 1457, and IgG and free secretory component for *E. coli* Nissle 1917. Generally, the percentage of bacterial cells detected positive for FITC was low, under 20%, with exception of β-LG and *S. epidermidis* 1457 M10, and sIgA.

7.2.3.3 Analysis of peak-progression along the X-axis: changes in signal intensity per cell

Figure 7.13 shows the shift in geometric mean of the titration curves for detected fluorescence, for the same protein concentrations as in Figure 7.12. The higher the value, the more label was detected per cell. Comparing the results for LF in Figure 7.12 and Figure 7.13 showed that only a small percentage of all bacteria bound labelled LF, but binding resulted in a comparably high load of protein per cell. Contrary, a higher percentage of cells bound β-LG but only few protein molecules adhered per cell (at this low level of titration, 0.05 µmol protein), particularly in *S. epidermidis* 1457 M10.

sIgA carried a different (brighter) fluorescent label (Cy5) compared to the other proteins (FITC). Although this difference does not allow a comparison of the shift in geometric mean between sIgA and the other proteins, the difference is of less importance for other graphs (i.e. initial histograms and binding curves). Generally, the difference in label brightness might be relevant at the lower detection limits of the labels and also close to the detector's saturation level (i.e. higher sensitivity for sIgA at a low level but lower accuracy at higher levels). The samples analysed here were mostly in the range of medium fluorophore levels, thus higher

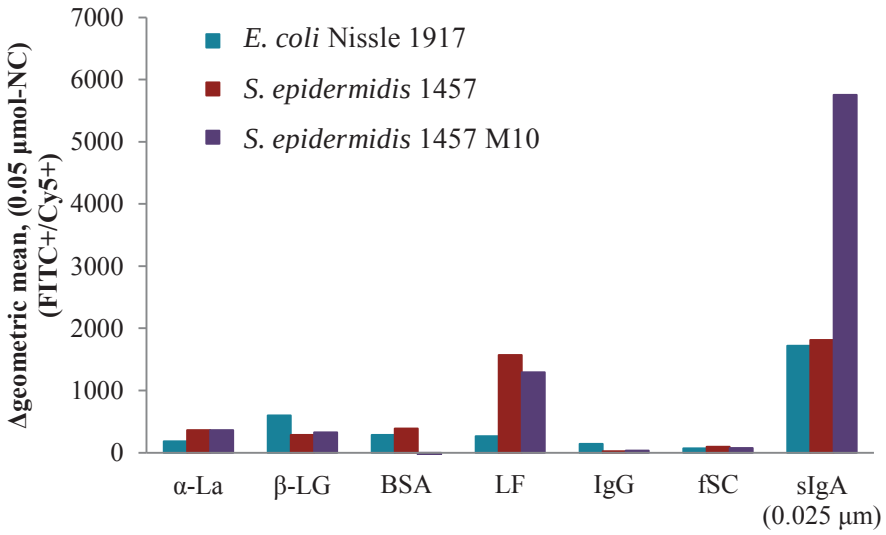

Figure 7.13: Overview of binding of tested proteins (0.05 µm) to all bacteria, as Δgeometric mean

Summary of the difference in geometric mean of FITC or Cy5 (sIgA) positive bacteria after titration of 0.05 µmol (0.025 µmol for sIgA) protein onto bacteria and the NC (untreated bacteria). As Cy5 is a brighter label than FITC, no comparison of degree of binding between sIgA and other proteins is possible. Also, free secretory component and IgG have not been corrected for the degree of FITC-labelling, thus they cannot compared with the other proteins in a quantitative manner.

sensitivity could increase the increments between the concentrations (therefore higher values for Δgeometric mean). Further, the degrees of FITC-labelling could not be determined for free secretory component and IgG.

7.3 Discussion

7.3.1 Binding of isolated proteins to human epithelial cells in culture

All tested proteins bound to both cell types used. Significant binding occurred already at medium protein concentrations from 0.4 to 1 μmol protein (Figure 7.6). Figure 7.5 shows that at comparable protein levels, the proportion of cells with bound protein (determined by the area under the initial titration curves (represented by Figure 7.1 to Figure 7.4), which is the total number of cells with bound protein, independent of the amount of protein per cell) was higher for HT29-MTX cells than for Caco-2 cells. This could have been due to the mucus produced by the former cells (Figure 7.5) and suggests that the proteins bound better to the mucin (proportion of cells with bound protein) than to the IEC surface, or that bound proteins were more efficiently retained in the mucus layer or the cell surface underneath, e.g. the proteins were protected from being washed away or from desorption in an equilibrium situation. Another reason could be the larger cell surface of Caco-2 cells compared to HT29-MTX cells that could accommodate more proteins per cell, and thus, under limited availably of proteins (i.e. before saturation), might leave some cells without bound protein. Also an emission quenching effect of Caco-2 cells was suggested in Section 7.2.2.2. Improved binding of β-LG in the presence of small amounts of mucin agreed with results from the Western blot experiments where β-LG bound best to the co-culture (90% Caco-2 and 10% HT29-MTX cells). Taken together with increased adhesion of α-LA to HT29-MTX cells, this suggests that the molecular size was a criterion in protein binding to cells partly covered with mucin or the mucin itself. It is possible that the smaller hydrodynamic radius favours the accommodation of small molecules on the cell-mucin-interface. This aspect requires future research as it could provide information whether the size of a protein or nutrient vehicle play a role in the targeting process or the target-ability of a surface layer, e.g. it might be beneficial to generate small vehicles to target mucin

covered cells. In the case that their small molecular size was responsible for binding of α-LA and β-LG, binding is likely to be impaired after the incorporation into a larger nutrient vehicle. In contrast, the proteins which bound best to Caco-2 cells are larger in molecular size and related to the immune system. BSA binding could not be assessed at higher concentrations and was thus not comparable with the other proteins. Post-translational modifications (e.g. glycosylation or phosphorylation [624]) often occur in whey proteins, e.g. high (e.g. LF or Igs [1]), little (α-LA [625]) or non (β-LG [533]). These modifications can influence the charge or the local polarity of a protein molecule and contribute to its binding properties.

Some proteins (β-LG, LF and IgG) showed the appearance of a bimodal distribution in titration curves for both cell types at higher protein concentrations. The onset concentration for the formation of the second peak was not the same for the different proteins or between the cell types (it could be dependent on the size of the protein or the surface area of the cells). At lower concentrations, the first peak showed an increase in tailing up to the formation of an almost triangular shape. This was also observed for BSA which is known for its non-specific binding [623]. Thus it was suggested that the triangular peak represented non-specific binding of proteins or smaller protein clusters to the cell surfaces. On the contrary, the second peak was possibly an indicator for a more structured protein organisation where higher order complexes of multiple units were being formed (no literature reference could be found). As the peak appeared suddenly and did not grow from the tailing (Figure 7.2 to Figure 7.4), there might have been a critical concentration (similar to critical micelle concentration [626, 627]) above which the proteins assembled and organised in clusters, before or after binding to cells, which adhered to the cells. Below this concentration, adhesion of protein monomers (first peak) would be favourable. This could be due to the energy requirements of an interface-like protein construct. The plateau observed in the binding curves (Figure 7.5) also agrees with this hypothesis. Once the critical concentration was reached, additional protein was incorporated into the organised structure until new excess protein was available to bind to further cells. Polymerisation could also be involved. However, the exact mechanism for each individual protein-cell type

combination is yet to be investigated. Experimental designs here could also include the analysis of gen up or down-regulation upon binding. This could enable profound insights into binding processes on a molecular level.

The plateau was only observed for LF and IgG, but not for β-LG. This might be due to the smaller molecular size of β-LG of the protein, which could allow more flexibility in the accommodation and release of molecules in the cluster, thus making the transition from one cluster to the next seamless. Further, β-LG is known for its surface activity and the associated unfolding on the interface [628]. This might also support the formation of protein bilayer structures [629-631]. A BLAST comparison of the two protein structures did not reveal any significant similarities between β-LG and LF (no sequence for the IgG Fc fragment could be found and the Fab fragments were too variable) [632]. Also, no common functionalities between these two proteins are known, thus it is likely that the observed bimodal distributions at higher protein concentrations are due to different reasons.

An alternative explanation which is compatible with a bimodal distribution is that specific or receptor based binding lead to the formation of the second peak. The reasons for the different types of binding were likely to be cell specific. Sanchez et al. [633] showed that human LF bound to 80% confluent and differentiated Caco-2 cultures in a similar experimental set-up to the one used in this thesis. Approximately half the LF molecules bound specifically while the other half bound non-specifically. This mix of specific and non-specific binding is a possible explanation for the bimodal distribution. However, the authors could not detect a receptor that exhibited a measurable affinity for LF.

β-LG was also shown to bind specifically to Caco-2 brush border membranes by Bolte et al. [468]. Rytkönen et al. [131] reported the transport of native β-LG through Caco-2 cells under limited protein degradation. No reports about LF or β-LG binding to HT29-MTX cells could be found. This is possibly due to a lack of research in the field and this specific cell type as the results in this thesis did show binding of the two proteins to HT29-MTX cells. However, these

results need to be considered carefully as detached cells were used for the experiments. Thus binding might have happened everywhere around the cell surfaces and not only the apical sides as it is the case for intact monolayers. In particular, the tight junction proteins between the Caco-2 cells [634], that are occupied in intact monolayers (forming intact tight junctions) but accessible in detached cells, might introduce additional binding capacities to the cells in the experiments here. Accordingly, freshly trypsinised Caco-2 cells have been reported as showing higher levels of WGA binding than confluent monolayers [635].

One study describing tight junctions in HT29-MTX cells was found [288]. The authors used FITC-phalloidin to visualise actin with a confocal laser scanning microscope. Actin was described to be present in cystic intracellular structures in the HT29-MTX-E12 and as a network on the apical side of the HT29-MTX-D1 cells in the study. The presence of actin was interpreted as the presence of tight junctions. This conclusion is questionable as actin filaments are present is many cell components (e.g. as web close to the cell membrane [45]) and not exclusively associated with tight junctions. Further, the actin in this study was located around the whole circumference of the cells which would indicate tight junctions in close proximity to each other. This would lead to high transepithelial electrical resistance values which were not confirmed in the study. Thus the results from Behrens et al. [288] do not prove the presence of tight junctions in HT29-MTX cells. As no further reports about tight junctions in HT29-MTX cells were found, it can was assumed that there were no free tight junction-related proteins in trypsinised HT29-MTX cells.

However, trypsin-treatment was likely to degrade cell surface structures on the IEC (Dr S. Amu, University College Cork, Cork, Ireland, April 2016). As IEC were used for the adhesion assay briefly after trypsin treatment, their binding potential could have been reduced. Thus, cell-adhesion of isolated whey proteins observed here might not show the full binding capacity of Caco-2 and HT29-MTX cells.

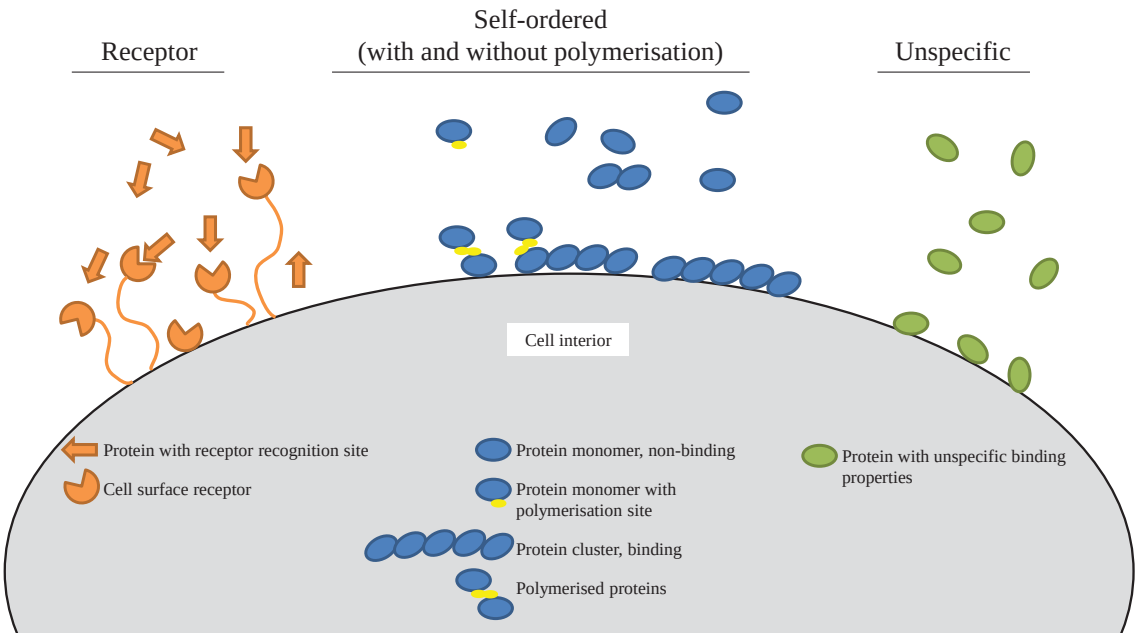

Figure 7.14: Schematic representation of the three suggested binding mechanisms for milk proteins adhering to (epithelial) cells in this study.

A comparison between Western blot analysis (Chapter 5) and flow cytometry was not possible. Western blot only showed significant binding for the co-culture, which was not used for flow cytometry due to protein restrictions, and for IgM which could not be acquired as isolate.

The three types of binding discussed – unspecific (e.g. BSA, first of two peaks in bimodal patterns), self-organised micro-structures, with or without polymerisation (suggested for second peaks in bimodal patters), or receptor-based (e.g. Igs) – are illustrated in Figure 7.14.

7.3.2 Binding of isolated proteins to bacterial cells

Contrary to Western blot, the flow cytometry results showed a difference in β-LG binding between the bacteria. Significant binding to the biofilm free cells but little (although significant) binding to the *E. coli* Nissle 1917 or *S. epidermidis* 1457 was observed. Further, β-LG was the only protein that showed an unusual binding pattern, i.e. the bimodal distribution for *E. coli* Nissle 1917 and *S. epidermidis* 1457 and the shift in geometric mean with little change in peak height for *S. epidermidis* 1457 M10. Here the peak shift observed for *S. epidermidis* 1457 M10 would indicate a strong display of ordered binding. The changes (in binding to *E. coli* Nissle 1917 *or S. epidermidis* 1457) might have been caused by different ways of binding, e.g. organised, receptor-based or non-specific (Figure 7.14), as already discussed for the IEC in culture. The change in distribution could also have been caused by a heterogeneous bacterial population, e.g. different degrees of extracellular matrix coverage, or different stages of growth. A possible explanation for the difference in binding between *S. epidermidis* 1457 M10 and all other tested cells (bacterial and epithelial) is that the mutant displayed an partially unprotected (pathogenic) cell surface [636] which was likely to be insufficiently protected from protein binding. Other proteins, including LF and IgG, did not show a bimodal distribution. A possible reason is the fact that both those proteins are related to the immune system and are evolved to interact with bacteria in a more specific manner [446, 637].

The binding behaviour for LF was in agreement with Western blot results, which showed superior binding *to S. epidermidis* 1457 M10. However, flow cytometry also indicated that only

10 to 15% of bacteria bound LF at the titration end point. The LF binding cells could have been older cells in a later growth phase. These cells have been reported to undergo structural changes [638] which could render the cells more 'visible' to the immune system. This could even be a type of decoy mechanism, aiming to occupy the host's system with the eradication of old bacterial cells while the fresher cells can reproduce stealthily. As the binding curves (Figure 7.11 D) plateaued towards the end of the titration, this indicates that LF can bind only to a sub-population of bacteria, independent of their propensity to form a biofilm. This also reflected in similar binding patterns between the two wild types and the mutant.

In comparison to Western blot, the flow cytometry experiments showed low levels of IgG-binding to bacteria, despite the lack of a competitive binding environment. If the decreased adhesion potential was caused by the purification of IgG (IgG detected by Western blot was from whey whereas IgG used for flow cytometry was purified), this is a strong indication for the importance of the native conditions in the adhesion of IgG to bacteria. Possible factors are a native milieu including other proteins, peptides, lactose or minerals that act as co-factors during IgG binding. In addition, the tertiary structure of IgG itself could be crucial and miniscule changes during purification can have adhesion-reducing effects.

sIgA showed a high proportion of binding to the biofilm free mutant at low protein levels. IgA results agree between those obtained with Western blot and the flow cytometry analysis, although the flow cytometry results were only significant for the mutant strain. Comparing the results for sIgA and free secretory component (a component of sIgA) suggests that free secretory component plays a more important role in sIgA binding to *E. coli* Nissle 1917 than to the pathogen (Figure 7.12, number of FITC or Cy5 positive cells). Free secretory component showed significant binding (compared to untreated cells) only to *E. coli* Nissle 1917 and almost no binding to *S. epidermidis* 1457 and its mutant. Contrary, binding of sIgA was increased to the two *S. epidermidis* 1457 strains, while binding to *E. coli* Nissle 1917 was comparable to that of free secretory component (although the concentration of free secretory component was double that of sIgA). This correlation suggests that, in sIgA, the *E. coli* Nissle 1917 binding

epitope is located on the free secretory component part whereas it is on the IgA dimer-backbone for the pathogens. Generally, the better adhesion to *S. epidermidis* 1457 M10 than to *S. epidermidis* 1457 agreed with the Western blot results and supports the concept of a (immuno)-protective biofilm [639]. However, the amount of protein molecules per cell (Figure 7.13) suggests that a comparable number of free secretory component proteins bound to all three bacteria investigated. Further, the levels of sIgA detected on *E. coli* Nissle 1917 and *S. epidermidis* 1457 were similar, while a higher number of sIgA dimers was observed to bind to the mutant, suggesting an (immuno)-protective effect of the wild types.

7.3.3 Lessons from flow cytometry

Some proteins might change their binding behaviour once all available (cell) surface is occupied and a critical concentration of unbound protein is available, e.g. β-LG, LF or IgG. The formation of such a 'conditioning' or 'base' film on the surface might also allow for improved adherence for secondary proteins. This would be worthy of further research as the use of a smaller quantity of minor or functional proteins (e.g. LF or Igs) could enhance the subsequent binding of major milk or whey proteins which did not show good binding in a mixed solution, such as β-LG or α-LA. For example, liposomes could be constructed with a small percentage of LF (good binding to most tested surfaces) and a larger percentage of α-LA (non-allergenic major whey protein with low demonstrated binding affinity) incorporated into its surface. The specific combination of different proteins might lead to an enhanced binding of the liposomes and reduce the cost of protein incorporated in the vehicle (synergy).

A change in binding mechanism at higer protein concentrations could, however, also be caused by a change in binding behaviour of bacterial cells or IEC once all available surface is occupied with proteins. Changes could be caused by the presentation of receptors, modified surface structures or a secretion response. As mentioned before (Section 7.3.1), answering these questions demands a molecular biologic approach.

Flow cytometry experiments also suggest that the protein size might be a factor in binding to mucin covered epithelial cells. α-LA and β-LG were the proteins showing most binding to HT29-MTX cells (results from binding curves representing all cells with bound protein independent of the amount of protein per cell). Further, during binding the ability of the protein to penetrate into and diffuse through the mucus is likely to be important. For diffusion speed the molecule size is relevant. This can be deduced from diffusion equations which contain the molecule radius as a diffusion enhancing factor (e.g. Equation 2) [640]

$$D = \frac{k_B \, \mathrm{T}}{6\pi\mu \mathrm{r}} \qquad \text{(Eq.2)}$$

where D is the diffusion coefficient, k_B is Boltzmann's constant, T is the absolute temperature, μ is medium viscosity and r is the radius of the diffusing molecule.

This partly agrees with findings from Olmsted *et al.* [286] who showed that smaller molecules move more freely through mucin compared to IgM which was 3 to 5-times slower. However, the group of small molecules also contained human IgG and IgA which are over 10-times larger than α-La and β-LG. The ability to penetrate into the mucin is likely to be dependent on the molecule size but also charge and hydrophobicity are relevant as the mucin layer in the human intestinal tract was reported to be covered with a phospholipid layer [275-279]. This layer might not be present in cell culture models but needs to be considered for *in vivo* applications.

7.4 Conclusions

The binding of whey proteins to human IEC in culture and bacteria was tested. The results support the hypothesis of this chapter, that the proteins identified as adhering to the different intestinal surface layers in previous chapters differ in their binding behaviour and also that binding to human IEC in culture differs from binding to bacterial cells. It was shown that most proteins bound better to the PIA-depleted mutant than to the to wild-type strains. Results were most striking for LF, sIgA and β-LG. Thereby a large number of LF molecules bound per bacterial cell (small percentage of cells), whereas β-LG bound to a large percentage of cells particularly the biofilm free mutant (few proteins per cell). sIgA bound to a large percentage of

bacterial cells, likely with a lot of molecules per cell. This agrees with documented function of LF and sIgA in innate immunity. Bacterial binding of β-LG is not well documented to date. However, results here suggest that β-LG is suitable to target bacteria due to its binding performance (in an isolated solution) and availability. Binding to Caco-2 and HT29-MTX cells was significant for all tested proteins. Thereby β-LG and α-LA adhered to a larger percentage of mucin covered cells, possibly due to their small molecular size. In contrast, LF and IgG appeared to bind to a larger percentage of Caco-2 cells. The protein size was an important factor regarding the number of molecules per cell; this effect was less prominent in the mucin covered cells.

The results here suggested that binding at low protein concentrations was non-specific. At higher concentrations a change in binding mode is proposed. This could either be receptor based or caused by polymerisation or self-organisation of the proteins. Proteins which showed a bimodal behaviour were β-LG (for both bacterial and epithelial), LF and IgG (for epithelial cells). In summary, results suggest that after isolation especially LF (preferably but not exclusively microorganisms), β-LG (preferably but not exclusively mucin covered cells), and to a lesser degree BSA are candidates for food grade protein ingredients which might serve as anchors for targeted delivery vehicles.

Chapter 8 General discussion

8.1 Objectives and hypothesis

Research in the recent years has contributed to the discovery of new, food-derived functional molecules. In contrast to minerals or vitamins, these molecules often have a higher molecular weight and complex structures (e.g. bioactive proteins) and may need to be protected in a delivery system, such as micelles, liposomes or capsules if they are to survive the passage of the GIT until they reach their desired target site. The delivery systems are typically designed to disintegrate at a predetermined site, e.g. the small intestine, and release the active ingredient, e.g. at its site of absorption.

In most cases, the desired target site for the delivery systems is the intestinal surface or one specific layer (bacterial biofilm, mucus layer, or absorptive IEC) thereof. Thus it would be desirable to incorporate anchor molecules at the surfaces of delivery systems that can bind to the intestinal surface to allow sufficient time for the delivery systems to degrade and release the active ingredient. Further, this would result in an accumulation of delivery vehicles at the site of action and prevent release of the active ingredient in the middle of the lumen where premature degradation through digestive enzymes may occur and reduce the amount of bioactivity.

Therefore this thesis aimed to develop an adhesion protocol to evaluate complex food systems and identify food protein molecules which adhere to one or several layers of the human intestinal surface. An assay was needed to determine if protein molecules adhere differently to the individual intestinal surface layers, depending on their structure. And further, whether or not these specificities can be harnessed to target delivery systems to a specific intestinal surface layer. Three different key components of the human intestinal surface layers were considered (epithelium (Chapter 5), mucus (Chapter 4) and bacteria with the propensity to form a biofilm (Chapter 6)) and model systems for each were adapted. The binding behaviour of individual proteins to IEC and bacterial cells was then investigated in Chapter 7 using flow cytometry. An *in vitro* partial gastric digestion protocol was developed to prepare whey proteins in an array of digestion profiles as it might occur *in vivo*, and a protocol to test for adhesion *in vitro* was set up (Chapter 3).

8.2 Adhesion protocol

Applicability and adaption of the developed adhesion protocol to other foods (e.g. different mineral composition to whey, or solid foods) were discussed in Chapter 3. In brief, an *in vitro* adhesion protocol, investigating adhesion of proteins from a liquid substrate to an intestinal surface layer model, was optimised for whey or milk and bacteria, IEC and their mucus layer. Additionally, an *in vitro* gastric digestion was adapted for whey and milk. For the adhesion assay, mucin-coated Sepharose-beads, bacteria or IEC were incubated with milk or whey and adhering proteins were observed using reducing SDS-PAGE analysis. Proteins of interest were identified using mass spectrometry and identification was confirmed with Western blot. Advantages and limitations of the analysis methods used are compared in Table 8.1. In combination, the methods used here are suitable for screening of adhering molecules (SDS-PAGE), protein identification (LC-MS/MS) and determination of preferentially binding proteins from a mix (SDS-PAGE and Western blot). Flow cytometry was then used to investigate binding profiles.

For in depth analysis of interactions in future research, native PAGE with or without mass spectrometry and atomic force microscopy [641, 642] could provide further information on the exact binding partners, identify non-protein adherents and measure binding forces, respectively. Thus, it might be possible to investigate the nature of interactions as the wash cycle, developed and used to determine the type of interaction, was not applicable to bacteria or epithelial cells in a culture.

For analysing non-protein components, different methods need to be used. Generally, mass spectrometric analysis of the whole pellet (i.e. beads or cells with bound molecules of interest) is an option. However, this seems un-feasible for the screening of a large number of samples. Therefore, other methods need to be chosen for a first assessment of adhesion (similar to SDS-PAGE analysis in this thesis) and to find candidate molecules for further investigation. Carbohydrate analysis could be done by combining SDS-PAGE analysis with glycoside staining

Table 8.1: Advantages and limitations of the analysis methods used in this thesis

	Advantages	Limitations	Suggested to use for
SDS-PAGE	Mixture of proteins Visualisation of all proteins Fast	Protein identification Often background (interference)	Screening Determination of selective binding
SDS-PAGE + MS	Mixture of proteins Visualisation of all proteins Protein identification	Slow Costly	Identification of specific proteins of interest
Western blot	Mixture of proteins Test for specific protein Quantitative	Antibody availability Labour intense	Quantification of known adhering proteins
Flow cytometry	Analysis at a cell level Determination of homogenous populations Fast Quantitative	Purified proteins Isolated in solution	Quantification of proteins binding per cell

[643] and mass spectrometric analysis of spots of interest. In addition, HPLC or ion-exchange chromatography of attached molecules after stripping from the surface component could be possible [644]. However, determining the origin of a detected sugar is difficult when sugars from both, the food under investigation and surface layer, are native and unmarked (e.g. in this thesis, proteins from whey and bacterial or epithelial cells were differentiated by adding a fluorescent tag to whey proteins). This can be addressed by using sugars labelled with isotopes and isotope-based detection methods [645]. Fats and phospholipids (hydrophobic components in general) could be analysed by solvent extraction followed by gas chromatography [646] or gas liquid chromatography [647].

Finally, it would be interesting to co-culture IEC and bacteria with the propensity to form biofilms, use everted gut sacs or *ex vivo* guts to take the assay a step closer to the *in vivo* situation before using an animal model. An overview of advantages and limitations of the applied protocol for the investigated surface layer models is given in Table 8.2.

8.3 Adhesive proteins and mechanisms of binding

Combining the results from SDS-PAGE analysis, Western blot and flow cytometry showed that milk proteins adhered differently to the tested model surface layers (bacteria with the propensity to form biofilms, mucin or IEC). A comparison of the results showed that the Ig-family, especially IgM, represents proteins that bind to different layers (Table 8.3).

8.3.1 Immune related proteins

Members of the Ig-family have different domains for specific binding purposes. The (hyper)variable regions, at the top end of the Y-shape [648], bind with high specificity to antigens whereas the other end (crystalisable domain [649]) can bind to a surface of a cell, e.g. B-cell, in a way that the antigen binding site is accessible for ligands [650]. Western blot analysis showed that the IgG heavy chain and a 75 kDa fragment of IgM which was likely to be a part of the heavy chain [651] bound to all three bacteria evaluated in this thesis. Further, a 50 kDa SDS-PAGE band, the molecular weight of heavy chains, was observed in mucin-coated

Table 8.2: Analysis of advantages, limitations and development potential of the developed adhesion assay

DTT: Dithiothreitol. IEC: Intestinal epithelial cells. GIT: Gastrointestinal tract.

	Advantages	Limitations	Options for development
***In vitro* gastric digestion**	Easy and fast Inhibition without denaturating proteins	Only gastric phase Only for protein	Should be extended to a two (gastric + duodenal) or three (gastric + duodenal + brush border) phase digestion More mechanical impact for solid foods
Adhesion assay with coated Sepharose beads	Easy and fast Adaptable to various ligands of interest Beads can be stored	Sepharose can bind molecules non-specifically and result in high background	Useful for screening, especially for molecules which do not bind to Sepharose beads
Adhesion assay with bacteria	Closer to *in vivo* situation than isolated biofilm components Can show differences between wild type bacteria and biofilm depleted mutant Adaptable to other strains	Not a full grown biofilm Binding to potential biofilm and bacterial cells (no 'clean' design) Slight variation between samples due to wash steps (some cells with proteins are removed during washing) Background for some Western blot antibodies	Bacteria in the GIT grow in an anaerobic environment [2]
Adhesion assay with cells in culture	Selecting the right cells allows to focus on IEC feature of interest	Duration Fractionation (mucin, cells) is imprecise and DTT might influence binding of some proteins Background in SDS-PAGE	Can be developed or adapted (e.g. anaerobic chamber [2] to mix IEC with intestinal bacteria)
Flow cytometry	Quantitative	Isolated proteins (purification might change proteins and a lack of competition)	Analyse several proteins with different fluorophores to create competitive environment

Sepharose beads after incubation with skim milk. Western blot analysis of experiments with IEC also suggests minimal binding of the IgG heavy chain, however only to Caco-2 cells. This agrees with reports that the V_H (variable, heavy) domains are the major antigen binding sites on the variable regions, with the H3 loop being the main contributor [652, 653]. Vermeer and Nord [650] also showed that the globular structure of the IgG monomer is hardly changed at temperatures up to 50°C. Thus the incubation of whey at 45°C to remove sediment was not predicted to impact on the protein structure.

IgG has been hypothesised to show dose-dependent binding to epithelial cells and bacteria. At low concentrations, it increased antigen binding to mucosal surfaces whereas at high concentrations it inhibited bacterial adhesion by binding to lipopolysaccharide [654]. Western blot analysis in this thesis showed binding of a 50 kDa fraction of IgG to all three bacteria but little or no binding was detected for IEC. Flow cytometry analysis confirmed binding of IgG to bacterial cells and IEC, whereby binding to IEC appeared to increase with increasing protein concentration (up to 2 $\mu mol.10^{-5}$ cells) while binding to bacteria plateaued when more than 0.01 $\mu mol.10^{-6}$ cells) IgG was added. As mentioned before, flow cytometry results for bacteria and IEC could not be compared due to different protein concentrations (0 to 8 $\mu mol.10^{-5}$ for IEC and 0 to 0.1 $\mu mol.10^{-6}$ cells for bacteria). Thus results here neither support nor reject the stated hypothesis that the concentration of IgG determines whether bacteria or IEC are targeted. However, a dose-dependent binding might determine the target specificity (IgG density on the microsphere surface) when IgG is used as an anchor molecule. This is relevant information for the design of targeted delivery systems and needs to be investigated further. Experiments could be undertaken to compare the IgG binding to IEC and bacteria after incubating a set number of cells with increasingly diluted whey preparations. In addition, studies with a mixed bacterial-IEC culture model would be a good approach to investigate (preferential) binding of IgG in a system in which both, bacteria and IEC, are available for binding. Using whey is preferable to isolated protein solutions as a competitive binding environment is desirable.

IgM showed the most adhesion potential in this thesis (Table 8.3). This correlates with the average glycoside content in bovine milk Igs as described by Marnila and Korhonen [655] in O'Riordan et al. [1]: IgG (2.6 to 3.1%), IgA (6 to 10%) and IgM (10 to 12%). However, there is little information about the glycosylation pattern of bovine Igs [1] and its role in Ig binding. In addition to the glycans on the conserved regions (Table 8.4), there are further saccharides randomly distributed on the variable region of the Fab fragment [656, 657]. These are reported to be more sialated than the glycans on the conserved regions, more complex or high in Man [658]. While the studies were carried out on human IgG molecules, Aoki et al. [659] confirmed that bovine IgG is similar in structure. In agreement with the findings here, IgM, but also IgG and IgA, represent a class of antibodies which can bind to proteins, carbohydrates, lipids and nucleic acids [660]. These molecules can bind equally well to different antigens [661], a property which was previously interpreted as low affinity. Generally, antibodies (a subset of all Igs) show binding specificity for one antigen, while Igs which are not selected for an antigen are expected to show a different, less specific binding behaviour (Dr S. Amu, University College Cork, Cork, Ireland, June 2016). Accessible glyco-epitopes show wide cross-reactivity and are preferential targets for IgM, which is thus able to bind to a range of different molecules [662]. *Vice versa*, IgMs of different individuals are able to bind to the same antigens [593]. Thus, if the binding of IgM to the mucin fraction of HT29-MTX cells (MUC5AC) shown in this thesis is based on epitopes in the glycoside side chains of the mucins, it is likely that IgM also binds to other mucins. These can be in the glycocalyx (MUC3) of IEC or the secreted intestinal mucin layer (MUC2). Additionally, IgM was shown to bind to bacterial cells in the GIT, rendering it a prime candidate for an anchor-molecule for broad spectrum targeting.

Flow cytometry experiments were the only set-up with the potential to give information about the mechanisms underlying the binding of the individual proteins. Results suggest that some proteins might have different binding sites for different surface layers. This was shown, in particular, for sIgA and isolated free secretory component (discussed in Section 7.3.2). The

Table 8.3: Comparison of identified adhesive proteins from Chapters 4 to 7

XOR: Xanthine oxidoreductase. IgA/G/M: Immunoglobulin A/G/M. sIgA: Secretory Immunoglobulin A. LF: Lactoferrin. fSC: Free secretory component. BSA: Bovine serum albumin. CNs: Caseins. β-LG: β-Lactoglobulin. α-LA: α-Lactalbumin. hc: heavy chain. Comp. PP3: Component proteose peptone 3. BTN: Butyrophilin. MS: Mass spectroscopy. WB: Western blot. FC: Flow cytometry. EcN: *E. coli* Nissle 1917. Se: *S. epidermidis* 1457. SeM: *S. epidermidis* 1457 M10. [1]PIGR (polymeric immunoglobulin receptor).

	Bacteria (SDS-PAGE)	Bacteria (MS)	Bacteria (WB)	Bacteria (FC)	Bacteria (Microscpy)	Mucus beads	Mucus cell culture (WB)	IEC (WB)	Detached cells (FC)
XOR	Se, SeM (150)	Yes	---						
IgM		hc, const.reg.	Yes (70)SeM (50,20)			Yes	Co-cult.	Caco-2	
IgA			SeM			No	No	No	
sIgA				SeM		No			
IgG			SeM (50, 23)	EcN		Yes hc	No	No	Yes
LF	Yes	Yes	EcN, SeM	SeM		Yes			Yes
fSC				EcN		Yes[1]			
BSA	Yes (70)	Yes (dig)		SeM			No	No	Yes
CNs	Yes (25)				?	Yes, α_{S1}, β			Yes, κ
β-LG	EcN (18)	Yes	---	EcN, Se		Yes	Co-cult.	No	Yes
α-LA	Yes (14)			SeM			No	HT29-MTX	Yes
other	Ig hc (70, 60) Unknown (10)	Ig hc, Ig lc Comp.PP3				BTN			

difference might have been caused either by the different characteristics of the bacteria (probiotic *E. coli* Nissle 1917 and pathogenic *S. epidermidis* 1457) and resultant surface features like receptors, or by their cell wall structure (Gram-negative *E. coli Nissle* 1917 and Gram-positive *S. epidermidis* 1457). In either scenario, it appeared that the pathogenic character or cell wall structure was more important than the ability to form a biofilm as the results *for S. epidermidis* 1457 wild type and mutant were similar, while *E. coli* Nissle 1917 showed a different behaviour. Results from Mathias and Corthesy [663] indicate that free secretory component is a key factor in binding of sIgA, and further that the Gram-type plays an important role in sIgA binding to bacteria. For example, native and deglycosylated sIgA bound equally well to *E. coli* Nissle 1917, whereas binding of the deglycosylated form was reduced for tested Gram-positive commensals. The authors also pointed out that pathogenic bacteria could display different surface features, such as intimins which depend on glycosides for adhesion. Taken together with observations from this thesis, this suggests that the protein component of free secretory component binds to *E. coli* Nissle 1917, whereas glycosides on the Ig-backbone mediate binding to *S. epidermidis* 1457 M10. This shows that binding of sIgA and free secretory component to bacteria differs between bacteria and it is reasonable to test binding for the relevant strain in each case.

Intact LF is unlikely to enter into membranes due to its size and cationic character. Its positive charge was suggested to enable binding to divalent cation-binding sites on the lipopolysaccharide layer of the Gram-negative bacteria or to the teichoic or lipoteichoic acid embedded in the peptidoglycan layer of the Gram-positive bacteria [664]. Additionally, LF can carry negative charges introduced through its accessories, for example the NeuNAc containing termini which carry a negative charge at physiological pH-value. Bovine LF is also high in Man and sialated N-glycans [665-668] on its four glycosylation sites (Asn233, Asn368 (GlcNAc), Asn476 (two GlcNAc and β-1,4-Man) and Asn545 (Man rich hexasachharide)) [669, 670]. Despite not containing any glycosylation sides, the lactoferricin fragment (17-41) [450] was also found to bind to lipopolysaccharides and lipoteichoic acid [671]. Thus it is likely that

binding is based on the amino acid sequence itself [672, 673]. Taken together this suggests that LF can undergo various types of interactions with bacteria. This agrees with results from Western blot and flow cytometry which showed adhesion of LF to bacteria and IEC. In agreement, Ashida et al. [674] describe binding of LF to differentiated Caco-2 cells with a dissociation constant to that of recombinant LF-receptors. The authors concluded that Caco-2 cells display LF-receptors on their apical surface. This suggests that LF is a good candidate for an anchor molecule. However, it needs to be protected from premature digestion and also potential antimicrobial effects also need to be considered.

8.3.2 Caseins

Adhesion of caseins was not the focus of this study. Thus few results regarding κ-casein (flow cytometry) and total casein from skim milk (fluorescent microscopy) are available for discussion.

Glycomacropeptide, derived from κ-casein, the only glycosylated casein [675], has glycoside chains of which 82% are mono- or di-sialated [11]. Nakajima et al. [676] demonstrated that the NeuAc component is of particular importance for glycomacropeptide's ability to bind pathogens. Despite being un-glycosylated, α_{S2}-casein fragment (183-207) was found to bind to lipopolysaccharides and lipoteichoic acid [671]. This shows that there is bacterial-binding potential of caseins which could have been observed in the fluorescent microscopy pictures (Figure 6.8). Further, flow cytometry analysis showed κ-casein binding to both, Caco-2 and HT29-MTX cells. Hira et al. [677] showed that α-casein (not further specified) and “casein sodium” bind to isolated rat small intestinal brush border membrane. Binding of caseins induced stronger signals than BSA adhesion, as observed with BIACORE (compare Chapter 3).

Depending on the degree of glycosylation, glycomacropeptide is partially protected from pancreatic digestion [678, 679]. If whey is produced through chymosin or pepsin action [675] glycomacropeptide makes up 15 to 20% of whey protein. This prevalence in secondary streams

of cheese production and stability during passage of the human GIT make glycomacropeptide an interesting molecule for targeted adhesion.

8.3.3 Other binding proteins

Detecting adhesion of β-LG was an unexpected finding. To date, binding of lipophilic compounds has been described for β-LG [584, 680], but no information about adhesive properties to bacteria, mucin or IEC was found. However, β-LG is the major whey protein, making up 50% of all whey proteins [493], and thus is likely to show detectable binding even at low binding affinity. For example, β-LG was shown by Western blot analysis to bind to *E. coli* Nissle 1917, and to the mucus of the Caco-2 and HT29-MTX co-culture in this thesis. Therefore, different approaches to increase β-LG binding and theories of the binding mechanism to individual intestinal surface layers are discussed below.

Two hypothesised methods to further increase β-LG adhesion to intestinal surface layers are controlled glycosylation (e.g. early products of the Maillard reaction) or selectively cleaving the intra-molecular bonds to display the hydrophobic core [680] and thus allow adherence based on hydrophobic interactions. Both mechanisms were also hypothesised to be involved in the binding of β-LG to the mucin fraction of the co-culture (90% Caco-2 and 10% HT29-MTX cells) due to activity of brush border membrane enzymes and discussed in detail in Chapter 5.

Observations in this thesis suggest that β-LG did bind to mucin glycoproteins directly, as indicated by results in Chapter 5. This agrees with results from Ouwehand and Salminen [681] who showed that β-LG from infant formula could prevent bacterial adhesion to glycoproteins from ileostomy effluent [682] pre-treated with β-LG, which suggests that β-LG did bind to the glycoproteins but did not show bacterial binding.

At neutral pH, β-LG binds palmitic acid, retinol, retinoic acid and several other hydrophobic compounds [683-689]. Barbiroli et al. [690] could further show that at neutral pH, the binding to β-LG was determined by the hydrophobicity of the ligands. This is supported by previous findings that molecules like palmitic or oleic acid which are known for β-LG binding, bind well

at neutral pH but are released at acidic pH [688, 689]. The binding buffer in this thesis had a neutral pH and binding of β-LG to hydrophobic molecules such as lipophilic components in or on the cell surface (e.g. lipoproteins) or lipid fraction of lipoteichoic acids on bacteria might have been possible.

α-LA is secreted as glycoprotein but rapidly de-glycosylated by milk hydrolases [12]. The initial form, glyco-α-LA, has been discussed (Section 6.3.2). Based on its wide spectrum of glycosides (compare Table 8.4), it is likely that this glyco-α-LA has the potential to bind to the small intestinal surface layers through glycoside mediated interactions. No information on glyco-α-LA binding was found in the literature.

Serum albumin, which is known to contain fatty acid-binding sites has previously been shown to be capable of binding to the lipid moieties of lipoteichoic acid [691]. Teichoic acid is a polyanionic cell wall glycopolymer [692] that shows high concentrations in the cell walls of Gram-positive bacteria [693] and increases *S. epidermidis* binding to fibronectin in a dose-dependent and saturable manner [694]. Results from Kulikov et al. [695] suggest that poly-cations bind to the cell wall of *S. aureus* and the authors hypothesise that teichoic acid is one binding partner. Most proteins in this thesis carry one or several charges at neutral pH and had the potential to directly bind to the bacterial cell walls if these were accessible. The positively charged proteins could directly bind to the teichoic acids while anionic proteins could use di-cationic ions such as Mg^{2+} as binding bridges [696].

8.3.4 Glycosylation of proteins

All proteins investigated in this thesis are secreted proteins. These proteins typically carry glycosides as cellular signals for secretion from the mammary cells and correct protein folding upon secretion [697]. Some of these glycosides are removed quickly from the protein by milk hydrolases after secretion, resulting in proteins with low or no glycosylation, e.g. α-LA and β-LG. Other proteins remain glycosylated, and in this thesis, most of the proteins which showed

Table 8.4: Overview of milk protein glycosylation

Data summarised from O'Riordan et al. [1] and as indicated. If not stated differently, data is derived from bovine proteins.

Yes: Glycoside is part of protein's glycome. No: Glycoside is nto part of protein's glyvome. n/a: No information found. --- Information for several cells

IgA/G/M: Immunoglobulin A/G/M. LF: Lactoferrin. GMP: Glycomacropeptide. α-LA: α-Lactalbumin. BTN: Butyrophilin. CPP3: Component proteose peptone 3. Neu5Ac: N-acetyl-neuraminic acid, sialic acid. Neu5Gc: N-glycolyl-neuraminic acid. GlcNAc: N-acetyl-glucosamine. GalNAc: N-acetyl-galactosamine. Man: Mannose. Fuc: Fucose. Gal: Galactose. [1]Data from the corresponding human protein [2] Data from the corresponding mouse protein

	Neu5Ac	Neu5Gc	GlcNAc	GalNac	Man	Fuc	Gal	Comment
IgM [3, 4]	Yes	n/a	Yes[1]	n/a	Yes[1]	Yes		
IgG	Mostly α_{2-6} linkage [5]	n/a	Yes, N-glycos. linked to Asn[1]	n/a	n/a	Yes[1]	Yes[1]	Most glycans on heavy chain Fc fragment [5, 6]
IgA [3, 7, 8]	Yes[1]	n/a	n/a	Yes[1]	n/a	Yes[2]	Yes[1]	
LF	Yes, terminal charge	Yes, 5% of Neu	Yes, N-glycosid. link to Asn	---------- Yes, glycoside core ---------- 65% Man chains (<Man8) 35% hybrid				76% neutral, 24% sialayted glycosides
GMP [9, 10]	Yes, terminal	No	No	Yes, O-glycosid. link to Thr	No	No	Yes	82% sialated [11]
α-LA [12, 13]	Low level	n/a	Yes	Yes	Yes	Low level	Low level	3-10% glycosylated, N-glycans Susceptible to hydrolase de-glycosylation
BTN [1, 14]	Yes	n/a	Yes	n/a	Yes	Yes	Yes	N-glycosylated [15] Also LacdiNAc
CPP3 [16, 17]	Yes, terminal	n/a	Yes, N-glycosid. link to Asn	Yes, O-glycosid. link	Yes	Yes	Yes, O-glycosid. link	Also phosphorylated [18] Also LacNAc and LacdiNAc Terminal sialaytion

adhesion (e.g. Igs, LF, κ-casein) were glycoproteins. Thus, it is likely that the sugar moieties were involved in some of the interactions. However, it needs to be emphasised that carrying glycosides does not automatically imply binding and each protein needs to be considered individually.

Glycosylation characteristics of milk proteins were reviewed by O'Riordan et al. [1] and are summarised in Table 8.4. Analysis of the total glycome of a whey protein product by van Leeuwen et al. [698] showed that all relevant glycans are listed in Table 8.4, except glucose of which there are only traces. Two MFGM proteins, butyrophilin and component PP3, were included as they were identified as binding proteins in the first set of mass spectrometry analysis from mucin-bead experiments. Especially component PP3, a phosphorylated glycoprotein of 28 kDa molecular weight, is of interest as it is present at high concentrations in bovine milk (300 $mg.l^{-1}$) and makes up to 10% of whey proteins [17, 18]. Current understanding is that glycosides have several functions, such as receptor-ligand interactions, protection from digestion, protein folding [1], tissue targeting [699] or secretion [700]. Thus, it is likely that a proportion of the adhesion observed in this thesis was glycoside-mediated. A possible set-up to test the effect of glycosides on protein binding to human intestinal surface layers is to compare the adhesion of native proteins and proteins treated with N- and O-glycosidases to remove glycosides from proteins. This could be done using the adhesion protocol developed in this thesis. A comparison of adhering proteins, e.g. using reducing SDS-PAGE or Western blot, can then show if de-glycosylation impacts the adhesion behaviour of milk or whey proteins, i.e. if binding is decreased after removal of glycosides. This could be complemented with a glycoside stain of the SDS-PAGE gels to quantify the degree of de-glycosylation.

8.5 Achievements and limitations

Reflecting on the objectives stated in Chapter 1, this thesis did succeed in developing a template adhesion protocol which can be adapted to test the binding of food molecules to the intestinal surface layers. Here the adhesion protocol was used to test the adherence of milk and whey proteins, but with adjustments to the binding buffer compositions or respective analysis methods

the assay could also be used for other foods or to analyse different food components, respectively (Section 8.2.1). Further, model systems for three intestinal surface layers (bacterial biofilm, mucin layer and IEC) were identified and optimised for the adhesion assay. Thereby one model, the mucin coated Sepharose beads, was shown to have performance deficiencies due to a low degree of mucin binding to the Sepharose beads. Thus it is recommended for future work to either optimise the beads by substituting the partially purified mucin used here with fresh porcine mucin, or to use alternative protocols such as a mucin particle adhesion assay, or mucin producing IEC in culture as it was done in this thesis. On the other hand, assays with bacterial pellets and cell culture worked well. The validity of the assay was confirmed by showing the binding of LF and Igs to bacterial cell surfaces. Finally, the hypothesis was supported in that different proteins bind specifically to one intestinal surface layer and several proteins which bind to one or several intestinal surface layers were identified.

However, this thesis did not answer the question from Chapter 1 about how the identified binding molecules behave when they are incorporated into nutrient delivery vehicles. Formulating the delivery systems might block binding domains or change the protein structure so that the adhesive properties of the final construct is reduced compared to theoretical values. Further the introduced model systems for the intestinal layers are *in vitro* systems and can only give indication of what happens when proteins or delivery systems enter the human GIT. Thus further research is required to answer these questions, and suggestions for these experiments are made in Section 8.7.

8.6 Summary and conclusions

In summary, an adhesion assay was developed which allows the screening of liquid foods for proteins adhering to the individual intestinal surface layers. By adjusting the sample preparation and binding buffer composition, the assay could also be applied for solid foods. By changing the analysis methods (e.g. database set up for analysing peptides identified with mass spectrometry) other food components like glycosides or fatty acids might also be detected.

Using the assay, several whey proteins which bind to the intestinal surface layers were identified. Selecting the right protein, if necessary in the right concentration (e.g. IgG), might even allow to target only one specific surface layer which is the desired site of action for an active ingredient. The most promising candidates for the different layers are shown in Table. 8.5.

This shows that the developed adhesion protocol does enable the discovery of a new range of adhering proteins that will facilitate the development of improved food delivery systems. These new food delivery systems can be used target functional ingredients (e.g. bioactive proteins) to their specific site of action, and thus increase the efficacy of the functional proteins.

8.7 Future research

Most research was done with whey to identify proteins that bind better than other proteins in their environment (competitive binding). However, isolated proteins showed different binding patterns. Isolated proteins will be incorporated into the nutrient vehicle surfaces and thus will be enriched but not isolated in their environment which is a state between the two extremes tested in this thesis. To test this intermediate state, the adhesion assay could be conducted with (labelled) isolated proteins spiked into a competitive food system like whey or milk, but also plant extracts would be of interest. The samples from candidate protein enriched whey and untreated whey can then be compared (e.g. Western blot) to evaluate the effect of protein enrichment on protein binding. In parallel, the adhesive molecules can be incorporated into nutrient delivery systems like micelles which can then be tested under competitive conditions. One crucial factor might be how to attach enough molecules into the surface to generate sufficient interactive forces with the intestinal surface to withstand the luminal flux.

Most of the experimental work in this thesis was done with intact proteins. However, exposing the proteins to *in vivo* conditions of the human GIT will result in degradation of most of the proteins which will also change their binding properties. Thus future research questions should consider how digestion (gastric and intestinal) changes the adhesion of molecules incorporated

Table 8.5: Summary of whey proteins adhering to one or all intestinal surface layer models in this thesis
GIT: Gastrointestinal tract.

GIT surface layer	Generally binding protein	Specifically binding proteins
Intestinal epithelial cells	IgM	α-lactalbumin
Mucin layer		β-lactoglobulin (observed in 90/10 co-culture)
Bacteria (and their biofilm)		Immunoglobulin fractions Lactoferrin

into the surfaces of nutreient delivery vehicles. Another option could be the introduction of a second surface layer to protect the anchor molecules from premature degradation. As mentioned before, such a layer should be designed to dissolve quickly in the small intestine, for example through pH-dependend solubility.

After *in vitro* adhesion of the nutrient vehicles is demonstrated, the next step is to test the compounds in more complex intestinal layer systems like an *ex vivo* intestinal sections or germ-free mice. These mice have a complete epithelial S-layer and mucus layer but no bacterial biofilm. Thus interactions between these two layers (e.g. synergies, blocking of binding site) can be explored. Comparing binding of nutrient vehicles between normal mice and germ-free mice might further allow investigating the effect of bacterial biofilms better than in *in vitro* experiments. A limitation here is the unusual GIT morphology of the germ-free mice. As a final step, the performance of the delivery system can be validated in pigs which are a more appropriate model animal than rodents as the porcine GIT resembles that of humans more closely. For all the models described here, the compounds need to be prepared in a way to recover them for analysis. This could be done by using indigestible nanosized beads instead of functional proteins encapsulated in the vehicles. Another option could be to include a rinse with fixative after the administration of the vehicles to stop all processes on the intestinal surface. In order to trace the actual anchor molecules (candidate proteins from this thesis), the proteins could be labelled with indigestible markers.

Regarding individual adhesive proteins, the adhesive potential of Igs might be enhanced by collecting them from animals which have been exposed to certain antigens. Their reactivity is strongly related to the immune challenge of the individual they are derived from (e.g. [701, 702]) and being sourced from different cows could cause a difference in binding ability. In addition, the adhesive properties of yet un-glycosylated (β-LG) or low glycosylated (α-LA) proteins might be enhanced by controlled glycosylation. This way more abundant whey proteins could be employed as anchors while others with known functionality like Igs or LF can be used in a more beneficial way. As described earlier (Section 8.3.4), determining the effect of

glycosylation on protein binding will be an important step in understanding protein binding to the intestinal surface layers. Further, if glycosides are shown to increase adherence, the assay will be a major tool in exploring the effect of controlled glycosylation of proteins and its effect on protein binding.

Another way to maximise the binding potential of delivery vehicles could be to incorporate a tailored mix of selected proteins into the micelle surface. Results here suggested that the use of a smaller quantity of functional proteins with high binding affinity (e.g. LF or Igs) could enhance the subsequent binding of major milk or whey proteins which did not show good binding in a mixed solution such as β-LG or α-LA (Section 7.3). Here the idea is that the proteins with high binding affinity generate a conditioning film on the intestinal surface which enables faster, secondary binding of the proteins with lower binding affinity.

Taken together, this thesis developed an *in vitro* adhesion protocol that can easily be adapted and expanded to enable further research in the field of targeted delivery of nutrients. Further, a set of adhesive proteins was identified. Some of them (e.g. α-LA or β-LG) showed low binding potential. However, they are major whey proteins and thus it would be of interest to increase their binding potential. Other proteins (e.g. IgM or LF) showed already good binding and can be used for immediate development nutrient vehicles. Working on both approaches in parallel could reduce the time required develop new targeted delivery systems which increase the overall time for degradation of the vehicle and facilitate the accumulation of functional nutrient on the site of absorption.

List of literature

1. O'Riordan, N., et al., *Structural and functional characteristics of bovine milk protein glycosylation.* Glycobiology, 2014. **24**(3): p. 220-236.
2. Ulluwishewa, D., et al., *Live Faecalibacterium prausnitzii in an apical anaerobic model of the intestinal epithelial barrier.* Cellular Microbiology, 2015. **17**(2): p. 226-240.
3. Krotkiewski, H., *Carbohydrate moiety of immunoglobulins in health and pathology.* Acta Biochimica Polonica, 1999. **46**(2): p. 341-350.
4. Arnold, J.N., et al., *Human serum IgM glycosylation: Identification of glycoforms that can bind to Mannan-binding lectin.* Journal of Biological Chemistry, 2005. **280**(32): p. 29080-29087.
5. Takimori, S., et al., *Alteration of the N-glycome of bovine milk glycoproteins during early lactation.* FEBS Journal, 2011. **278**(19): p. 3769-3781.
6. Wright, A. and S.L. Morrison, *Effect of glycosylation on antibody function: Implications for genetic engineering.* Trends in Biotechnology, 1997. **15**(1): p. 26-32.
7. Rudd, P.M., et al., *Glycosylation and the immune system.* Science, 2001. **291**(5512): p. 2370-2376.
8. Mattu, T.S., et al., *The glycosylation and structure of human serum IgA1, Fab, and Fc regions and the role of N-glycosylation on Fcα receptor interactions.* Journal of Biological Chemistry, 1998. **273**(4): p. 2260-2272.
9. Alais, C. and P. Jollès, *Étude comparée des caséino-glycopeptides formés par action de la présure sur les caséines de vache, de brebis et de chèvre. II. Étude de la partie non-peptidique.* BBA - Biochimica et Biophysica Acta, 1961. **51**(2): p. 315-322.
10. Keller, S.J., T.W. Keenan, and W.N. Eigel, *Glycosylation of κ-casein. I. Localization and characterization of sialyltransferase in bovine mammary gland.* BBA - Enzymology, 1979. **566**(2): p. 266-273.
11. Hua, S., et al., *Site-specific protein glycosylation analysis with glycan isomer differentiation.* Analytical and Bioanalytical Chemistry, 2012. **403**(5): p. 1291-1302.
12. Barman, T.E., *Purification and properties of bovine milk glyco-α-lactalbumin.* BBA - Protein Structure, 1970. **214**(1): p. 242-244.
13. Hindle, E.J. and J.V. Wheelock, *Carbohydrates of bovine alpha-lactalbumin preparations.* Biochemical Journal, 1970. **119**(3).
14. Sato, T., et al., *Site-specific glycosylation of bovine butyrophilin.* Journal of Biochemistry, 1995. **117**(1): p. 147-157.
15. Valivullah, H.M. and T.W. Keenan, *Butyrophilin of milk lipid globule membrane contains N-linked carbohydrates and cross-links with xanthine oxidase.* International Journal of Biochemistry, 1989. **21**(1): p. 103-107.
16. Girardet, J.M., et al., *Structure of glycopeptides isolated from bovine milk component PP3.* European Journal of Biochemistry, 1995. **234**(3): p. 939-946.
17. Sorensen, E.S. and T.E. Petersen, *Phosphorylation, glycosylation and amino acid sequence of component PP3 from the proteose peptone fraction of bovine milk.* Journal of Dairy Research, 1993. **60**(4): p. 535-542.
18. Girardet, J.M. and G. Linden, *PP3 component of bovine milk: A phosphorylated whey glycoprotein.* Journal of Dairy Research, 1996. **63**(2): p. 333-350.
19. Backstrand, J.R., *The history and future of food fortification in the United States: A public health perspective.* Nutrition Reviews, 2002. **60**(1): p. 15-26.
20. De Lourdes Samaniego-Vaesken, M., E. Alonso-Aperte, and G. Varela-Moreiras, *Vitamin food fortification today.* Food and Nutrition Research, 2012. **56**.
21. Thomas, J. *Functional foods market increases in size*. 2014 [cited 2016 30 May]; Available from: https://www.leatherheadfood.com/functional-foods-market-increases-in-size.
22. Legrand, D., *Lactoferrin, a key molecule in immune and inflammatory processes.* Biochemistry and Cell Biology, 2012. **90**(3): p. 252-268.

23. Furlund, C.B., et al., *Identification of lactoferrin peptides generated by digestion with human gastrointestinal enzymes.* Journal of Dairy Science, 2013. **96**(1): p. 75-88.
24. Shoaf-Sweeney, K.D. and R.W. Hutkins, *Adherence, Anti-Adherence, and Oligosaccharides: Preventing Pathogens from Sticking to the Host.* Advances in Food and Nutrition Research, 2009. **55**: p. 101-161.
25. Ashkenazi, S., *A review of the effect of human milk fractions on the adherence of diarrheogenic Escherichia coli to the gut in an animal model.* Israel Journal of Medical Sciences, 1994. **30**(5-6): p. 335-338.
26. Palmeira, P., et al., *Inhibition of enteropathogenic Escherichia coli (EPEC) adherence to HEp-2 cells by bovine colostrums and milk.* Allergologia and Immunopathologia, 2001. **29**: p. 229-237.
27. Schroten, H., F.G. Hanisch, and R. Plogmann, *Inhibition of adhesion of S-fimbriated Escherichia coli to buccal epithelial cells by human milk fat globule membrane components: a novel aspect of the protective function of mucins in the noimmunoglobulin fraction.* Infection and Immunity, 1992. **60**: p. 2893-2899.
28. Stromqvist, M., et al., *Human milk k-casein and inhibition of Helicobacter pylori adhesion to human gastric mucosa.* Journal of Pediatric Gastroenterology and Nutrition, 1995. **21**(3): p. 288-296.
29. Hall, T., et al., *Bacterial invasion of HT29-MTX-E12 monolayers: Effects of human breast milk.* Journal of Pediatric Surgery, 2013. **48**(2): p. 353-358.
30. Van Amersfoort, E.S., T.J.C. Van Berkel, and J. Kuiper, *Receptors, mediators, and mechanisms involved in bacterial sepsis and septic shock.* Clinical Microbiology Reviews, 2003. **16**(3): p. 379-414.
31. Peterfi, Z. and B. Kocsis, *Comparison of blocking agents for an ELISA for LPS.* J Immunoassay, 2000. **21**(4): p. 341-54.
32. Shahadir, F., J.R. Gordon, and E. Simko, *Identification of lipopolysaccharide-binding proteins in porcine milk.* The Canadian Journal of Veterinary Research, 2006. **70**: p. 243-250.
33. Cravioto, A., et al., *Inhibition of localized adhesion of enteropathogenic Escherichia coli to HEp-2 cells by immunoglobulin and oligosaccharide fractions of human colostrum and breast milk.* J Infect Dis, 1991. **163**(6): p. 1247-55.
34. Idota, T. and H. Kawakami, *Inhibitory effects of milk gangliosides on the adhesion of Escherichia coli to human intestinal carcinoma cells.* Bioscience Biotechnology Biochemistry, 1995. **59**(1): p. 69-72.
35. Coppa, G.V., et al., *Human milk oligosaccharides inhibit the adhesion to Caco-2 cells of diarrheal pathogens: Escherichia coli, Vibrio cholerae, and Salmonella fyris.* Pediatr Res, 2006. **59**(3): p. 377-82.
36. Cywes, C., I. Stamenkovic, and M.R. Wessels, *CD44 as a receptor for colonization of the pharynx by group A Streptococcus.* Journal of Clinical Investigation, 2000. **106**(8): p. 995-1002.
37. Burger, O., et al., *Inhibition of Helicobacter pylori adhesion to human gastric mucus by a high-molecular-weight constituent of cranberry juice.* Critical Reviews in Food Science and Nutrition, 2002. **42**: p. 279-284.
38. HOWELL, A.B., *Bioactive compounds in cranberries and their role in prevention of urinary tract infections.* Molecular Nutrition & Food Research, 2007. **51**: p. 732-737.
39. Puupponen-Pimia, R., et al., *Bioactive berry compounds-novel tools against human pathogens.* Applied Microbiology and Biotechnology, 2005. **67**: p. 8-18.
40. Georgiades, P., et al., *Tea derived galloylated polyphenols cross-link purified gastrointestinal mucins.* PLoS ONE, 2014. **9**(8).
41. Jacobs, C., *Neue Nanosuspensionsformulierungen fur verschiedene Appliaktionsformen*, in *Biology, Chemistry, Pharmacy*2003, Freie Universitat: Berlin.
42. Mortazavi, S.A., *An in vitro assessment of mucus/mucoadhesive interactions.* International Journal of Pharmaceutics, 1995. **124**(2): p. 173-182.
43. Patti, J.M., et al., *MSCRAMM-mediated adherence of microorganisms to host tissues.* Annual Review of Microbiology, 1994. **48**: p. 585-617.

44. Kenyon, E.M. and M.F. Hughes, *Oral Exposure and Absorption of Toxins*, in *Comprehensive Toxicology*, C.A. McQueen, Editor. 2010, Elsevier Ltd.: Kidlington, UK.
45. Fahlke, C., et al., *Taschenatlas Physiologie*. Vol. 1. 2008, Munich: Elsevier Urban & Fischer.
46. Riemann, J.F., et al., eds. *Gastroentreologie: Das Refernzwerk fuer Klinik und Praxis, Band 1 Intestinum*. 2010, Georg Thieme Verlag KG: Stuttgart.
47. Sherwood, L., *Fundamentals of Physiology: A Human Perspective*. 3rd ed. 2006, Belmont, USA: Thomason Books/Cole.
48. Tortora, G.J. and B.H. Derrickson, *Principles of Anatomy and Physiology*. 13. ed. 2011: John Wiley & Sons.
49. Javadzadeh, Y. and S. Hamedeyazdan, *Novel Drug Delivery Systems for Modulation of Gastrointestinal Transit Time*, in *Recent Advances in Nocel Drug Carrier Systems*, A. Demir, Editor. 2012, InTech.
50. Dockray, G.J., *Topical review. Gastrin and gastric epithelial physiology.* The Journal of physiology, 1999. **518**.
51. Khurana, I., *Physiological Activities in Stomach*, in *Textbook of Human Physiology for Dental Students*. 2013, Reed Elsevier India Private Limited: Gurgaon, Haryana.
52. Corfield, A.P., et al., *Mucins and mucosal protection in the gastrointestinal tract: New prospects for mucins in the pathology of gastrointestinal disease.* Gut, 2000. **47**(4): p. 589-594.
53. Macfarlane, S. and J.F. Dillon, *Microbial biofilms in the human gastrointestinal tract.* Microbial biofilms in the human gastrointestinal tract, 2007. **102**: p. 1187-1196.
54. van Aken, G.A., *Relating Food Emulsion Structure and Composition to the way It Is Processed in the Gastrointestinal Tract and Physiological Responses: What Are the Opportunities?* Food Biophysics, 2010. **5**: p. 258-283.
55. CenciČ, A. and T. Langerholc, *Functional cell models of the gut and their applications in food microbiology - A review.* International Journal of Food Microbiology, 2010. **141**(SUPPL.): p. S4-S14.
56. Pinto, J.F., *Site-specific drug delivery systems within the gastro-intestinal tract: from the mouth to the colon.* Int J Pharm, 2010. **395**(1-2): p. 44-52.
57. Schwegler, J. and R. Lucius, eds. *Der Mensch - Anatomie und Physiologie*. 4th ed. 2006, Georg Thieme Verlag: Stuttgart.
58. Schmidt, R.F. and G. Thews, *Physiologie des Menschen* 1997, Springer Verlag. p. 889.
59. Pinto, J.F., *Site-specific drug delivery systems within the gastrointestinal tract: From the mouth to the colon.* International Journal of Pharmaceutics, 2010. **395**: p. 44-52.
60. Johansson, M.E., J.M. Larsson, and G.C. Hansson, *The two mucus layers of colon are organized by the MUC2 mucin, whereas the outer layer is a legislator of host-microbial interactions.* Proc Natl Acad Sci U S A, 2011. **108 Suppl 1**: p. 4659-65.
61. Tso, P., *Overview of digestion and absorption*, in *Biochemical and Physiological Aspects of Human Nutrition*, K.D. Crissinger and M.H. Stipanuk, Editors. 2000, W.B. Saunders Company: Philadelphia, Pennsylvania. p. 75-90.
62. Moon, H.H., et al., *MSC-based VEGF gene therapy in rat myocardial infarction model using facial amphipathic bile acid-conjugated polyethyleneimine.* Biomaterials, 2014. **35**(5): p. 1744-1754.
63. Macierzanka, A., et al., *Enzymatically Structured Emulsions in Simulated Gastrointestinal Environment: Impact on Interfacial Proteolysis and Diffusion in Intestinal Mucus.* Langimur, 2012. **28**(50): p. 17349-17362.
64. Johnson, L.R., Ed., *Physiology of the gastrointestinal tract*. 3rd ed. 1994, New York: Raven Press.
65. Balimane, P.V., S. Chong, and R.A. Morrison, *Current methodologies used for evaluation of intestinal permeability and absorption.* Journal of Pharmacological and Toxicological Methods, 2000. **44**(1): p. 301-312.
66. Shimizu, M., *Interaction between Food Substances and the Intestinal Epithelium.* Bioscience Biotechnology Biochemistry, 2010. **74**(2): p. 232-241.

67. Hagerman, E.M., et al., *Surface modification and initial adhesion events for intestinal epithelial cells.* Journal of Biomedical Materials Research Part A, 2005. **76A**(2): p. 272-278.
68. Versantvoort, C.H.M., et al., *Monolayers of IEC-18 cells as an in vitro model for screening the passive transcellular and paracellular transport across the intestinal barrier: comparison of active and passive transport with the human colon carcinoma Caco-2 cell line.* Environmental Toxicology and Pharmacy, 2002. **11**: p. 335-344.
69. van Itallie, C.M., et al., *The density of small tight junction pores varies among cell types and is increased by expression of claudin-2.* Journal of Cell Science, 2008. **121**(3): p. 298-305.
70. Watson, C.J., et al., *Interferon-γ selectively increases epithelial permeability to large molecules by activating different populations of paracellular pores.* Journal of Cell Science, 2005. **118**(22): p. 5221-5230.
71. Turner, J.R., *Intestinal mucosal barrier function in health and disease.* Nature Reviews Immunology, 2009. **9**: p. 799-809.
72. Bronner, F., *Calcium absorption - A paradigm for mineral absorption.* Journal of Nutrition, 1998. **128**(5): p. 917-920.
73. Pappenheimer, J.R. and K.Z. Reiss, *Contribution of solvent drag through intercellular junctions to absorption of nutrients by the small intestine of the rat.* J Membr Biol, 1987. **100**(1): p. 123-136.
74. Fine, K.D., et al., *Mechanism by which glucose stimulates the passive absorption of small solutes by the human jejunum in vivo.* Gastroenterology, 1994. **107**(2): p. 389-395.
75. Hossain, Z. and T. Hirata, *Molecular mechanism of intestinal permeability: Interaction at tight junctions.* Mol Biosyst, 2008. **4**(12): p. 1181-1185.
76. Deplancke, B. and H.R. Gaskins, *Microbial modulation of innate defense - goblet cells and the intestinal mucus layer.* Am J Clin Nutr, 2001. **73**(Suppl): p. 1131S-41S.
77. Benet, L.Z. and C.L. Cummins, *The drug efflux-metabolism alliance: Biochemical aspects.* Adv Drug Deliv Rev, 2001. **50**(SUPPL. 1): p. S3-S11.
78. McGuckin, M., et al., *Mucin dynamics and enteric pathogens.* Nature Reviews - Microbiology, Focus on Mucosal Microbiology, 2011. **9**: p. 265-278.
79. Gill, N., M. Wlodarska, and B.B. Finlay, *Roadblocks in the gut: Barriers to enteric infection.* Cellular Microbiology, 2011. **13**(5): p. 660-669.
80. Forchielli, M.L. and W.A. Walker, *The role of gut-associated lymphoid tissues and mucosal defence.* British Journal of Nutrition, 2005. **93**(SUPP): p. S41-S48.
81. Wehkamp, J., M. Schmid, and E.F. Stange, *Defensins and other antimicrobial peptides in inflammatory bowel disease.* Current Opinion in Gastroenterology, 2007. **23**(4): p. 370-378.
82. Yoo, E.M. and S.L. Morrison, *IgA: An immune glycoprotein.* Clinical Immunology, 2005. **116**(1): p. 3-10.
83. Pearson, J.P. and I.A. Brownlee, *Structure and function of mucosal surfaces*, in *Colonization of Mucosal Surfaces*, J.P. Nataro, et al., Editors. 2005, ASM Press: Washingtion D.C. p. 3-16.
84. Autnrieth, I.B., *Die Oekologie der humanen Darmflora: physiologische und pathophysiologische Aspekte.* Journal fuer Gastroenterologische und Hepatologische Erkrankungen, 2003. **1**(1): p. 14-17.
85. Dockray, G.J., *Luminal sensing in the gut: an overview.* Journal of physiology and pharmacology : an official journal of the Polish Physiological Society, 2003. **54 Suppl 4**: p. 9-17.
86. *Encyclopaedia Britannica*, in *Cecum, Anatomy*.
87. Backhed, F., et al., *Host-bacterial mutualism in the human intestine.* Science, 2005. **307**(5717): p. 1915-20.
88. Dressman, J.B., et al., *Dissolution Testing as a Prognostic Tool for oral Drug Absorption: Immediate Release Dosage Forms.* Pharmaceutical Research, 1998. **15**(1): p. 11-22.

89. Bauer, E., S. Jakob, and R. Mosenthin, *Principles of physiology of lipid digestion.* Asian-Australasian Journal of Animal Sciences, 2005. **18**(2): p. 282-295.
90. Payne, A.N., et al., *Advances and perspectives in in vitro human gut fermentation modeling.* Trends in Biotechnology, 2012. **30**(1): p. 17-25.
91. Atuma, C., et al., *The adherent gastrointestinal mucus gel layer: thickness and physical state in vivo.* American Journal of Physiology Gastrointestinal and Liver Physiology, 2001. **280**: p. G922-929.
92. Johansson, M.E.V., et al., *The inner of two Muc2 mucin-dependent mucus layers in colon is devoid of bacteria.* PNAS, 2008. **105**(39): p. 15064-10569.
93. Lindahl, A., et al., *Characterization of fluids from the stomach and proximal jejunum in men and women.* Pharmaceutical Research, 1997. **14**(4): p. 497-502.
94. Kalantzi, L., et al., *Characterization of the Human Upper Gastrointestinal Contents Under Conditions Simulating Bioavailability/Bioequivalence Studies.* Pharmaceutical Research, 2006. **23**(1): p. 165-176.
95. Karam, S.M., *Lineage commitment and maturation of epithelial cells in the gut.* Frontiers in bioscience : a journal and virtual library, 1999. **4**: p. D286-298.
96. Kastner, U., et al., *Saure Oligosaccharide als Wirkprinzip von waessrigen Zubereitungen aus der Karotte in der Prophylaxe und Therapie von gastrointestinalen Infektionen.* Wiener Medizinische Wochenschrift, 2002. **152**: p. 379-381.
97. Kim, Y.S. and S.B. Ho, *Intestinal Goblet Cells and Mucin in Health and Disease: Recent Insights and Progress.* Current Gastroenterology Reports, 2010. **12**: p. 319-330.
98. Carroll, I.M., D.W. Threadgill, and D.S. Threadgill, *The gastrointestinal microbiome: A malleable, third genome of mammals.* Mammalian Genome, 2009. **20**(7): p. 395-403.
99. Bongaerts, G.P.A. and R.S.V.M. Severijnen, *The beneficial, antimicrobial effect of probiotics.* Medical Hypotheses, 2001. **56**(2): p. 174-177.
100. Turroni, F., et al., *Human gut microbiota and bifidobacteria: from composition to functionality.* Antonie Van Leeuwenhoek, 2008. **94**(1): p. 35-50.
101. Wang, M., et al., *Comparison of bacterial diversity along the human intestinal tract by direct cloning and sequencing of 16S rRNA genes.* FEMS Microbiol Ecol, 2005. **54**(2): p. 219-31.
102. Zoetendal, E.G., et al., *Mucosa-associated bacteria in the human gastrointestinal tract are uniformly distributed along the colon and differ from the community recovered from feces.* Applied and Environmental Microbiology, 2002. **68**(7): p. 3401-3407.
103. Croucher, S.C., et al., *Bacterial Populations associated with Different Regions of the Human Colon Wall.* Applied and Environmental Microbiology, 1983. **45**(3): p. 1025-1033.
104. Rajilic-Stojanovic, M., H. Smidt, and W.M. De Vos, *Diversity of the human gastrointestinal tract microbiota revisited.* Environmental Microbiology, 2007. **9**(9): p. 2125-2136.
105. Bik, E.M., *Composition and function of the human-associated microbiota.* Nutrition Reviews, 2009. **67**(Suppl.2): p. 164-171.
106. Courtney, H.S., D.L. Hasty, and I. Ofek, *Hydrophobicity of a group A streptococci and its relationship to adhesion of streptococci to host cells*, in *Microbial Cell Surface Hydrophobicity*, R.J. Doyle and M. Rosenberg, Editors. 1990, ASM Press: Washington, D.C. p. 361-386.
107. Hasty, D.L., et al., *Multiple adhesins of streptococci.* Infection and Immunity, 1992. **60**(6): p. 2147-2152.
108. Mo, H.Z., Y.; Nout, M. J. R. , *In vitro digestion enhances anti-adhesion effect of tempe and tofu against Escherichia coli.* Letters in Applied Microbiology, 2011. **54**(2): p. 166-168.
109. Roubus-van dem Hil, P.J., et al., *Fermented soya bean (tempe) extracts reduce adhesion of enterotoxigenic Escherichia coli to intestinal epithelial cells.* Journal of Applied Microbiology, 2009. **106**: p. 1013-1021.
110. Stipanuk, M.H. and M. Caudill, *Biochemical, Physiological, and Molecular Aspects of Human Nutrition*. 3rd ed. 2012: Saunders / Elsevier.

111. Singh, H. and A. Sarkar, *Behaviour of protein-stabilised emulsions under various physiological conditions.* Adv Colloid Interface Sci, 2011. **165**(1): p. 47-57.
112. Malone, M.E., I.A.M. Appelqvist, and I.T. Norton, *Oral behaviour of food hydrocolloids and emulsions. Part 1. Lubrication and deposition considerations.* Food Hydrocolloids, 2003. **17**(6): p. 763-773.
113. Vingerhoeds, M.H., et al., *Emulsion flocculation induced by saliva and mucin.* Food Hydrocolloids, 2005. **19**(5): p. 915-922.
114. De Wijk, R.A., et al., *The role of α-amylase in the perception of oral texture and flavour in custards.* Physiology and Behavior, 2004. **83**(1 SPEC. ISS.): p. 81-91.
115. Miettinen, S.M., et al., *Effect of emulsion characteristics on the release of aroma as detected by sensory evaluation, static headspace gas chromatography, and electronic nose.* Journal of Agricultural and Food Chemistry, 2002. **50**(15): p. 4232-4239.
116. Sarkar, A., K.K.T. Goh, and H. Singh, *Colloidal stability and interactions of milk-protein-stabilized emulsions in an artificial saliva.* Food Hydrocolloids, 2009. **23**(5): p. 1270-1278.
117. Jantratid, E., et al., *Dissolution media simulating conditions in the proximal human gastrointestinal tract: an update.* Pharm Res, 2008. **25**(7): p. 1663-76.
118. Gass, J., et al., *Enhancement of dietary protein digestion by conjugated bile acids.* Gastroenterology, 2007. **133**(1): p. 16-23.
119. Maldonado-Valderrama, J., et al., *Interfacial characterization of β-lactoglobulin networks: Displacement by bile salts.* Langmuir, 2008. **24**(13): p. 6759-6767.
120. Singh, H., A. Ye, and D. Horne, *Structuring food emulsions in the gastrointestinal tract to modify lipid digestion.* Prog Lipid Res, 2009. **48**(2): p. 92-100.
121. McClements, D.J., et al., *Designing food structure to control stability, digestion, release and absorption of lipophilic food components.* Food Biophysics, 2008. **3**(2): p. 219-228.
122. Goodman, B.E., *Insights into digestion and absorption of major nutrients in humans.* Adv Physiol Educ, 2010. **34**(2): p. 44-53.
123. Binder, H.J. and A. Reuben, *Nutrient Digestion and Absorption*. Medical Physiology: A Cellular and Molecular Approach. Vol. 2nd. 2009, Philadelphia: Saunders / Elsevier.
124. Clark Jr, S.L., *The ingestion of proteins and colloidal materials by columnar absorptive cells of the small intestine in suckling rats and mice.* The Journal of biophysical and biochemical cytology, 1959. **5**(1): p. 41-50.
125. Casley-Smith, J.R., *The passage of ferritin into jejunal epithelial cells.* Experientia, 1967. **23**(5): p. 370-371.
126. Warshaw, A.L., et al., *Small intestinal permeability to macromolecules. Transmission of horseradish peroxidase into mesenteric lymph and portal blood.* Laboratory Investigation, 1971. **25**(6): p. 675-684.
127. Warshaw, A.L., W.A. Walker, and K.J. Isselbacher, *Protein uptake by the intestine: evidence for absorption of intact macromolecules.* Gastroenterology, 1974. **66**(5): p. 987-992.
128. Heyman, M., et al., *Horseradish peroxidase transport across adult rabbit jejunum in vitro.* American Journal of Physiology - Gastrointestinal and Liver Physiology, 1982. **5**(6): p. G558-G564.
129. Weber, E. and H.J. Ehrlein, *Relationships between gastric emptying and intestinal absorption of nutrients and energy in mini pigs.* Digestive Diseases and Sciences, 1998. **43**(6): p. 1141-1153.
130. Heyman, M. and J.F. Desjeux, *Significance of intestinal food protein transport.* Journal of Pediatric Gastroenterology and Nutrition, 1992. **15**(1): p. 48-57.
131. Rytkönen, J., et al., *Enterocyte and M-cell transport of native and heat-denatured bovine β-lactoglobulin: Significance of heat denaturation.* Journal of Agricultural and Food Chemistry, 2006. **54**(4): p. 1500-1507.
132. Caillard, I. and D. Tome, *Transport des antigenes proteiques majeurs du lacto-serum bovin dans l'epithelium intestinal.* Cahiers de nutrition et de dietetique, 1995. **30**(5): p. 306-312.

133. Walker, W.A. and K.J. Isselbacher, *Uptake and transport of macromolecules by the intestine. Possible role in clinical disorders.* Gastroenterology, 1974. **67**(3): p. 531-550.
134. Paganelli, R. and R.J. Levinsky, *Solid phase radioimmunoassay for detection of circulating food protein antigens in human serum.* Journal of Immunological Methods, 1980. **37**(3-4): p. 333-341.
135. Gardner, M.L.G., *Gastrointestinal absorption of intact proteins.* Annual Review of Nutrition, 1988. **8**: p. 329-350.
136. Husby, S., J.C. Jensenius, and S.E. Svehag, *Passage of undegraded dietary antigen into the blood of healthy adults. Further characterization of the kinetics of uptake and the size distribution of the antigen.* Scandinavian Journal of Immunology, 1986. **24**(4): p. 447-455.
137. Lovegrove, J.A., et al., *Transfer of cow's milk β-lactoglobulin to human serum after a milk load: a pilot study.* Gut, 1993. **34**: p. 203-207.
138. El-Loly, M.M., *Bovine milk immunoglobulins in relation to human health.* International Journal of Dairy Science, 2007. **2**(3): p. 183-195.
139. Reilly, R.M., R. Domingo, and J. Sandhu, *Oral delivery of antibodies. Future pharmacokinetic trends.* Clinical Pharmacokinetics, 1997. **32**(4): p. 313-323.
140. Roos, N., et al., *15N-labeled immunoglobulins from bovine colostrum are partially resistant to digestion in human intestine.* Journal of Nutrition, 1995. **125**(5): p. 1238-1244.
141. Picariello, G., et al., *Peptides surviving the simulated gastrointestinal digestion of milk proteins: biological and toxicological implications.* J Chromatogr B Analyt Technol Biomed Life Sci, 2010. **878**(3-4): p. 295-308.
142. Bockman, D.E. and M.D. Cooper, *Pinocytosis by epithelium associated with lymphoid follicles in the bursa of Fabricius, appendix, and Peyer's patches. An electron microscopic study.* American Journal of Anatomy, 1973. **136**(4): p. 455-477.
143. Owen, R.L., *Sequential uptake of horseradish peroxidase by lymphoid follicle epithelium of Peyer's patches in the normal unobstructed mouse intestine: An ultrastructural study.* Gastroenterology, 1977. **72**(3): p. 440-451.
144. Bernasconi, E., R. Fritsche, and B. Corthesy, *Specific effects of denaturation, hydrolysis and exposure to Lactococcus lactis on bovine beta-lactoglobulin transepithelial transport, antigenicity and allergenicity.* Clin Exp Allergy, 2006. **36**(6): p. 803-14.
145. Delie, F. and M.J. Blanco-Príeto, *Polymeric particulates to improve oral bioavailability of peptide drugs.* Molecules, 2005. **10**(1): p. 65-80.
146. Florence, A.T., *The oral absorption of micro- and nanoparticulates: Neither exceptional nor unusual.* Pharmaceutical Research, 1997. **14**(3): p. 259-266.
147. Chen, H. and R. Langer, *Oral particulate delivery: Status and future trends.* Adv Drug Deliv Rev, 1998. **34**(2-3): p. 339-350.
148. Delie, F., *Evaluation of nano- and microparticle uptake by the gastrointestinal tract.* Adv Drug Deliv Rev, 1998. **34**(2-3): p. 221-233.
149. McClean, S., et al., *Binding and uptake of biodegradable poly-DL-lactide micro- and nanoparticles in intestinal epithelia.* European Journal of Pharmaceutical Sciences, 1998. **6**(2): p. 153-163.
150. Norris, D.A., N. Puri, and P.J. Sinko, *The effect of physical barriers and properties on the oral absorption of particulates.* Adv Drug Deliv Rev, 1998. **34**(2-3): p. 135-154.
151. Yeh, P.Y., H. Ellens, and P.L. Smith, *Physiological considerations in the design of particulate dosage forms for oral vaccine delivery.* Adv Drug Deliv Rev, 1998. **34**(2-3): p. 123-133.
152. Stutzmann, J., et al., *Adhesion Complexes Implicated in Intestinal Epithelial Cell-Matrix Interactions.* Microscopy Research and Techniques, 2000. **51**: p. 179-190.
153. Johansson, M.E.V., K.A. Thomsson, and G.C. Hansson, *Proteomic Analysis of the Two Mucus Layers of the Colon Barrier Reveal That Their Main Component, the Muc2 Mucin, Is Strongly Bound to the Fcgbp Protein.* Journal of Proteome Research, 2009. **8**: p. 3549-3557.

154. Johansson, M.E.V., et al., *Composition and functional role of the mucus layers in the intestine.* Cellular and Molecular Life Sciences, 2011. **68**: p. 3635-3641.
155. Savage, D.C., *Microorganisms associated with epithelial surfaces and stability of the indigenous gastrointestinal microflora.* Die Nahrung, 1987. **31**(5-6): p. 383-395.
156. Macfarlane, S., A.J. Mcbain, and G.T. Macfarlane, *Consequneces of Biofilm and Sessile Growth in the Large Intestine.* Advances in Dental Research, 1997. **11**(1): p. 59-68.
157. Allen, A., D.A. Hutton, and J.P. Pearson, *The MUC2 gene product: a human intestinal mucin.* The International Journal of Biochemistry & Cell Biology, 1998. **30**: p. 797-801.
158. Roger, E., et al., *Biopharmaceutical parameters to consider in order to alter the fate of nanocarriers after oral delivery.* Nanomedicine, 2010. **5**(2): p. 287-306.
159. McClements, D.J. and Y. Li, *Review of in vitro digestion models for rapid screening of emulsion-based systems.* Food & Function, 2010. **1**: p. 32-59.
160. Forstner, J.F., M.G. Oliver, and F.A. Sylvester, *Production, structure, and biologic relevance of gastrointestinal mucins*, in *Infections of the Gastrointestinal Tract*, M.J. Blaser, et al., Editors. 1995, Raven Press: New York. p. 71-88.
161. Gagnon, M., et al., *Comparison of the Caco-2, HT-29 and the mucus-secreting HT29-MTX intestinal cell models to investigate Salmonella adhesion and invasion.* Journal of Microbiological Methods, 2013. **94**(3): p. 274-279.
162. Johansson, M.E.V., J.M. Holmen-Larsson, and G.C. Hansson, *The two mucus layers of colon are organized by the MUC2 mucin, whereas the outer layer is a legislator of host-microbial interactions.* PNAS, 2011. **108**(Suppl. 1): p. 4659-4665.
163. Wang, X., et al., *Impact of biofilm matrix components on interaction of commensal Escherichia coli with the gastrointestinal cell line HT-29.* Cell Mol Life Sci, 2006. **63**(19-20): p. 2352-63.
164. Quaroni, A. and J. Hochman, *Development of intestinal cell culture models for drug transport and metabolism studies.* Adv Drug Deliv Rev, 1996. **22**(1-2): p. 3-52.
165. Linden, S.K., et al., *Mucins in the mucosal barrier to infection.* Mucosal Immunol, 2008. **1**(3): p. 183-97.
166. Lievin-Le Moal, V. and A.L. Servin, *The front line of enteric host defense against unwelcome intrusion of harmful microorganisms: mucins, antimicrobial peptides, and microbiota.* Clin Microbiol Rev, 2006. **19**(2): p. 315-37.
167. Dharmani, P., et al., *Role of intestinal mucins in innate host defense mechanisms against pathogens.* Journal of Innate Immunity, 2009. **1**(2): p. 123-135.
168. Pfannkuche, H. and G. Gaebel, *Glucose, epithelium, and enteric nervous system: dialogue in the dark.* Journal of Animal Physiology and animal Nutrition, 2009. **93**: p. 277-286.
169. Kraehenbuhl, J.P., E. Pringault, and M.R. Neutra, *Review article: Intestinal epithelia and barrier functions.* Alimentary Pharmacology and Therapeutics, Supplement, 1997. **11**(3): p. 3-9.
170. Ewaschuk, J.B., et al., *Secreted bioactive factors from Bifidobacterium infantis enhance epithelial cell barrier function.* American Journal of Physiology - Gastrointestinal and Liver Physiology, 2008. **295**(5): p. G1025-G1034.
171. Ismail, A.S. and L.V. Hooper, *Epithelial Cells and Their Neighbours – IV Bacterial contributions to intestinal epithelial barrier integrity.* American Journal of Physiology Gastrointestiology Liver Physiology, 2005. **289**: p. G779-784.
172. Turner, J.R., *Molecular Basis of Epithelial Barrier Regulation – From Basic Mechanisms to Clinical Application.* American Journal of Pathology, 2006. **169**(6): p. 1901-1909.
173. Maldonado-Contreras, A.L. and B.A. McCormick, *Intestinal epithelial cells and their role in innate mucosal immunity.* Cell Tissue Research, 2010. **343**: p. 5-12.
174. Zasloff, M., *Antimicrobial peptides of multicellular organisms.* Nature, 2002. **415**(6870): p. 389-395.
175. Csaki, K.F., *Synthetic surfactant food additives can cause intestinal barrier dysfunction.* Medical Hypotheses, 2011. **76**: p. 676-681.

176. Lehr, C.-M., *Lectin-mediated drug delivery: The second generation of bioadhesives.* Journal of Controlled Release, 2000. **65**: p. 19-29.
177. Kedinger, M., et al., *Fetal gut mesenchyme induces differentiation of cultured intestinal endodermal and crypt cells.* Developmental Biology, 1986. **113**(2): p. 474-483.
178. Potten, C.S., et al., *Proliferation in human gastrointestinal epithelium using bromodeoxyuridine in vivo: Data for different sites, proximity to a tumour, and polyposis coli.* Gut, 1993. **33**(4): p. 524-529.
179. Schmidt, G.H., M.M. Wilkinson, and B.A.J. Ponder, *Cell migration pathway in the intestinal epithelium: An in situ marker system using mouse aggregation chimeras.* Cell, 1985. **40**(2): p. 425-429.
180. Cheng, H. and C.P. Leblond, *Origin, differentiation and renewal of the four main epithelial cell types in the mouse small intestine. III. Entero endocrine cells.* American Journal of Anatomy, 1974. **141**(4): p. 503-520.
181. Goke, M. and D.K. Podolsky, *Regulation of the mucosal epithelial barrier.* Baillière's Clinical Gastroenterology, 1996. **10**(3): p. 393-405.
182. Gavrieli, Y., Y. Sherman, and S.A. Ben-Sasson, *Identification of programmed cell death in situ via specific labeling of nuclear DNA fragmentation.* Journal of Cell Biology, 1992. **119**(3): p. 493-501.
183. Noah, T.K., B. Donahue, and N.F. Shroyer, *Intestinal development and differentiation.* Experimental Cell Research, 2011. **317**(19): p. 2702-2710.
184. Trier, J.S. and J.L. Madara, *Functional morphology of the mucosa of the small intestine.* Physiology of the gastrointestinal tract, ed. I.R. Johnson. 1981, New York: Raven Press.
185. Cheng, H. and C.P. Leblond, *Origin, differentiation and renewal of the four main epithelial cell types in the mouse small intestine. V. Unitarian theory of the origin of the four epithelial cell types.* American Journal of Anatomy, 1974. **141**(4): p. 537-562.
186. Moe, H., *On Goblet Cells, Especially of the Intestine of Some Mammalian Species*, in *International Review of Cytology*1955. p. 299-334.
187. Ayabe, T., et al., *Sectretion of microbial a-defensis by intestinal paneth cells in response to beacteria.* Nature Immunology, 2000. **1**(2): p. 113-118.
188. Erlandsen, S.L. and D.G. Chase, *Paneth cell function: phagocytosis and intracellular digestion of intestinal microorganisms. II. Spiral microorganism.* Journal of Ultrasructure Research, 1972. **41**(3-4): p. 319-333.
189. Clark, M.A., B.H. Hirst, and M.A. Jepson, *M-cell surface β1 integrin expression and invasin-mediated targeting of Yersinia pseudotuberculosis to mouse Peyer's patch M cells.* Infection and Immunity, 1998. **66**(3): p. 1237-1243.
190. Neutra, M.S.P. and J.P. Kraehenbuhl, *Role of intestinal M cells in microbial pathogenesis*, in *Microbial pathogenesis and the intestinal cell*, G. Hecht, Editor. 2003, ASM: Washingtpn, DC. p. 23-42.
191. Man, A.L., M.E. Pietro-Garcia, and C. Nicoletti, *Improving M cell mediated transport across mucosal barriers: do certain bacteria hold the key?* Immunulogy, 2004. **1113**(1): p. 15-22.
192. Van den Berg, B.M., H. Vink, and J.A.E. Spaan, *The endothelial glycocalyx protects against myocardial edema.* Circulation Research, 2003. **92**(6): p. 592-594.
193. Kleessen, B. and M. Blaut, *Modulation of gut mucosal biofilms.* British Journal of Nutrition, 2005. **93**(Suppl.1): p. S35-S40.
194. Ou, G., et al., *Contribution of intestinal epithelial cells to innate immunity of the human gut - Studies on polarized monolayers of colon carcinoma cells.* Scandinavian Journal of Immunology, 2009. **69**(2): p. 150-161.
195. Johansson, M.E., et al., *Composition and functional role of the mucus layers in the intestine.* Cell Mol Life Sci, 2011. **68**(22): p. 3635-41.
196. Huang, J.Y., S.M. Lee, and S.K. Mazmanian, *The human commensal Bacteroides fragilis binds intestinal mucin.* Anaerobe, 2011.
197. Pelaseyed, T., et al., *The mucus and mucins of the goblet cells and enterocytes provide the first defense line of the gastrointestinal tract and interact with the immune system.* Immunological Reviews, 2014. **260**(1): p. 8-20.

198. Moran, A.P., A. Gupta, and L. Joshi, *Sweet-talk: Role of host glycosylation in bacterial pathogenesis of the gastrointestinal tract.* Gut, 2011. **60**(10): p. 1412-1425.
199. Falk, P., T. Boren, and S. Normark, *Characterization of microbial host receptors.* Methods in Enzymology, 1994. **236**: p. 353-374.
200. Lane, J.A., et al., *The food glycome: A source of protection against pathogen colonization in the gastrointestinal tract.* International Journal of Food Microbiology, 2010. **142**: p. 1-13.
201. Sturm, A. and A.U. Dignass, *Epithelial restitution and wound healing in inflammatory bowel disease.* World Journal of Gastroenterology, 2008. **14**(3): p. 348-353.
202. Maury, J., et al., *The filamentous brush border glycocalyx, a mucin-like marker of enterocyte hyper-polarization.* European Journal of Biochemistry, 1995. **228**(2): p. 323-331.
203. De O. Ferreira, E., et al., *A Bacteroides fragilis surface glycoprotein mediates the interaction between the bacterium and the extracellular matrix component laminin-1.* Research in microbiology, 2006. **157**: p. 960-966.
204. Wexler, H.M., *Outer-membrane pore-forming proteins in gram-negative anaerobic bacteria.* Clinical Infectious Diseases, 2002. **35**(SUPPL. 1): p. S65-S71.
205. Brandley, B.K. and R.L. Schnaar, *Cell-surface carbohydrates in cell recognition and response.* Journal of Leukocyte Biology, 1986. **40**(1): p. 97-111.
206. Roseman, S., *Studies on specific intercellular adhesion.* Journal of Biochemistry, 1985. **97**(3): p. 709-718.
207. Hakamori, S., et al., *Novel fucolipids accumulating in human adenocarcinoma. I. Glycolipids with DI- or trifucosylated type 2 chain.* Journal of Biological Chemistry, 1984. **259**(7): p. 4672-4680.
208. Stutzmann, J., et al., *Adhesion complexes implicated in intestinal epithelial cell-matrix interactions.* Microsc Res Tech, 2000. **51**(2): p. 179-190.
209. Ruoslahti, E. and B. Öbrink, *Common principles in cell adhesion.* Experimental Cell Research, 1996. **227**(1): p. 1-11.
210. Timpl, R. and J.C. Brown, *Supramolecular assembly of basement membranes.* Bioessays, 1996. **18**(2): p. 123-132.
211. Hanai, N., et al., *Ganglioside-mediated modulation of cell growth. Specific effects of GM3 and lyso-GM3 in tyrosine phosphorylation of the epidermal growth factor receptor.* Journal of Biological Chemistry, 1988. **263**(22): p. 10915-10921.
212. Uski, T.K., *Further characterization of the contraction-mediating prostanoid receptors in feline cerebral arteries. Effects of the thromboxane-receptor antagonist AH 23848.* Acta Physiologica Scandinavica, 1988. **133**(4): p. 519-524.
213. Levine, H.A., M.P. McGee, and S. Serna, *Diffusion and reaction in the cell glycocalyx and the extracellular matrix.* J Math Biol, 2010. **60**(1): p. 1-26.
214. Mirelman, D. and I. Ofek, *Introduction to microbial lectins and agglutinins*, in *Microbial Lectins and Agglutinins*, D. Mirelman, Editor. 1986, John Wiley & Sons: New York. p. 1-19.
215. Sava, I.G., et al., *Novel Interactions of Glycosaminoglycans and Bacterial Glycolipids Mediate Binding of Enterococci to Human Cells.* Journal of Biological Chemistry, 2009. **284**(27): p. 18194-18201.
216. Gornik, O., et al., *Glycoscience - A new frontier in rational drug design.* Acta Pharmaceutica, 2006. **56**(1): p. 19-30.
217. Eimhoff, W.G.J., et al., *Metabolic aspects of isolated cells from rat small intestinal epithelium.* BBA - General Subjects, 1970. **215**(2): p. 229-241.
218. Norval, M., et al., *Growth in culture of adenocarcinoma cells from the small intestine of sheep.* British Journal of Experimental Pathology, 1981. **62**(3): p. 270-282.
219. Debons-Guillemin, M.C., et al., *Serotonin and histamine production by human carcinoid cells in culture.* Cancer Research, 1982. **42**(4): p. 1513-1516.
220. Vachon, P.H. and J.F. Beaulieu, *Transient mosaic patterns of morphological and functional differentiation in the Caco-2 cell line.* Gastroenterology, 1992. **103**(2): p. 414-423.

221. Huet, C., et al., *Absorptive and mucus-secreting subclones isolated from a multipotent intestinal cell line (HT-29) provide new models for cell polarity and terminal differentiation.* Journal of Cell Biology, 1987. **105**(1): p. 345-357.
222. Lesuffleur, T., et al., *Growth Adaption to Methotrexate of HT-29 Human Colon Carcinoma Cells Is Associated with Their Ability to Differentiate into Absorptive and Mucus-secreting Cells.* Cancer Res, 1990. **50**(19): p. 6334-6343.
223. Matthes, I., F. Nimmerfall, and H. Sucker, *Mucus models for investigation of intestinal absorption. Part: Validation and optimization.* MUCUSMODELLE ZUR UNTERSUCHUNG VON INTESTINALEN ABSORPTIONSMECHANISMEN. 1. MITTEILUNG: VALIDIERUNG UND OPTIMIERUNG DER MODELLE, 1992. **47**(7): p. 505-515.
224. Lesuffleur, T., et al., *Dihydrofolate reductase gene amplification-associated shift of differentiation in methotrexate-adapted HT-29 cells.* Journal of Cell Biology, 1991. **115**(5): p. 1409-1418.
225. Lesuffleur, T., et al., *Differential expression of the human mucin genes MUC1 to MUC5 in relation to growth and differentiation of different mucus-secreting HT-29 cell subpopulations.* Journal of Cell Science, 1993. **106**(3): p. 771-783.
226. Walter, E., et al., *HT29-MTX/Caco-2 cocultures as an in vitro model for the intestinal epithelium: In vitro-in vivo correlation with permeability data from rats and humans.* J Pharm Sci, 1996. **85**(10): p. 1070-1076.
227. Leteurtre, E., et al., *Differential mucin expression in colon carcinoma HT-29 clones with variable resistance to 5-fluorouracil and methotrexate.* Biology of the Cell, 2004. **96**(2): p. 145-151.
228. Wickström, C., et al., *MUC5B is a major gel-forming, oligomeric mucin from human salivary gland, respiratory tract and endocervix: Identification of glycoforms and C-terminal cleavage.* Biochemical Journal, 1998. **334**(3): p. 685-693.
229. Ajioka, Y., L.J. Allison, and J.R. Jass, *Significance of MUC1 and MUC2 mucin expression in colorectal cancer.* Journal of Clinical Pathology, 1996. **49**(7): p. 560-564.
230. Desseyn, J.L., et al., *Evolution of the large secreted gel-forming mucins.* Molecular Biology and Evolution, 2000. **17**(8): p. 1175-1184.
231. Buisine, M.P., et al., *Mucin gene expression in human embryonic and fetal intestine.* Gut, 1998. **43**(4): p. 519-524.
232. Roussel, P. and P. Delmotte, *The diversity of epithelial secreted mucins.* Current Organic Chemistry, 2004. **8**(5): p. 413-437.
233. Sellers, L.A., et al., *Mucus glycoprotein gels. Role of glycoprotein polymeric structure and carbohydrate side-chains in gel-formation.* Carbohydrate Research, 1988. **178**(1): p. 93-110.
234. Thornton, D.J., K. Rousseau, and M.A. McGuckin, *Structure and function of the polymeric mucins in airways mucus*, in *Annual Review of Physiology*2008. p. 459-486.
235. Lesuffleur, T., A. Zweibaum, and F.X. Real, *Mucins in normal and neoplastic human gastrointestinal tissues.* Critical Reviews in Oncology and Hematology, 1994. **17**(3): p. 153-180.
236. Hennebicq-Reig, S., et al., *O-glycosylation and cellular differentiation in a subpopulation of mucin-secreting HT-29 cell line.* Experimental Cell Research, 1997. **235**(1): p. 100-107.
237. Boland, G.R. and G.D. Deshmukh, *The carbohydrate composition of mucin in colonic cancer.* Gastroenterology, 1990. **98**(5 PART I): p. 1170-1177.
238. Kim, Y.S., J. Gum Jr, and I. Brockhausen, *Mucin glycoproteins in neoplasia.* Glycoconj J, 1996. **13**(5): p. 693-707.
239. Capon, C., et al., *Oligosaccharide structures of mucins secreted by the human colonic cancer cell line Cl.16E.* Journal of Biological Chemistry, 1992. **267**(27): p. 19248-19257.
240. Malagolini, N., D. Cavallone, and F. Serafini-Cessi, *Differentiation-dependent glycosylation of gp190, an oncofetal crypt cell antigen expressed by Caco-2 cells.* Glycoconj J, 2000. **17**(5): p. 307-314.

241. Dall'Olio, F. and D. Trerè, *Expression of alpha 2,6-sialylated sugar chains in normal and neoplastic colon tissues. Detection by digoxigenin-conjugated Sambucus nigra agglutinin.* European journal of histochemistry : EJH, 1993. **37**(3): p. 257-265.
242. Cui, M.I.N., et al., *The effect of differentiation on 1,25 dihydroxyvitamin d-mediated gene expression in the enterocyte-like cell line, Caco-2.* Journal of Cellular Physiology, 2009. **218**(1): p. 113-121.
243. Jalal, F., et al., *Polarized distribution of neutral endopeptidase 24.11 at the cell surface of cultured human intestinal epithelial Caco-2 cells.* Biochemical Journal, 1992. **288**(3): p. 945-951.
244. Schnabl, K.L., C. Field, and M.T. Clandinin, *Ganglioside composition of differentiated Caco-2 cells resembles human colostrum and neonatal rat intestine.* British Journal of Nutrition, 2009. **101**(5): p. 694-700.
245. Lee, I.J., et al., *NMR metabolomic analysis of Caco-2 cell differentiation.* Journal of Proteome Research, 2009. **8**(8): p. 4104-4108.
246. Pinto, M., S. Robine Leon, and M.D. Appay, *Enterocyte-like differentiation and polarization of the human colon carcinoma cell line Caco-2 in culture.* Biology of the Cell, 1983. **47**(3): p. 323-330.
247. Hidalgo, I.J., T.J. Raub, and R.T. Borchardt, *Characterization of the human colon carcinoma cell line (Caco-2) as a model system for intestinal epithelial permeability.* Gastroenterology, 1989. **96**(3): p. 736-749.
248. Artursson, P., *Cell cultures as models for drug absorption across the intestinal mucosa.* Critical Reviews in Therapeutic Drug Carrier Systems, 1991. **8**(4): p. 305-330.
249. Lenaerts, K., et al., *Comparative proteomic analysis of cell lines and scrapings of the human intestinal epithelium.* BMC Genomics, 2007. **8**.
250. Sambuy, Y., et al., *The Caco-2 cell line as a model of the intestinal barrier: Influence of cell and culture-related factors on Caco-2 cell functional characteristics.* Cell Biology and Toxicology, 2005. **21**(1): p. 1-26.
251. Pinto, M., M.D. Appay, and P. Simon-Assmann, *Enterocytic differentiation of cultured human colon cancer cells by replacement of glucose by galactose in the medium.* Biology of the Cell, 1982. **44**(2): p. 193-196.
252. Le Bivic, A., et al., *Biogenetic pathways of plasma membrane proteins in Caco-2, a human intestinal epithelial cell line.* Journal of Cell Biology, 1990. **111**(4): p. 1351-1361.
253. Hauri, H.P., et al., *Expression and intracellular transport of microvillus membrane hydrolases in human intestinal epithelial cells.* Journal of Cell Biology, 1985. **101**(3): p. 838-851.
254. Duizer, E., et al., *Comparison of permeability characteristics of the human colonic Caco-2 and rat small intestinal IEC-18 cell lines.* Journal of Controlled Release, 1997. **49**(1): p. 39-49.
255. Hunter, J., et al., *Functional expression of P-glycoprotein in apical membranes of human intestinal Caco-2 cells. Kinetics of vinblastine secretion and interaction with modulators.* Journal of Biological Chemistry, 1993. **268**(20): p. 14991-14997.
256. Thwaites, D.T., B.H. Hirst, and N.L. Simmons, *Substrate specificity of the di/tripeptide transporter in human intestinal epithelia (Caco-2): Identification of substrates that undergo H+-coupled absorption.* British Journal of Pharmacology, 1994. **113**(3): p. 1050-1056.
257. Saito, H. and K.I. Inui, *Dipeptide transporters in apical and basolateral membranes of the human intestinal cell line Caco-2.* American Journal of Physiology - Gastrointestinal and Liver Physiology, 1993. **265**(2 28-2): p. G289-G294.
258. Gu, L., et al., *Heparin blocks the adhesion of E. coli O157:H7 to human colonic epithelial cells.* Biochemical and Biophysical Research Communications, 2008. **369**(4): p. 1061-1064.
259. Quaroni, A., *Crypt cell antigen expression in human colon tumor cell lines: Analysis with a panel of monoclonal antibodies to CaCo-2 luminal membrane components.* Journal of the National Cancer Institute, 1986. **76**(4): p. 571-585.

260. Frizzell, R.A. and S.G. Schultz, *Ionic conductances of extracellular shunt pathway in rabbit ileum. Influence of shunt on transmural sodium transport and electrical potential differences.* Journal of General Physiology, 1972. **59**(3): p. 318-346.
261. Engle, M.J., G.S. Goetz, and D.H. Alpers, *Caco-2 cells express a combination of colonocyte and enterocyte phenotypes.* Journal of Cellular Physiology, 1998. **174**(3): p. 362-369.
262. Macfarlane, S., E.J. Woodmansey, and G.T. Macfarlane, *Colonization of Mucin by Human Intestinal Bacteria and Establishment of Biofilm Communities in a two-Stage Continuous Culture System.* Applied and Environmental Microbiology, 2005. **71**(11): p. 7483-7492.
263. Allen, A. and J.P. Pearson, *Mucus glycoproteins of the gastrointestinal tract.* European Journal of Gastroenterology & Hepatology, 1993. **5**(4): p. 193-199.
264. Allen, A., et al., *The structure and physiology of gastrointestinal mucus.* Advances in Experimental Medicine and Biology, 1982. **144**: p. 115-133.
265. Laboisse, C., et al., *Recent aspects of the regulation of intestinal mucus secretion.* Proceedings of the Nutrition Society, 1996. **55**(1): p. 259-264.
266. Perez-Vilar, J. and R.L. Hill, *The Structure and Assembly of Secreted Mucins.* Journal of Biological Chemistry, 1999. **274**: p. 31751-31754.
267. Johansson, M.E.V., et al., *Bacteria penetrate the inner mucus layer before inflammation in the dextran sulfate colitis model.* PLoS ONE, 2010. **5**(8).
268. Kindon, H., et al., *Trefoil peptide protection of intestinal epithelial barrier function: Cooperative interaction with mucin glycoprotein.* Gastroenterology, 1995. **109**(2): p. 516-523.
269. De Repentigny, L., et al., *Characterization of binding of Candida albicans to small intestinal mucin and its role in adherence to mucosal epithelial cells.* Infection and Immunity, 2000. **68**(6): p. 3172-3179.
270. Kalabis, J., I. Rosenberg, and D.K. Podolsky, *Vangl1 protein acts as a downstream effector of intestinal trefoil factor (ITF)/TFF3 signaling and regulates wound healing of intestinal epithelium.* Journal of Biological Chemistry, 2006. **281**(10): p. 6434-6441.
271. Slomiany, A., M. Grabska, and B.L. Slomiany, *Essential Components of Antimicrobial Gastrointestinal Epithelial Barrier: Specific Interaction of Mucin with an Integral Apical Membrane Protein of Gastric Mucosa.* Molecular Medicine, 2001. **7**(1): p. 1-10.
272. Akiba, Y., et al., *Dynamic regulation of mucus gel thickness in rat duodenum.* American Journal of Physiology - Gastrointestinal and Liver Physiology, 2000. **279**(2 42-2): p. G437-G447.
273. McAuley, J.L., et al., *MUC1 cell surface mucin is a critical element of the mucosal barrier to infection.* Journal of Clinical Investigation, 2007. **117**(8): p. 2313-2324.
274. Godl, K., et al., *The N Terminus of the MUC2 Mucin Forms Trimers That are Held Together within a Trypsin-resistant Core Fragment.* The Journal of Biological Chemistry, 2002. **277**(49): p. 47248-47256.
275. Qin, X., et al., *Hydrophobicity of mucosal surface and its relationship to gut barrier function.* Shock, 2008. **29**(3): p. 372-376.
276. Butler, B.D., L.M. Lichtenberger, and B.A. Hills, *Distribution of surfactants in the canine gastrointestinal tract and their ability to lubricate.* American Journal of Physiology - Gastrointestinal and Liver Physiology, 1983. **7**(6): p. G645-651.
277. DeSchryver-Kecskemeti, K., et al., *Intestinal surfactant-like material. A novel secretory product of the rat enterocyte.* Journal of Clinical Investigation, 1989. **84**(4): p. 1355-1361.
278. Hicks, A.M., et al., *Unique molecular signatures of glycerophospholipid species in different rat tissues analyzed by tandem mass spectrometry.* Biochimica et Biophysica Acta - Molecular and Cell Biology of Lipids, 2006. **1761**(9): p. 1022-1029.
279. Lugea, A., et al., *Surface hydrophobicity of the rat colonic mucosa is a defensive barrier against macromolecules and toxins.* Gut, 2000. **46**(4): p. 515-521.
280. Lichtenberger, L.M., *The hydrophobic barrier properties of gastrointestinal mucus.* Annual Reviews in Physiology, 1995. **57**: p. 565-583.

281. Willumeit, R., et al., *Phospholipids as implant coatings.* Journal of Materials Science: Materials in Medicine, 2007. **18**(2): p. 367-380.
282. Guo, W., et al., *Phospholipid impregnation of abdominal rubber drains: resistance to bacterial adherence but no effect on drain-induced bacterial translocation.* Research in Experimental Medicine, 1993. **193**(1): p. 285-296.
283. Drusch, S., et al., *Surface accumulation of milk proteins and milk protein hydrolysates at the air-water interface on a time-scale relevant for spray-drying.* Food Research International, 2012. **47**(2): p. 140-145.
284. Tanaka, S., et al., *Regional differences of H +, HCO 3 -, and CO 2 diffusion through native porcine gastroduodenal mucus.* Digestive Diseases and Sciences, 2002. **47**(5): p. 967-973.
285. Allen, A. and J.P. Pearson, *Mucus glycoproteins of the normal gastrointestinal tract.* European Journal of Gastroenterology and Hepatology, 1993. **5**(4): p. 193-199.
286. Olmsted, S.S., et al., *Diffusion of macromolecules and virus-like particles in human cervical mucus.* Biophys J, 2001. **81**(4): p. 1930-1937.
287. Macierzanaka, A., et al., *Adsorption of bile salts to particles allows penetration of intestinal mucus.* Soft Matter, 2011. **7**: p. 8077-8084.
288. Behrens, I., et al., *Transport of lipophilic drug molecules in a new mucus-secreting cell culture model based on HT29-MTX cells.* Pharmaceutical Research, 2001. **18**(8): p. 1138-1145.
289. Bertolazzi, S., et al., *Bio-physical characteristics of gastrointestinal mucosa of celiac patients: comparison with control subjects and effect of gluten free diet.* BMC Gastroenterol, 2011. **11**: p. 119.
290. Corfield, A.P., et al., *Mucin degradation in the human colon: Production of sialidase, sialate O- acetylesterase, N-acetylneuraminate lyase, arylesterase, and glycosulfatase activities by strains of fecal bacteria.* Infection and Immunity, 1992. **60**(10): p. 3971-3978.
291. Van Tassell, M.L. and M.J. Miller, *Lactobacillus adhesion to mucus.* Nutrients, 2011. **3**(5): p. 613-36.
292. Carlstedt, I., et al., *Mucous glycoproteins: a gel of a problem.* Essays in Biochemistry, 1985. **20**: p. 40-76.
293. Desseyn, J.L., D. Tetaert, and V. Gouyer, *Architecture of the large membrane-bound mucins.* Gene, 2008. **410**(2): p. 215-22.
294. Hazlett, L.D., M. Moon, and R.S. Berk, *In vivo identification of sialic acid as the ocular receptor for Pseudomonas aeruginosa.* Infection and Immunity, 1986. **51**(2): p. 687-689.
295. Ellingham, R.B., et al., *Secreted human conjunctival mucus contains MUC5AC glycoforms.* Glycobiology, 1999. **9**(11): p. 1181-1189.
296. Sanchez, B., et al., *Lactobacillus plantarum extracellular chitin-binding protein and its role in the interaction between chitin, Caco-2 cells, and mucin.* Appl Environ Microbiol, 2011. **77**(3): p. 1123-6.
297. Kim, Y.S. and S.B. Ho, *Intestinal goblet cells and mucins in health and disease: recent insights and progress.* Curr Gastroenterol Rep, 2010. **12**(5): p. 319-30.
298. Gum Jr, J.R., et al., *MUC3 human intestinal mucin. Analysis of gene structure, the carboxyl terminus, and a novel upstream repetitive region.* Journal of Biological Chemistry, 1997. **272**(42): p. 26678-26686.
299. Crawley, S.C., et al., *Genomic organization and structure of the 3' region of human MUC3: Alternative splicing predicts membrane-bound and soluble forms of the mucin.* Biochemical and Biophysical Research Communications, 1999. **263**(3): p. 728-736.
300. Axelsson, M.G., N. Asker, and G.C. Hansson, *O-glycosylated MUC2 Monomer and Dimer from LS 174T Cells Are Water-soluble, whereas Larger MUC2 Species Formed Early during Biosynthesis Are Insoluble and Contain Nonreducible Intermolecular Bonds.* The Journal of Biological Chemistry, 1998. **273**(30): p. 18864-18870.
301. Sheehan, J.K., K. Oates, and I. Carlstedt, *Electron microscopy of cervical, gastric and bronchial mucus glycoproteins.* Biochemical Journal, 1986. **239**(1): p. 147-153.

302. Sheehan, J.K., et al., *Biosynthesis of the MUC2 mucin: Evidence for a slow assembly of fully glycosylated units.* Biochemical Journal, 1996. **315**(3): p. 1055-1060.
303. Thornton, D.J., et al., *Mucus glycoproteins from 'normal' human tracheobronchial secretion.* Biochemical Journal, 1990. **265**(1): p. 179-186.
304. Jaques, L.W., et al., *Sialic Acid – A Calcium-Binding Carbohydrate.* The Journal of Biological Chemistry, 1977. **22**(13): p. 4533-4538.
305. Eylar, E.H., et al., *The contribution of sialic acid to the surface charge of the erythrocyte.* The Journal of Biological Chemistry, 1962. **237**: p. 1992-2000.
306. Behr, J.P. and J.M. Lehn, *The binding of divalent cations by purified gangliosides.* FEBS Letters, 1973. **31**(3): p. 297-300.
307. Forstner, J.F. and G.G. Forstner, *Calcium binding to intestinal goblet cell mucin.* Biochimica et Biophysica Acta, 1975. **386**: p. 283-292.
308. Thongborisute, J. and H. Takeuchi, *Evaluation of mucoadhesiveness of polymers by BIACORE method and mucin-particle method.* International Journal of Pharmaceutics, 2008. **354**(1-2): p. 204-209.
309. Suknuntha, K., et al., *Characterization of muco- and bioadhesive properties of chitosan, PVP, and chitosan/PVP blends and release of amoxicillin from alginate beads coated with chitosan/PVP.* Drug Development and Industrial Pharmacy, 2011. **37**(4): p. 408-418.
310. Han, H.K., H.J. Shin, and D.H. Ha, *Improved oral bioavailability of alendronate via the mucoadhesive liposomal delivery system.* European Journal of Pharmaceutical Sciences, 2012. **46**(5): p. 500-507.
311. Maierhofer, C., K. Rohmer, and V. Wittmann, *Probing multivalent carbohydrate-lectin interactions by an enzyme-linked lectin assay employing covalently immobilized carbohydrates.* Bioorg Med Chem, 2007. **15**(24): p. 7661-76.
312. Alvarez, J.R. and R. Torres-Pinedo, *Interactions of soybean lectin, soyasaponins, and glycinin with rabbit jejunal mucosa in vitro.* Pediatric Research, 1982. **16**(9): p. 728-731.
313. Klemetsrud, T., et al., *Studies on pectin-coated liposomes and their interaction with mucin.* Colloids and Surfaces B: Biointerfaces, 2013. **103**: p. 158-165.
314. D'Agostino, E.M., et al., *Intercation of Tea Polyphenoles and Food Constituents with Model Gut Epithelia: The Protective Role of the Mucus Layer.* Agricultural and Food Chemistry, 2012. **60**: p. 3318-3328.
315. MacAdam, A., *The effect of gastro-intestinal mucus on drug absorption.* Adv Drug Deliv Rev, 1993. **11**(3): p. 201-220.
316. Flemming, H.-C. and J. Wingender, *Flocken, Filme und Schlämme - Biofilme - die bevorzugte Lebensform der Bakterien.* Biologie in unserer Zeit, 2001. **31**(3): p. 169-180.
317. Costerton, J.W., P.S. Stewart, and E.P. Greenberg, *Bacterial Biofilms: A COmmon Cause of Persistent Infections.* Science, 1999. **284**: p. 1318-1322.
318. Donlan, R.M., *Biofilms: microbial Life on Surfaces.* Emerging Infectious Diseases, 2002. **8**(9): p. 881-890.
319. Branda, S.S., et al., *Biofilms: the matrix revisited.* Trends in Microbiology, 2005. **13**(1): p. 20-26.
320. Costerton, J.W., et al., *Microbial biofilms.* Annu. Rev. Microbiol., 1995. **49**: p. 711-45.
321. Sutherland, I.W., *The biofilm matrix – an immobilized but dynamic microbial environment.* Trends in Microbiology, 2001. **9**(5): p. 221-227.
322. Sanders, R. *Discovery opens door to attacking biofilms that cause chronic infections.* 2012; Available from: http://newscenter.berkeley.edu/2012/07/12/discovery-opens-door-to-attacking-biofilms-that-cause-chronic-infections/.
323. Bjarnsholt, T., et al., *The in vivo biofilm.* Trends in Microbiology, 2013.
324. O'Toole, G.A. and R. Kolter, *Initiation of biofilm formation in Pseudomonas fluorescens WCS365 proceeds via multiple, convergent signalling pathways: A genetic analysis.* Molecular Microbiology, 1998. **28**(3): p. 449-461.

325. Lee, O.O., et al., *In situ environment rather than substrate type dictates microbial community structure of biofilms in a cold seep system.* Scientific Reports, 2014. **4**.
326. Xu, Z., et al. *Modeling framework for investigating the influence of amino acids on the planktonic-biofilm transition of Pseudomonas aeruginosa*. in *IFAC Proceedings Volumes (IFAC-PapersOnline)*. 2014.
327. Sims, I.M., et al., *Structure and functions of exopolysaccharide produced by gut commensal Lactobacillus reuteri 100-23.* The ISME Journal, 2011. **5**: p. 1115-1124.
328. Schwab, C. and M.G. Gänzle, *Effect of membrane lateral pressure on the expression of fructosyltransferases in Lactobacillus reuteri.* Systematic and Applied Microbiology, 2006. **29**(2): p. 89-99.
329. Creti, R., et al., *Enterococcal colonization of the gastro-intestinal tract: role of biofilm and environmental oligosaccharides.* BMC Microbiol, 2006. **6**: p. 60.
330. Van Houdt, R. and C.W. Michiels, *Role of bacterial cell surface structures in Escherichia coli biofilm formation.* Research in microbiology, 2005. **256**: p. 626-633.
331. Sutherland, I.W., *Biofilm exopolysaccharides: A strong and sticky framework.* Microbiology, 2001. **147**(1): p. 3-9.
332. Silverstein, A. and C.F. Donatucci, *Bacterial Biofilms and implantable prosthetic devices.* International Journal of Impotence Research, 2003. **15**(Suppl5): p. S150-S154.
333. Beloin, C., A. Roux, and J.-M. Ghigo, *Escherichia coli biofilms.* Current Topics in Microbiology and Immunulogy, 2008. **322**: p. 249-289.
334. Mack, D., et al., *The Intercellular Adhesin Involved in Biofilm Accumulation of Staphylococcus epidermis Is a linear β-1,6-Linked Glucosaminoglycan: Purification and Structural analysis.* Journal of Bacteriology, 1996. **178**(1): p. 175-183.
335. Mack, D., et al., *Association of Biofilm Production of Coagulase-Negative Staphylococci with Expression of a Specific Polysaccharide Intercellular Adhesin.* Journal of Infectious Diseases, 1996. **174**(4): p. 881-884.
336. Beenken, K.E., et al., *Global Gene Expression in Staphylococcus aureus Biofilms.* Journal of Bacteriology, 2004. **186**(14): p. 4665-4685.
337. Herrmann, M., et al., *Fibronectin, fibrinogen, and laminin act as mediators of adherence of clinical staphylococcal isolates to foreign material.* Journal of Infectious Diseases, 1988. **158**(4): p. 693-701.
338. Mack, D., et al., *Mechanisms of biofilm formation in Stphylococcus epidermidis and Staphylococcus aureus: functional molecules, regulatory circuits, and adaptive responses.* International Journal of Medical Microbiology, 2004. **294**: p. 203-212.
339. Costerton, J.W., et al., *Bacterial biofilms in nature and disease.* Ann. Rev. Microbiol., 1987. **41**: p. 435-64.
340. Tojo, M., et al., *Isolation and characterization of a capsular polysaccharide adhesin from Staphylococcus epidermidis.* Journal of Infectious Diseases, 1988. **157**(4): p. 713-722.
341. Timmerman, C.P., et al., *Characterization of a proteinaceous adhesin of Staphylococcus epidermidis which mediates attachment to polystyrene.* Infection and Immunity, 1991. **59**(11): p. 4187-4192.
342. Ledeboer, N.A. and B.D. Jones, *Exopolysaccharide Suagrs Contribute to Biofilm Formation by Salmonella enterica Serovar Typhimurium on HEp-2 Cells and Chicken Intestinal Epithelium.* Journal of Bacteriology, 2005. **187**(9): p. 3214-3226.
343. Sauer, K., *The genomics and proteomics of biofilm formation.* Genome Biology, 2003. **4**(6).
344. Heilman, C., et al., *Evidence for autolysin-mediated primary attachment of staphylococcus epidermis to a polystyrene surface.* Molecular Biology, 1997. **24**(5): p. 1013-1024.
345. Mack, D., et al., *Characterization of transposon mutants of biofilm-producing Staphylococcus epidermidis impaired in the accumulative phase of biofilm production: Genetic identification of a hexosamine-containing polysaccharide intercellular adhesin* Infection and Immunity, 1994. **62**(8): p. 3244-3253.

346. Inoue, T., et al., *Biofilm Formation by a Fimbriae-Deficient Mutant of Actinobacillus actinomycetemcomitans.* Microbiol Immunol, 2003. **47**(11): p. 877-881.
347. Vu, B., et al., *Bacterial extracellular polysaccharides involved in biofilm formation.* Molecules, 2009. **14**(7): p. 2535-54.
348. Lecuyer, S., et al., *Shear stress increases the residence time of adhesion of Pseudomonas aeruginosa.* Biophys J, 2011. **100**(2): p. 341-350.
349. Berk, V., et al., *Molecular architecture and assembly principles of Vibrio cholerae biofilms.* Science, 2012. **337**(6091): p. 236-239.
350. Busscher, H.J., R. Bos, and H.C. van der Mei, *Initial microbial adhesion is a determinant for the strength if biofilm adhesion.* FEMS Microbiology Letters, 1995. **128**(3): p. 229-234.
351. Dufour, D., V. Leung, and C.M. Lévesque, *Bacterial biofilm: structure, function, and antimicrobial resistance.* Endodontic Topics, 2010. **22**(1): p. 2-16.
352. Vuong, C., et al., *A crucial role for exopolysaccharide modification in bacterial biofilm formation, immune evasion, and virulence.* J Biol Chem, 2004. **279**(52): p. 54881-6.
353. Brooks, J.D. and S.H. Flint, *Biofilms in the food industry: Problems and potential solutions.* International Journal of Food Science and Technology, 2008. **43**(12): p. 2163-2176.
354. Latasa, C., et al., *Biofilm-associated proteins.* Comptes Rendus Biologies, 2006. **329**: p. 849-857.
355. Hancock, V., I.L. Witso, and P. Klemm, *Biofilm formation as a function of adhesin, growth medium, substratum and strain type.* Int J Med Microbiol, 2011. **301**(7): p. 570-6.
356. Stewart, P.S. and M.J. Franklin, *Physiological heterogeneity in biofilms.* Nature Reviews Microbiology, 2008. **6**(3): p. 199-210.
357. Dal Bello, F., et al., *In vitro study of prebiotic properties of levan-type exopolysaccharides from Lactobacilli and non-digestible carbohydrates using denaturing gradient gel electrophoresis.* Systematic and Applied Microbiology, 2001. **24**(2): p. 232-237.
358. Kokare, C.R., et al., *Biofilm: Importance and applications.* . Indian Journal of Biotechnology, 2008. **8**(2): p. 159-168.
359. Hancock, V., R. Munk Vejborg, and P. Klemm, *Functional genomics of probiotic Escherichia coli Nissle 1917 and 83972, and UPEC strain CFT073: comparison of transcriptomes, growth and biofilm formation.* Molecular Genetics & Genomics, 2010. **284**: p. 437-454.
360. Mayer, C., et al., *The role of intermolecular interactions: studies on model systems for bacterial biofilms.* . International Journal of Biological Macromolecules, 1999. **26**: p. 3-16.
361. Macfarlane, S., et al., *Chemotaxonomic analysis of bacterial populations colonizing the rectal mucosa in patients with ulcerative colitis.* Clinical Infectious Diseases, 2004. **38**: p. 1697-1699.
362. Roux, A., C. Beloin, and J.-M. Ghigo, *Combined Inactivation and Expression Strategy To Study Gene Function under Physiological Conditions: Application to Identification of New Escherichia coli Adhesins.* Journal of Bacteriology, 2005. **187**(3): p. 1001-1013.
363. Reisner, A., et al., *In Vitro Biofilm Formation of Commersal and Pathogenic Escherichia coli Strains: Impact of Environmental and Genetic Factors.* Journal of Bacteriology, 2006. **188**(10): p. 3572-3581.
364. Solano, C., et al., *Genetic analysis of Salomonella enteritidis biofilm formation: critical role of cellulose.* Molecular Microbiology, 2002. **43**(3): p. 793-808.
365. Zogaj, X., et al., *Production of Cellulose and Curli Fimbriae by Members of the Family Enterobacteriaceae Isolated from the Human Gastrointestinal Tract.* Infection and Immunity, 2003. **71**(7): p. 4151-4158.
366. Navasa, N., et al., *Temperature has reciprocal effects on colanic acid and polysialic acid biosynthesis in E. coli K92.* Applied Microbiology and Biotechnology, 2009. **82**(4): p. 721-729.

367. Sonnenborn, U. and J. Schulze, *The non-pathogenic escherichia coli strain nissle 1917 - features of a versatile probiotic.* Microbial Ecology in Health and Disease, 2009. **21**: p. 122-158.
368. Monteiro, C., et al., *Characterization of cellulose production in Escherichia coli Nissle 1917 and its biological consequences.* Environmental Microbiology, 2009. **11**(5): p. 1105-1116.
369. Bokranz, W., et al., *Expression of cellulose and curli fimbriae by Escherichia coli isolated from the gastrointestinal tract.* Journal of Medical Microbiology, 2005. **54**: p. 1171-1182.
370. Romling, U., et al., *Multicellular and aggregative behaviour of Salmonella typhimurium strains is controlled by mutations in the agfD promoter.* Molecular Microbiology, 1998. **28**: p. 249-264.
371. Costa, A.R., et al., *The role of polysaccharide intercellular adhesion (PIA) in Staphylococcus epidermidis adhesion to host tissues and subsequent antibiotic tolerance.* European Journal of Clinical Microbiology and Infectious Diseases, 2009. **28**(6): p. 623-629.
372. Sousa, C., P. Teixeira, and R. Oliveira, *The role of extracellular polymers on Staphylococcus epidermidis biofilm biomass and metabolic activity.* Journal of Basic Microbiology, 2009. **49**: p. 363-370.
373. Spiliopoulou, A.I., et al., *An extracellular Staphylococcus epidermidis polysaccharide: relation to Polysaccharide Intercellular Adhesin and its implication in phagocytosis.* BMC Microbiology, 2012. **12**: p. art.no. 76.
374. Vuong, C., et al., *Polysaccharide intercellular adhesin (PIA) protects Staphylococcus epidermidis against major components of the human innate immune system.* Cellular Microbiology, 2004. **6**(3): p. 269-275.
375. Mack, D., et al., *Biofilm formation in medical device-related infection.* International Journal of Artificial Organs, 2006. **29**(4): p. 343-359.
376. Karatan, E. and P. Watnick, *Signals, regulatory networks, and materials that build and break bacterial biofilms.* Microbiol Mol Biol Rev, 2009. **73**(2): p. 310-47.
377. Da Re, S. and J.M. Ghigo, *A CsgD-independent pathway for cellulose production and biofilm formation in Escherichia coli.* J Bacteriol, 2006. **188**(8): p. 3073-87.
378. Solano, C., et al., *Genetic analysis of Salmonella enteritidis biofilm formation: Critical role of cellulose.* Molecular Microbiology, 2002. **43**(3): p. 793-808.
379. Zogaj, X., et al., *The multicellular morphotypes of Salmonella typhimurium and Escherichia coli produce cellulose as the second component of the extracellular matrix.* Molecular Microbiology, 2001. **39**(6): p. 1452-1463.
380. Spiers, A.J., et al., *Biofilm formation at the air-liquid interface by the Pseudomonas fluorescens SBW25 wrinkly spreader requires an acetylated form of cellulose.* Molecular Microbiology, 2003. **50**(1): p. 15-27.
381. Ude, S., et al., *Biofilm formation and cellulose expression among diverse environmental Pseudomonas isolates.* Environmental Microbiology, 2006. **8**(11): p. 1997-2011.
382. Hungund, B.S. and S.G. Gupta, *Production of bacterial cellulose from Enterobacter amnigenus GH-1 isolated from rotten apple.* World Journal of Microbiology and Biotechnology, 2010. **26**: p. 1823-1828.
383. Yamane, C., K. Okajima, and M. Otsuka, *Cellulose-Type Material*, 2009: United States Patent, US
384. Gibson, L.J., *The hierarchical structure and mechanics of plant materials*. Vol. 9. 2012. 2749-2766.
385. Watanabe, K., et al., *Structural Features and Properties of Bacterial Cellulose Produced in Agitated Culture.* Cellulose, 1998. **5**(3): p. 187-200.
386. Ago, M., et al., *Characterization of Morphology and Physical strength for Bacterial Cellulose Produced by an Enterobacter sp.* Sen'I Gakkaishi, 2006. **62**(11): p. 258-262.
387. O'Sullivan, A.C., *Cellulose: the structure slowly unravels.* Cellulose, 1997. **4**: p. 173-207.

388. Bielecki, S., et al., *Bacterial cellulose*, in *Biopolymers Online*. 2005, Wiley-VCH Verlag GmbH&Co.KGaA.
389. Zimmerley, M., et al., *Molecular Orientation in Dry and Hydrated Cellulose Fibers: A Coherent Anti-Stokes Raman Scattering microscopy Study.* Journal of Physical Chemistry, 2010. **114**: p. 10200-10208.
390. Götz, F., *Staphylococcus and biofilms.* Molecular Microbiology, 2002. **43**(6): p. 1367-1378.
391. Wang, X., J.F.I. Preston, and T. Romeo, *The pgaABCD Locus of Escherichia coli Promotes the Synthesis of a Polysaccharide Adhesion Required for Biofilm Formation.* Journal of Bacteriology, 2004. **186**(9): p. 2724-2734.
392. Heilmann, C., et al., *Molecular basis of intercellular adhesion in the biofilm-forming Staphylococcus epidermidis.* Molecular Microbiology, 1996. **20**(5): p. 1083-1091.
393. Deighton, M.A., R. Borland, and J.A. Capstick, *Virulence of Staphylococcus epidermidis in a mouse model: Significance of extracellular slime.* Epidemiology and Infection, 1996. **117**(2): p. 267-280.
394. Rodgers, J., F. Phillips, and C. Olliff, *The effects of extracellular slime from Staphylococcus epidermidis on phagocytic ingestion and killing.* FEMS Immunology and Medical Microbiology, 1994. **9**(2): p. 109-115.
395. Izano, E.A., et al., *Poly-N-acetylglucosamine mediates biofilm formation and detergent resistance in Aggregatibacter actinomycetemcomitans.* Microb Pathog, 2008. **44**(1): p. 52-60.
396. Agladze, K., X. Wang, and T. Romeo, *Spatial periodicity of Escherichia coli K-12 biofilm microstructure initiates during a reversible, polar attachment phase of development and requires the polysaccharide adhesin PGA.* J Bacteriol, 2005. **187**(24): p. 8237-46.
397. Joyce, J.G., et al., *Isolation, structural characterization, and immunological evaluation of a high-molecular-weight exoplysaccharide from Staphylococcus aureus.* Carbohydrate Research, 2003. **228**: p. 903-922.
398. Izano, E.A., et al., *Poly-N-acetylglucosamine mediates biofilm formation and antibiotic resistance in Actinobacillus pleuropneumoniae.* Microb Pathog, 2007. **43**(1): p. 1-9.
399. Gerke, C., et al., *Characterization of the N-Acetylglucosaminyltransferase activity involved in the biosynthesis of the Staphylococcus epidermidis polysaccharide intercellular adhesin.* Journal of Biological Chemistry, 1998. **273**(29): p. 18586-18593.
400. Fredheim, E.G., et al., *Staphylococcus epidermidis polysaccharide intercellular adhesin activates complement.* FEMS Immunol Med Microbiol, 2011. **63**(2): p. 269-80.
401. Cramton, S.E., et al., *The intercellular adhesion (ica) locus is present in Staphylococcus aureus and is required for biofilm formation.* Infection and Immunity, 1999. **67**(10): p. 5427-5433.
402. Mack, D., et al., *Characterization of transposon mutants of biofilm-producing Staphylococcus epidermidis impaired in the accumulative phase of biofilm production: Genetic identification of a hexosamine-containing polysaccharide intercellular adhesin.* Infection and Immunity, 1994. **62**(8): p. 3244-3253.
403. Mack, D., et al., *Staphylococcus epidermidis biofilms:Functional molecules, relation to virulence, and vaccine potential*, in *Topics in Current Chemistry*, T.K. Lindhorst and S. Oscarson, Editors. 2009. p. 157-182.
404. Borges, O., et al., *Evaluation of the immune response following a short oral vaccination schedule with hepatitis B antigen encapsulated into alginate-coated chitosan nanoparticles.* Eur J Pharm Sci, 2007. **32**(4-5): p. 278-90.
405. Amin, M., M.R. Jaafari, and M. Tafaghodi, *Impact of chitosan coating of anionic liposomes on clearance rate, mucosal and systemic immune responses following nasal administration in rabbits.* Colloids Surf B Biointerfaces, 2009. **74**(1): p. 225-9.
406. Katz, D.E., et al., *Oral immunization of adult volunteers with microencapsulated enterotoxigenic Escherichia coli (ETEC) CS6 antigen.* Vaccine, 2003. **21**(5-6): p. 341-346.

407. Frey, A., et al., *Role of the glycocalyx in regulating access of microparticles to apical plasma membranes of intestinal epithelial cells: Implications for microbial attachment and oral vaccine targeting.* Journal of Experimental Medicine, 1996. **184**(3): p. 1045-1059.
408. Mann, J.F.S., et al., *Lipid vesicle size of an oral influenza vaccine delivery vehicle influences the Th1/Th2 bias in the immune response and protection against infection.* Vaccine, 2009. **27**(27): p. 3643-3649.
409. Azizi, A., et al., *Enhancing Oral Vaccine Potency by Targeting Intestinal M Cells.* PLoS Pathogens, 2010. **6**(1): p. e1001147.
410. Gupta, P.K., S.-H.S. Leung, and J.R. Robinson, *Bioadhesives/Mucoadhesives in Drug Delivery to the Gastrointestinal Tract*, in *Bioadhesive Drug Delivery Systems*, V. Lenaertes and R. Gurny, Editors. 1990, CRC Press Inc.: Boca Raton, Florida.
411. Wirth, M., et al., *Lectin-mediated drug delivery: Influence of mucin on cytoadhesion of plant lectins in vitro.* Journal of Controlled Release, 2002. **79**(1-3): p. 183-191.
412. Islam, M.A., et al., *Mucoadhesive chitosan derivatives as novel drug carriers.* Current Pharmaceutical Design, 2015. **21**(29): p. 4285-4309.
413. Bernkop-Schnürch, A., *Thiomers: A new generation of mucoadhesive polymers.* Adv Drug Deliv Rev, 2005. **57**(11): p. 1569-1582.
414. Peppas, N.A. and Y. Huang, *Nanoscale technology of mucoadhesive interactions.* Adv Drug Deliv Rev, 2004. **56**(11): p. 1675-1687.
415. Peppas, N.A. and P.A. Buri, *Surface, interfacial and molecular aspects of polymer bioadhesion on soft tissues.* Journal of Controlled Release, 1985. **2**(C): p. 257-275.
416. Liu, Y.-H., et al., *pH-sensitive and mucoadhesive microspheres for duodenum-specific drug delivery system.* Drug Development and Industrial Pharmacy, 2011. **37**(7): p. 868-874.
417. Lembre, P., C. Lorentz, and P. Di Martino, *Exopolysaccharides of the Biofilm Matrix: A Complex Biophysical World*, in *The Complex World of Polysaccharides*, D.N. Karunaratne, Editor. 2012, InTech.
418. Safinya, C.R. and K.K. Ewert, *Materials chemistry: Liposomes derived from molecular vases.* Nature, 2012. **489**(7416): p. 372-374.
419. Kubitschke, J., S. Javor, and J. Rebek, *Deep cavitand vesicles - Multicompartmental hosts.* Chemical Communications, 2012. **48**(74): p. 9251-9253.
420. Yin Win, K. and S.S. Feng, *Effects of particle size and surface coating on cellular uptake of polymeric nanoparticles for oral delivery of anticancer drugs.* Biomaterials, 2005. **26**(15): p. 2713-2722.
421. Gaumet, M., et al., *Nanoparticles for drug delivery: The need for precision in reporting particle size parameters.* European Journal of Pharmaceutics and Biopharmaceutics, 2008. **69**(1): p. 1-9.
422. Lince, F., D.L. Marchisio, and A.A. Barresi, *Strategies to control the particle size distribution of poly-ε-caprolactone nanoparticles for pharmaceutical applications.* J Colloid Interface Sci, 2008. **322**(2): p. 505-515.
423. Gref, R., et al., *Biodegradable long-circulating polymeric nanospheres.* Science, 1994. **263**(5153): p. 1600-1603.
424. Surh, J., Y.G. Jeong, and G.T. Vladisavljević, *On the preparation of lecithin-stabilized oil-in-water emulsions by multi-stage premix membrane emulsification.* Journal of Food Engineering, 2008. **89**(2): p. 164-170.
425. Toorisaka, E., et al., *Hypoglycemic effect of surfactant-coated insulin solubilized in a novel solid-in-oil-in-water (S/O/W) emulsion.* International Journal of Pharmaceutics, 2003. **252**(1-2): p. 271-274.
426. Kukizaki, M. and M. Goto, *Size control of nanobubbles generated from Shirasu-porous-glass (SPG) membranes.* Journal of Membrane Science, 2006. **281**(1-2): p. 386-396.
427. Couvreur, P. and F. Puisieux, *Nano- and microparticles for the delivery of polypeptides and proteins.* Adv Drug Deliv Rev, 1993. **10**(2-3): p. 141-162.

428. Prego, C., et al., *Efficacy and mechanism of action of chitosan nanocapsules for oral peptide delivery.* Pharm Res, 2006. **23**(3): p. 549-56.
429. Kawashima, Y., et al., *Mucoadhesive DL-lactide/glycolide copolymer nanospheres coated with chitosan to improve oral delivery of elcatonin.* Pharmaceutical Development and Technology, 2000. **5**(1): p. 77-85.
430. Schipper, N.G.M., et al., *Chitosans as absorption enhancers of poorly absorbable drugs. 3: Influence of mucus on absorption enhancement.* European Journal of Pharmaceutical Sciences, 1999. **8**(4): p. 335-343.
431. Furda, I., *Chitin and Chitosan - Special Class of Dietary Fiber*, in *CRC Hanbook of Dietary Fiber in Human Nutrition*, G.A. Spiller, Editor. 2001, CRC Press LLC: Boca Raton, Florida.
432. Smart, J.D., *The Role of Water Movement and Polymer Hydration in Mucoadhesion*, in *Bioadhesive Drug Delivery Systems*. 1999, CRC Press. p. 11-23.
433. Grabovac, V., D. Guggi, and A. Bernkop-Schnürch, *Comparison of the mucoadhesive properties of various polymers.* Adv Drug Deliv Rev, 2005. **57**(11): p. 1713-1723.
434. Behrens, I., et al., *Comparative uptake studies of bioadhesive and non-bioadhesive nanoparticles in human intestinal cell lines and rats: The effect of mucus on particle adsorption and transport.* Pharmaceutical Research, 2002. **19**(8): p. 1185-1193.
435. Bhattacherjee, S., et al., *Surface charge-specific interactions between polymer nanoparticles and ABC transporters in CaCo-2 cells.* Journal of Nanoparticle Research, 2013. **15**: p. 1695.
436. Thompson, A.K. and H. Singh, *Preparation of liposomes from milk fat globule membrane phospholipids using a microfluidizer.* Journal of Dairy Science, 2006. **89**(2): p. 410-419.
437. Zeisig, R. and B. Caemmerer, *Liposomes in the food industry*, in *Microencapsulation of Food Ingredients*, P. Vilstrup, Editor. 2001, Leatherhead Publishing: London, UK. p. 101-119.
438. Lasic, D.D., *Novel applications of liposomes.* Trends in Biotechnology, 1998. **16**(7): p. 307-321.
439. Laginha, K., D. Mumbengegwi, and T. Allen, *Liposomes targeted via two different antibodies: Assay, B-cell binding and cytotoxicity.* Biochimica et Biophysica Acta - Biomembranes, 2005. **1711**(1): p. 25-32.
440. Tsai, M.S., et al., *Binding patterns of peptide-containing liposomes in liver and spleen of developing mice: Comparison with heparan sulfate immunoreactivity.* Journal of Drug Targeting, 2011. **19**(7): p. 506-515.
441. Clark, M.A., B.H. Hirst, and M.A. Jepson, *Lectin-mediated mucosal delivery of drugs and microparticles.* Adv Drug Deliv Rev, 2000. **43**(2-3): p. 207-223.
442. Clark, M.A., et al., *Targeting polymerized liposome vaccine carriers to intestinal M cells.* Vaccine, 2001. **20**: p. 208-217.
443. Woodley, J.F., *Lectins for gastrointestinal targeting - 15 Years on.* Journal of Drug Targeting, 2000. **7**(5): p. 325-333.
444. Lavelle, E.C., et al., *Mucosal immunogenicity of plant lectins in mice.* Immunology, 2000. **99**(1): p. 30-37.
445. Kunz, C., et al., *Oligosaccharides in human milk: structural, functional, and metabolic aspects.* Annu Rev Nutr, 2000. **20**: p. 699-722.
446. Valenti, P. and G. Antonini, *Lactoferrin: An important host defence against microbial and viral attack.* Cellular and Molecular Life Sciences, 2005. **62**(22): p. 2576-2587.
447. Adlerova, L., A. Bartoskova, and M. Flaldyna, *Lactoferrin: a review.* Veterinarni Medicina, 2008. **53**(9): p. 457-468.
448. Orsi, N., *The antimicrobial activity of lactoferrin: Current status and perspectives.* BioMetals, 2004. **17**(3): p. 189-196.
449. Ward, P.P., E. Paz, and O.M. Conneely, *Multifunctional roles of lactoferrin: A critical overview.* Cellular and Molecular Life Sciences, 2005. **62**(22): p. 2540-2548.

450. Bellamy, W., et al., *Antibacterial spectrum of lactoferricin B, a potent bactericidal peptide derived from the N-terminal region of bovine lactoferrin.* Journal of Applied Bacteriology, 1992. **73**(6): p. 472-479.
451. Sugita-Konishi, Y., et al., *Inhibition of bacterial adhesins and salmonella infection in BALB/c mice by sialyloligosaccharides and their derivates from chicken egg yolk.* Journal of Agricultural and Food Chemistry, 2002. **50**: p. 3607-3613.
452. Sinclair, H.R., et al., *Sialyloligosaccharides inhibit cholera toxin binding to the GM1 receptor.* Carbohydr Res, 2008. **343**(15): p. 2589-94.
453. Sharon, N., *Carbohydrates as future anti-adherence drugs for infectious diseases.* Biochimica et Biophysica Acta, 2006. **1760**: p. 527-537.
454. Bouckaert, J., et al., *The affinity of the FimH fimbrial adhesin is receptor-driven and quasi-independent of Escherichia coli pathotypes.* Molecular Microbiology, 2006. **61**(6): p. 1556-1568.
455. Zafriri, D., et al., *Inhibitory activity of cranberry juice on adherence of type 1 and type P fimbriated Escherichia coli to eucaryotic cells.* Antimicrobial Agents and Chemotherapy, 1989. **33**(1): p. 92-98.
456. Howell, A.B., et al., *A-type cranberry proanthocyanidins and uropathogenic bacterial anti-adhesion activity.* Phytochemistry, 2005. **66**(18 SPEC. ISS.): p. 2281-2291.
457. Howell, A.B., *Bioactive compounds in cranberries and their role in prevention of urinary tract infections.* Mol Nutr Food Res, 2007. **51**(6): p. 732-7.
458. Guggenbichler, J.P., et al., *Acidic oligosaccharides from natural sources block adherence of Escherichia coli on uroepithelial cells.* Pharmaceutical and Pharmacological Letters, 1997. **7**: p. 35-38.
459. Lee, J.H., et al., *Inhibition of pathogenic bacterial adhesion by acidic polysaccharide from green tea (Camellia sinensis).* Journal of Agricultural and Food Chemistry, 2006. **54**: p. 8717-8722.
460. Alvarez, R.A., M.W. Blaylock, and J.B. Baseman, *Surface localized glyceraldehyde-3-phosphate dehydrogenase of Mycoplasma genitalium binds mucin.* Molecular Microbiology, 2003. **48**(5): p. 1417-1425.
461. *GE Healthcare - 2-D Quant Kit*. 2014; Available from: https://www.gelifesciences.com/gehcls_images/GELS/Related%20Content/Files/1314729545976/litdoc28954714AE_20110830215136.pdf.
462. Niv, Y., et al., *Human HT-29 colon carcinoma cells: Mucin production and tumorigenicity in relation to growth phases.* Anticancer Research, 1995. **15**(5 B): p. 2023-2027.
463. Hilgendorf, C., et al., *Caco-2 versus Caco-2/HT29-MTX co-cultured cell lines: Permeabilities via diffusion, inside- and outside-directed carrier-mediated transport.* J Pharm Sci, 2000. **89**(1): p. 63-75.
464. *Protein Detection & Quantification - Direct Detect® Spectrometer*. 2014; Available from: http://www.merckmillipore.com/NZ/en/life-science-research/protein-detection-quantification/direct-detect-spectrometer/NWGb.qB.NtgAAAFBfBwRRkwm,nav?cid=BI-XX-BSP-P-GOOG-DIDE-B328-1005.
465. *US pharmacopeia - Gastric digestion*.
466. Wessel, D. and U.I. Flügge, *A method for the quantitative recovery of protein in dilute solution in the presence of detergents and lipids.* Anal Biochem, 1984. **138**(1): p. 141-143.
467. Bendix, U., et al., *Effect of γ-interferon on binding of gliadin and other food peptides to the human intestinal cell line HT-29.* Clinica Chimica Acta, 1997. **261**(1): p. 69-80.
468. Bolte, G., et al., *Specific interaction of food proteins with apical membranes of the human intestinal cell lines Caco-2 and T84.* Clinica Chimica Acta, 1998. **270**(2): p. 151-167.
469. Arentz-Hansen, H., et al., *The intestinal T cell response to α-gliadin in adult celiac disease is focused on a single deamidated glutamine targeted by tissue transglutaminase.* Journal of Experimental Medicine, 2000. **191**(4): p. 603-612.

470. Barnes, L.M., et al., *Correlated XPS, AFM and bacterial adhesion studies on milk and milk proteins adherent to stainless steel.* Biofouling, 2001. **17**(1): p. 1-22.
471. Parker, P., et al., *Bovine Muc1 inhibits binding of enteric bacteria to Caco-2 cells.* Glycoconj J, 2010. **27**(1): p. 89-97.
472. Lane, J.A., et al., *Anti-infective bovine colostrum oligosaccharides: Campylobacter jejuni as a case study.* International Journal of Food Microbiology, 2012. **157**(2): p. 182-188.
473. Hiramoto, S., et al., *Melanoidin, a food protein-derived advanced Maillard reaction product, suppresses Helicobacter pylori in vitro and in vivo.* Helicobacter, 2004. **9**(5): p. 429-435.
474. Davidson, L.A. and B. Lonnerdal, *Persistence of human milk proteins in the breast-fed infant.* Acta Paediatrica Scandinavica, 1987. **76**(5): p. 733-740.
475. *BioRad Instruction Manual - Quick Start™Bradford Protein Assay.*
476. Mahe, S., et al., *Gastroileal nitrogen and electrolyte movements after bovine milk ingestion in humans.* American Journal of Clinical Nutrition, 1992. **56**(2): p. 410-416.
477. Hur, S.J., E.A. Decker, and D.J. McClements, *Influence of initial emulsifier type on microstructural changes occurring in emulsified lipids during in vitro digestion.* Food Chemistry, 2009. **114**(1): p. 253-262.
478. Georgiades, P., et al., *Particle tracking microrheology of purified gastrointestinal mucins.* Biopolymers, 2014. **101**(4): p. 366-377.
479. Moreno, F.J., A.R. Mackie, and E.N.C. Mills, *Phospholipid interactions protect the milk allergen α-lactalbumin from proteolysis during in vitro digestion.* Journal of Agricultural and Food Chemistry, 2005. **53**(25): p. 9810-9816.
480. Eriksen, E.K., et al., *Different digestion of caprine whey proteins by human and porcine gastrointestinal enzymes.* Br J Nutr, 2010. **104**(3): p. 374-81.
481. Lee, S., et al., *Porcine gastric mucin (PGM) at the water/poly(dimethylsiloxane) (PDMS) interface: Influence of pH and ionic strength on its conformation, adsorption, and aqueous lubrication properties.* Langmuir, 2005. **21**(18): p. 8344-8353.
482. Bansil, R. and B.S. Turner, *Mucin structure, aggregation, physiological functions and biomedical applications.* Current Opinion in Colloid & Interface Science, 2006. **11**(2–3): p. 164-170.
483. Mantle, M. and A. Allen, *Isolation and characterization of the native glycoprotein from pig small-intestinal mucus.* Biochemical Journal, 1981. **195**(1): p. 267-275.
484. Kočevar-Nared, J., J. Kristl, and J. Šmid-Korbar, *Comparative theological investigation of crude gastric mucin and natural gastric mucus.* Biomaterials, 1997. **18**(9): p. 677-681.
485. Glenister, D.A., et al., *Enhanced growth of complex communities of dental plaque bacteria in mucin-limited continuous culture.* Microbial Ecology in Health and Disease, 1988. **1**(1): p. 31-38.
486. Takeuchi, H., et al., *Novel mucoadhesion tests for polymers and polymer-coated particles to design optimal mucoadhesive drug delivery systems.* Adv Drug Deliv Rev, 2005. **57**(11): p. 1583-1594.
487. *BIACORE - Technology*. 2015 24 November 2015]; Available from: https://www.biacore.com/lifesciences/technology/introduction/data_interaction/index.html.
488. Lafitte, G., K. Thuresson, and O. Söderman, *Diffusion of nutrients molecules and model drug carriers through mucin layer investigated by magnetic resonance imaging with chemical shift resolution.* J Pharm Sci, 2007. **96**(2): p. 258-263.
489. Aksoy, N., et al., *A study of the intracellular and secreted forms of the MUC2 mucin from the PC/AA intestinal cell line.* Glycobiology, 1999. **9**(7): p. 739-746.
490. *The Sahlgrenska Academy - Mucin Biology Group*. 05 November 2015]; Available from: http://www.medkem.gu.se/mucinbiology/index.php?jumpto=research.
491. Tailford, L.E., et al., *Mucin glycan foraging in the human gut microbiome.* Frontiers in Genetics, 2015. **5**(FEB).

492. Slotta, D.J., M.A. McFarland, and S.P. Markey, *MassSieve: Panning MS/MS peptide data for proteins.* Proteomics, 2010. **10**(16): p. 3035-3039.
493. Toepel, A., *Chemie und Physik der Milch*. Vol. 1. 2004, Hamburg, Germany: B. Behr's Verlag.
494. Swaisgood, H.E., *Chemistry of the caseins*, in *Dairy Chemistry-1: Proteins*, P.F. Fox and P.L.H. McSweeney, Editors. 2003, Kluwer Academic/Plenum Press: New York. p. 139-201.
495. Dalgleish, D.G., *On the structural models of bovine casein micelles - Review and possible improvements.* Soft Matter, 2011. **7**(6): p. 2265-2272.
496. Powell, J.J., R. Jugdaohsingh, and R.P.H. Thompson, *The regulation of mineral absorption in the gastrointestinal tract.* Proceedings of the Nutrition Society, 1999. **58**(1): p. 147-153.
497. Horne, D.S., *Casein micelle structure and stability*, in *Milk Proteins: From Expression to Food*, A. Thompson, M. Boland, and H. Singh, Editors. 2009, Academic Press/Elsevier: New York, N.Y. p. 133-162.
498. Soares, R.V., et al., *MG2 and lactoferrin form a heterotypic complex in salivary secretions.* Journal of Dental Research, 2003. **82**(6): p. 471-475.
499. *UniProtKB - Q8WML4 (MUC1_BOVIN)*. 05 November 2015]; Available from: http://www.uniprot.org/uniprot/Q8WML4.
500. Pallesen, L.T., et al., *Purification of MUC1 from bovine milk-fat globules and characterization of a corresponding full-length cDNA clone.* Journal of Dairy Science, 2001. **84**(12): p. 2591-2598.
501. Liu, C., A.K. Erickson, and D.R. Henning, *Distribution and carbohydrate structures of high molecular weight glycoproteins, MUC1 and MUCX, in bovine milk.* Journal of Dairy Science, 2005. **88**(12): p. 4288-4294.
502. Nylander, T. and N.M. Wahlgren, *Competitive and Sequential Adsorption of β-Casein and β-Lactoglobulin on Hydrophobic Surfaces and the Interfacial Structure of β-Casein.* J Colloid Interface Sci, 1994. **162**(1): p. 151-162.
503. Bernardi, G. and T. Kawasaki, *Chromatography of polypeptides and proteins on hydroxyapatite columns.* BBA - Protein Structure, 1968. **160**(3): p. 301-310.
504. Withers, C.A., et al., *Investigation of milk proteins binding to the oral mucosa.* Food and Function, 2013. **4**(11): p. 1668-1674.
505. Imafidon, G.I., N.Y. Farkye, and A.M. Spanier, *Isolation, purification, and alteration of some functional groups of major milk proteins: A review.* Critical Reviews in Food Science and Nutrition, 1997. **37**(7): p. 663-689.
506. Paz, H.B., et al., *The role of calcium in mucin packaging within goblet cells.* Experimental Eye Research, 2003. **77**(1): p. 69-75.
507. Dang, C.V., et al., *Fibrinogen sialic acid residues are low affinity calcium-binding sites that influence fibrin assembly.* Journal of Biological Chemistry, 1989. **264**(25): p. 15104-15108.
508. Roefs, S.P.F.M., et al., *Preliminary note on the change in casein micelles caused by acidification.* Neth. Milk Dairy J., 1985. **39**.
509. Walstra, P., *On the Stability of Casein Micelles.* Journal of Dairy Science, 1990. **73**(8): p. 1965-1979.
510. Bake, K., A. Hoffrichter, and R. Sonssna, *Hanbuch der Milch- und Molkereitechnik*, ed. G.T.P.P. GmbH. 2003, Essen: Th.-Mann Verlag.
511. Chen, H., *Surface Fouling During Heating*, in *Encyclopedia of Agricultural, Food, and Biological Engineering*, D.R. Heldman, Editor. 2003, Marcel Dekker Inc.: Basel, Switzerland. p. 975-978.
512. Wang, K., et al., *Theoretical analysis of protein effects on calcium phosphate precipitation in simulated body fluid.* CrystEngComm, 2012. **14**(18): p. 5870-5878.
513. Mekmene, O., Y. Le Graët, and F. Gaucheron, *A model for predicting salt equilibria in milk and mineral-enriched milks.* Food Chemistry, 2009. **116**(1): p. 233-239.
514. Mortimer, C.E. and U. Mueller, *Chemie - Das Basiswissen der Chemie*. Vol. 8. 2003, Stuttgart: Thieme Verlag.

515. Dybing, S.T. and D.E. Smith, *The Ability of Phosphates or κ-Carrageenan to Coagulate Whey Proteins and the Possible Uses of Such Coagula in Cheese Manufacture.* Journal of Dairy Science, 1998. **81**(2): p. 309-317.
516. Saulnier, F., et al., *Variation of the composition and nature of the insoluble precipitate from industrial wheys.* Le Lait, 1995. **75**(1): p. 93-100.
517. Tercinier, L., et al., *Adsorption of milk proteins on to calcium phosphate particles.* J Colloid Interface Sci, 2013. **394**(1): p. 458-466.
518. Tercinier, L., et al., *Effects of Ionic Strength, pH and Milk Serum Composition on Adsorption of Milk Proteins on to Hydroxyapatite Particles.* Food Biophysics, 2014. **9**(4): p. 341-348.
519. Laparra, J.M. and Y. Sanz, *Comparison of in vitro models to study bacterial adhesion to the intestinal epithelium.* Lett Appl Microbiol, 2009. **49**(6): p. 695-701.
520. Maestracci, D., et al., *Enzymes of the human intestinal brush border membrane. Identification after gel electrophoretic separation.* BBA - Biomembranes, 1975. **382**(2): p. 147-156.
521. Wikman-Larhed, A. and P. Artursson, *Co-cultures of human intestinal goblet (HT29-H) and absorptive (Caco-2) cells for studies of drug and peptide absorption.* European Journal of Pharmaceutical Sciences, 1995. **3**(3): p. 171-183.
522. Matthes, I., et al., *Mucus models for investigation of intestinal absorption. Part 4: Comparison of the in vitro mucus model with absorption models in vivo and in situ to predict intestinal absorption.* MUSCUSMODELLE ZUR UNTERSUCHUNG VON INTESTINALEN ABSORPTIONSMECHANISMEN. 4. MITTEILUNG: VERGLEICH DES MUCUSMODELLS MIT ABSORPTIONSMODELLEN IN VIVO UND IN SITU ZUR VORHERSAGE INTESTINALER WIRKSTOFFABSORPTION, 1992. **47**(10): p. 787-791.
523. Song, J., et al., *PROSPER: An Integrated Feature-Based Tool for Predicting Protease Substrate Cleavage Sites.* PLoS ONE, 2012. **7**(11).
524. *Degradome Enzyme Database*. [cited 2016 18 June]; Available from: http://degradome.uniovi.es/.
525. Shah, R.B. and M.A. Khan, *Protection of Salmon Calcitonin Breakdown with Serine Proteases by Various Ovomucoid Species for Oral Drug Delivery.* J Pharm Sci, 2004. **93**(2): p. 392-406.
526. Howell, S., A.J. Kenny, and A.J. Turner, *A survey of membrane peptidases in two human colonic cell lines, Caco-2 and HT-29.* Biochemical Journal, 1992. **284**(2): p. 595-601.
527. Alfalah, M., R. Jacob, and H.Y. Naim, *Intestinal dipeptidyl peptidase IV is efficiently sorted to the apical membrane through the concerted action of N- and O-glycans as well as association with lipid microdomains.* Journal of Biological Chemistry, 2002. **277**(12): p. 10683-10690.
528. Brockhausen, I., P.A. Romero, and A. Herscovics, *Glycosyltransferase changes upon differentiation of CaCo-2 human colonic adenocarcinoma cells.* Cancer Research, 1991. **51**(12): p. 3136-3142.
529. Malagolini, N., et al., *Effect of ethanol on human colon carcinoma CaCo-2 and HT-29 cell lines during the maturation process.* Alcoholism: Clinical and Experimental Research, 1994. **18**(6): p. 1386-1391.
530. Kleene, R. and E.G. Berger, *The molecular and cell biology of glycosyltransferases.* BBA - Reviews on Biomembranes, 1993. **1154**(3-4): p. 283-325.
531. Whitfield, D.M., *Plausible transition states for glycosylation reactions.* Carbohydrate Research, 2012. **356**: p. 180-190.
532. Galonić, D.P. and D.Y. Gin, *Chemical glycosylation in the synthesis of glycoconjugate antitumour vaccines.* Nature, 2007. **446**(7139): p. 1000-1007.
533. *UniProtKB - P02754 (LACB_BOVIN)*. 2015 17 November 2015]; Available from: http://www.uniprot.org/uniprot/P02754.
534. Spiro, R.G., *Protein glycosylation: Nature, distribution, enzymatic formation, and disease implications of glycopeptide bonds.* Glycobiology, 2002. **12**(4): p. 43R-56R.

535. Elhammer, A.P., et al., *The specificity of UDP-GalNAc:polypeptide N-acetylgalactosaminyltransferase as inferred from a database of in vivo substrates and from the in vitro glycosylation of proteins and peptides.* Journal of Biological Chemistry, 1993. **268**(14): p. 10029-10038.
536. Brownlow, S., et al., *Bovine β-lactoglobulin at 1.8 Å resolution — still an enigmatic lipocalin.* Structure, 1997. **5**(4): p. 481-495.
537. Snyder, J.D. and W.A. Walker, *Structure and function of intestinal mucin: Developmental aspects.* International Archives of Allergy and Applied Immunology, 1987. **82**(3-4): p. 351-356.
538. Carre, A. and K.L. Mittal, eds. *Surafce and Interfacial Aspects of Cell Adhesion*. 2011, CRC Prsee, Taylor & Francis Group: Boca Raton, FL.
539. Imberty, A., *Bacterial lectins and adhesins: Structures, ligands and functions*. 2011, Bentham Science Publishers Ltd. p. 3-11.
540. Korea, C.G., J.M. Ghigo, and C. Beloin, *The sweet connection: Solving the riddle of multiple sugar-binding fimbrial adhesins in Escherichia coli: Multiple E. coli fimbriae form a versatile arsenal of sugar-binding lectins potentially involved in surface-colonisation and tissue tropism.* Bioessays, 2011. **33**(4): p. 300-11.
541. Krogfelt, K.A., H. Bergmans, and P. Klemm, *Direct evidence that the FimH protein is the mannose specific adhesin of Escherichia coli type 1 fimbriae.* Infection and Immunity, 1990. **58**: p. 1995-1998.
542. Jones, C.H., et al., *FimH adhesin of the type 1 pili is assembled into a fimbrillar tip structure in the Enterobacteriaceae.* Proceedings in the National Academy of Sciences USA, 1995. **92**: p. 2081-2085.
543. Lin, C.-C., et al., *Selective binding of mannose-encapsulated gold nanoparticles to type 1 pili in Escherichia coli.* Journal of the American Chemical Society, 2002. **124**: p. 3508-3509.
544. Le Bouguenec, C., *Adhesions and invasions of pathogenic Escherichia coli.* International Journal of Medical Microbiology, 2005. **295**: p. 471-478.
545. Pouttu, R., et al., *Amino acid residue Ala-62 in the FimH fimbrial adhesin is critical for the adhesiveness of meningitis-associated Escherichia coli to collagens.* Molecular Microbiology, 1999. **31**: p. 1747-1757.
546. Sokurenko, E.V., et al., *Diversity of the Escherichia coli type 1 fimbrial lectin. Differential binding to mannosides and uroepithelial cells.* Journal of Biological Chemistry, 1997. **272**: p. 17880-17886.
547. Sokurenko, E.V., et al., *Quantitative differences in the adhesiveness of type 1 fimbriated Escherichia coli due to structural differences in fimH genes.* Journal of Bacteriology, 1995. **176**: p. 748-755.
548. Sharon, N. and I. Ofek, *Fighting infectious diseases with inhibitors of microbial adhesion to host tissues.* Critical Reviews in Food Science and Nutrition, 2002. **42**(3 Suppl): p. 267-272.
549. Westerlund-Wikstrom, B. and T.K. Korhonen, *Molecular structure of adhesion domains in Escherichia coli fimbriae.* International Journal of Medical Microbiology, 2005. **295**: p. 479-486.
550. Klemm, P., R. Munk Vejborg, and V. Hankock, *Prevention of bacterial adhesion.* Applied Microbiology and Biotechnology, 2010. **88**: p. 421-459.
551. Latasa, I. and J.R. Penades, *Bap: A family of surface proteins involved in biofilm formation.* Research in microbiology, 2005. **157**: p. 99-107.
552. Latasa, C., et al., *BapA, a large secreted protein for biofilm formation and host colonization of Salmonella enterica serovar Enteritidis.* Molecular Microbiology, 2005. **58**(5): p. 1322-1339.
553. Sansonetti, P.J., *To be or not to be a pathogen: that is the mucosally relevant question.* Mucosal Immunology, 2011. **4**(1): p. 8-14.
554. Tendolkar, P.M., A.S. Baghdayan, and N. Shankar, *The N-Terminal Domain of Enterococcal Surface Protein, Esp, Is Sufficient for Esp-Mediated Biofilm Enhancment in Enetrococcus faecalis.* Journal of Bacteriology, 2005. **187**(17): p. 6213-6222.

555. Lasa, I., *Towards the identification of the common features of bacterial biofilm development.* International Microbiology, 2006. **9**(1): p. 21-23.
556. Sadovskaya, I., et al., *Extracellular carbohydrate-containing polymers of a model biofilm-producing strain, Staphylococcus epidermidis RP62A.* Infect Immun, 2005. **73**(5): p. 3007-17.
557. Olsen, A., et al., *The RpoS sigma factor relieves H-NS-mediated transcriptional repression of csgA, the subunit gene of fibronectin-binding curli in Escherichia coli.* Molecular Microbiology, 1993. **7**(4): p. 523-536.
558. Olsen, A., A. Jonsson, and S. Normark, *Fibronectin binding mediated by a novel class of surface organelles on Escherichia coli.* Nature, 1989. **338**(6217): p. 652-655.
559. Prigent-Combaret, C., et al., *Developmental pathway for biofilm formation in curli-producing Escherichia coli strains: Role of flagella, curli and colanic acid.* Environmental Microbiology, 2000. **2**(4): p. 450-464.
560. Markovitz, A., *Genetics and regulation of bacterial capsular polysaccharide synthesis and radiation sensitivity*, in *Surface carbohydrates of the prokaryotic cell*, I.W. Sutherland, Editor. 1977, Academic Press Inc.: NewYor, N.Y. p. 415-462.
561. Danese, P.N., et al., *The outer membrane protein, Antigen 43, mediates cell-to-cell interactions within Escherichia coli biofilms.* Molecular Microbiology, 2000. **37**(2): p. 424-432.
562. Sugita-Konishi, Y., et al., *Preventive effect of sialylglycopeptide - Nondigestive polysaccharide conjugates on Salmonella infection.* Journal of Agricultural and Food Chemistry, 2004. **52**(17): p. 5443-5448.
563. Cebo, C., *Milk fat globule membrane proteomics: A 'snapshot' of mammary epithelial cell biology.* Food Technology and Biotechnology, 2012. **50**(3): p. 306-314.
564. Petschow, B.W., R.D. Talbott, and R.P. Batema, *Ability of lactoferrin to promote the growth of Bifidobacterium spp. in vitro is independent of receptor binding capacity and iron saturation level.* Journal of Medical Microbiology, 1999. **48**(6): p. 541-549.
565. McKenney, D., et al., *The ica locus of Staphylococcus epidermidis encodes production of the capsular polysaccharide/adhesin.* Infection and Immunity, 1998. **66**(10): p. 4711-4720.
566. Sánchez, B., et al., *Identification of surface-associated proteins in the probiotic bacterium Lactobacillus rhamnosus GG.* International Dairy Journal, 2009. **19**(2): p. 85-88.
567. Tiong, H.K., S. Hartson, and P.M. Muriana, *Comparison of five methods for direct extraction of surface proteins from Listeria monocytogenes for proteomic analysis by orbitrap mass spectrometry.* Journal of Microbiological Methods, 2015. **110**: p. 54-60.
568. Kaveti, S. and J.R. Engen, *Protein interactions probed with mass spectrometry.* Methods in molecular biology (Clifton, N.J.), 2006. **316**: p. 179-197.
569. Perham, M., J. Liao, and P. Wittung-Stafshede, *Differential effects of alcohols on conformational switchovers in α-helical and β-sheet protein models.* Biochemistry, 2006. **45**(25): p. 7740-7749.
570. Dufour, E., et al., *Conformation changes of β-lactoglobulin: An ATR infrared spectroscopic study of the effect of pH and ethanol.* Journal of Protein Chemistry, 1994. **13**(2): p. 143-149.
571. Wehbi, Z., et al., *Study of ethanol-induced conformational changes of holo and apo α-lactalbumin by spectroscopy and limited proteolysis.* Molecular Nutrition and Food Research, 2006. **50**(1): p. 34-43.
572. Beddek, A.J. and A.B. Schrvyers, *The lactoferrin receptor complex in gram negative bacteria.* BioMetals, 2010. **23**: p. 377-386.
573. Ling, J.M.L. and A.B. Schryvers, *Perspectives on interactions between lactoferrin and bacteria.* Biochemistry and Cell Biology, 2006. **84**(3): p. 275-281.
574. Tian, H., et al., *Influence of bovine lactoferrin on selected probiotic bacteria and intestinal pathogens.* BioMetals, 2010. **23**(3): p. 593-596.

575. Huang, X.H., et al., *Specific IgG activity of bovine immune milk against diarrhea bacteria and its protective effects on pathogen-infected intestinal damages.* Vaccine, 2008. **26**(47): p. 5973-5980.
576. Tsuruta, T., et al., *Commensal bacteria coated by secretory immunoglobulin A and immunoglobulin G in the gastrointestinal tract of pigs and calves.* Animal Science Journal, 2012. **83**(12): p. 799-804.
577. Van Der Waaij, L.A., et al., *Immunoglobulin coating of faecal bacteria in inflammatory.* European Journal of Gastroenterology and Hepatology, 2004. **16**(7): p. 669-674.
578. Keenan, T.W. and S. Patton, *The structure of milk: Implications for sampling and storage. A. The milk lipid globule membrane*, in *Handbook of milk composition*, R.G. Jensen, Editor. 1995, Academic Press Inc.: New York, n.Y. p. 5-50.
579. Martin, H.M., et al., *Role of xanthine oxidoreductase as an antimicrobial agent.* Infection and Immunity, 2004. **72**(9): p. 4933-4939.
580. Singh, H., *The milk fat globule membrane-A biophysical system for food applications.* Current Opinion in Colloid and Interface Science, 2006. **11**(2-3): p. 154-163.
581. Vorbach, C., R. Harrison, and M.R. Capecchi, *Xanthine oxidoreductase is central to the evolution and function of the innate immune system.* Trends in Immunology, 2003. **24**(9): p. 512-517.
582. El-Sayed, M.M.H. and H.A. Chase, *Purification of the two major proteins from whey concentrate using a cation-exchange selective adsorption process.* Biotechnology Progress, 2010. **26**(1): p. 192-199.
583. Le Maux, S., et al., *Bovine β-lactoglobulin/fatty acid complexes: Binding, structural, and biological properties.* Dairy Science and Technology, 2014. **94**(5): p. 409-426.
584. Kontopidis, G., C. Holt, and L. Sawyer, *Invited review: β-lactoglobulin: Binding properties, structure, and function.* Journal of Dairy Science, 2004. **87**(4): p. 785-796.
585. Kontopidis, G., C. Holt, and L. Sawyer, *The ligand-binding site of bovine β-lactoglobulin: Evidence for a function?* Journal of Molecular Biology, 2002. **318**(4): p. 1043-1055.
586. Ji, Y.K. and J.Q. Ling, *Spatial distribution of dead and vital bacteria in the native dental biofilm.* Zhonghua kou qiang yi xue za zhi = Zhonghua kouqiang yixue zazhi = Chinese journal of stomatology, 2007. **42**(5): p. 294-297.
587. Laspidou, C.S. and B.E. Rittmann, *Modeling the development of biofilm density including active bacteria, inert biomass, and extracellular polymeric substances.* Water Research, 2004. **38**(14-15): p. 3349-3361.
588. Zhang, T.C. and P.L. Bishop, *Density, porosity, and pore structure of biofilms.* Water Research, 1994. **28**(11): p. 2267-2277.
589. Ammann, C.G., et al., *Influence of poly-N-acetylglucosamine in the extracellular matrix on N-chlorotaurine mediated killing of Staphylococcus epidermidis.* New Microbiologica, 2014. **37**(3): p. 383-386.
590. Bouvet, J.P., *Immunoglobulin Fab fragment-binding proteins.* International Journal of Immunopharmacology, 1994. **16**(5-6): p. 419-424.
591. Bjorck, L. and G. Kronvall, *Purification and some properties of streptococcal protein G, a novel IgG-binding reagent.* Journal of Immunology, 1984. **133**(2): p. 969-974.
592. Forsgren, A. and J. Sjöquist, *"Protein A" from S. aureus. I. Pseudo-immune reaction with human gamma-globulin.* Journal of Immunology, 1966. **97**(6): p. 822-827.
593. Harboe, M. and I. Folling, *Recognition of two distinct groups of human IgM and IgA based on different binding to staphylococci.* Scandinavian Journal of Immunology, 1974. **3**(4): p. 471-482.
594. Eliasson, M., et al., *Differential IgG-binding characteristics of staphylococcal protein A, streptococcal protein G, and a chimeric protein AG.* Journal of Immunology, 1989. **142**(2): p. 575-581.
595. Moshier, A., M.S. Reddy, and F.A. Scannapieco, *Role of type 1 fimbriae in the adhesion of Escherichia coli to salivary mucin and secretory immunoglobulin A.* Curr Microbiol, 1996. **33**(3): p. 200-208.

596. Harrison, R., *Milk xanthine oxidase: Hazard or benefit?* Journal of Nutritional and Environmental Medicine, 2002. **12**(3): p. 231-238.
597. Adachi, T., et al., *Binding of human xanthine oxidase to sulphated glycosaminoglycans on the endothelial-cell surface.* Biochemical Journal, 1993. **289**(2): p. 523-527.
598. Barboza, M., et al., *Glycosylation of human milk lactoferrin exhibits dynamic changes during early lactation enhancing its role in pathogenic bacteria-host interactions.* Molecular and Cellular Proteomics, 2012. **11**(6).
599. Ling, J.M.L. and A.B. Schryvers, *Perspectives on interactions between lactoferrin and bacteria.* Biochemistry and Cell Biology, 2006. **84**: p. 275-281.
600. Baveye, S., et al., *Lactoferrin: A multifunctional glycoprotein involved in the modulation of the inflammatory process.* Clinical Chemistry and Laboratory Medicine, 1999. **37**(3): p. 281-286.
601. Beddek, A.J. and A.B. Schryvers, *The lactoferrin receptor complex in gram negative bacteria.* BioMetals, 2010. **23**(3): p. 377-386.
602. Naidu, A.S., et al., *Bovine lactoferrin binding to six species of coagulase-negative staphylococci isolated from bovine intramammary infections.* Journal of Clinical Microbiology, 1990. **28**(10): p. 2312-2319.
603. Naidu, A.S., et al., *Comparison between lactoferrin and subepithelial matrix protein binding in Staphylococcus aureus associated with bovine mastitis.* Journal of Dairy Science, 1991. **74**(10): p. 3353-3359.
604. Nascimento de Araujo, A. and L. Gimenes Giugliano, *Lactoferrin and free secretory component of human milk inhibit the adhesion of enteropathogenic Escherichai coli to HeLa cells.* BMC Microbiology, 2001. **1**(25).
605. De Araújo, A.N. and L. Gimenes Giugliano, *Lactoferrin and free secretory component of human milk inhibit the adhesion of enteropathogenic Escherichia coli to HeLa cells.* BMC Microbiology, 2001. **1**: p. 1-6.
606. Berlutti, F., et al., *Both lactoferrin and iron influence aggregation and biofilm formation in Streptococcus mutans.* BioMetals, 2004. **17**(3): p. 271-278.
607. Orndorff, P.E., et al., *Immunoglobulin-Mediated Agglutination of and Biofilm Formation by Escherichia coli K-12 Require the Type 1 Pilus Fiber.* Infection and Immunity, 2004. **72**(4): p. 1929-1938.
608. Shida, K., et al., *Enterotoxin-binding glycoproteins in a proteose-peptone fraction of heated bovine milk.* Journal of Dairy Science, 1994. **77**(4): p. 930-939.
609. Brück, W.M., et al., *The effects of α-lactalbumin and glycomacropeptide on the association of CaCo-2 cells by enteropathogenic Escherichia coli, Salmonella typhimuriumand Shigella flexneri.* FEMS Microbiology Letters, 2006. **259**(1): p. 158-162.
610. Muller, E., et al., *Blood Proteins Do Not Promote Adherence of Coagulase-Negative Staphylococci to Biomaterials.* Infection and Immunity, 1991. **59**(9): p. 3323-3326.
611. Bulard, E., et al., *Competition of bovine serum albumin adsorption and bacterial adhesion onto surface-grafted ODT: In situ study by vibrational SFG and fluorescence confocal microscopy.* Langmuir, 2012. **28**(49): p. 17001-17010.
612. Fletcher, M., *The effects of proteins on bacterial attachment to polystyrene.* Journal of General Microbiology, 1976. **94**(2): p. 400-404.
613. Ovchinnikova, E.S., et al., *Exchange of adsorbed serum proteins during adhesion of Staphylococcus aureus to an abiotic surface and Candida albicans hyphae-An AFM study.* Colloids and Surfaces B: Biointerfaces, 2013. **110**: p. 45-50.
614. Sjobring, U., et al., *Isolation and characterization of a 14-kDa albumin-binding fragment of streptococcal protein G.* Journal of Immunology, 1988. **140**(5): p. 1595-1599.
615. Myhre, E.B. and G. Kronvall, *Demonstration of specific binding sites for human serum albumin in group C and G streptococci.* Infection and Immunity, 1980. **27**(1): p. 6-14.
616. Schmidt, K.H. and T. Wadstrom, *A secreted receptor related to M1 protein of Streptococcus pyogenes binds to fibrinogen, IgG, and albumin.* Zentralblatt fur Bakteriologie, 1990. **273**(2): p. 216-228.

617. Vacca-Smith, A.M., et al., *The effect of milk and casein proteins on the adherence of Streptococcus mutans to saliva-coated hydroxyapatite.* Archives of Oral Biology, 1994. **39**(12): p. 1063-1069.
618. Neeser, J.R., et al., *In vitro modulation of oral bacterial adhesion to saliva-coated hydroxyapatite beads by milk casein derivatives.* Oral Microbiology and Immunology, 1994. **9**(4): p. 193-201.
619. Hytönen, J., S. Haataja, and J. Finne, *Use of flow cytometry for the adhesion analysis of Streptococcus pyogenes mutant strains to epithelial cells: Investigation of the possible role of surface pullulanase and cysteine protease, and the transcriptional regulator Rgg.* BMC Microbiology, 2006. **6**.
620. *Cy5 dye.* accessed 02/02/2015.
621. *Fluorescein (FITC).* accessed 02/02/2015; Available from: https://www.lifetechnologies.com/nz/en/home/life-science/cell-analysis/fluorophores/fluorescein.html.
622. Stegen, J., et al., *Mass-action driven conformational switching of proteins: Investigation of beta-lactoglobulin dimerisation by infrared spectroscopy.* Journal of Physics D: Applied Physics, 2015. **48**(38).
623. Gunning, A.P., et al., *Mapping specific adhesive interactions on living human intestinal epithelial cells with atomic force microscopy.* FASEB J, 2008. **22**(7): p. 2331-9.
624. Koolman, J. and K.-H. Rohm, *Taschenatlas der Biochemie*. 3rd ed. 2003, Stuttgart: Georg Thieme Verlag.
625. *UniProtKB - P00711 (LALBA_BOVIN)*. 2015 17 November 2015]; Available from: http://www.uniprot.org/uniprot/P00711.
626. Chakraborty, T., I. Chakraborty, and S. Ghosh, *The methods of determination of critical micellar concentrations of the amphiphilic systems in aqueous medium.* Arabian Journal of Chemistry, 2011. **4**(3): p. 265-270.
627. Scientific, B. *Critical Micelle Concentration*. 2015 17 November 2015]; Available from: http://www.biolinscientific.com/attension/applications/?card=AA8.
628. Dufour, E., M. Dalgalarrondo, and L. Adam, *Conformation of β-lactoglobulin at an oil/water interface as determined from proteolysis and spectroscopic methods.* J Colloid Interface Sci, 1998. **207**(2): p. 264-272.
629. Benattar, J.J., et al., *Adhesion of a free-standing Newton black film onto a solid substrate.* Angewandte Chemie - International Edition, 2006. **45**(25): p. 4186-4188.
630. Nedyalkov, M., C. Sultanem, and J.J. Benattar, *Contact angles of protein black foam films under dynamic and equilibrium conditions.* Central European Journal of Chemistry, 2007. **5**(3): p. 748-765.
631. Cascão Pereira, L.G., et al., *A bike-wheel microcell for measurement of thin-film forces.* Colloids and Surfaces A: Physicochemical and Engineering Aspects, 2001. **186**(1-2): p. 103-111.
632. 09 November 2015]; Available from: https://blast.ncbi.nlm.nih.gov/Blast.cgi?PROGRAM=blastp&PAGE_TYPE=BlastSearch&BLAST_SPEC=blast2seq&LINK_LOC=blasttab.
633. Sánchez, L., et al., *Iron transport across Caco-2 cell monolayers. Effect of transferrin, lactoferrin and nitric oxide.* Biochimica et Biophysica Acta - General Subjects, 1996. **1289**(2): p. 291-297.
634. Yu, Q., et al., *The effect of various absorption enhancers on tight junction in the human intestinal Caco-2 cell line.* Drug Development and Industrial Pharmacy, 2013. **39**(4): p. 587-592.
635. Gabor, F., A. Schwarzbauer, and M. Wirth, *Lectin-mediated drug delivery: Binding and uptake of BSA-WGA conjugates using the Caco-2 model.* International Journal of Pharmaceutics, 2002. **237**(1-2): p. 227-239.
636. Spiliopoulou, A.I., et al., *An extracellular Staphylococcus epidermidis polysaccharide: Relation to Polysaccharide Intercellular Adhesin and its implication in phagocytosis.* BMC Microbiology, 2012. **12**.

637. Myhre, E.B. and G. Kronvall, *Specific binding of bovine, ovine, caprine and equine IgG subclasses to defined types of immunoglobulin receptors in gram-positive cocci.* Comparative Immunology, Microbiology and Infectious Diseases, 1981. **4**(3-4): p. 317-328.
638. Gao, S., *Bacterial survival during long-term stationary phase*, in *Biology Education Centre and Department of Cell and Molecular Biology*2010, Uppsala Universitet: Uppsala.
639. Alhede, M., et al., *Pseudomonas aeruginosa biofilms. Mechanisms of immune evasion*, in *Adv Appl Microbiol*2014. p. 1-40.
640. Cu, Y. and W.M. Saltzman, *Mathematical modeling of molecular diffusion through mucus.* Adv Drug Deliv Rev, 2009. **61**(2): p. 101-114.
641. Baumgartner, W., et al., *Cadherin interaction probed by atomic force microscopy.* Proc Natl Acad Sci U S A, 2000. **97**(8): p. 4005-4010.
642. McNamee, C.E., et al., *Determination of the binding of non-cross-linked and cross-linked gels to living cells by atomic force microscopy.* Langmuir, 2009. **25**(12): p. 6977-6984.
643. Roth, Z., G. Yehezkel, and I. Khalaila, *Identification and Quantification of Protein Glycosylation.* International Journal of Carbohydrate Chemistry, 2012. **2012**: p. 10.
644. Novotny, M.V. and Y. Mechref, *New hyphenated methodologies in high-sensitivity glycoprotein analysis.* Journal of Separation Science, 2005. **28**(15): p. 1956-1968.
645. Bond, M.R. and J.J. Kohler, *Chemical methods for glycoprotein discovery.* Current Opinion in Chemical Biology, 2007. **11**(1): p. 52-58.
646. Ulberth, F., R. Gabernig, and D. Roubicek, *Gas Chromatographie triglyceride profiling of milk fat; comparison of packed and short metal capillary columns.* European Food Research and Technology, 1998. **206**(1): p. 21-24.
647. Destaillats, F., et al., *Authenticity of milk fat by fast analysis of triacylglycerols. Application to the detection of partially hydrogenated vegetable oils.* Journal of Chromatography A, 2006. **1131**(1-2): p. 227-234.
648. Guenther, H.O., *immunochemische Nachweismethoden fuer Milchproteine*, in *Milchproteine Bd.4 der Schriftenreihe Lebensmittelchemie, Lebensmittelqualitaet*. 1991, Behr's Verlag GmbH: Hamburg.
649. Janeway, C.A., Jr., et al., *Chapter 3 - Antigen recognition by B-cell and T-cell receptors*. 5th ed. Immunobiology, The Immune System in Health and Disease. 2001, New York: Garland Science.
650. Vermeer, A.W.P. and W. Norde, *The Thermal Stability of Immunoglobulin: Unfolding and Aggregation of a Multi-Domain Protein.* Biophys J, 2000. **78**(1): p. 394-404.
651. Hill, K.E., et al., *Cerebellar Purkinje cells incorporate immunoglobulins and immunotoxins in vitro: Implications for human neurological disease and immunotherapeutics.* Journal of Neuroinflammation, 2009. **6**: p. 31.
652. Morea, V., et al., *Conformations of the third hypervariable region in the VH domain of immunoglobulins.* Journal of Molecular Biology, 1998. **275**(2): p. 269-294.
653. Xu, J.L. and M.M. Davis, *Diversity in the CDR3 region of V(H) is sufficient for most antibody specificities.* Immunity, 2000. **13**(1): p. 37-45.
654. Svanborg-Eden, C. and A.M. Svennerholm, *Secretory immunoglobulin A and G antibodies prevent adhesion of Escherichia coli to human urinary tract epithelial cells.* Infection and Immunity, 1978. **22**(3): p. 790-797.
655. Marnila, P. and H. Korhonen, *Immunoglobulins*, in *Encyclopedia of Dairy Science*, H. Roginski, Editor. 2002, Academic Press: New York. p. 1950-1956.
656. Labeta, M.O., et al., *Structure of asymmetric non-precipitating antibody: Presence of a carbohydrate residue in only one Fab region of the molecule.* Immunology, 1986. **57**(2): p. 311-317.
657. Grebenau, R.C., et al., *Microheterogeneity of a purified IgG1, due to asymmetric fab glycosylation.* Molecular Immunology, 1992. **29**(6): p. 751-758.

658. Spiegelberg, H.L., et al., *Localization of the carbohydrate within the variable region of light and heavy chains of human γG myeloma proteins.* Biochemistry, 1970. **9**(21): p. 4217-4223.
659. Aoki, N., et al., *A bovine IgG heavy chain contains N-acetylgalactosaminylated N-linked sugar chains.* Biochemical and Biophysical Research Communications, 1995. **210**(2): p. 275-280.
660. Marchalonis, J.J., et al., *Exquisite specificity and peptide epitope recognition promiscuity, properties shared by antibodies from sharks to humans.* Journal of Molecular Recognition, 2001. **14**(2): p. 110-121.
661. Prabhakar, B.S., et al., *Lymphocytes capable of making monoclonal autoantibodies that react with multiple organs are a common feature of the normal B cell repertoire.* Journal of Immunology, 1984. **133**(6): p. 2815-2817.
662. Vollmers, H.P. and S. Brändlein, *Natural IgM antibodies: The orphaned molecules in immune surveillance.* Adv Drug Deliv Rev, 2006. **58**(5-6): p. 755-765.
663. Mathias, A. and B. Corthésy, *Recognition of gram-positive intestinal bacteria by hybridoma- and colostrum-derived secretory immunoglobulin A is mediated by carbohydrates.* Journal of Biological Chemistry, 2011. **286**(19): p. 17239-17247.
664. Pan, Y., et al., *Enhancing the antimicrobial and antiviral properties of whey proteins by chemical modification.* Australian Journal of Dairy Technology, 2007. **62**(2): p. 9-10.
665. Nwosu, C.C., et al., *Comparison of the human and bovine milk N-Glycome via high-performance microfluidic chip liquid chromatography and tandem mass spectrometry.* Journal of Proteome Research, 2012. **11**(5): p. 2912-2924.
666. Hurley, W.L., et al., *Electrophoretic comparisons of lactoferrin from bovine mammary secretions, milk neutrophils, and human milk.* Journal of Dairy Science, 1993. **76**(2): p. 377-387.
667. Le Parc, A., et al., *Characterization of goat milk lactoferrin N-glycans and comparison with the N-glycomes of human and bovine milk.* Electrophoresis, 2014. **35**(11): p. 1560-1570.
668. El-Loly, M. and M.B. Mahfouz, *Lactoferrin in relation to biological functions and applications: A review.* International Journal of Dairy Science, 2011. **6**(2): p. 79-111.
669. Baker, E.N. and H.M. Baker, *A structural framework for understanding the multifunctional character of lactoferrin.* Biochimie, 2009. **91**(1): p. 3-10.
670. Moore, S.A., et al., *Three-dimensional structure of diferric bovine lactoferrin at 2.8 Å resolution.* Journal of Molecular Biology, 1997. **274**(2): p. 222-236.
671. López-Expósito, I., L. Amigo, and I. Recio, *Identification of the initial binding sites of αs2-casein f(183-207) and effect on bacterial membranes and cell morphology.* Biochimica et Biophysica Acta - Biomembranes, 2008. **1778**(10): p. 2444-2449.
672. Sinha, M., et al., *Antimicrobial lactoferrin peptides: The hidden players in the protective function of a multifunctional protein.* International Journal of Peptides, 2013. **2013**.
673. Bellamy, W.R., et al., *Role of cell-binding in the antibacterial mechanism of lactoferricin B.* Journal of Applied Bacteriology, 1993. **75**(5): p. 478-484.
674. Ashida, K., et al., *Cellular internalization of lactoferrin in intestinal epithelial cells.* BioMetals, 2004. **17**(3): p. 311-315.
675. Delfour, A., et al., *Caseino-glycopeptides: Characterization of a methionine residue and of the N-terminal sequence.* Biochemical and Biophysical Research Communications, 1965. **19**(4): p. 452-455.
676. Nakajima, K., et al., *Prevention of intestinal infection by glycomacropeptide.* Bioscience, Biotechnology and Biochemistry, 2005. **69**(12): p. 2294-2301.
677. Hira, T., H. Hara, and F. Tomita, *Characterization of Binding between the Rat Small Intestinal Brush-border Membrane and Dietary Proteins in the Sensory Mechanism of Luminal Dietary Proteins.* Bioscience, Biotechnology and Biochemistry, 2001. **65**(5): p. 1007-1015.

678. Boutrou, R., et al., *Glycosylations of κ-casein-derived caseinomacropeptide reduce its accessibility to endo- but not exointestinal brush border membrane peptidases.* Journal of Agricultural and Food Chemistry, 2008. **56**(17): p. 8166-8173.
679. Fosset, S., et al., *Peptide fragments released from Phe-caseinomacropeptide in vivo in the rat.* Peptides, 2002. **23**(10): p. 1773-1781.
680. Jameson, G.B., J.J. Adams, and L.K. Creamer, *Flexibility, functionality and hydrophobicity of bovine β-lactoglobulin.* International Dairy Journal, 2002. **12**(4): p. 319-329.
681. Ouwehand, A.C. and S.J. Salminen, *Adhesion inhibitory activity of β-lactoglobulin isolated from infant formulae.* Acta Paediatrica, International Journal of Paediatrics, 1998. **87**(5): p. 491-493.
682. Ruseler-Van Embden, J.G.H., et al., *Changes in bacterial composition and enzymatic activity in ileostomy and ileal reservoir during intermittent occlusion: A study using dogs.* Applied and Environmental Microbiology, 1992. **58**(1): p. 111-118.
683. Perez, M.D., et al., *Interaction of fatty acids with β-lactoglobulin and albumin from ruminant milk.* Journal of Biochemistry, 1989. **106**(6): p. 1094-1097.
684. Wu, S.Y., et al., *β-Lactoglobulin binds palmitate within its central cavity.* Journal of Biological Chemistry, 1999. **274**(1): p. 170-174.
685. Dufour, E. and T. Haertlé, *Binding of retinoids and β-carotene to β-lactoglobulin. Influence of protein modifications.* Biochimica et Biophysica Acta (BBA)/Protein Structure and Molecular, 1991. **1079**(3): p. 316-320.
686. Narayan, M. and L.J. Berliner, *Fatty acids and retinoids bind independently and simultaneously to β- lactoglobulin.* Biochemistry, 1997. **36**(7): p. 1906-1911.
687. Wang, Q., J.C. Allen, and H.E. Swaisgood, *Binding of Vitamin D and Cholesterol to β-Lactoglobulin.* Journal of Dairy Science, 1997. **80**(6): p. 1054-1059.
688. Ragona, L., et al., *Bovine β-lactoglobulin: Interaction studies with palmitic acid.* Protein Science, 2000. **9**(7): p. 1347-1356.
689. Beringhelli, T., et al., *pH and ionic strength dependence of protein (Un)folding and ligand binding to bovine β-lactoglobulins A and B.* Biochemistry, 2002. **41**(51): p. 15415-15422.
690. Barbiroli, A., et al., *Bovine β-lactoglobulin acts as an acid-resistant drug carrier by exploiting its diverse binding regions.* Biological Chemistry, 2010. **391**(1): p. 21-32.
691. Courtney, H.S., W.A. Simpson, and E.H. Beachey, *Binding of streptococcal lipoteichoic acid to fatty acid-binding sites on human plasma fibronectin.* Journal of Bacteriology, 1983. **153**(2): p. 763-770.
692. Weidenmaier, C. and A. Peschel, *Teichoic acids and related cell-wall glycopolymers in Gram-positive physiology and host interactions.* Nature Reviews Microbiology, 2008. **6**(4): p. 276-287.
693. Brown, S., J.P. Santa Maria Jr, and S. Walker, *Wall teichoic acids of gram-positive bacteria*, in *Annual Review of Microbiology*2013. p. 313-336.
694. Hussain, M., et al., *Teichoic acid enhances adhesion of Staphylococcus epidermidis to immobilized fibronectin.* Microb Pathog, 2001. **31**(6): p. 261-270.
695. Kulikov, S.N., R.Z. Khairullin, and V.P. Varlamov, *Influence of polycations on antibacterial activity of lysostaphin.* Applied Biochemistry and Microbiology, 2015. **51**(6): p. 683-687.
696. Lambert, P.A., I.C. Hancock, and J. Baddiley, *Influence of alanyl ester residues on the binding of magnesium ions to teichoic acids.* Biochemical Journal, 1975. **151**(3): p. 671-676.
697. Sakaguchi, M., *Eukaryotic protein secretion.* Current Opinion in Biotechnology, 1997. **8**(5): p. 595-601.
698. Van Leeuwen, S.S., et al., *N -and O -Glycosylation of a Commercial Bovine Whey Protein Product.* Journal of Agricultural and Food Chemistry, 2012. **60**(51): p. 12553-12564.
699. Recio, I., F.J. Moreno, and R. Lopez-Fandino, *Glycosylated dairy components: Their roles in nature and ways to make use of their biofunctionality in dairy products*, in

Dairy-Derived Ingerdients - Food and Nutraceutical Uses, M. Corredig, Editor. 2009, CRC Press & Woodhead Publishing Limited. p. 170-211.

700. Alexander, D.B., et al., *Lactoferrin: An alternative view of its role in human biological fluids.* Biochemistry and Cell Biology, 2012. **90**(3): p. 279-306.

701. Hammarström, L. and C.K. Weiner, *Targeted antibodies in dairy-based products*, in *Advances in Experimental Medicine and Biology*, Z. Bosze, Editor 2008. p. 321-343.

702. Fayer, R. and M.C. Jenkins, *Colostrum from cows immunized with Eimeria acervulina antigens reduces parasite development in vivo and in vitro.* Poultry science, 1992. **71**(10): p. 1637-1645.